



**GOUT AS AN AUTOINFLAMMATORY DISEASE:  
FROM CELLULAR TO GENETIC MECHANISMS**

Emma García Melchor

*Ph.D. Thesis*  
Ph.D. in Medicine

Supervisors:  
Manel Juan Otero  
Mònica Gumà Uriel

Academic tutor:  
Miquel Sabrià Leal

Department of Medicine  
Universitat Autònoma de Barcelona

**2014**



*Al Joan i la Nora,  
per haver-me canviat la vida*



## Abstract

Gout has been classified as an autoinflammatory disease because of its self-remitting course and the involvement of the innate immune system and IL-1 $\beta$  in its pathogenesis. During the last years, the evidence of NLRP3 inflammasome activation by monosodium urate (MSU) crystals and the beneficial effect of IL-1 blockade for the treatment of patients with gout, have reaffirmed the concept of gout as an autoinflammatory disease. However, some questions regarding its pathogenesis remain still unanswered. The presence of MSU crystals in asymptomatic joints or why not all individuals with hyperuricemia develop clinical gout, are some examples. In this thesis we centred our attention in the mononuclear phagocyte system with the hypothesis that the state of activation or maturation of monocytes and macrophages modulates the inflammatory response to MSU crystals.

Regarding macrophages, our hypothesis is that resident macrophages, after contact with MSU crystals, acquire an inflammatory phenotype, being able to produce inflammatory cytokines in the presence of a second signal or trigger. Therefore, to test it, we used an *in vitro* model of human monocyte-derived macrophages polarized towards M1 or M2 phenotypes in the presence of GM-CSF and M-CSF respectively, considering M2 macrophages a model of resident synovial macrophages. M1 and M2 macrophages failed to produce IL-1 $\beta$  after stimulation with MSU crystals or LPS. However, in the presence of MSU, M2 macrophages produced IL-1 $\beta$  and decreased IL-10 secretion when LPS was added. Surprisingly, soluble uric acid had a suppressive effect for expression of both cytokines. The production of IL-1 $\beta$  was explained because MSU crystals increased the presence of active caspase-1, reflecting inflammasome activation, whereas LPS induced pro-IL-1 $\beta$  and inactive caspase-1 production. Analysis of inflammasome activation in M1 and M2 macrophages revealed differences in inflammasome proteins, that could account for their different IL-1 $\beta$  production.

To investigate if the capacity of monocytes to react to MSU crystals could explain why some individuals develop gout, we compared the inflammasome activation induced by MSU crystals in PBMCs from gouty patients with healthy controls. PBMCs of patients with gout exhibited enhanced inflammasome activation after culture with MSU. Therefore, our results suggest that patients with gout have an increased reactivity to MSU crystals. To provide further insight, we genotyped exon 3 of *NLRP3* gene in gout patients, without finding any association of gout with polymorphisms in this gene. Finally, we analyzed the distribution of different monocyte phenotypes or blood subpopulations in patients with gout. We observed an expansion of the intermediate subpopulation (CD14<sup>++</sup>CD16<sup>+</sup>) during gout flares, but no differences were observed in any of the subpopulations between asymptomatic patients and healthy controls.



# Table of Contents

ABBREVIATIONS .....	XIII
<b>1. INTRODUCTION .....</b>	<b>1</b>
1.1. An overview of gout	3
1.1.1. Gout is an ancient disease	3
1.1.2. Uric acid and hyperuricemia	3
1.1.3. Epidemiology of gout	4
1.1.4. Risk factors for the development of gout	5
1.1.4.1. Gender and age	5
1.1.4.2. Ethnicity	5
1.1.4.3. Diet	6
1.1.4.4. Alcohol consumption	6
1.1.4.5. Drugs	6
1.1.4.6. Hypertension and chronic kidney disease	7
1.1.4.7. Other uric acid comorbidities	7
1.1.4.8. Genetic factors	8
1.1.5. Clinical manifestations	9
1.1.5.1. Acute clinical manifestations	9
1.1.5.2. Persistent clinical manifestations	10
1.1.6. Diagnostic elements and factors to heed	12
1.1.7. Treatment	15
1.1.7.1. Treatment of acute gout arthritis	15
1.1.7.2. Long-term management of gout	17
1.1.7.2.1. Education and lifestyle modifications	18
1.1.7.2.2. Urate-lowering therapy (ULT)	18
1.1.7.2.3. Prophylaxis of gout flares during ULT therapy	20
1.2. Gout as an autoinflammatory disease	20
1.2.1. Autoinflammatory diseases	20
1.2.2. The innate immune system	22
1.2.3. Inflammasomes: NLRP3, the paradigm	24
1.2.4. Interleukin-1 $\beta$	27
1.2.5. Uric acid as a danger signal	29
1.2.6. MSU crystals activate the NLRP3 inflammasome	29
1.3. Role of the mononuclear phagocyte system in gout	30
1.3.1. The mononuclear phagocyte system	30
1.3.2. The concept of macrophage polarization	31

1.3.2.1. M1 macrophages	31
1.3.2.2. M2 macrophages	32
1.3.3. Role of M-CSF and GM-CSF in macrophage polarization	33
1.3.3.1. M-CSF biology and functions	34
1.3.3.2. GM-CSF biology and functions	36
1.3.4. Monocyte subpopulations	37
1.3.5. Role of monocytes and macrophages in gouty arthritis	39
<b>2. HYPOTHESIS</b> .....	<b>43</b>
<b>3. OBJECTIVES</b> .....	<b>47</b>
<b>4. MATERIALS AND METHODS</b> .....	<b>51</b>
4.1. Cell culture	53
4.1.1. Culture of M1 and M2 macrophages	53
4.1.1.1. Isolation of peripheral blood mononuclear cells (PBMCs)	54
4.1.1.2. Isolation of monocytes from PBMCs	54
4.1.1.3. Macrophage polarization	55
4.1.1.4. Culture of macrophages with soluble uric acid (SUA)	55
4.1.1.5. Stimulation with MSU crystals and LPS	56
4.1.1.6. Detachment of macrophages	56
4.1.2. THP-1 cells	56
4.2. MSU preparation	57
4.3. Phagocytosis assays	57
4.3.1. Phagocytosis of fluorescent beads	57
4.3.2. Phagocytosis of MSU crystals	58
4.4. Cytokine analyses	60
4.4.1. Enzyme-linked immunosorbent assay (ELISA)	60
4.4.1.1. IL-1 $\beta$ ELISA	60
4.4.1.2. IL-10 ELISA	60
4.4.2. Luminex assays	61
4.5. Flow cytometry	62
4.5.1. Cell surface antigens	62
4.5.2. Caspase-1 activity in macrophages	62
4.6. Western Blot	63
4.6.1. Sample preparation	63
4.6.1.1. Isolation of cytoplasmic protein	64



4.6.1.2. Protein quantification with Bio-Rad DC™ Protein Assay	64
4.6.2. SDS-PAGE	65
4.6.3. Transferring to PVDF membrane	65
4.6.4. Western Blotting	65
4.7. Expression of genes involved in inflammation	66
4.7.1. Preparation of samples	66
4.7.2. RNA extraction	66
4.7.3. RNA quantification	68
4.7.4. Assessment of RNA quality	68
4.7.5. First strand cDNA synthesis	68
4.7.6. Real time PCR (RT-PCR)	70
4.7.6.1. Taqman probes for IL-1 $\beta$ and caspase-1 RT-PCR	70
4.7.6.2. RT-PCR with SYBR Green for IL-10 and NLRP3 expression	70
4.7.6.3. Universal Probe Library for GAPD expression	71
4.7.6.4. Analysis of RT-PCR results	72
4.7.6.5. Agarose gel electrophoresis	72
4.8. Patients and controls	73
4.8.1. Determination of uric acid, creatinine and CRP in sera	73
4.9. Inflammasome activity in monocytes from patients with gout	74
4.9.1. Selection of samples	74
4.9.2. Quantification of active caspase-1 in monocytes	74
4.10. Monocyte subpopulations in patients with gout	75
4.10.1. Selection of samples	75
4.10.2. Assessment of monocyte subpopulations in peripheral blood	75
4.11. Analysis of <i>NLRP3</i> gene in patients with gout	77
4.11.1. Sample preparation	77
4.11.2. Genomic DNA amplification	77
4.11.3. PCR sequencing reaction	77
4.11.4. Analysis of results	78
4.12. Statistical analysis	78
<b>5. ROLE OF M2 MACROPHAGES IN EARLY STAGES OF GOUT FLARES</b> .....	<b>79</b>
5.1. Characterization of M1 and M2 macrophages	82
5.1.1. Differences in macrophage morphology	82
5.1.2. Expression of cell surface antigens in polarized macrophages	84
5.1.3. Phagocytic capacity of M1 and M2 macrophages	85
5.1.3.1. Phagocytosis of fluorescent beads	85
5.1.3.2. Phagocytosis of MSU crystals	87

5.1.4. Cytokine profile in response to LPS	90
5.1.5. Differential IL-10 gene expression	91
5.2. Role of M2 macrophages in gout initiation	92
5.2.1. Effect of MSU crystals on cytokine production	92
5.2.1.1. Macrophages and MSU	92
5.2.1.2. THP-1 cells and MSU	96
5.2.2. Effect of MSU crystals in cell surface markers	97
5.2.3. Effect of CPP crystals on M2 macrophages	98
5.2.4. Effect of SUA on macrophage function	100
5.2.4.1. Effect of chronic exposure to SUA on macrophage polarization	101
5.2.4.2. Effect of acute exposure to SUA	102
5.2.4.3. Effect of SUA on viability and phagocytic capacity of M2	103
5.3. The inflammasome in the inflammatory response of M2 macrophages	104
5.3.1. Analysis of intracellular active caspase-1	104
5.3.2. Inactive forms of caspase-1, IL-1 $\beta$ and ASC	109
5.3.3. Expression of inflammasome related genes	110
5.3.3.1. Caspase-1 gene expression	111
5.3.3.2. IL-1 $\beta$ gene expression	112
5.3.3.3. <i>NLRP3</i> gene expression	113
<b>6. THE MONONUCLEAR PHAGOCYTE SYSTEM IN PATIENTS WITH GOUT</b>	<b>115</b>
6.1. Demographic data	118
6.2. Caspase-1 activity in patients with gout	119
6.2.1. Demographic data	119
6.2.2. Assessment of inflammasome activity	120
6.2.2.1. Baseline levels of active caspase-1	120
6.2.2.2. Caspase-1 activation in stimulated monocytes	121
6.2.3. IL-1 $\beta$ production after MSU stimulation	123
6.2.4. Polymorphisms of <i>NLRP3</i> gene in gouty patients	125
6.3. Monocyte subpopulations in gout	126
6.3.1. Analysis of monocyte subpopulations	126
6.3.1.1. Relation of monocytes with uric acid, creatinine and CRP	130
6.3.1.2. Influence of gender on monocytes	131
6.3.1.3. Monocyte subpopulations in synovial fluid	132

<b>7. DISCUSSION</b> .....	<b>133</b>
7.1. Role of M2 macrophages in gout initiation	135
7.2. The mononuclear phagocyte system in patients with gout	145
7.3. Future work	150
<b>8. CONCLUSIONS</b> .....	<b>151</b>
<b>BIBLIOGRAPHY</b> .....	<b>155</b>



## Abbreviations

aa	Aminoacid
ACR	American College of Rheumatology
ACR-TFP	ACR Task Force Panels
ACTH	Adrenocorticotropic hormone
ADP	Adenosine diphosphate
AIM2	Absent in melanoma 2
APC	Allophycocyanin
APC	Antigen presenting cell
ASC	Apoptosis-associated speck-like protein containing a caspase recruitment domain
ATP	Adenosine triphosphate
BIR	Baculovirus inhibitor repeat
BMI	Body mass index
BSA	Bovine serum albumin
CAPS	Cryopyrin associated periodic syndromes
CARD	Caspase recruitment domain
CD	Cluster of differentiation
CD	Cluster of differentiation
CI	Confidence interval
CIITA	Class II MHC transactivator
CINCA	Chronic infantile neurologic, cutaneous, articular syndrome
CKD	Chronic kidney disease
CLE	Cutaneous lupus erythematosus
COX	Cyclooxygenase
CPP	Calcium pyrophosphate
CRP	C-reactive protein
cRPMI	Complete RPMI medium
CS	Corticosteroids
CSF-1	Colony stimulating factor 1
CYP3A4	Cytochrome P450 3A4
DAMP	Danger-associated molecular pattern
DC	Dendritic cell
DECT	Dual-energy computed tomography
DIRA	Deficiency of IL-1 receptor antagonist

DNA	Deoxyribonucleic acid
dsDNA	Double-stranded DNA
dsRNA	Double-stranded RNA
EDTA	Ethylenediaminetetraacetic acid
eGFR	Estimated glomerular filtration rate
ELISA	Enzyme-Linked ImmunoSorbent Assay
EMA	European Medicines Agency
ERK	Extracellular signal-regulated kinase
EU	Endotoxin units
FACS	Fluorescent activated cell sorting
FBS	Fetal bovine serum
FC	Fragment crystallisable region
FCAS	Familial cold autoinflammatory syndrome
FCS	Fetal calf serum
FDA	Food and Drug Administration
FITC	Fluorescein isothiocyanate
FMF	Familial Mediterranean fever
FSC	Forward scatter
GM-CSF	Granulocyte macrophage colony-stimulating factor
GMP	Glycomacropeptide
GWAS	Genome-wide association studies
HBSS	Hank's Buffered Saline Solution
HEPES	4-(2-hydroxyethyl)-1-piperazineethanesulfonic acid
HGPRT	Hypoxanthine-guanine phosphoribosyl transpherase
HIDS	Hyperimmunoglobulin-D syndrome
HLA	Human leukocyte antigen
IC	Immune complexes
ICAM-1	Intercellular adhesion molecule-1
IFN	Interferon
IgG	Immunoglobulin G
IL	Interleukin
IL-1R	Interleukin-1 receptor
IL-1Ra	Interleukin-1 receptor antagonist
IL-1RAcP	Interleukin-1 receptor accessory protein

IM	Intramuscular
iNOS	Inducible nitric oxide synthase
IP10	Interferon gamma-induced protein 10 or CXCL10
IRAK	Interleukin-1 receptor associated kinase
IRF	Interferon regulatory factor
IV	Intravenous
JNK	C-Jun N-terminal kinase
LGP2	Laboratory of genetics and physiology 2
LPS	Lipopolysaccharide
LPS	Lipopolysaccharide
LRR	Leucine rich repeat
MAPK	Mitogen-activated kinase
mBSA	Methylated bovine serum albumin
MCP1	Monocyte chemoattractant protein 1 or CCL2
M-CSF	Macrophage colony-stimulating factor
MDA5	Melanoma differentiation-associated protein
MES	2-(N-morpholino) ethanesulfonic acid
MFI	Mean fluorescence intensity
MHC	Major histocompatibility complex
MIG	Monokine induced by gamma interferon or CXCL9
MRI	Magnetic resonance imaging
mRNA	Messenger RNA
MSU	monosodium urate crystals
MW	Muckle-Wells syndrome
MYD88	Myeloid differentiation primary response 88
NACHT	NAIP (neuronal apoptosis inhibitory protein), CIITA (MHC class II transcription activator), HET-E (incompatibility locus protein from <i>Podospora anserina</i> ) and TP1 (telomerase-associated protein)
NAIP	NLR family CARD domain-containing protein 4
NALP	NACHT-leucine rich repeat-pyrin domain-containing protein
NF- $\kappa$ B	Nuclear factor kappa-light-chain-enhancer of activated B cells
NHANES	National Health and Nutrition Examination Survey
NK	Natural killer
NLR	NOD-like receptor

NLRP3	NOD-like receptor family, pyrin domain containing 3 gene
NO	Nitric oxide
NOD	Nucleotide-binding oligomerization domain
NOMID	Neonatal-onset multisystem inflammatory disease
NSAIDS	Non-steroidal anti-inflammatory analgesics
OR	Odds ratio
P2X7R	Purinergic receptor P2X ligand-gated ion channel 7
PAMP	Pathogen-associated molecular pattern
PBMCs	Peripheral blood mononuclear cells
PBS	Phosphate buffered solution
PGN	Peptidoglycan
pKa	Acidic dissociation constant
PMA	Phorbol 12-myristate 13-acetate
PMSF	Phenylmethyl
PRPS1	5-phosphoribosyl-1-pyrophosphate synthetase
PRR	Pattern recognition receptor
PVDF	Ployvinylidene difluoride
PYD	Pyrin
RA	Rheumatoid arthritis
RANK-L	Receptor activator of nuclear factor-kappa B ligand
RIG-1	Retinoic acid-inducible gene 1
RLH	RIG-like helicase
RLR	RIG-like receptor
RNA	Ribonucleic acid
ROS	Reactive oxygen species
Rpm	Revolutions per minute
RPMI	Roswell Park Memorial Institute-1640 medium
RR	Relative risk
RT	Room temperature
RT-PCR	Reverse transcriptase polymerase chain reaction
SAA	Serum amyloid A protein
SD	Standard deviation
SDS	Sodium dodecyl sulfate
SDS-PAGE	SDS polyacrylamide gel electrophoresis



SIGIRR	Single IG IL-1-related receptor
SJS	Stevens-Johnson syndrome
SSC	Side scatter
SUA	Soluble uric acid
TEN	Toxic epidermal necrolysis
TGF- $\beta$	Transforming growth factor beta
Th1	T helper cells 1
Th17	T helper cells 17
Th2	T helper cells 2
THP-1	Human monocytic leukemia cell line
TIR	Toll/Interleukin-1 receptor
TLR	Toll-like receptor
TMB	3,3', 5,5' tetramethylbenzidine (TMB)
TNF	Tumour necrosis factor
TRAF	TNF receptor-associated factor
TRAPS	TNF receptor-associated periodic syndrome
TXNIP	Thioredoxin-interacting protein
UA	Uric acid
UK	United Kingdom
ULT	Urate lowering therapy
US	Ultrasonography
XOI	Xantine oxidase inhibitors



*"Men love to wonder,  
and that is the seed of science"*

Ralph Waldo Emerson

1.

**Introduction**



## 1.1. An overview of gout

Gout is a disease caused by the deposition of monosodium urate (MSU) crystals in tissues such as cartilage, synovial membranes, bone and skin<sup>[1]</sup>. In the musculoskeletal system gout affects both articular and extra-articular structures, resulting in arthritis, tendinitis and bursitis. This deposition occurs when serum uric acid levels exceed the saturation point for MSU crystal formation, a condition referred as hyperuricemia<sup>[2,3]</sup>.

### 1.1.1. Gout is an ancient disease

A good proof of that is that bone erosions suggestive of gout have been found in phalanges from *Tyrannosaurus rex* specimens<sup>[4]</sup>. First descriptions of gout come from Hippocrates in the fifth century BC, who referred to it as 'the un-walkable disease' and linked gout to lifestyle. In the ancient Greek medicine, gout received the name of *podagra* from the words *pous* meaning food and *agra* a seizure<sup>[5]</sup>. It was also the Greek physician Galen who described for the first time the macroscopic deposits of MSU crystals, or tophi, and who recognized an hereditary trait in gout. The term gout, from the Latin word *gutta*, was first used by the dominican monk Randolphus of Bocking from the medieval belief that when one of the four humours was in excess, it could flow into a joint like a drop, causing inflammation<sup>[6]</sup>. Antoni van Leeuwenhoek, considered the father of microbiology, described the appearance of MSU crystals in a tophus<sup>[7]</sup>. These crystals were identified as urate by Wollaston in a tophus from his own ear in 1797<sup>[8]</sup>. Sir Alfred Garrod linked the condition of hyperuricemia with gout, developing a semi-quantitative method for the measure of uric acid in serum and urine, considered the first clinical chemical tester ever undertaken<sup>[6,9]</sup>. MSU crystals in synovial fluid of patients were identified by McCarty and Hollander using the polarized light microscope<sup>[10]</sup>. Moreover, they confirmed the role of MSU crystals in gout by injecting them in their own joints<sup>[11]</sup>.

### 1.1.2. Uric acid and hyperuricemia

Uric acid is the final product of the metabolic breakdown of purines. It is a weak acid with an acidic dissociation constant ( $pK_a$ ) of 5.5, meaning that at the physiological pH 7.4, uric acid predominantly acquires the urate-ionised form. As sodium is the most abundant extracellular ion, most of this urate is found as monosodium urate. Two-thirds of the uric acid produced daily is eliminated through the kidneys, whereas other routes such as saliva, gastric juice, pancreatic secretions and bowel account for the other third. Impaired renal excretion of uric acid is the main cause of hyperuricemia. When urate concentrations exceed its solubility limit (380  $\mu\text{mol/l}$  or 6.8  $\text{mg/dL}$  at 37°C), urate precipitates and forms crystals in tissues<sup>[3,12]</sup>.

Primates, birds, some reptiles and most insects lack the enzyme uricase that in other species is responsible of the breakdown of uric acid into the soluble compound allantoin<sup>[13,14]</sup>. This fact explains that other mammals exhibit uric acid levels below 2 mg/dL and do not suffer gout. The loss of the uricase gene occurred during the Miocene epoch, approximately 15-20 million of years ago, a period of progressive cooling that affected the diet of our ancestors, that was mainly vegetarian and low in sodium<sup>[15]</sup>. Repeated mutations in promoter and sequencing regions resulted in the loss of activity<sup>[16]</sup>. It has been proposed that the raise in uric acid levels could have had an evolutionary advantage, maintaining blood pressure and protecting from dehydration, stimulating hypertriglyceridemia, fatty acid liver and weight gain to re-establish fat stores, inducing insulin resistance that could have preserve glucose for utilization by the brain and preventing oxidative brain damage<sup>[17,18]</sup>. Nowadays, this advantage seems to have disappeared, as in western countries the intake of fructose and purine-rich foods has increased uric acid levels to the point that are harmful and associated with morbidity and an increased mortality.

Hyperuricemia is defined in a physiochemical sense, when serum urate concentration exceeds the solubility limit of MSU, which is 6.8 mg/dL at 37°C. In a relative sense hyperuricemia is considered when this concentration exceeds the upper limit of the normal range, defined as the mean serum urate value plus two standard deviation in sex and age-matched healthy population. In this case, the upper limit is different in men (7 mg/dL) and in women (6 mg/dL)<sup>[3]</sup>. The risk of gouty arthritis increases with uric acid concentrations: yearly incidence of gout is 0.1% with uric acid levels below 7 mg/dL, 0.5% between 7 and 8.9 mg/dL and 4.9% when higher than 9 mg/dL<sup>[19]</sup>. With urate levels of 9 mg/dL the cumulative incidence of gout arthritis is 22% after five years, suggesting that for unknown reasons not all patients with hyperuricemia will develop symptoms of gout.

### 1.1.3. Epidemiology of gout

Gout is a frequent condition, being the first cause of arthritis in men in the Western countries<sup>[20]</sup>. Its prevalence has experienced an increase over the last decades due to factors such as ageing of the population, changes in lifestyle, increased prevalence of advanced chronic kidney disease and use of drugs associated with gout.<sup>[21]</sup> In United States prevalence of gout doubled from 1969 to 1985, experiencing a slower increase thereafter<sup>[22,23]</sup>. According to the latest National Health and Nutrition Examination Survey (NHANES) study, self-reported lifetime prevalence of gout in 2007-2008 was 3.9%, which corresponded to 8.3 million of adults with gout<sup>[24]</sup>. This prevalence was higher in men than in women (5.9% versus 2%) and increased with age, with a peak of 12.6% above 80 years old. When comparing with the first NHANES study from 1988 to 1994, gout increased 1.2% and hyperuricemia 3.2%. This trend

was observed in United Kingdom (UK) too, where prevalence increased from 2.6/1000 in 1987 to 9.5/1000 in 1993.<sup>[25-27]</sup> More recent epidemiological studies have estimated a lifetime prevalence of 1.4% in UK and Germany during the years 2000-2004<sup>[28]</sup>. In Italy prevalence increased from 6.7/1000 in 2005 to 9.1/1000 in 2009<sup>[29]</sup>, as well as in China, where prevalence was 3.6/1000 and 5.3/1000 in 2002 and 2004 respectively<sup>[30,31]</sup>. In New Zealand estimated prevalence during the years 1998-2009 was 2.69%, increasing with age and affecting 25% of Māori men older than 65 years old<sup>[32]</sup>.

Regarding the incidence of gout, in the Rochester Epidemiology Project, age and sex-adjusted annual incidence rates of gout increased from 45/100.000 during the years 1977-1978 to 62.3/100.000 during the years 1995-1996. While the incidence of secondary gout did not change over time, the incidence of primary gout doubled. In this study, the fact that more cases of atypical gout were diagnosed during the last period prompted the authors to suggest that the ascertain of atypical cases and the use of arthrocentesis could contribute to this increase in gout incidence<sup>[33]</sup>. In Italy, an incidence around 0.9/1000 person per year remained stable from 2005 to 2009<sup>[29]</sup>.

#### **1.1.4. Risk factors for the development of gout**

##### **1.1.4.1. Gender and age**

Uric acid levels in children are low, around 3-4 mg/dL, because of their high renal uric acid clearance. At puberty, concentrations increase 1-2 mg/dL in males, whereas females exhibit little change due to the uricosuric effect of sex hormones. This fact explains that gout is more frequent in men and increases in women after menopause<sup>[3]</sup>. Gout prevalence increases with age secondary to a decrease in renal function that results in higher uric acid levels, the use of diuretics and other drugs associated with hyperuricemia and changes in connective tissues, such as the higher prevalence of osteoarthritis, that can facilitate MSU crystal deposition.

##### **1.1.4.2. Ethnicity**

As previously described, prevalence of gout varies between countries and ethnicities, being infrequent in African countries whereas a higher prevalence is observed in aboriginal populations of Asia and Australasia<sup>[20]</sup>. In New Zealand prevalence ranges from 3.24% in European ancestry population to 7.63% in Pacific Islands population. Moreover, in Māoris gout has a stronger familiar association, an early onset and it is more severe, with higher frequencies of tophi and polyarticular disease<sup>[34]</sup>.

#### 1.1.4.3. Diet

Since antiquity, gouty arthritis has been linked to a lifestyle characterized by a high-fat diet and alcohol consumption. But it not has been until recently that epidemiological studies have provided evidence on dietary risk factors. Purine rich foods, especially meat and to a lesser extend seafood, have been associated with a higher risk of gout and with the precipitation of gout flares<sup>[35,36]</sup>. Fructose and sugar-sweetened soft drinks, but not diet drinks, increase the risk of gout as fructose induces uric acid production by increasing ATP (adenosine triphosphate) degradation and increases insulin levels and resistance<sup>[37,38]</sup>. Contrary to popular belief, this association has not been found with purine-rich vegetables, and current guidelines encourage the consumption of vegetables as part of a healthy diet<sup>[35,39]</sup>. Low-fat dairy products and coffee, but not tea, have a protective role in the incidence of gout and this effect is moderate with decaffeinated coffee<sup>[35,40-42]</sup>. Two fractions of skim milk, glycomacropeptide (GMP) and G600 milk fat extract, have been associated with clinical improvement and a decrease in the frequency of gout flares, probably through an anti-inflammatory effect<sup>[43]</sup>. Consumption of cherries has a beneficial anti-inflammatory and urate-lowering effect, decreasing the recurrence of flares<sup>[44,45]</sup>. Vitamin C has an uricosuric effect that decreases uric acid levels, exerting a protective effect on gout<sup>[46,47]</sup>.

#### 1.1.4.4. Alcohol consumption

Alcohol intake has been associated with gout and this effect increases with the ingested amount and depends on the type of alcoholic beverage. Relative risk (RR) and 95% confidence interval (CI) for beer, spirits and wine 2.51 (CI 1.77-3.55), 1.60 (CI 1.19-2.16) and 1.05 (CI 0.64-1.72) respectively. Higher effects of beer consumption can be explained by its content in the purine guanosine<sup>[48]</sup>. However, it seems that moderate wine drinking is not associated with gout. Alcohol increases uric acid production by increasing ATP degradation to ADP (adenosine diphosphate) and because its conversion to acid lactic inhibits uric acid secretion by the renal proximal tubule<sup>[49-51]</sup>.

#### 1.1.4.5. Drugs

Drugs that induce hyperuricemia by a renal mechanism, and are therefore associated with gout include: loop and thiazide diuretics, aspirin, pyrazinamide, nicotinic acid, ethambutol, ethanol, levodopa, cyclosporine, tacrolimus, ribavirin and interferon, teriparatide and cytotoxic chemotherapy<sup>[3,12,21]</sup>. Aspirin has a bimodal effect, at high doses (>3 g per day) is uricosuric, whereas at low doses (<1 g per day) causes uric acid retention. On the other hand, losartan and fenofibrate lower serum urate concentrations and thus, should be considered for the treatment of hypertension and hyperlipidaemia in patients with gout<sup>[52]</sup>.



#### 1.1.4.6. Hypertension and chronic kidney disease

Hyperuricemia has been associated with high blood pressure in several epidemiological studies. In NHANES 2007-2008 prevalence of hypertension was 74% in patients with gout, 47% in hyperuricemic individuals, 24% in normouricemic, increasing with uric acid levels and reaching a prevalence of 83.8% with uric acid levels above 10 mg/dL<sup>[53]</sup>. In animal models, uric acid induces afferent arteriopathy in the kidney through proliferation of vascular smooth muscle cells, inflammation, suppression of nitric oxide (NO) and activation of the renin-angiotensin system, leading to ischemia in postglomerular circulation<sup>[12,54,55]</sup>. A two-stage model has been suggested to explain the development of hypertension in the setting of high uric acid levels. In the first stage hypertension is uric acid dependent, as uric acid raises blood pressure through an increase of renal renin activity and a decrease of circulating plasma nitrates. The second stage is characterized by anatomic changes induced by uric acid, such as wall thickening and smooth muscle proliferation, resulting in high blood pressure that is urate-independent but sodium dependent<sup>[56]</sup>. This theory could explain that the reduction in uric acid levels is more efficient in adolescents with essential hyperuricemia than in adults with established hyperuricemia<sup>[57]</sup>. A decrease in blood pressure has been observed after treatment with allopurinol and probenecid, suggesting that the positive effect of urate-lowering therapy is independent of the inhibition of xanthine oxidase activity<sup>[58]</sup>. However, even these results, nowadays there is no indication of urate-lowering therapy in patients with hypertension<sup>[59]</sup>.

Gout has been associated with urolithiasis, and the most important risk factor for uric acid stones in urine pH, as acidic urine favours the precipitation of urate<sup>[21]</sup>. Hyperuricemia has been associated with chronic kidney disease (CKD) but the role of uric acid is not easy to establish as uric acid has a renal excretion and so, is difficult to ascertain if high uric acid levels are cause or effect of decreased renal clearance<sup>[56]</sup>.

#### 1.1.4.7. Other uric acid comorbidities

Metabolic syndrome represents a cluster of physiological and anthropometric abnormalities that are regarded as risk factors for the development of diabetes and cardiovascular diseases. It comprises insulin resistance, high blood pressure and dyslipoproteinemia, the later characterized by high plasma triglycerides and low high-density lipoprotein cholesterol<sup>[3]</sup>. Hyperuricemia has been associated with insulin resistance and cardiovascular disease, and thus it has been included as part of metabolic syndrome. Data from 2 generations of the Framingham Heart Study provide evidence that individuals with higher serum uric acid exhibit high risk of future type 2 diabetes independent of other risk factors<sup>[60]</sup>.

The effect of uric acid in vascular smooth muscle cells secondary to reduced NO production and its effect on blood hypertension may explain the link between uric acid concentrations and cardiovascular diseases<sup>[61]</sup>. Uric acid levels have been associated with an increased carotid intima-media thickness measured by ultrasonography, a surrogate marker of atherosclerosis that is associated with cardiovascular disease risk<sup>[62,63]</sup>. However, conflicting results exist about its association with coronary artery disease<sup>[64,65]</sup>. NHANES 2007-2008 study reported an age and sex-adjusted odds ratio (OR) for myocardial infarction of 2.37 and 1.45 in patients with gout and hyperuricemic individuals respectively and higher risk of heart failure with an OR of 2.68 in gout and 2.52 in hyperuricemic individuals. Prevalence of myocardial infarction and heart failure increased with serum uric acid levels<sup>[53]</sup>. One meta-analysis of 26 studies reported an increased cardiovascular mortality related to uric acid in the group of women<sup>[66]</sup>. In the same line, a recent meta-analysis has showed that high uric acid levels increase the risk of all-cause mortality in men and the risk of cardiovascular mortality in women<sup>[67]</sup>.

#### 1.1.4.8. Genetic factors

Rare familiar forms of gout and hyperuricemia are associated with monogenic inborn errors of purine metabolism, such as hypoxanthine-guanine phosphoribosyl transferase (HGPRT) deficiency, also known as Lesh-Nyhan syndrome, and 5-phosphoribosyl-1-pyrophosphate synthetase (PRPS1) superactivity. Both are X-linked diseases characterized by hyperuricemia with hyperuricosuria and a spectrum of possible neurological manifestations<sup>[12]</sup>. Hereditary renal disorders, such as autosomal dominant familial juvenile hyperuricemic nephropathy or medullary cystic kidney disease type 1 and 2, predispose to hyperuricemia and gout<sup>[68]</sup>.

Twin studies have demonstrated that the risk of gout is determined by the environment and genetic factors are not important contributors. On the other hand, 60% of phenotypic variance in hyperuricemia has been attributable to hereditary factors<sup>[69]</sup>.

Genome-wide association studies (GWAS) have identified genes associated with uric acid levels and the development of gout. GWAS meta-analyses have reported associations of serum urate and gout with the following genes: *SLC2A9*, *ABCG2*, *SLC17A1*, *SLC22A11*, *SLC22A12*, *SLC16A9*, *GCKR*, *LRRC16A*, *PDZK1*, *R3HDM2-INHBC* region, *RREB1*, *PDZK1*, *SGK1-SLC2A12* region and *MAF*. For some additional comments about these genes see next paragraphs<sup>[70-73]</sup>. A recent GWAS meta-analysis performed by Köttgen *et al.* in 2013 confirmed the association of 10 previously described loci and identified 18 new loci, some of them associated with inhibins-activins growth factor system and glycolysis pathways<sup>[74]</sup>. An Icelandic GWAS found association of *ALDH16A1*, encoding aldehyde dehydrogenase 16 family member A1, with uric acid levels<sup>[75]</sup>.

Most of these genes are involved in renal urate transport, as more than 90% of patients with gout have reduced renal urate clearance leading to hyperuricemia<sup>[76]</sup>. Genetic variants in *SLC2A9* gene are associated with lower uric acid levels and lower risk of gout, especially among women. *SLC2A9* encodes the urate transporter GLUT-9 that is involved in reabsorption of filtered urate by proximal tubules and seems to be a fructose-urate exchanger. It is partially inhibited by probenecid, benzbromarone and losartan. Another urate transporter involved in urate absorption in proximal tubule is URAT-1, which is encoded by *SLC22A12* and is also a target of uricosuric agents. Mutations in this gene have been associated with a reduction of urate absorption and decreased uric acid levels. Human ATP-binding cassette, subfamily G 2 (ABCG2), encoded by the *ABCG2* gene, is an urate efflux transporter that has a role in the apical secretion of urate. Variations in this gene have been associated with high uric acid levels.

### 1.1.5. Clinical manifestations

Although gout is characterized by acute and recurrent inflammatory episodes, signs of persistent inflammation such as tophi, limitation, joint swelling and deformity can be present from the beginning of the disease, even before the first flare of arthritis. Therefore, Pérez-Ruiz *et al.* propose that, instead of dividing clinical manifestations of gout into stages, gout should be considered a chronic disease from the beginning as acute and persistent manifestations can coexist<sup>[1]</sup>.

#### 1.1.5.1. Acute clinical manifestations

The hallmark of gout is the self-limiting episodes of inflammation. MSU crystals can deposit anywhere in the musculoskeletal system and inflammation can manifest in form of arthritis, tendinitis and bursitis. First attack usually occurs in middle-aged men, around 40-60 years, and in women after menopause, when they have lost the uricosuric effect of estrogens<sup>[77,78]</sup>. An onset before the age of 25 should raise the possibility on an enzymatic disorder<sup>[3]</sup>.

Factors that modify uric acid levels or the deposition of MSU crystals, such as the initiation of urate-lowering therapy, drugs like diuretics or cyclosporine, purine or alcohol intake, fasting, surgery and local trauma may trigger the onset of an episode of arthritis.

Flares are monoarticular in more than 90%<sup>[79]</sup> and affect peripherally located joints, with predilection of the lower limbs, although centrally located joints and axial skeleton can also be involved<sup>[80]</sup>. Gout has predilection for previously damaged joints, such as hands of women with osteoarthritis and Heberden nodules<sup>[81,82]</sup>. Arthritis of the first metatarsophalangeal joint, also termed *podagra* (Figure 1.1), is the first presentation of gout in the 50% of cases, occurring during the course of the disease in more 80% of untreated patients. Is followed in frequency by

tarsus, ankle, knee and olecranon bursa inflammation. No differences exist in the distribution of arthritis between men and women<sup>[1]</sup>.

Although episodes of arthritis typically have an abrupt onset, sometimes there is an "aura" of discomfort that precedes the onset of arthritis and that allows to start treatment early<sup>[1]</sup>, with a "pill-in-the-pocket" approach similar to the one used to treat episodes of angina. Frequently flares start at night, probably because lower temperatures and dehydration state can favour precipitation of uric acid<sup>[12]</sup>. Affected structures become warm, swollen, tender and red, resembling septic arthritis<sup>[83]</sup>. Moreover, systemic symptoms like malaise or low-grade fever can occur. The episode resolves within a few days, even without treatment. Sometimes the skin over joints peels. Other acute manifestations include Baker cyst rupture, joint blockade caused by intra-articular tophi or rupture of intradermal tophi<sup>[1]</sup>.

If left untreated, attacks become more frequent, have a less abrupt onset affecting more joints, spread to upper limb, last longer with a slower healing, and persistent clinical manifestations appear<sup>[3]</sup>.

#### 1.1.5.2. Persistent clinical manifestations

Tophi are macroscopic deposits of MSU crystals that can occur in virtually every place in the body, but especially in cartilage, synovial membranes, tendons and soft tissues, with a predilection for friction areas (Figure 1.2). Tophi are painless, but can ulcerate and extrude a white chalky material. They usually appear after long-standing and untreated gout, as the degree and duration of hyperuricemia are determinant for tophi formation. However, tophi may be the first clinical manifestation and occasionally appear in asymptomatic joints<sup>[84]</sup>. Other factors that seem to influence tophi formation are the severity of renal disease and the use of diuretics, being especially present in patients with severe renal disease, after allograft transplantation in patients treated with cyclosporine in gout secondary to myeloproliferative diseases, glycogen storage disease and Lesh-Nyhan syndrome<sup>[3]</sup>. The importance of the assessment of tophi in the follow-up of patients with gout is that palpable tophi correlate with tophi in bone and joints and consequently with higher radiographic scores and poorer function.

The presence of joint limitation in the absence of swelling or deformity, termed as gout arthropathy, can be related to MSU deposition in joint structures. These crystals induce a granulomatous inflammation of synovial membrane and persistent swelling of the joint that can be assessed in asymptomatic joints with doppler ultrasonography (US) or gadolinium magnetic resonance imaging (MRI). Finally, MSU deposits are associated with joint and bone damage, leading to deformity and loss of function<sup>[1]</sup>.



**Figure 1.1. Acute gout.** Arthritis of the first metatarsophalangeal joint, or *podagra*, and tarsal affection of the left foot.



**Figure 1.2. Tophi in chronic gout.** Man of 55 years old, who had suffered recurrent attacks of gout for 20 years. St Bartholomew's Hospital Archives & Museum (1908).

### 1.1.6. Diagnostic elements and factors to heed

The definitive diagnosis of gout is established after joint aspiration and identification of MSU crystals through microscopic examination. Routine search for MSU crystals is recommended in all synovial fluid samples obtained from undiagnosed patients<sup>[85]</sup>. Joint aspiration of asymptomatic joints yields to the diagnosis especially in the absence of hypouricemic treatment<sup>[86]</sup>. Synovial fluid samples should be examined as soon as possible at room temperature. Observed under the microscope, MSU crystals are thin needle-shaped structure with pointed ends<sup>[12]</sup>. In the compensated polarizing microscope are negatively birefringent, as shown in Figure 1.3, being yellow when long crystal axis is aligned parallel to the compensator axis, and blue when aligned perpendicular<sup>[87]</sup>.

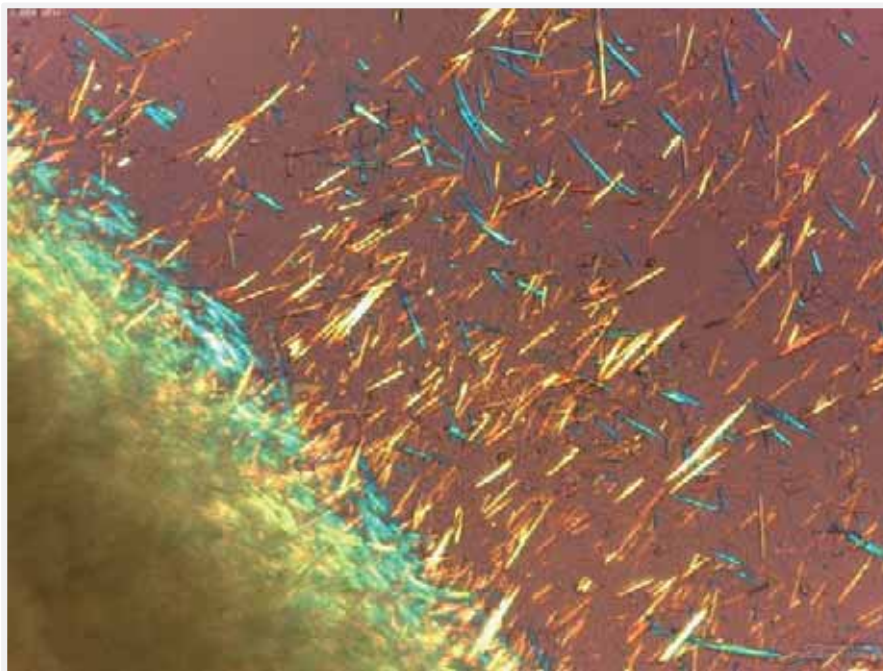


Figure 1.3. MSU crystals on polarized microscope. © Fondo de Imagen de la Sociedad Española de Reumatología. Author: Clara Méndez Perles.

However, in certain circumstances, when joint aspiration or microscopic examination are not available, clinical diagnosis can be considered as accurate, although not definitive, in the presence of typical presentations such as podagra<sup>[88]</sup>. This clinical diagnosis can be made based on clinical history, risk factors, examination, laboratory tests and imaging techniques. Several classification criteria have been designed for gout (Figure 1.4). However, their use should be restrained to research studies.



<b>Rome 1963</b>	<ol style="list-style-type: none"> <li>1. Serum UA &gt;7 mg/dL in men and &gt;6 mg/dL in women</li> <li>2. Presence of tophi</li> <li>3. MSU crystals in SF or tissue</li> <li>4. History of attacks of painful joint swelling with abrupt onset and resolution within 2 weeks</li> </ol> <p>Case definition: two or more criteria</p>
<b>New York 1966</b>	<ol style="list-style-type: none"> <li>1. At least two attacks of painful joint swelling with complete resolution with 2 weeks</li> <li>2. History or observation of podagra</li> <li>3. Presence of tophi</li> <li>4. Rapid response to colchicine treatment, defined as a major reduction in the objective signs of inflammation within 48 hours</li> </ol> <p>Case definition: <math>\geq 2</math> criteria or the presence of MSU crystals in SF or on deposition</p>
<b>ACR 1977</b>	<ol style="list-style-type: none"> <li>1. More than one attack of acute arthritis</li> <li>2. Maximum inflammation developed within 1 day</li> <li>3. Oligoarthritis attack</li> <li>4. Redness observed over joints</li> <li>5. First MTP joint painful or swollen</li> <li>6. Unilateral first MTP joint attack</li> <li>7. Unilateral tarsal joint attack</li> <li>8. Tophus (suspected or proven)</li> <li>9. Hyperuricemia (more than 2 S.D. greater than the normal population average)</li> <li>10. Asymmetric swelling within a joint on X-ray</li> <li>11. Subcortical cysts without erosions on X-ray</li> <li>12. Complete termination of an attack</li> </ol> <p>Case definition: 6 of 12 clinical criteria or MSU identification in SF or tophus</p>
<b>Mexico 2010</b>	<ol style="list-style-type: none"> <li>1. Current or past history of more than one attack of arthritis</li> <li>2. Rapid onset of pain and swelling (less than 24 hours)</li> <li>3. Mono and/or oligoarticular attacks</li> <li>4. Podagra</li> <li>5. Joint erythema</li> <li>6. Unilateral tarsal joint attack</li> <li>7. Tophus (suspected or proven)</li> <li>8. Hyperuricemia (more than 2 S.D. greater than the normal population average)</li> </ol> <p>Case definition: 4 of 8 criteria or MSU crystal identification</p>
<b>Netherlands 2010</b>	<ol style="list-style-type: none"> <li>2 Male sex</li> <li>2 Previous patient-reported arthritis attack</li> <li>0.5 Onset within 1 day</li> <li>1 Joint redness</li> <li>2.5 MTP1 involvement</li> <li>1.5 Hypertension or more than one cardiovascular disease</li> <li>3.5 Serum UA &gt; 5.8 mg/dL</li> <li>13 Presence of a tophus</li> </ol> <p>Case definition: A summed score of 4 or less excludes gout, 8 or more suggests gout, between 4 and 8 suggests the need for SF analysis</p>

**Figure 1.4. Classification criteria for gout.** (Adapted from Dalbeth *et al.*, 2013)<sup>[89]</sup>. SF: synovial fluid, MTP: metatarsophalangeal, UA: uric acid, SD: standard deviation, ACR: American College of Rheumatology.

Plain radiographs, although are not useful for diagnose during the acute attack as in most of the cases only show soft tissue oedema, are of utility in patients with long standing gout or to initially evaluate joint damage. Typically erosions in gout are punched out, located along the long axis of the bone, with overhanging edges and sclerotic rims, and joint space is well preserved until late (Figure 1.5 A). New imaging techniques such as US or Dual-Energy computed tomography (DECT) are being evaluated to be used for gout diagnosis and follow-up.

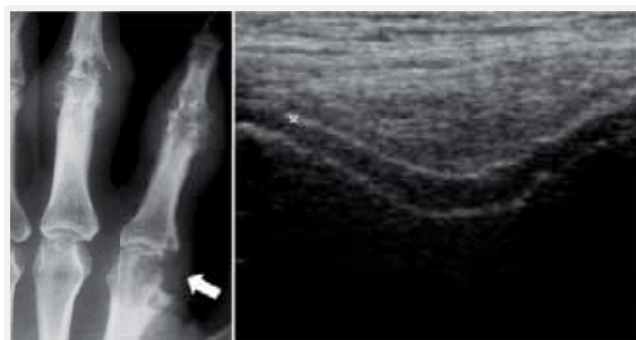


**Figure 1.5. Imaging in gout.** (A) Plain radiography of typical bone erosions (white arrow). (B) Transversal ultrasound imaging of the knee joint showing the double-contour sign (white cross) as a result of MSU deposit on the surface of the hyaline cartilage. © Fondo de Imagen de la Sociedad Española de Reumatología, (A) M<sup>a</sup> Luisa Muñoz Guillén and Juan José García Borrás; (B) Juan J. Alegre.

Determination of serum uric acid levels is of little help in making the diagnosis, as uric acid levels decrease during the acute episode, and may even be normal<sup>[90]</sup>. On the other hand, quantification of urinary excretion of uric acid, although not necessary for diagnostic, is useful to decide therapeutic options.

Differential diagnosis should be established with rheumatoid arthritis when the presentation is polyarticular, keeping in mind that sometimes tophi can be misdiagnosed as rheumatoid nodules. The possibility of spondyloarthropathy has to be taken into account in cases of oligoarthritis affecting lower limbs. In the setting of an acute monoarthritis, pyrophosphate (PPC) crystal arthritis and septic arthritis should be ruled out. However, the presence of MSU crystals does not exclude these diagnosis as they can coexist with gout<sup>[83,91,92]</sup>.

Once the diagnosis is established, it is important to evaluate the burden of the disease considering number of acute inflammation episodes, affected joints, presence of tophi and persistent manifestations such as pain, swelling, limitation or deformity. Moreover, it is recommended an evaluation of potentially modifiable risk factors and associated coexisting illnesses such as hypertension or dyslipemia.



### 1.1.7. Treatment

Two different settings have to be considered when treating gout. The first is the treatment of acute flares, which is mainly symptomatic and anti-inflammatory. But as gout is caused by the deposition of MSU crystals, the ultimate goal is to remove these deposits in order to avoid joint destruction and recurrence of gout flares. For this purpose, urate-lowering therapy (ULT) is recommended to finally cure gout.

#### 1.1.7.1. Treatment of acute arthritis gout

Although gout flares usually are self-limited, it can take more than one week until their resolution<sup>[93]</sup>, and thus attacks should be treated with pharmacologic therapy<sup>[94]</sup>. Therefore, the aim of treatment is to rapidly relief pain and disability caused by the inflammation<sup>[95]</sup>. It is important to initiate it as soon as possible, ideally within the first 24 hours, as it has been associated with better outcomes<sup>[94]</sup>.

I- **Non-pharmacological treatment** that helps to ameliorate inflammatory signs and must be taken into account are joint rest and application of local cold<sup>[96,97]</sup>. If the patient is on ULT, this treatment should be continued without interruption<sup>[94]</sup>.

II- **Pharmacological treatment** includes non-steroidal anti-inflammatory drugs (NSAIDs), colchicine and systemic or intra-articular corticosteroids (CS). The election of the treatment should be done depending on patient comorbidities, previous response to treatments and patient preferences. The American College of Rheumatology (ACR) Task Force Panels (TFP) has not ranked one therapeutic class over another, recommending to start with monotherapy in mild to moderate flares. In severe flares (defined as polyarticular flares, involvement of 1 or 2 large joints or severe pain, defined as intensity >6 in a visual analogue scale), combination therapy with colchicine and NSAIDs, colchicine and corticoids or intra-articular corticoids with any other treatment should be considered.

II.a) NSAIDs have an anti-inflammatory action by inhibiting cyclooxygenase (COX), an enzyme that is responsible for prostaglandins, prostacyclin and thromboxane production<sup>[96]</sup>. Although the only NSAIDs approved by the Food and Drug Administration (FDA) for the treatment of acute gout are indomethacin, naproxen and sulindac, there is no consensus to recommend one specific NSAID. It is important to initiate treatment at full doses and maintain it until the acute gouty attack has resolved<sup>[94]</sup>.

II.b) Colchicine is an alkaloid derived from extracts of meadow saffron (*Crocus autoimmale*), that acts through inhibition of microtubule formation and suppresses MSU crystal-induced NLRP3 inflammasome activation<sup>[96,98]</sup>. It was approved by the FDA for treatment of gout in

2009. ACR guidelines recommends its use when the onset of the attack is no greater than 36 hours<sup>[94]</sup>. The low-dose regimen (loading dose of 1.2 mg followed by 0.6 mg 1 hour later, 1.8 mg total) is preferred to the high-dose regimen (4.8 mg total), as is equally effective and associated with fewer adverse effects<sup>[99]</sup>. Colchicine has hepatic metabolism and urinary excretion and thus, especial caution is required in patients with renal or hepatic impairment. The same applies with patients treated with drugs that are substrates for cytochrome P450 3A4 (CYP3A4) or P-glycoprotein transporters, such as cyclosporine, erythromycin, calcium-channel antagonists ketoconazole, itraconazole and human immunodeficiency virus protease inhibitors, as they can enhance colchicine levels, increasing the risk of toxicity<sup>[96]</sup>.

II.c) Corticosteroids (CS). Intra-articular CS are an option to consider when 1 or 2 accessible joints are affected, and in severe flares they can be followed by an oral anti-inflammatory regimen. Systemic CS, 0.5 mg/kg/day for 5 to 10 days or 2 to 5 days followed by a taper<sup>[94]</sup>, are recommended for severe oligoarticular or polyarticular attacks, when injection is not possible or when NSAIDs and colchicine are contraindicated<sup>[52]</sup>. An alternative regimen of intramuscular single-dose triamcinolone acetonide (60 mg) followed by oral prednisone or prednisolone has been suggested by the ACR-TFP. When oral administration is not possible, patients can be treated with intravenous (IV) or intramuscular (IM) methylprednisolone, 0.5 to 2 mg/kg, repeated as needed, or subcutaneous adrenocorticotrophic hormone or ACTH (25-40 UI and repeated as necessary)<sup>[94]</sup>. The latter could be an alternative in patients with contraindication to colchicine and NSAIDs and comorbidities like diabetes that limit the use of CS<sup>[100-103]</sup>.

III.d) IL-1 blocking agents. As the inflammatory cytokine interleukin-1 $\beta$  (IL-1 $\beta$ ) has a central role in the initiation of gout flares, novel therapies targeting IL-1 $\beta$  blockade have been developed, as shown in Figure 1.6. Riloncept and canakinumab have been approved for treatment of CAPS (cryopyrin associated periodic syndromes). In gout, these treatments are reserved for patients with contraindications or who are resistant to traditional treatments. Riloncept is a soluble receptor-Fc (Fragment Crystallizable region) fusion protein that inhibits both interleukin-1 $\alpha$  (IL-1 $\alpha$ ) and IL-1 $\beta$  and is administered at doses of 160 mg weekly, with a loading dose of 320 mg. One placebo-controlled pilot study analyzed the effect of riloncept in treatment of patients with active gout who were contraindicated or refractory to other treatments. Although injection site reaction was the most frequent adverse event, patients treated with riloncept reported an improvement in pain and severity of joint symptoms and experienced a decrease in C-reactive protein (CRP) levels<sup>[104]</sup>. Canakinumab is a human monoclonal anti-IL-1 $\beta$  antibody with a long half-life that has been approved in Europe for the treatment of patients with acute gout who have contraindications or are refractory to colchicine, NSAIDs and corticosteroids<sup>[105]</sup> and has showed superiority compared with

triamcinolone in the treatment of acute gout in these difficult-to-treat patients<sup>[106–108]</sup>. Anakinra, a recombinant nonglycosylated form of the human IL-1 receptor antagonist, was initially approved for treatment of rheumatoid arthritis and has showed its efficacy in the treatment of gout flares in small series and case reports at doses of 100 mg daily usually for 3 days<sup>[109–114]</sup>.

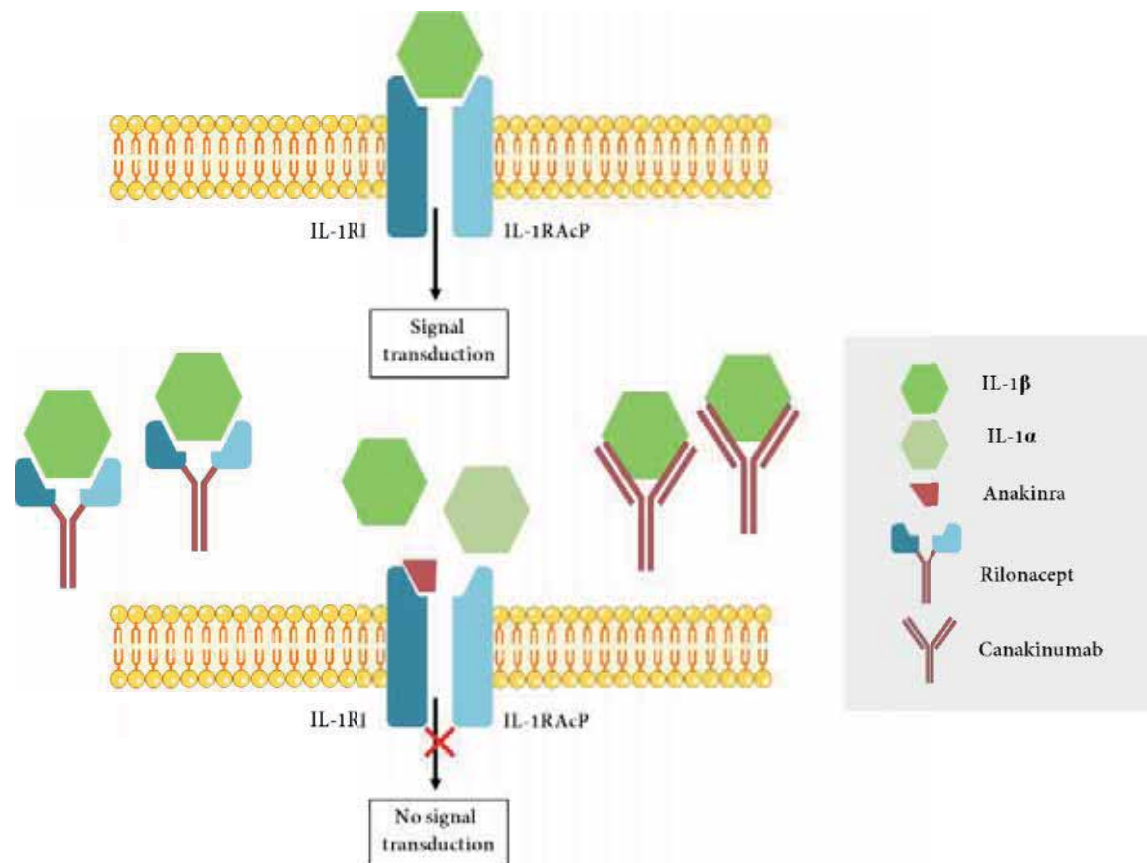


Figure 1.6. Mechanisms of action of IL-1 blocking agents. (Adapted from So *et al.*, 2009 and Doherty *et al.*, 2011)<sup>[115,116]</sup>

### 1.1.7.2. Long-term management of gout

The aim of the long-term treatment of gout is to maintain uric acid levels below the saturation point for monosodium urate crystallization in order to dissolve crystal deposits, as this can lead to a resolution and even a reversal of the signs and symptoms of gout<sup>[117]</sup>. This point is important, as states that gout can be cured if we manage to eliminate the deposits of MSU, that are the responsible of the burden<sup>[2]</sup>.

The recommended goal is to achieve serum urate levels < 6 mg/dL, and in patients with tophi levels < 5 mg/dL should be desirable, as the lower the serum urate levels achieved, the faster the reduction of tophaceous deposits<sup>[39,118]</sup>.

#### **1.7.2.1.1. Education and lifestyle modifications**

All patients should receive information about the disease and its treatment, especially its objectives and adverse events. Patient education increases adherence to treatment and encourages lifestyle modifications, not only to improve gout outcomes, but to increase quality of life<sup>[119]</sup>. The aim of lifestyle modifications is to reduce the impact of risk factors in the expression and severity of gout. Suggested measures are: maintain a body mass index (BMI) in the normal range, quit smoking, practice exercise, stay well-hydrated and to follow a healthy diet.

Regarding diet, ACR-TSF recommends avoidance of organ meats with high purine content, high fructose corn syrup-sweetened beverages or foods, alcohol overuse and any alcohol use during periods of frequent gout attacks or in gout under poor control. Patients with gout should limit beef, lamb, pork, seafood with high purine content, naturally sweet fruit juices, table sugar and sweetened beverages and desserts, table salt, and alcohol. On the other hand, ACR guidelines encourage consumption of low-fat or non-fat dairy products as well as vegetables<sup>[39]</sup>.

Comorbidities associated with hyperuricemia and gout, such as hypertension or dyslipemia, should be assessed and correctly managed in an attempt to an holistic care. When possible, drugs associated with an increase of uric acid levels should be substituted by other treatments. Accordingly, losartan and fenofibrate, because of their uricosuric effects, should be considered in the treatment of hypertension and hypertriglyceridemia respectively. Unlike the effect of low doses of aspirin on uric acid, discontinuation of low-dose acetylsalicylic acid when prescribed for cardiovascular disease prophylaxis is not recommended<sup>[39]</sup>.

#### **1.7.2.1.2. Urate-lowering therapy (ULT)**

Although non-pharmacological approach is recommended to improve quality of life and optimal management of comorbidities, it is usually not enough for reaching the goal serum urate levels<sup>[39]</sup>. According to ACR guidelines, ULT<sup>[39]</sup> should be indicated in any patient with established diagnosis of gouty arthritis and tophi, 2 or more attacks per year, chronic kidney disease (CKD) stage 2 or worse or in patients with urolithiasis. Although it has been often recommended that ULT should be started once the flare has resolved, there is no contraindication, and current guidelines state that it can be started during an acute flare.

However, sometimes it is easier to wait until resolution and then discuss with the patient the modality and goals of treatment<sup>[39,120]</sup>. Slow reduction of urate levels is recommended to avoid gout flares.

Three different strategies are available as ULT: to reduce of uric acid production with the xanthine oxidase inhibitors (XOI) allopurinol or febuxostat, to increase uric acid renal excretion with uricosuric agents such as probenecid, benzbromarone and sulfinpyrazone and finally to convert uric acid to allantoin with pegloticase, a recombinant uricase. Allopurinol and febuxostat are recommended as first-line therapies and uricosurics should be considered in the setting of contraindication or intolerance of at least 1 XOI agent, especially in patients with low uric acid excretion. During treatment, uric acid levels should be monitored 2 to 5 weeks after each dose adjustment and twice a year once the goal target is achieved<sup>[39]</sup>.

- **Allopurinol**, and its active metabolite oxypurinol, are purine analogues of xanthine and hypoxanthine that competitively inhibit the enzyme xanthine oxidase. It has to be initiated at low doses (100 mg daily if normal renal function) with a slow titration of 100 mg every 2-4 weeks until reaching the minimum dose necessary to maintain goal uric acid levels, up to the maximum approved dose in Europe (900 mg). In patients with renal impairment, allopurinol should be initiated at lower doses (1.5 mg per mL/min estimated glomerular filtration rate or eGFR), increasing 50 mg every 4 weeks. The purpose of this slow titration and adjustment based in renal function is to avoid hypersensitivity reactions, such as Stevens-Johnson syndrome (SJS) and Toxic Epidermal Necrolysis (TEN), which although not common, are associated with an increased mortality. These reactions occur during the first few months of treatment initiation, being associated factors female gender, age, CKD, diuretic therapy and HLA-B\*5801 haplotype, which is common in Han Chinese, Korean and Thai populations, in whom screening is recommended<sup>[39]</sup>.

- **Febuxostat** is a thiazolecarboxylic acid derivative that selectively inhibits oxidized and reduced forms of xanthine oxidoreductase, being more selective than allopurinol<sup>[117]</sup>. It was approved by the European Medicines Agency or EMA in 2008 at 80 mg or 120 mg daily<sup>[121]</sup> after two randomized trials<sup>[122,123]</sup>. As its metabolism is mainly hepatic, it is preferred in the setting of mild or moderate renal impairment, as there is no need of dose adjustment<sup>[124]</sup>, and in patients with antecedent of allopurinol hypersensitivity reaction<sup>[117]</sup>.

- **Uricosuric drugs** prevent uptake of uric acid at the proximal renal tubule, increasing its renal excretion and thus, they can predispose to uric acid stone formation. That is why patients should be well hydrated and urine alkalisation (pH>6) should be considered<sup>[120]</sup>. According to ACR guidelines, uricosuric treatment is recommended as an alternative first-line therapy in

the setting of contraindication or intolerance to at least 1 XOI agent, being contraindicated in patients with urolithiasis. Probenecid is the only uricosuric drug available in United States but is ineffective in patients with renal impairment. Benzbromarone is a powerful uricosuric drug, especially in patients with decreased urinary uric acid excretion, and may be used in patients with mild-to-moderate renal insufficiency, but monitoring hepatic function<sup>[95,125]</sup>.

- The recombinant uricase **pegloticase** is recommended only in cases of severe gout and refractoriness or intolerance of other ULT treatments. It is intravenously administered, at doses of 8 mg biweekly, with no maximum duration of treatment yet defined. The formation of antibodies against this drug is associated with infusion reactions and loss of urate-lowering responsiveness<sup>[126]</sup>. Thus, discontinuation of pegloticase is recommended if pre-infusion urate levels exceed 6 mg/dl on two successive occasions<sup>[117]</sup>.

Duration of ULT treatment depends on achievement of target serum uric acid levels and tophi dissolution, and should be continued for the greater of: 6 months of duration or 3 months after achieving the target serum uric acid in patients without tophi or 6 months after achieving the target serum uric acid levels when tophi have already dissolved<sup>[94]</sup>.

#### *1.7.2.1.3. Prophylaxis of attacks of acute gout during ULT therapy*

Anti-inflammatory prophylaxis should be started with ULT, as the decrease of uric acid levels caused by this treatment has been associated with a higher risk of gout attacks. First-line therapy agents are colchicine (0.5 or 0.6 mg orally once or twice a day with dose adjustment if renal impairment), or low-dose NSAIDs (such as 250 mg Naproxen orally twice a day). In patients intolerant or contraindicated to previous treatments, low doses of prednisone or prednisolone (<10 mg/day) can be considered. Blocking IL-1 $\beta$  with riloncept and canakinumab has demonstrated its effectiveness in the prophylaxis of gout flares associated with ULT<sup>[127-130]</sup>.

## **1.2. Gout as an autoinflammatory disease**

### **1.2.1. Autoinflammatory diseases**

The concept of autoinflammatory diseases appeared in 1999<sup>[126]</sup> to include those entities that are characterized by recurrent episodes of unexplained inflammation in which, unlike autoimmune diseases, there is no association with autoantibodies, antigen-specific T cells or Major Histocompatibility Complex (MHC) class II haplotypes<sup>[132]</sup>. A common feature of autoimmune and autoinflammatory diseases is self-directed inflammation, but its origin differs. In **autoimmune diseases** the adaptive immune system has a central role, with aberrant



dendritic cell (DC), B and T cell responses that lead to a break of tolerance and reactivity against self-antigens. On the other hand, **autoinflammatory diseases** are initiated by local factors at sites predisposed to disease, leading to activation of the innate immune system and tissue damage. Autoinflammation has been associated with the inflammatory cytokine IL-1 $\beta$  and consequently, autoinflammatory diseases are highly responsive to IL-1 $\beta$  blockade and, in contrast to autoimmune diseases, not to TNF- $\alpha$  neutralization<sup>[133]</sup>.

However, the boundary between autoimmune and autoinflammatory diseases is not always easy to define and physiopathogenic limits between both mechanisms appear progressively more faint in the last years. Besides pure monogenic autoinflammatory diseases and pure monogenic autoimmune diseases, many common clinical entities present a combination of autoinflammatory and autoimmune mechanisms. Therefore immunological diseases may represent a continuum that is depicted in Figure 1.7.

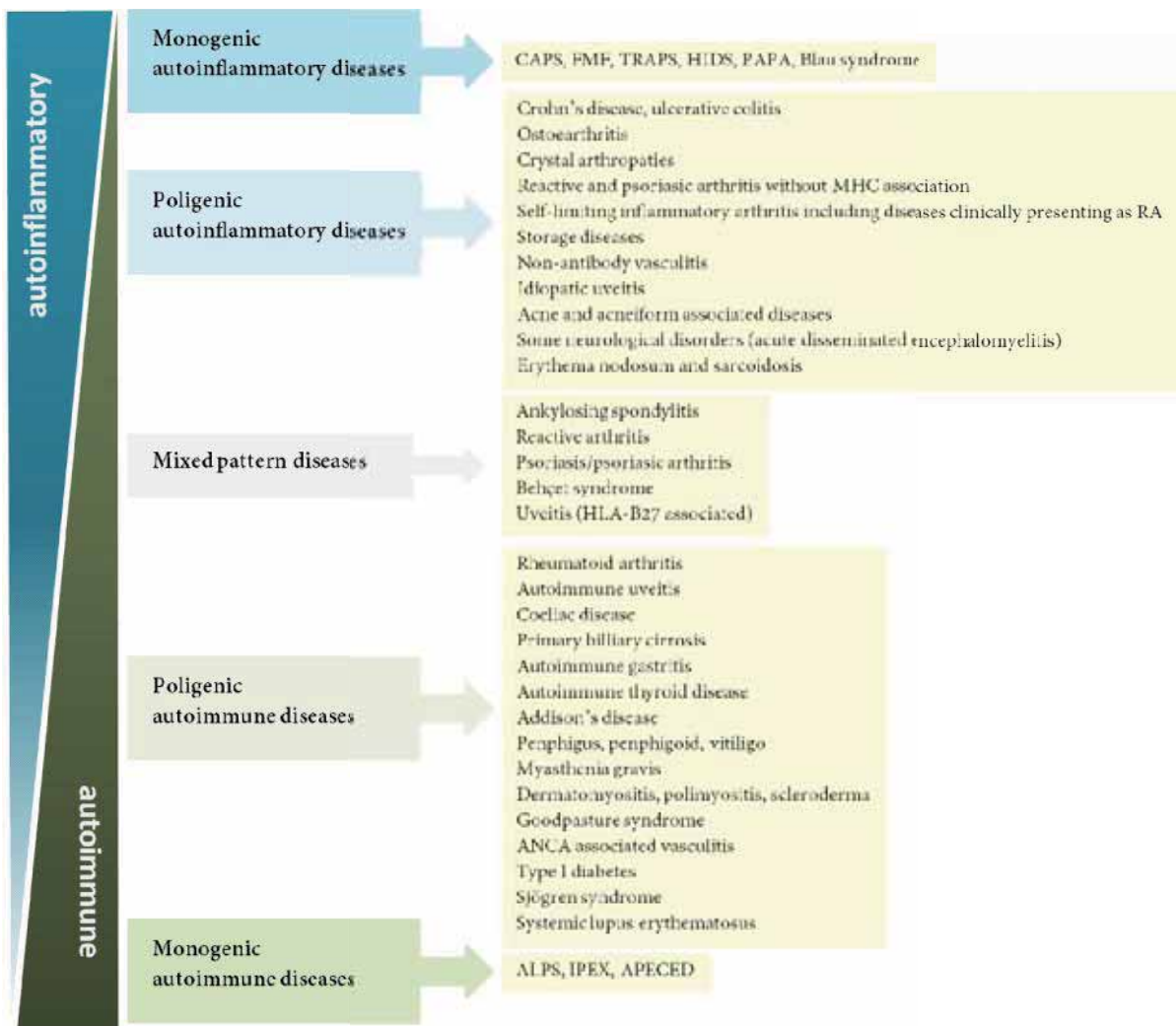


Figure 1.7. The spectrum of immunological diseases. (Adapted from McGonagle *et al.*)<sup>[134]</sup>

Monogenic autoinflammatory diseases or hereditary periodic fever syndromes, as their name suggests, are hereditary and have a known genetic basis. These comprise CAPS or cryopyrin-associated periodic syndromes (including familial cold autoinflammatory syndrome or FCAS, Muckle-Wells syndrome or MW and neonatal-onset multisystem inflammatory disease or NOMID, also known as chronic infantile neurologic, cutaneous, articular syndrome or CINCA), familial Mediterranean fever (FMF), hyperimmunoglobulin-D with periodic fever syndrome (HIDS), TNF receptor-associated periodic syndrome (TRAPS), pyogenic arthritis with pyoderma gangrenosum and acne syndrome (PAPA) and paediatric granulomatous arthritis that includes Blau syndrome and early onset sarcoidosis<sup>[135]</sup>. Nevertheless, autoinflammation is involved in a wide spectrum of complex genetic diseases such as Crohn's disease, psoriasis, hereditary angioedema, Still's disease or in storage diseases (such as Gaucher's disease)<sup>[134]</sup>.

Gout was considered from the beginning a possible autoinflammatory disease<sup>[132]</sup> because its recurrent nature, self-limiting course, involvement of innate immune cells, such as monocytes, macrophages and neutrophils, and the presence of IL-1 $\beta$  during inflammatory episodes<sup>[136]</sup>.

### 1.2.2. The innate immune system

The innate immune system is our first line of defence against pathogens and other foreign molecules<sup>[137]</sup>. Contrary to the adaptive immune system, in which lymphocytes express specific receptors generated by a unique genomic recombination in each lymphocyte, cells of the innate immune system recognise a wide range of pathogens through a limited number of germline-encoded receptors. These are termed pattern-recognition receptors (PRR), and are mainly expressed in macrophages, DCs, neutrophils and epithelial cells<sup>[138]</sup>. PRRs recognise structures shared by many pathogens that are necessary for their viability and less prone to modifications, known as pathogen-associated molecular patterns (PAMPs). Examples of PAMPs are the cell wall components peptidoglycan (PGN) and lipopolysaccharide (LPS). Additionally, innate immune system can be activated by endogenous danger-associated molecular patterns (DAMPs) such as double-stranded ribonucleic acid (dsRNA) or ATP. All these danger signals are recognised by PRRs located in the cytoplasm, cell membrane or secreted. Based on their structure and location, 3 major groups of PRRs can be distinguish: Toll-like receptors (TLRs) in cell surface and vesicles, and NOD-like receptors (NLRs) and RIG-like receptors (RLRs) surveying the cytoplasm<sup>[139]</sup>.

- TLRs are type I transmembrane receptors characterized by an extracellular leucine-rich repeat (LRR) domain and an intracellular Toll/IL-1 receptor (TIR) domain. This TIR domain is also present in the cytoplasmic portions of the members of IL-1R family IL-1R or IL-18R. As



membrane proteins, TLRs survey extracellular fluids and endosomal compartments and their stimulation activates signalling cascades such as NF- $\kappa$ B (nuclear factor kappa-light-chain-enhancer of activated B cells) or type I interferon synthesis<sup>[140,141]</sup>.

- RIG-1 (Retinoic acid-Inducible gene 1) and MDA5 (Melanoma Differentiation-associated protein 5) belong to the RLRs (or RLHs from RIG-like helicases) family and are viral sensors that upon stimulation by dsRNA, activate NF- $\kappa$ B and IRF3/7 (Interferon Regulatory Factors 3 and 7) pathways, resulting in type I interferon transcription<sup>[139]</sup>. Considered by some authors as a third member of these RLR family, RIG-I-like receptor 3 (RLR-3 also known as LGP2 from Laboratory of Genetics and Physiology 2) contains a RNA binding domain but lacks the CARD domain and thus acts as a negative feedback regulator of RIG-I and MDA-5.

- NLR, which have high structural and functional homology to resistance genes (R-genes) in plants, are characterized by three structural domains: a C-terminal region with series of LRRs, a central nucleotide domain NACHT and an N-terminal effector domain. The LRR domain has been implicated in sensing, probably because of the homology with TLR receptors. The NACHT domain [NAIP (neuronal apoptosis inhibitory protein), CIITA (MHC class II transcription activator), HET-E (incompatibility locus protein from *Podospora anserina*) and TP1 (telomerase-associated protein)] is essential for oligomerization and activation, forming high molecular weight complexes. Finally, the effector domain can be a pyrin domain (PYD), a caspase recruitment domain (CARD) or a baculovirus inhibitor repeat (BIR) domain, which interacts with accessory proteins. NLRs are divided into subfamilies based in their molecular structure (Figure 1.8). NALPs (NACHT Leucine rich repeats and Pyrin domains-containing proteins) are the largest subfamily with 14 genes identified in humans. All but NALP1 have a N-terminal PYD domain. The IPAF and NAIP groups contain a N-terminal CARD and BIR respectively, and are involved in the formation of inflammasomes. The third class includes the remaining CARD-containing NLRs such as NODs (nucleotide-binding oligomerization domain): NOD1, NOD2, NOD3, NOD4, NOD5/NLRX1 and CIITA (class II MHC transactivator)<sup>[139]</sup>.

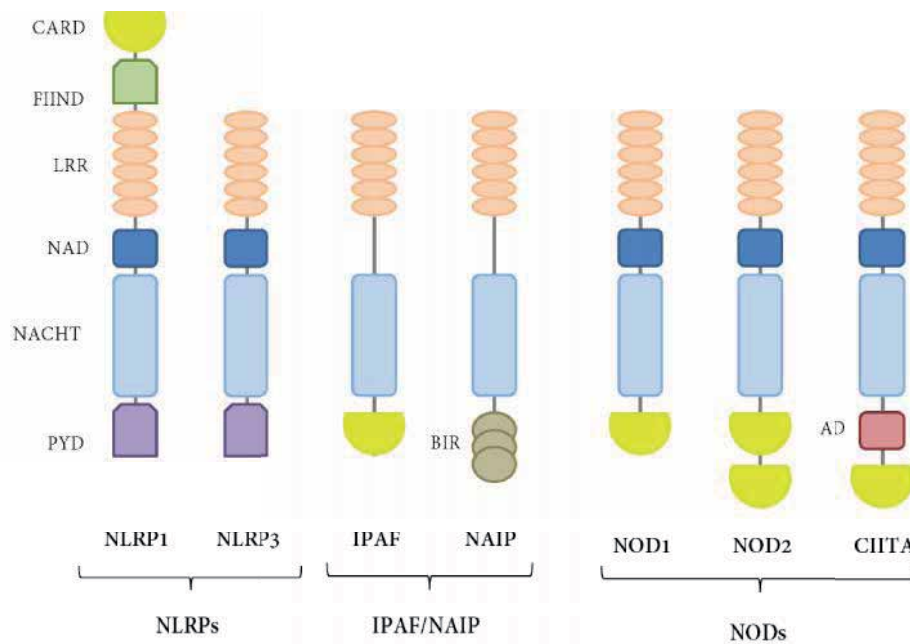


**Figure 1.8. The NLRs family.** NLR share the same structure consisting in a LRR domain involved in sensing, a central oligomerization NACHT domain and an effector domain. Differences in the effector domain further differentiate NLR into subfamilies. (Adapted from Martinon *et al.*, 2009)<sup>[139]</sup>

### 1.2.3. Inflammasomes: NLRP3, the paradigm

The term inflammasome was assembled from the words inflammation and the Greek suffix *soma*, to define a molecular complex involved in inflammation<sup>[139]</sup>. Inflammasomes were first described in 2002 as multiprotein cytoplasmic complexes of NLRs receptors and adaptor proteins that mediate the cleavage and activation of the inflammatory caspases<sup>[142]</sup>. Caspases are proteases that need proteolytic processing to be activated. Executioner caspases cleave substrates during apoptosis, whereas inflammatory caspases (caspase-1, caspase-4 and caspase-5) are involved in inflammation. Once activated by the inflammasome, the main substrate of inflammatory caspases are inflammatory cytokines such as IL-1 $\beta$ , IL-18 and possibly IL-33<sup>[143]</sup>. The prototypic inflammasomes are NLRP1, NLRP3, IPAF and AIM2 (Absent In Melanoma 2).

**NLRP3 inflammasome** is composed by the oligomerization of the intracellular receptor NLRP3, also known as cryopyrin, the adaptor protein ASC (apoptosis-associated speck-like protein containing a caspase recruitment domain) and caspase-1. NLRP3 and ASC interact by their PYD domain, whereas ASC recruits caspase-1 as they both have a CARD domain. Once activated, caspase-1 cleaves the inactive form of IL-1 $\beta$  (pro-IL-1 $\beta$ ), resulting in activation and secretion of the active cytokine. Gain-of-function mutations in *NLRP3* (NOD-like receptor family pyrin domain containing 3) gene have been recognized in the cryopyrin-associated periodic syndromes or CAPS<sup>[144,145]</sup>. Patients with mutations exhibit higher IL-1 $\beta$  production, even in non-stimulated cells<sup>[146]</sup>.

Several danger signals are responsible of NLRP3 inflammasome activation (Figure 1.9): ATP, RNA or dsDNA, particles such as silica, asbestos and alum and pore-forming toxins such as nigericin<sup>[147-153]</sup>. Mechanisms involved in inflammasome activation are not fully understood but it is possible that several activators share the same pathways and that, for one single activator, several pathways could converge to inflammasome activation. The first mechanism described was K<sup>+</sup> efflux<sup>[154]</sup>, as spontaneous assembly and activation of the inflammasome occurs at K<sup>+</sup> concentrations below 90 mM and its activation is prevented with higher concentrations. Physiological intracellular concentrations of K<sup>+</sup> inhibit the inflammasome assembly and the efflux of K<sup>+</sup> to the extracellular compartment triggers its activation<sup>[155]</sup>. Nigericin, maioitotoxin and ATP, the later through its P2X7 receptor, share this mechanism and the requirement of pannexin-1, that seems to be involved in membrane permeabilization<sup>[156]</sup>. A second theory proposed for particulate molecules suggests that the process of phagocytosis or frustrated phagocytosis could activate the inflammasome by non-well known mechanisms, being supported by the fact that inhibition of cytoskeletal filament generation with cytochalasin D or colchicine inhibits IL-1 $\beta$  activation<sup>[98,149]</sup>. A third mechanism involves phagosomal destabilization by these particles and the release of cathepsin proteases to the cytosol<sup>[149]</sup>. Reactive Oxygen Species (ROS) production is shared by many inflammasome activators such as ATP, nigericine, silica or asbestos, but contradictory results exist about its role in inflammasome activation. Although in the absence of ROS production caspase-1 activation is impaired, patients with chronic granulomatous disease and impaired ROS production show normal NLRP3 activation<sup>[157]</sup>. Other redox-related factors involved in inflammasome activation are the thioredoxin-interactin protein (TXNIP) and oxidised mitochondrial DNA. Antioxidants have also been proposed as inflammasome activators, and these contradictory results could be explained by the balance between oxidants and antioxidants, as a oxidative insult is followed by a rapid antioxidant response<sup>[158]</sup>. How inflammasome sense all these signals remains unknown, but it has been suggested that, as the TLRs, the LRR domain of NLRs could be involved<sup>[159]</sup>.

Various proteins interfere with inflammasome assembly and activation, acting like inflammasome regulators. PYD-containing regulators are believed to interfere with the interaction between NLRPs and ASC and include pyrin, POP1, POP2 and viral PYDs. Mutations in the pyrin protein are associated with the hereditary autoinflammatory syndrome familial Mediterranean fever<sup>[160]</sup>. It is suggested that wild-type pyrin blocks ASC and mutations result in a lack of its suppressive effect. CARD-containing regulators presumably interfere the activation of the caspase-1 by the adaptor protein ASC, and include iceberg, INCA, COP and caspase-12<sup>[139]</sup>.

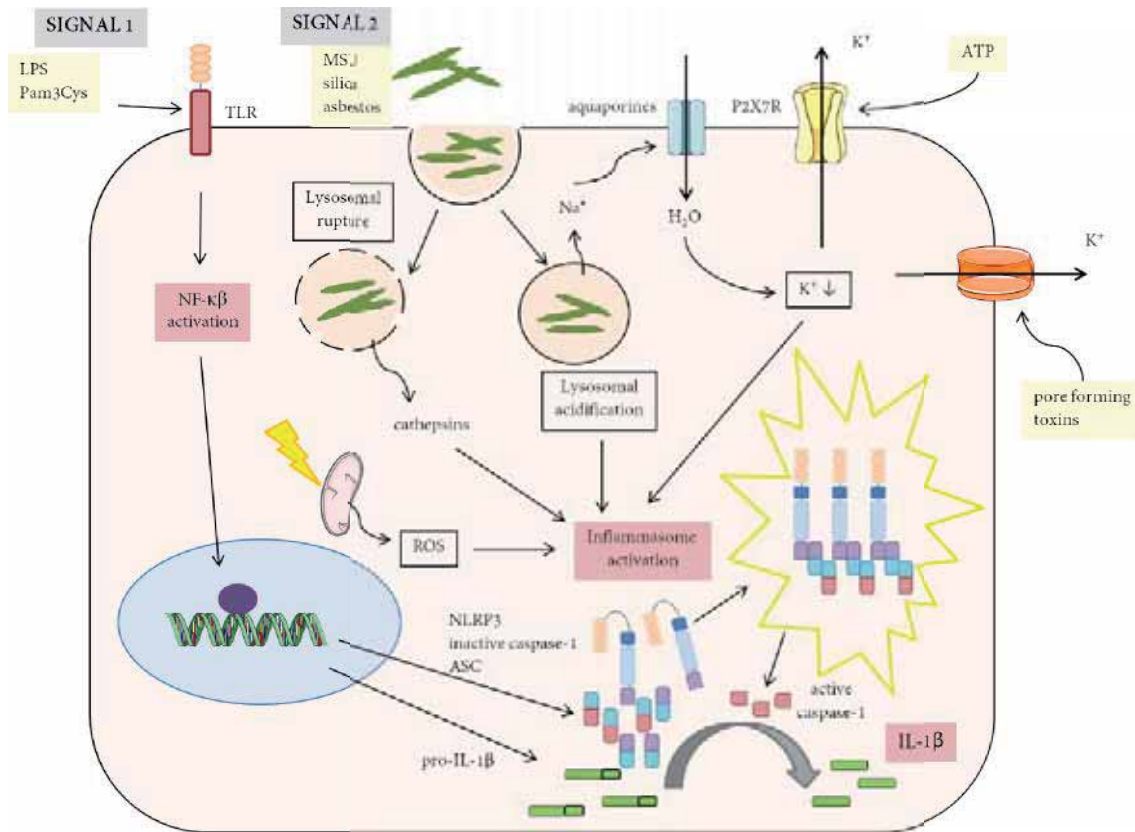


**Figure 1.9. NLRP3 inflammasome activation.** IL-1 $\beta$  production is tightly regulated and requires the presence of pro-IL-1 $\beta$  and its cleavage by active caspase-1. TLR agonists provide signal 1, inducing NF- $\kappa$ B activation and nuclear translocation of p65/p50 heterodimers that promote transcription and translation of inflammasome proteins and pro-IL-1 $\beta$ . Signal 2 is responsible of inflammasome assembly and activation of caspase-1. Inflammasome is activated by the drop in intracellular K<sup>+</sup> concentrations induced by pore forming toxins and ATP. Phagocytosis of MSU crystals activates NLRP3 inflammasome due to lysosomal rupture and release of cathepsins. Another suggested mechanism is that lysosomal acidification would result in Na<sup>+</sup> release to the cytoplasm and secondary water influx, decreasing K<sup>+</sup> intracellular concentrations. (Adapted from Contassot *et al.*, 2012)<sup>[161]</sup>

### 1.2.4. Interleukin-1 $\beta$

The Interleukin-1 family comprises 11 members that probably arose from the duplication of a common ancestral gene: IL-1 $\alpha$ , IL-1 $\beta$ , IL-1 receptor antagonist (IL-1Ra), IL-18, IL-33 and IL-1F (from F5 to F10). All genes encoding IL-1 family members, except IL-18 and IL-33, are located in chromosome 2<sup>[133]</sup>.

IL-1 $\alpha$  and IL-1 $\beta$  exert their activities binding to the same IL-1 receptor type I (IL-1RI), expressed at the surface of a wide variety of cell types. IL-1RI contains three extracellular immunoglobulin-like (Ig-like) domains and an intracellular Toll-like/IL-1R (TIR) domain, that is also present in the structure of TLRs. Binding of this cytokines to their receptor induces the recruitment of IL-1R accessory protein (IL-1RAcP) and this complex recruits the intracellular adaptors myeloid differentiation factor 88 (MyD88), IL-1R-associated kinases (IRAK) and TNF receptor-associated factor 6 (TRAF6) to activate the NF- $\kappa$ B, p38, extracellular signal-regulated kinases (ERKs), c-Jun N-terminal kinases (JNKs) and mitogen-activated protein kinases (MAPKs) pathways<sup>[162]</sup>.

Both cytokines are synthesized as 31 KDa precursor peptides (pro-IL-1 $\alpha$  and pro-IL-1 $\beta$ ) that can be cleaved to generate a 17 KDa mature form. Calpain, a calcium-activated cystein protease associated with the plasma membrane, cleaves the IL-1 $\alpha$  precursor into a mature molecule, but this process scarcely occurs as is not required for its biological activity. Conversely, IL-1 $\beta$  needs to be cleaved by caspase-1 to exert its activity, a process that involves the assembly and activation of the inflammasome. Generation of active IL-1 $\beta$  is tightly regulated, being necessary two signals. The first one is generated by activation of TLR or IL-1R by their ligands, and is responsible of the transcription and translation of the inactive protein. The second signal activates the inflammasome, which in turn, activates caspase-1 to cleave pro-IL-1 $\beta$  to mature IL-1 $\beta$ . Pro-IL-1 $\beta$  can also be cleaved in the extracellular media by different proteases, such as the neutrophil proteases proteinase 3 or elastase, in a caspase-1 independent process<sup>[163]</sup>.

However, synthesis and release of IL-1 $\beta$  depends on the type of cell and the *in vitro* stimulation protocol used: monocytes have constitutively activated caspase-1 and thus they can secrete IL-1 $\beta$  by only the first signal (through TLR receptors in response to LPS). On the other hand, THP-1 cells and macrophages need the two stimuli for IL-1 $\beta$  release. According to Netea *et al.*, this could be explained as monocytes circulate in the blood, that is a pathogen-free environment, and must respond promptly to any danger signal, whereas resident macrophages are more exposed to microbial signals and the requirement of two signals could prevent for excessive activation<sup>[164]</sup>.

Secretion of IL-1 $\alpha$  and IL-1 $\beta$  is independent of the endoplasmic reticulum and Golgi apparatus, as both lack signal peptides. Mechanisms proposed for their secretion are exocytosis of secretory lysosomes, shedding of plasma membrane microvesicles and direct release via transporters or multivesicular bodies containing exosomes, and it seems to be activated after an intracellular increase of calcium<sup>[133]</sup>.

As IL-1 $\alpha$  and IL-1 $\beta$  share the same receptor they have identical biological activities. In some of these actions IL-1 cytokines have a direct effect, whereas in others they act in an indirect manner through the induction of downstream cytokines and other mediators, such as prostaglandin E2 and NO. Both cytokines induce the expression of adhesion molecules on endothelial cells and the release of chemokines, promoting the recruitment of inflammatory cells at the site of inflammation. Acting on bone marrow stem cells, they promote differentiation of myeloid series of progenitor cells. They also induce hypotension, fever, neutrophilia, thrombocytosis and the production of acute-phase proteins. In the musculoskeletal system, IL-1 $\alpha$  and IL-1 $\beta$  stimulate the production of metalloproteinases, inhibit proteoglycans and type II collagen synthesis and stimulate the maturation of osteoclasts, resulting in a negative effect on articular cartilage and bone. Both have co-stimulatory T cell functions, contributing to Th2 polarization, and an important role in Th17 responses<sup>[133,165]</sup>.

However, these cytokines differ in some aspects. Interleukin-1 $\alpha$  is produced by diverse types of cells that contain constitutive levels, acting locally as an autocrine growth factor. It is rarely found in the circulation or in body fluids, except when is released from dying cells. The precursor of IL-1 $\alpha$  plays a role in inflammation and can be found in the membrane of monocytes and B-lymphocytes. The pro-domain of this cytokine has a nuclear localization sequence that can influence gene expression and cell survival. On the other hand, IL-1 $\beta$  is produced mainly by macrophages and monocytes, but not in the steady state, and once secreted circulates systemically. Another differential fact is that their genes are differentially regulated along development and in response to the environment, giving to each cytokine a different contribution<sup>[133,162,165]</sup>.

IL-1 Receptor antagonist (IL-1Ra) is a natural competitive inhibitor for the binding of IL-1 to IL-1RI. The importance of this molecule in controlling IL-1 $\beta$  effects is provided by the observation of the effects of its depletion. Knockout mice lacking IL-1Ra exhibit excessive inflammatory responses and develop chronic inflammatory polyarthropathy resembling rheumatoid arthritis<sup>[166]</sup>. DIRA (Deficiency of Interleukin-1 Receptor Antagonist) syndrome, caused by autosomal recessive loss of function mutations in *IL1RN* gene which encodes IL-1Ra, is characterized by early-onset pustular dermatitis and multifocal osteomyelitis and



periostitis, with marked elevations of acute phase reactants and responds to the administration of the recombinant IL-1Ra anakinra<sup>[167]</sup>.

Other regulators of IL-1 $\beta$  activity are IL-1RII, SIGGIR, sIL-1RAcP and IL-1RAcPb. IL-1RII is a decoy IL-1R that lack TIR domain. SIGIRR (Single Ig IL-1-related receptor) has a TIR domain that inhibits the activation of downstream pathways such as NF- $\kappa$ B. The soluble protein sIL-1RAcP is a splice variant of IL-1RAcP that inactivates the complex IL-1-IL-1RI and enhances the binding affinity of IL-1 $\alpha$  and IL-1 $\beta$  to the decoy receptor IL-1RII. IL-1RAcPb is expressed in the central nervous system and forms a complex with IL-1RI but does not lead to the recruitment of MyD88 and IRAKs<sup>[165]</sup>.

### 1.2.5. Uric acid as a danger signal

Historically, it has been considered that the immune system is responsible to differentiate between self and nonself, generating an immune response in the latter case<sup>[168]</sup>. This theory of self-nonsel has been questioned because does not explain some situations such as tolerance to the fetus during pregnancy or the failure to reject tumours containing cells with mutations that should be considered as foreign. The **danger theory** proposed by Dr. Polly Matzinger, tried to give explanation to these situations, suggesting that the immune system is activated in the presence of danger signals rather than foreignness<sup>[169]</sup>. Damaged cells contain in their cytoplasm signals that activate Antigen Presenting Cells (APCs). This activation, together with processing and presentation of the antigen, allows APCs to activate in turn lymphocytes and initiate an adaptive immune response. This theory explains the role of adjuvants, like alum, that are necessary for immunization to an antigen.

In 2003, Shy *et al.* identified uric acid as the component responsible for the adjuvant effect of necrotic cells, inducing activation of DCs and priming of CD8<sup>+</sup> T-cell responses when co-injected with an antigen. Once injured, cells degrade their RNA and DNA and purines are converted to uric acid that finally crystallizes into MSU crystals, its biological active form, acting like an endogenous danger signal<sup>[170]</sup>.

### 1.2.6. MSU crystals activate the NLRP3 inflammasome

Once MSU crystals were considered DAMPs, and as inflammasomes are activated by these signals, Martinon *et al.* had the hypothesis that these crystals could activate the inflammasome. In 2006, they demonstrated that MSU crystals activate the NLRP3 inflammasome, resulting in IL-1 $\beta$  production<sup>[98]</sup>. In their mice peritoneal model, the inflammasome was necessary for the induction of an inflammatory response. Their results confirmed the participation of the innate immune system and the central role of the inflammatory cytokine IL-1 $\beta$  in gout, linking the

role of uric acid as a danger signal with the concept of gout as an autoinflammatory disease. Subsequently, the effectiveness of IL-1 $\beta$  blocking treatments in patients with gouty arthritis has reaffirmed the consideration of gout as autoinflammatory disease<sup>[171]</sup>.

How MSU crystals activate the inflammasome is not fully understood. The presence of the membrane protein CD14 seems to be required<sup>[172]</sup>, suggesting that MSU crystals could bind this receptor, whereas the role of associated TLRs, namely TLR2 and TLR4, is controversial. What it seems clear is that IL-1R and MyD88, possibly as an adaptor of IL-1R, in non-hematopoietic cells are necessary for the amplification of the IL-1 $\beta$  response and the inflammatory reaction *in vivo*<sup>[173-175]</sup>. Apart from CD14 and TLR recognition, frustrated phagocytosis, disruption of lysosomes<sup>[149]</sup>, ATP<sup>[176]</sup> and ROS production have been proposed as mechanisms by which MSU crystals could activate the NLRP3 inflammasome. One interesting model was proposed by Schorn *et al.* in 2011 that links K<sup>+</sup> efflux with crystal phagocytosis: in this model, monocytes phagocytose MSU crystals in endocytic vesicles that then fuse with acidic lysosomes, leading to a drop in the pH. The acidic conditions convert MSU crystals in uric acid crystals, with the release of sodium into the cytoplasm. This sodium overload causes hyperosmolarity of the cytoplasm and is followed by the water influx through aquaporines, resulting in cell swelling and a drop in K<sup>+</sup> intracellular levels that activates NLRP3 inflammasome<sup>[177]</sup>.

### 1.3. Role of the mononuclear phagocyte system in gout

#### 1.3.1. The mononuclear phagocyte system

The mononuclear phagocyte system represents a population of bone marrow-derived myeloid cells that are distributed via the blood stream as monocytes to all tissues. Once there, monocytes undergo maturation and adapt to the local environment, giving rise to various cell types such as macrophages, myeloid-derived DCs and osteoclasts<sup>[178,179]</sup>.

With a half life of 1-2 days, **monocytes** circulate in the bloodstream, bone marrow and spleen and then migrate into tissues<sup>[180]</sup>. They are effector cells that uptake cells and toxic molecules, produce inflammatory cytokines and express chemokine and adhesion receptors that mediate migration from blood to tissue during an infectious or inflammatory process<sup>[178]</sup>.

**Macrophages** are resident phagocytic cells in lymphoid and non-lymphoid tissues. Although in the initial definition of the mononuclear phagocyte system van Furth *et al.* stated that macrophages originate from blood monocytes<sup>[181,182]</sup>, actual evidence suggests that some populations such as Langerhans cells, microglia, splenic red pulp, alveolar and peritoneal macrophages have a prenatal origin and do not depend on monocytes for their renewal in



steady-state conditions. Moreover, some tissue resident populations can proliferate and contribute to their self-renewal<sup>[183,184]</sup>. Macrophage phenotype is modulated by the tissue environment, giving rise to different populations of resident macrophages in the steady state such as Kupffer cells in the liver, lung alveolar macrophages, microglia, skin Langerhans cells and osteoclasts. The great plasticity of macrophages is confirmed by the variety of functions performed, such as maintenance of tissue homeostasis with removal of aged blood cells, necrotic tissues and toxic molecules, wound healing and angiogenesis, metabolic functions regulating adipocyte function, insulin-sensitivity and glucose tolerance, initiation of innate immune responses and activation of adaptive immune system<sup>[185]</sup>.

### 1.3.2. The concept of macrophage polarization

Macrophages are characterized by their plasticity as the environment modulates their phenotype exerting inflammatory or anti-inflammatory functions depending on their activation or polarization state. These polarization states differ in receptor expression, chemokine production and effector functions (Figure 1.10).

Early studies on macrophage function showed that these cells can be activated to increase their antimicrobial activity<sup>[186]</sup>. When exposed to microbial products and IFN- $\gamma$  produced by Th1 lymphocytes and NK cells, macrophages increase their ability to kill intracellular pathogens, as a result of what is known "classical activation"<sup>[187-189]</sup>. On the other hand, in 1982 Gordon *et al.* observed that IL-4 produced by Th2 cells had the opposite effect on macrophages, an "alternative activation"<sup>[190]</sup>. Mirroring Th1/Th2 nomenclature, classical and alternatively activated macrophages are commonly termed M1 and M2 macrophages respectively, as they represent extremes of a spectrum of possible forms of polarization.

Recent complex transcriptomic analysis has revealed that the distinction of only two subtypes of polarized macrophages is probably too simplistic and it is better to consider the concept of an spectrum of polarization states, with the typical IFN- $\gamma$  and IL-4 exposed macrophages as opposite ends, but with intermediate phenotypes that result from different stimulations<sup>[191]</sup>.

#### 1.3.2.1. M1 macrophages

Classical activation requires two signals: (1) IFN- $\gamma$  which primes macrophages for activation and (2) exogenous TNF- $\alpha$  or an inducer of TNF- $\alpha$ , such as LPS, that through activation of TLR induces endogenous production of TNF<sup>[192]</sup>. M1 macrophages develop 3 main functions: specialization in killing intracellular pathogens, induction of type I immune responses and development and expansion of Th17 cells<sup>[193-195]</sup>. They produce inflammatory cytokines such as IL-1 $\beta$ , IL-6, TNF- $\alpha$ , IL-12 and IL-23, up-regulating CD86, IL-1RI, IL-1RAcP, HLA-II, and

increasing their antigen presenting functions and opsonic receptors such as CD16. Their arginine metabolism is characterized by high levels of Nitric Oxide Synthase (iNOS) that produces NO from arginine<sup>[192,193,196]</sup>. Chemokines produced by M1 macrophages are related to IFN- $\gamma$  and Th1 responses, such as interferon gamma-induced protein 10 (IP-10 or CXCL10) or monokine induced by  $\gamma$ -interferon (MIG or CXCL9)<sup>[196]</sup>.

### 1.3.2.2. M2 macrophages

These cells have anti-inflammatory or suppressive functions, scavenge debris and promote angiogenesis, tissue remodelling and wound healing. Unlike M1, M2 macrophages up-regulate non-opsonic receptors, such as CD163 and the mannose receptor (MR), increasing their endocytic capacity. They express the decoy receptor IL-1RII and IL-1Ra and secrete the chemokines CXCR1, CXCR2, CCL17, CCL18, CCL22, and CCL24 that attract Th2 and regulatory cells. Regarding arginine metabolism, in M2 macrophages arginase is induced, which metabolizes arginine to urea and ornithine, a precursor of polyamines and proline. Polyamines are involved in growth and cell division whereas proline is a key component of collagen. Additionally, M2 macrophages have compromised the ability to kill intracellular microbes, as they fail to produce NO<sup>[192,193,196,197]</sup>.

Although alternative activation was originally described after culture with IL-4, other stimuli such as the presence of IL-13, IL-10, TGF- $\beta$ , IgG-IC (immune-complexes), vitamin D3, M-CSF and the uptake of apoptotic cells lead to activation of macrophages with similar phenotypes. They have in common the production of the anti-inflammatory cytokine IL-10 but not IL-12 and the involvement in type II responses, immune regulation and tissue remodelling. Therefore, these different conditions have been put together under the concept M2 or alternatively activated macrophages, as opposite to classical activation. However, macrophages polarized with these different stimuli differ in their patterns of gene expression, showing specialized functions<sup>[189,193,196]</sup>. Activation with IL-4 or IL-13, that share a common receptor chain and have similar effects on macrophages, results in **M2a macrophages** specialized in Th2 responses, type II inflammation, allergy and killing and encapsulation of parasites. Type II activated or **M2b macrophages** are the result of the combined exposure to IgG-IC and TLR or IL-1R ligands and they need two signals for their activation: one is the ligation to Fc $\gamma$ Rs and the second involves TLR, CD40 or CD44<sup>[192]</sup>. These macrophages generate great amounts of IL-10 although they produce also the inflammatory cytokines TNF- $\alpha$ , IL-1 $\beta$  and IL-6. Globally, M2b induce Th2 activation, showing anti-inflammatory functions and preventing acute pathologies such as LPS endotoxemia by avoiding the induction of arginase. In the presence of IL-10, **M2c macrophages** exhibit a deactivated phenotype characterized by the production of IL-10 and TGF- $\beta$  and they are involved in immune regulation, matrix deposition and tissue remodelling.

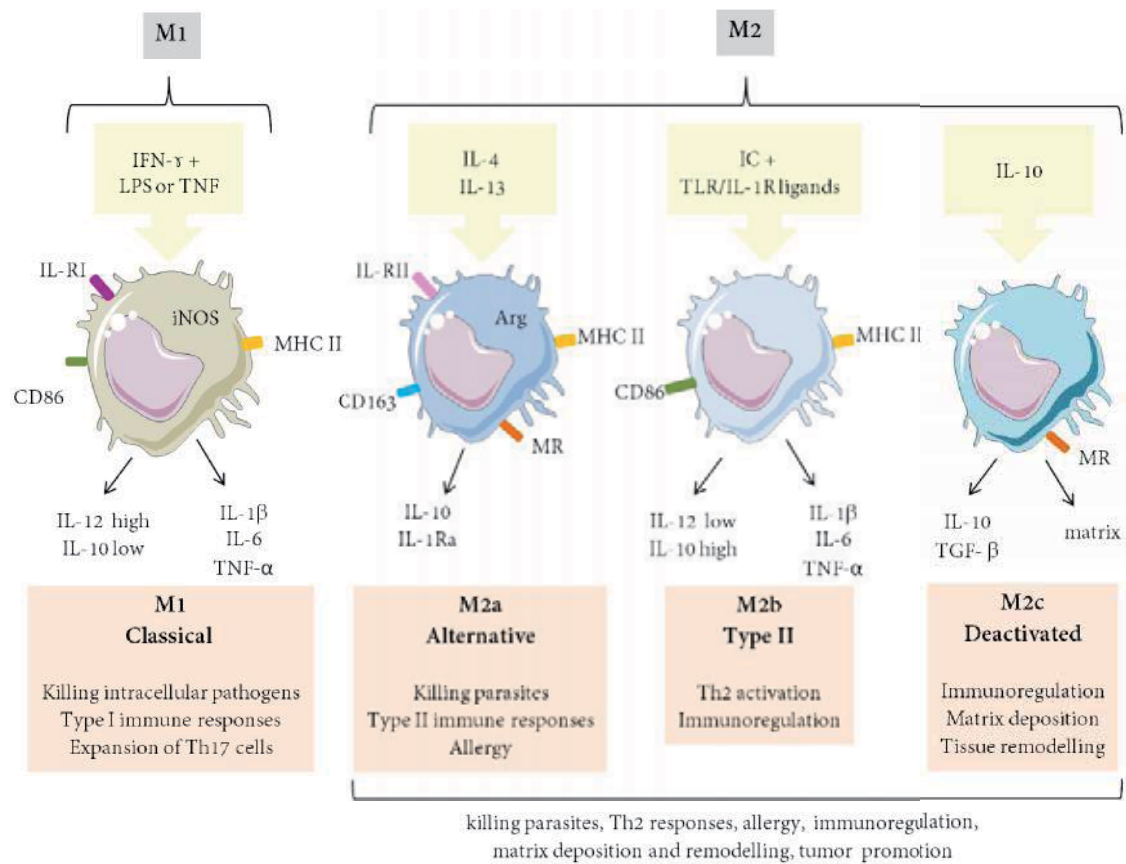


Figure 1.10. Macrophage polarization. (Adapted from Mantovani *et al.*, 2004)<sup>[196]</sup>

### 1.3.3. Role of M-CSF and GM-CSF in macrophage polarization

Colony-stimulating factors were first defined by their abilities to generate colonies of mature myeloid cells, such as granulocytes with granulocyte colony-stimulating factor (G-CSF), macrophages with macrophage colony-stimulating factor (M-CSF) or granulocytes and macrophages in the case of granulocyte/macrophage colony stimulating factor (GM-CSF), from bone-marrow precursors<sup>[198]</sup>. Apart from this haematopoietic function, these growth factors can act on mature myeloid cells and have a role during immune responses<sup>[199]</sup>.

In 2004, Verreck *et al.* confirmed previous observations, suggesting that macrophages polarized *in vitro* with GM-CSF or M-CSF exhibit different phenotypes and resemble M1 and M2 macrophages, respectively<sup>[200,201]</sup>. These macrophages can be distinguished by their morphology, surface markers, phagocytic capacity, cytokine secretion and gene expression. Although both are adherent cells, GM-CSF macrophages have rounded 'fried-egg' morphology, whereas M-CSF macrophages are stretched, spindle-like cells. The later exhibit higher phagocytic capacity and increased expression of cell surface antigen CD14, whereas GM-CSF

macrophages express higher levels of CD11b. The scavenger receptor CD163 is only present in M-CSF macrophages and helps to differentiate both subtypes. The surface antigen repertoire of macrophages polarized with M-CSF mimic the phenotype of IL-10 M2 macrophages<sup>[202]</sup>. Accordingly with their inflammatory and anti-inflammatory functions, GM-CSF macrophages are characterized by production of inflammatory cytokines and up-regulation of inflammatory genes such as TNF- $\alpha$ , whereas M-CSF macrophages up-regulate the expression of the anti-inflammatory cytokine IL-10<sup>[203]</sup>. As M-CSF is a homeostatic growth factor circulating in normal blood, some authors consider that macrophages polarized with M-CSF, instead of being activated, could represent the steady state resident macrophages in tissues<sup>[197,199,204]</sup>.

#### 1.3.3.1. M-CSF biology and functions

M-CSF, also known as colony stimulating factor-1 (CSF-1), regulates the survival, proliferation and differentiation of monocyte lineage cells like tissue macrophages, DCs, osteoclasts and microglia<sup>[205]</sup>. It is found in the circulation at detectable levels in the steady state, being constitutively produced *in vitro* by several cell types such as fibroblasts, endothelial cells, stromal cells, macrophages, smooth muscle cells and osteoblasts<sup>[199]</sup>. This protein is a disulfide-linked dimer, with each monomer consisting of 4 alpha-helical bundles and 1 anti-parallel beta-sheet. Full length human M-CSF protein has 522 amino acids (aa), and of them, the 150 N-terminal aa represent the minimal sequence required for full *in vitro* biological activity, whereas the remaining 372 aa determine how this biologically active region is expressed in cells. Three major M-CSF isoforms (a secreted glycoprotein, a cell-surface protein and a proteoglycan)<sup>[199]</sup> result from alternative splicing in exon 6 and alternative usages of the 3'-untranslated regions of exons 9 and 10. The mRNA containing the full length of exon 6 encodes a protein initially glycosylated in the endoplasmic reticulum and afterwards, in the Golgi, N-glycosyl units and O-linked sugars (like chondroitin sulphate) are added. These glycosylated precursors are then incorporated in secretory vesicles where, depending on whether the peptide chain is cleaved N-terminally or C-terminally, the glycoprotein or the proteoglycan forms will be released respectively. The chondroitin sulphate chains favour the location of the protein in extracellular matrices. On the other hand, the shorter precursor, that lack the proteolytic cleavage sites in exon 6, is not cleaved in the secretory vesicle and is expressed as a membrane-spanning glycoprotein, having a local action in cell-cell interactions<sup>[205]</sup>.

M-CSF receptor (CSF1R), encoded by the *FMS* proto-oncogene<sup>[206]</sup>, is a homodimeric type III receptor tyrosine kinase with 5 extracellular Ig-like domains, a transmembrane domain and an intracellular interrupted Src-related tyrosine kinase domain that possesses intrinsic tyrosine kinase activity being able to initiate several signalling cascades once activated. It is expressed in

mononuclear phagocytes and cells of the female reproductive tract<sup>[205]</sup>. Once activated by M-CSF, the complex is internalized and degraded in lysosomes to prevent ongoing signalling<sup>[205]</sup>. Of note, IL-34 is also a ligand for the M-CSF receptor and explains the more severe phenotype of the M-CSF receptor knockout mice compared to the M-CSF deficient mice. Thus, IL-34 have to be taken into account when analyzing the effects of M-CSF blockade<sup>[204]</sup>.

*In vitro*, M-CSF acts on cells of macrophage lineage, increasing their survival and proliferation. M-CSF is required *in vivo* for the maintenance of tissue macrophage populations in the steady state and could play a role in tissue homeostasis following injury or inflammatory damage, e.g. with the clearance of injured tissue by phagocytosis. Moreover, M-CSF may promote resistance to inflammatory signals in resident macrophages<sup>[204]</sup>. Acting at later stages of macrophage development, M-CSF regulates macrophage numbers in the steady state and during inflammation, probably through an effect in more mature peripheral monocytes, decreasing their migration to tissues, more than an effect on bone-marrow cells<sup>[207]</sup>. The importance of M-CSF *in vivo* for the maintenance of tissue macrophage populations has been demonstrated by the phenotype of the osteopetrotic *Csf1<sup>op</sup>/Csf1<sup>op</sup>* mutant mice, that lacks M-CSF due to an inactivating mutation. This mice exhibit a severe deficiency in mononuclear phagocytes, skeletal abnormalities characterized by osteopetrosis (due to the absence of osteoclasts), absence of teeth, decreased sensory processing, low body weight, defects in male and female fertility and short life span<sup>[208]</sup>. Partial restoration of macrophage population after systemic administration of recombinant human M-CSF (rhM-CSF), compared with the complete restoration with the transgenic expression of the full-length CSF-1 gene demonstrate that local M-CSF is required to restore tissue macrophages in muscle, tendon, periosteum, synovial membrane, adrenals, digestive tract, dermis, bladder, bone-marrow and salivary glands<sup>[209,210]</sup>. However, some tissue macrophages may develop independently of M-CSF and are present in the osteopetrotic mice, such as macrophages from lymphoid tissues and Langerhans cells of the skin, and this could explain that these mice are not immunologically compromised<sup>[205]</sup>.

M-CSF has been associated with deleterious effects in arthritis, nephritis, lung fibrosis, atherosclerosis, obesity, cutaneous lupus erythematosus (CLE), inflammatory bowel disease and cancer metastasis and consequently, clinical trials targeting M-CSF in rheumatoid arthritis, cancer and CLE are ongoing<sup>[204]</sup>. M-CSF is produced constitutively by synovial fibroblasts from rheumatoid arthritis and osteoarthritis patients and, in collaboration with RANK-L (receptor activator of nuclear factor kappa B ligand), contributes to the differentiation of synovial macrophages into osteoclasts, which are involved in bone destruction in rheumatoid arthritis<sup>[211]</sup>. In the model of collagen-induced arthritis, osteopetrotic mice are protected from the development of arthritis and M-CSF blockade decreases its incidence and disease severity whereas administration of M-CSF exacerbates

disease<sup>[212–214]</sup>. In the model of arthritis induced by methylated bovine serum albumin (mBSA), osteopetrotic mice did not develop arthritis but M-CSF blockade was not effective in normal mice<sup>[215]</sup>. In cancer, M-CSF has a dual role, as membrane-spanning M-CSF elicits anti-tumoral activity on macrophages in glioblastoma, glioma, hepatocellular carcinoma and breast cancer, whereas the secreted form promotes cell growth and tumour invasion. Similarly, anti-atherogenic effects of M-CSF are mediated by its circulating isoform and pro-atherogenic effects by local cell-surface protein<sup>[211]</sup>. M-CSF has a deleterious effect in lung fibrosis and lupus nephritis, as deficient mice have reduced renal injury after ureter obstruction or in mice model of lupus nephritis<sup>[216–218]</sup>. On the other hand, this growth factor has a therapeutic benefit in models of Alzheimer's disease, kidney repair, chronic graft-versus-host disease and gastric ulcer healing<sup>[204]</sup>.

### 1.3.3.2. GM-CSF biology and functions

GM-CSF is a glycosylated secreted protein that consists of a single polypeptide secreted chain. Its receptor (CSF2R) is a heterodimer composed of a ligand-binding subunit (CSF2R $\alpha$ ) and a signal-transduction subunit (CSF2R $\beta$ ) that is common with the receptor for IL-3 and IL-5. Mice with inactivated  $\beta$ -subunit exhibit the similar phenotype than the GM-CSF<sup>-/-</sup> mouse, whereas the specificity of functionality depends on different  $\alpha$ -chains. Unlike what happens with M-CSF, no circulating levels of GM-CSF are detected in the blood stream in the absence of inflammation. Besides its role in generating colonies of granulocytes and macrophages *in vitro*, GM-CSF is involved in emergency haematopoiesis in response to infection and in maintenance, survival and activation of granulocytes and macrophages at sites of injury or insult. GM-CSF acts on monocytes, macrophages, neutrophils, eosinophils and basophils. *In vitro*, it is involved in survival, proliferation and activation of macrophages and granulocytes and it is used for the generation of monocyte-derived DCs. Macrophages activated with GM-CSF produce IL-23, IL-1 and IL-6 that drive differentiation of Th17 and Th1 cells, that in turn produce GM-CSF<sup>[199,204,219]</sup>. Data from GM-CSF deficient mice have showed that *in vivo* this growth factor is required for the maturation of alveolar macrophages and invariant NK-T cells. Deficient mice exhibit pulmonary defects that resemble the human disorder alveolar proteinosis<sup>[220]</sup>. Its systemic administration mobilizes myeloid cells from bone-marrow to blood and primes monocytes for a increased response *in vitro* to LPS<sup>[199]</sup>.

Its blockade has benefits in arthritis<sup>[215,221,222]</sup>, encephalitis<sup>[223]</sup>, Alzheimer's disease<sup>[224]</sup>, myocardial infarction<sup>[225]</sup> and peripheral insulin resistance<sup>[226]</sup>. In the lung, ameliorates asthma, chronic obstructive pulmonary disease and lung inflammation<sup>[227,228]</sup>. Conflicting results have been reported in atherosclerosis, as administration of GM-CSF exacerbates disease and inversely its deficiency aggravates disease progression<sup>[229,230]</sup>. In cancer its administration has a



beneficial role, and it is clinically used to increase neutrophil numbers after chemotherapy and in mobilization of myeloid stem cells in transplantation. However, endogenous GM-CSF has been linked to the presence of myeloid suppressor cells that promote tumour growth<sup>[231,232]</sup>.

On the other hand, GM-CSF administration has benefits in myasthenia gravis<sup>[233]</sup>, wound healing<sup>[234]</sup>, brain injury, with a neuroprotective role restoring cerebral blood supply<sup>[235]</sup>, and vascular injury by promoting mobilization of endothelial cells and neovascularisation<sup>[236]</sup>. GM-CSF seems to have a protective role in intestinal immune responses and it has adjuvant properties<sup>[204]</sup>.

### 1.3.4. Monocyte subpopulations

Monocytes, in addition to being the origin of tissue macrophages, have multiple functions in the organism such as the defence from pathogenic microorganisms, anti-tumoral effects and participate in tissue homeostasis and repair. In accordance with these multiple functions, different monocyte subpopulations have been described according to their activity and the expression of cell surface antigens CD14 (LPS co-receptor) and CD16 (FcγRIIIa) (Figure 1.11): classical monocytes CD14<sup>++</sup>CD16<sup>-</sup>, intermediate CD14<sup>++</sup>CD16<sup>+</sup> and non-classical CD14<sup>+</sup>CD16<sup>++</sup>. They represent the 85%, 5% and 7% from total blood monocytes respectively<sup>[237,238]</sup>. Classical and intermediate monocytes are the human homologs of "inflammatory" Ly-6C<sup>high</sup>/Gr1<sup>+</sup> monocytes, whereas non-classical human monocytes resemble Ly-6C<sup>low</sup>/Gr1<sup>-</sup> murine monocytes<sup>[239]</sup>.

Both classical and intermediate monocytes exhibit an enhanced capacity for phagocytosis and inflammation, produce moderate amounts of the anti-inflammatory cytokine IL-10, but they differ in the repertoire of other secreted cytokines. **Classical monocytes** produce high levels of ROS, mRNA for myeloperoxidase and lysozyme and, in the presence of the TLR4 agonist LPS, produce IL-6, IL-8, CCL2 and CCL3. **Intermediate monocytes** do not produce ROS, express low levels of myeloperoxidase and lysozyme and secrete IL-1β, IL-1α and TNF-α after TLR2 and TLR4 stimulation. The intermediate population exhibits higher presenting activity and higher pro-angiogenic capacity. **Non-classical** or CD14<sup>+</sup>CD16<sup>++</sup> monocytes patrol the endothelium looking for danger signals and have anti-inflammatory and repair functions. They are less phagocytic, do not produce ROS, express little mRNA for myeloperoxidase and lysozyme, CCR1, CCR2, CCR5, IL-17RA, apolipoprotein B48 and CD36, but high amounts of IL-10 receptor and IL-1Ra. In response to viruses, that bind TLR7 and TLR8 receptors, produce high amounts of the inflammatory cytokines IL-1β, TNF-α and CCL3<sup>[239,240]</sup>.

In addition to CD14 and CD16, Shantsila *et al.* used the expression of CCR2 to discriminate between CD16<sup>+</sup> monocytes, and proposed the existence of three populations: CD14<sup>+</sup>CD16<sup>-</sup>

CCR2<sup>+</sup>, CD14<sup>+</sup>CD16<sup>+</sup>CCR2<sup>+</sup> and CD14<sup>low</sup>CD16<sup>+</sup>CCR2<sup>-</sup>[241]. CCR2 is the chemokine receptor for monocyte chemoattractant protein-1 (MCP-1 or CCL2), a chemokine that mediates monocyte chemotaxis. Because of the low levels of CCR2 in non-classical monocytes, their transendothelial migration is independent of CCL2. Instead, CD16<sup>+</sup> monocytes express high levels of CX<sub>3</sub>CR1, the receptor for fractalkine, a chemokine expressed as a transmembrane molecule on the surface of endothelial cells activated by inflammatory cytokines such as IL-1 $\beta$  or TNF- $\alpha$ . Thus, CD16<sup>+</sup> monocytes preferentially migrate to inflamed tissues and amplify the inflammatory response<sup>[242]</sup>.

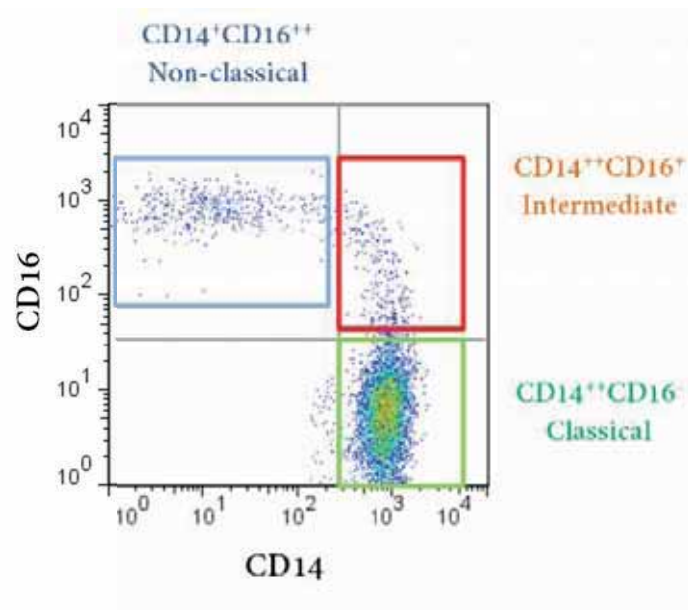


Figure 1.11. Analysis of peripheral blood monocyte subpopulations by flow cytometry. (Adapted from Cros *et al.*, 2010)<sup>[239]</sup>

Numerous studies have observed an expansion of the population CD16<sup>+</sup> monocytes in pathologies such as sepsis, cancer, coronary heart diseases, sarcoidosis and asthma and after exercise<sup>[243–249]</sup>. CD16<sup>+</sup> population is decreased after treatment with glucocorticoids, intravenous immunoglobulins and M-CSF blockade<sup>[248–252]</sup>. In rheumatoid arthritis this population correlates with disease activity. In particular, CD14<sup>++</sup>CD16<sup>+</sup> monocytes, that produce inflammatory cytokines such as IL-1 $\alpha$ , IL-1 $\beta$ , TNF- $\alpha$  and promote *in vitro* Th17 differentiation, are expanded and decrease after treatment<sup>[180,240,252,253]</sup>. Recently, a case report of a patient with rheumatoid arthritis receiving M-CSF blockade has showed that after the disappearance of this population, treatment recuperation starts with the intermediate and then the non-classical monocytes, suggesting a continuum of differentiation between monocyte subpopulations. This intermediate population has been involved too in the generation of atherosclerotic plaques. The increase of the same population in patients with chronic kidney



disease has led to hypothesise that this subset could be involved in the greater cardiovascular risk of these patients<sup>[254]</sup>.

### 1.3.5. Role of monocytes and macrophages in the initiation of gouty arthritis flares

The mononuclear phagocyte system in synovial tissue is represented by type A synoviocytes and macrophages in subintima and synovial fluid. The normal synovium comprises a continuum layer of cells, or intima, and the underlying tissue, or subintima. The intimal layer is one to two cell thick and is composed by type A (macrophage like cells) and type B synoviocytes (fibroblasts like cells)<sup>[255]</sup>. Staining of mice synovial membrane with the macrophage marker F4/80 shows that 40-50% of synovial lining cells correspond to macrophages<sup>[256]</sup>. On the other hand, subintima layer is relatively acellular and contains blood vessels, fat cells, fibroblasts, lymphocytes and macrophages. Synovial macrophages express nonspecific esterase activity, CD163 and CD68 and, to a lesser extent, CD14. Intimal macrophages also express the immunoglobulin receptor Fc $\gamma$ RIIIa, while subintimal macrophages usually express low levels<sup>[257]</sup>. Synovial macrophages derive from blood monocytes that migrate to the synovium through subintimal venules<sup>[258]</sup>.

Joint resident macrophages are in direct contact with MSU intraarticular deposits and have been involved in the initiation of the inflammatory response to MSU crystals; time course studies from Harper's group in the mice peritonitis model provide evidence of that concept<sup>[259]</sup>. They observed that, whereas infiltration of the peritoneal cavity with monocytes and neutrophils started after 4 hours of MSU injection, peaking at 16 hours, inflammatory cytokines (IL6, IL-1 $\beta$  and TNF- $\alpha$ ) were detectable in the peritoneal lavage in the first 2 hours and peaked at 4 hours. Moreover, monocytes and neutrophils isolated at 4 hour time point failed to produce IL-6 in response to MSU. All these facts suggested that these infiltrating cells could not be the origin of the inflammatory response and that resident macrophages could be the source of these cytokines. When analyzing this cell population, they observed the disappearance of the population of resident macrophages after MSU injection secondary to adhesion to the peritoneal membrane and depletion of macrophages by clodronate liposomes resulted in a decrease in inflammatory cytokines and neutrophil infiltration. *Ex vivo* these cells produced inflammatory cytokines in response to MSU crystals. Together, these findings demonstrate the role of resident macrophages in the initiation of the inflammatory response to MSU crystals.

Once activated by MSU, macrophages produce inflammatory cytokines and chemokines that induce activation of endothelial cells and recruitment of monocytes and neutrophils toward the

inflammatory site to further amplify the inflammatory response. Inflammatory cytokines produced by monocytes and macrophages in response to MSU and that have been found in synovial tissues or synovial fluids of patients with gout are: IL-1  $\beta$  [136,260,261], IL-6 [262], TNF- $\alpha$  [263]. Moreover, inflammatory cytokines, such as IL-1 $\beta$  and TNF- $\alpha$  activate vascular endothelial cell expression of E-selectin and intercellular adhesion molecule 1 (ICAM-1), promoting chemotaxis of leukocytes. Macrophages produce the chemokines IL-8 [264], the CXC chemokines CXCL1, CXCL2 that share the common receptor CXCR2 [265], CCL3, CCL4, CXCL2 and CCL2 [266]. CCL2 or monocyte chemoattractant protein 1 (MCP1), as its name suggests, is involved in monocyte chemotaxis: this chemokine is produced by synovial fibroblasts that contain vesicles with this chemokine, releasing its content after MSU stimulation [267–269]. Other secreted proteins are matrix metalloproteinases, such as MMP-9 and MMP-2. MSU induce also iNOS and NO production. . All these molecules are key elements of the inflammatory process in which the gout is developed.

However, clinical evidence suggests that the contact between macrophages and MSU crystals is not enough to initiate an inflammatory reaction, as MSU deposits can be detected in individuals with asymptomatic hyperuricemia [19] and in asymptomatic gouty patients. One example of that is the work of Pascual *et al.* analyzing synovial fluid samples from asymptomatic joints of gouty patients. Surprisingly, they found intracellular MSU crystals in 19 of 20 SF examined and 0.5% were inside neutrophils and the rest in mononuclear cells [270]. Evidence of this non-inflammatory phagocytosis of MSU crystals by macrophages has been also provided by Yagnik *et al.* After a series of experiments, they proposed that the state of maturation of monocytes/macrophages influences the response to MSU crystals. Using mice macrophage cell lines, they observed that cells with more mature phenotype, although being more phagocytic, failed to produce inflammatory cytokines and to induce ICAM in endothelial cells in response to MSU crystals. Conversely, less mature macrophages were able to induce E-selectin expression and to produce inflammatory cytokines [271]. These results were confirmed in human cells, in which fresh monocytes produced inflammatory cytokines whereas monocyte-derived macrophages produced the anti-inflammatory cytokine TGF- $\beta$  [272,273]. For further confirmation, they analyzed the production of cytokines in response to MSU crystals in cells from cantharidin-induced skin blisters, an *in vivo* model of acute and resolving inflammation [274]. Leukocytes from 16-hour blisters secreted TNF- $\alpha$ , but not TGF- $\beta$ , whereas leukocytes from 40-hour blisters secreted TGF- $\beta$  but not TNF- $\alpha$ . CD14<sup>+</sup> cells in the later time point were predominantly CD163 positive, that could suggest an M2 or non-inflammatory macrophage phenotype, whereas at 16 hours these cells represented <5%. As a conclusion, their results showed that the transition of monocyte/macrophages towards different activation states modulates the inflammatory response to MSU.

Apart from the effect of the state of macrophage differentiation in the initiation of gout flares, other studies have suggested the necessity of a second signal to trigger an inflammatory reaction to MSU crystals. These facts are in agreement with the episodic nature of gouty arthritis and with the identification of triggers such as traumatism, alcohol consumption or infection, which are followed by gouty arthritis flares. In this line, work from Netea *et al.* showed that intra-articular injection of MSU crystal in mice was not followed by the detection of inflammatory cytokines, joint swelling or histologic changes<sup>[275]</sup>. The addition of fatty acids, linked to alcohol consumption and great meals, resulted in IL-1 $\beta$  and KC production and cellular infiltration. As previously exposed in section 2.6, the same group had previously reported that macrophages need two signals for IL-1 $\beta$  production: one through TLR receptors for pro-IL-1 $\beta$  production, and the second signal would activate the inflammasome and in turn caspase-1 to cleave pro-IL-1  $\beta$  into its mature form IL-1  $\beta$ <sup>[164]</sup>. Free fatty acids could represent the first signal through TLR2 receptor. Similarly, serum amyloid A protein (SAA), in the presence of MSU crystals, triggers an inflammatory reaction<sup>[276]</sup>.

Bloodstream monocytes are recruited into the synovial tissue in response to chemokines and endothelial cell adhesion and there they differentiate towards macrophages. The inflammatory environment modulates the phenotype of these macrophages, turning them more inflammatory or anti-inflammatory depending on the stage of the inflammatory process. Harper's group demonstrated in the animal model of peritonitis, that monocytes recruited after MSU challenging are polarized towards an inflammatory or M1-like macrophage phenotype<sup>[277]</sup>. Mononuclear cells isolated 72 hours after intraperitoneal injection of MSU crystals were characterized by the expression of macrophage markers, the increased phagocytosis activity, production of inflammatory cytokines and up-regulation of proteins involved in inflammasome assembly. The production of GM-CSF by synovial cells, probably fibroblasts, seems to be the responsible for the acquisition of this inflammatory phenotype. In the same mice peritonitis model, GM-CSF blockade reduced L-1 $\beta$ , CXCL-1 and infiltrating neutrophils. Monocyte infiltration was unaffected, but these monocytes exhibited decrease expression of macrophage surface markers, M-CSF receptor and CD14, suggesting that GM-CSF is required for their maturation. Moreover, their inflammatory phenotype was impaired too, as they produced less IL-1 $\beta$  and had lower levels of pro/active IL-1  $\beta$  and pro/active caspase-1.

In conclusion, inflammation mediated by monocytes and macrophages is a key process in the pathogenesis of gout. A better understanding of this involvement remains still very relevant as the mechanisms of gout initiation are largely unknown. As previously mentioned, the phenotype of macrophages seems to affect the inflammatory response to MSU crystals,

however, data is lacking about the effect of these crystals on M1 and M2 macrophages. Moreover, the distribution of monocyte subpopulations in gout or the state of activation of monocytes in gouty patients have not yet been assessed. This thesis tries to expand the knowledge of the role of monocytes and macrophages in gout together with an insight into the autoinflammatory mechanisms involved in MSU inflammation.

*"The scientist is not a person who gives the right answers,  
he's one who asks the right questions".*

Claude Lévi-Strauss

# 2.

## Hypothesis



Although gout is an ancient disease, important basic mechanisms remain still unclear. The involvement of macrophages and monocytes is evident, but data about how this role is produced and how inflammatory mechanisms are coordinated are incomplete by now.

The main hypothesis of this thesis is that modulation of monocyte and macrophages' phenotype by the environment and the extent of their inflammatory reaction to MSU crystals are involved in the initiation of gout flares.

As secondary and more specific hypothesis:

(a) M2 macrophages would phagocyte MSU crystals without initiating an inflammatory response, in accordance with the presence of MSU crystals in asymptomatic joints. However, once phagocytosed, MSU crystals would induce changes in macrophage phenotype, turning them inflammatory. The incidence of a trigger, such as alcohol consumption or a copious meal, would result in activation of TLR receptors. These "M1-like" macrophages would then produce inflammatory cytokines such as IL-1 $\beta$ , initiating an inflammatory response.

(b) Blood monocytes could be influenced by factors released from inflamed joints during a gout flare. Such factors could expand the subpopulation of intermediate monocytes (CD14<sup>++</sup>CD16<sup>+</sup>), which exhibit an enhanced expression of chemokine receptors and produce inflammatory cytokines. These monocytes would migrate preferentially towards affected joints, amplifying the inflammatory response. Differences in the reactivity of monocytes to MSU crystals could explain why not all individuals with hyperuricemia develop clinical gout. As intermediate monocytes have been involved in atherosclerosis, this monocyte subset could represent a link between gout and the increase in cardiovascular risk observed in gouty patients.





*"I keep six honest serving-men,  
They taught me all I knew;  
Their names are What and Why and When  
And How and Where and Who".*

Rudyard Kipling

# 3.

## Objectives



To evaluate the previous hypothesis, I propose the following objectives for this study:

1. To define how changes in polarization state of resident macrophages could be involved in initiation of gout flares
2. To disclose how differences in inflammasome activation of M1 and M2 macrophages at steady state explain their specific behaviours regarding IL-1 $\beta$  production
3. To prove differences of inflammasome activation in response to MSU crystals between gouty patients and healthy controls
4. To determine the distribution of monocyte subpopulations in asymptomatic gout and during an acute flare of arthritis



*"I have had my results for a long time:  
but I do not yet know how I am to arrive at them".*

*Karl Friedrich Gauss*

4.

## **Materials and Methods**



## 4.1. Cell culture

### 4.1.1. Culture of M1 and M2 macrophages

Macrophages were derived *in vitro* from peripheral blood monocytes of healthy donors. Briefly, peripheral blood mononuclear cells (PBMCs) were separated from blood after centrifugation with a density gradient. Monocytes were then isolated by negative selection with magnetic beads and cultured at 37°C, 5% CO<sub>2</sub> in cRPMI for 6 days. For macrophage polarization, growth factors GM-CSF or M-CSF were added to obtain M1 or M2 macrophages respectively. Experiments were performed in a laminar flow hood to ensure the sterility (see more detailed protocols in next paragraphs).

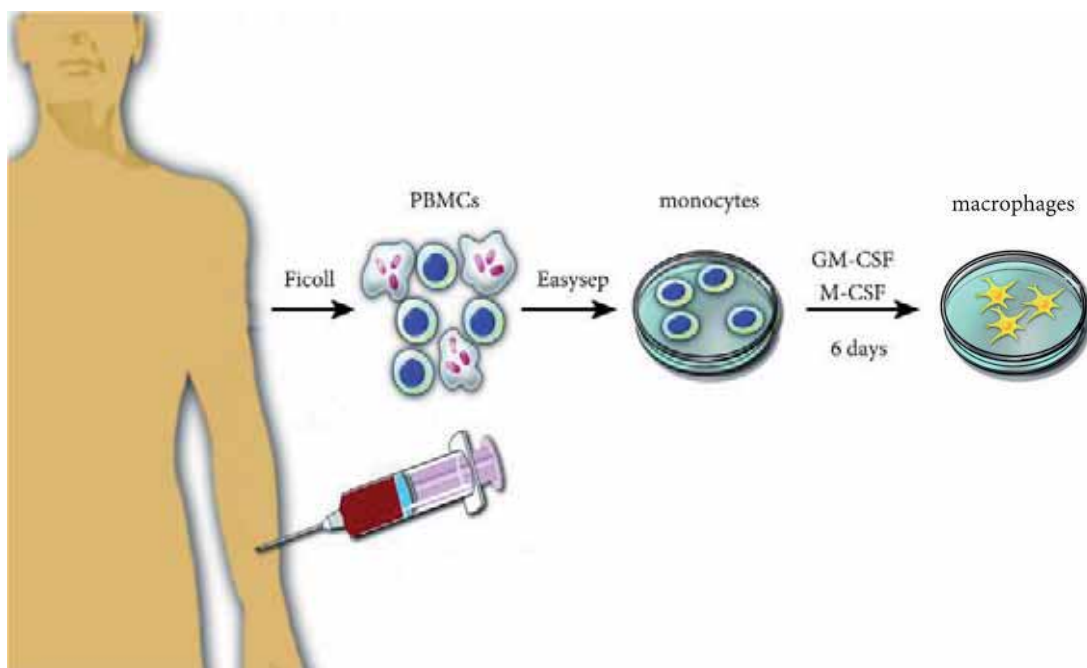


Figure 4.1. Overview of protocol for culture of *in vitro* monocyte-derived macrophages

#### 4.1.1.1. Isolation of peripheral blood mononuclear cells

Fifty millilitres of blood were collected into EDTA tubes (BD Vacutainer®) by vein puncture. Blood was then diluted with PBS (Roche), double volume of the one from blood, up to a total volume of 150 mL. 20 mL of diluted blood were overlaid on 7 mL of Ficoll-Paque PLUS (GE Healthcare). Tubes were centrifuged at room temperature (RT) with no brake (1800 rpm, 25 minutes). Mononuclear cells were harvested and washed three times with PBS at 1800 rpm for 5 minutes, 1500 rpm for 5 minutes and finally 1200 rpm for 10 minutes to discard platelets.

#### 4.1.1.2. Isolation of monocytes from PBMCs

For the isolation of monocytes from PBMCs, EasySep™ Human Monocyte Enrichment Kit (StemCell™ Technologies), a manual negative selection system based on magnetic beads, was used. In some experiments, EasySep™ Human Monocyte Enrichment Kit without CD16 Depletion was employed. With these kits, unwanted cells are specifically labelled with dextran-coated magnetic particles using bispecific TACs (Tetrameric Antibody Complexes). These TACs (Figure 4.2) recognize both dextran and the cell surface antigen expressed on the unwanted cells (CD2, CD3, CD19, CD20, CD56, CD66b, CD123 and glycophorin A).

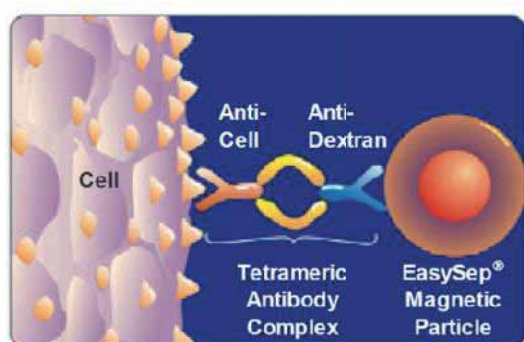


Figure 4.2. Tetrameric antibody Complexes (TACs) for magnetic cell isolation

Magnetic field separates cells that bind to the beads (positive unwanted fraction) from cells without magnetic beads (untouched monocytes). The specific protocol is the following one (Figure 4.3):

PBMCs were suspended at a concentration of  $50 \times 10^6$  cells/mL in recommended medium (PBS supplemented with 2% FBS and 1mM EDTA) and placed in a 5 mL polystyrene tube. EasySep™ Human Monocyte Enrichment Cocktail was added at 50  $\mu$ L/mL cells and the tube was incubated at 4°C for 10 minutes. After ensuring the uniform suspension of beads by vortex, EasySep™ D Magnetic Particles for Monocytes were added at 50  $\mu$ L/mL cells and incubated at 4°C for 5 minutes. Cells were brought to a total volume of 2.5 mL by adding recommended medium. After mixing carefully by pipetting up and down 2-3 times, the tube was placed into



the magnet and set aside for 2.5 minutes at RT. Then, the magnet and the tube were inverted, pouring off the desired fraction into a new tube. Monocytes were washed in PBS at 1500 rpm for 5 minutes and then counted in a Neubauer chamber, evaluating viability by using dye trypan blue to exclude dead cells.

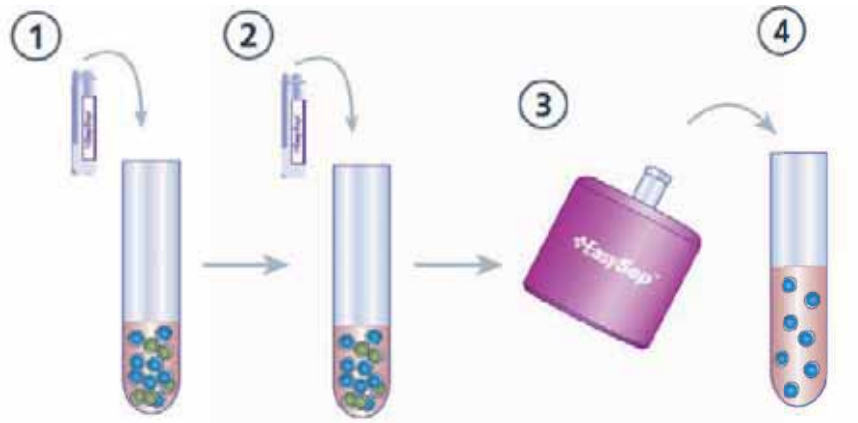


**Figure 4.3. Monocyte isolation using the EasySep™ method.** A cocktail with Tetrameric Antibody Complexes is added (1) and the sample is incubated at 4 °C for 10 minutes. After that, a solution with magnetic beads that bind to TACs is added (2) and cells are incubated again at 4 °C for 5 minutes. Cells are then diluted with recommended medium to 2.5 mL and the tube is placed in the magnet (3). Unwanted cells, labelled with TACs and magnetic beads, stick to the wall of the tube, so when the tube is inverted, the negative fraction of desired cells is poured off to a new tube (4).

#### 4.1.1.3. Macrophage polarization

Monocytes were resuspended at a concentration of  $0.5-1 \times 10^6$  cells/mL in cRPMI (RPMI supplemented with 10% FBS, penicillin 100 I.U./ml, streptomycin 100  $\mu$ g/ml, glutamax 2 mM) and cultured in 96, 24 or 12 well plates depending on the experiment. Plates were then incubated at 37°C, 5% CO<sub>2</sub> for 1 hour to allow cell attachment to the plate. On days 0, 2 and 5 half of the media was removed and replaced by new cRPMI, and growth factors GM-CSF (1000 I.U./mL, Miltenyi Biotech) and M-CSF (20 ng/mL, Prepotech) were added to obtain M1 and M2 macrophages respectively. After 6 days, macrophages were ready to be used in the experiments.

#### 4.1.1.4. Culture of macrophages with soluble uric acid

To study the effects of the chronic presence of high uric acid concentrations on macrophage function, peripheral blood monocytes from healthy volunteers were cultured in 96 well plates at  $1 \times 10^6$  cells/mL (200,000 monocytes per well) in cRPMI and different concentrations of uric acid (0.3 and 0.6 mM, Sigma-Aldrich). Monocytes were then polarized to M1 or M2 macrophages as previously described. On the other hand, to assess the effects of an acute

increase of uric acid concentrations, M1 and M2 macrophages cultured without uric acid for 6 days were exposed to the same concentrations of uric acid for 24 hours prior to stimulation.

#### 4.1.1.5. Stimulation with MSU crystals and LPS

On day 6, after washing each well twice with HBSS (Gibco) or PBS at 37°C, media was replaced by new cRPMI or Macrophage Medium without FBS (Gibco) depending on the experiment. As it has been reported that it is possible to find MSU crystals in asymptomatic joints of patients with gout and that a second signal through TLR receptors would be the trigger of a gout attack, in our experiments *in vitro* macrophages were stimulated first with MSU crystals (200 µg/mL, Invivogen) for 1 hour to allow phagocytosis of crystals, and then TLR4 agonist LPS (100 ng/mL, Invivogen) was added. After 18 hours, plates were centrifuged (1500 rpm, 5 minutes) and supernatants collected and stored at -20°C for further analysis. In some experiments calcium pyrophosphate (CPP) crystals (200 µg/mL) were used instead of MSU.

#### 4.1.1.6. Detachment of macrophages

Accutase™ (Millipore) is a solution of proteolytic and collagenolytic enzymes used for the detachment of adherent cells that changes minimally cell-surfaces, obtaining a suspension of cells that can be then analyzed by techniques such as flow cytometry. For macrophage detachment, an Accutase™ aliquot was thawed at room temperature. Cells were rinsed once with PBS and Accutase™ was added to each well at 10 mL per 75 cm<sup>2</sup> surface area. Plates were incubated at 37°C until detachment of cells (30-45 minutes in the case of macrophages). Cells were collected in a new tube through consecutive washes with PBS at 4°C to ensure complete recovery.

#### 4.1.2. THP-1 cells

THP-1 is a human monocytic cell line derived from an acute monocytic leukemia patient. These cells provide continuous grown (average doubling time 35-50 hours) in suspension cell culture, and can be differentiated into macrophage-like cells using PMA (Phorbol 12-myristate 13-acetate) and thus, have been widely used to study the regulation and function of macrophages.

In our assays, THP-1 cells were adjusted to  $2 \times 10^5$  cells/mL in cRPMI, plated in 12 well culture plates (400,000 cells per well) and then stimulated with 200 nM PMA (Sigma-Aldrich). Cells were incubated at 37°C, 5% CO<sub>2</sub> for 3 days, observing an increase in their size and adhesion to the surface of the plate, acquiring a macrophage appearance. On day 3, media was removed and, after washing with HBSS, 2 mL of new cRPMI media were added. Growth factors GM-CSF (1000 I.U./mL) and M-CSF (20 ng/mL) were added on days 3, 5 and 8. On day 9, cells

were detached with Accutase™, adjusted to  $0.5 \times 10^6$  cells/mL and placed in a 96 well culture plate (100,000 cells per well). After resting 24 hours at 37°C, 5% CO<sub>2</sub>, cells were stimulated with MSU and LPS as previously described for macrophages.

## 4.2. MSU preparation

Some of the experiments were performed using commercial MSU crystals (Invivogen). But for the experiments performed in Harper's group in New Zealand, crystals were prepared in the laboratory. Briefly, 250 mg uric acid and 300 µl of NaOH 5M were diluted in 45 mL of double distilled water. Mixture was boiled until complete dissolution of uric acid and filtered through a 0.2 µm filter. Then 1 mL NaCl 5M was added and the solution stored at 26°C for 7 days. The resulting crystals were washed with ethanol and acetone. Absence of endotoxin (<0.01 EU/10 mg) was confirmed with LAL (*Limulus amoebocyte*) assay. On polarized light microscope, MSU crystals were needle-shaped, with a crystal length of 5-20 µm and showed optical birefringence.

## 4.3. Phagocytosis assays

### 4.3.1. Phagocytosis of fluorescent beads

Phagocytic activity of macrophages was assessed using fluorescent beads (FluoSpheres® fluorescent microspheres, Invitrogen). Once inside the cell, these particles send out a fluorescent signal than can be detected by the flow cytometer in the FL-1 channel.

M1 and M2 macrophages were cultured as previously described for 7 days in 96 well culture plates. Fluorescent beads were diluted (2 µl beads in 4 mL cRPMI medium) and 50 µl of medium in each well were replaced by 50 µl of diluted beads. Plates were incubated at 37°C, 5% CO<sub>2</sub> for one hour and then washed with HBSS to remove unphagocytosed beads. Macrophages were detached with Accutase™. After two washes with PBS, cells were resuspended in 5 mL polystyrene tubes with FACS Buffer (0.1% BSA, 0.01% sodium azide in PBS) and run in a FACScan flow cytometer (BD Biosciences). Propidium Iodide (PI) was used to exclude dead cells. Macrophages were analyzed by gating by Forward Scatter(FSC)/Side Scatter (SSC) (Figure 4.5). The percentage of FL-1 positive cells, indicating cells that had phagocytosed fluorescent beads, and mean intensity of FL-1 fluorescence, suggesting the capability of phagocytosis of each cell, were analyzed.

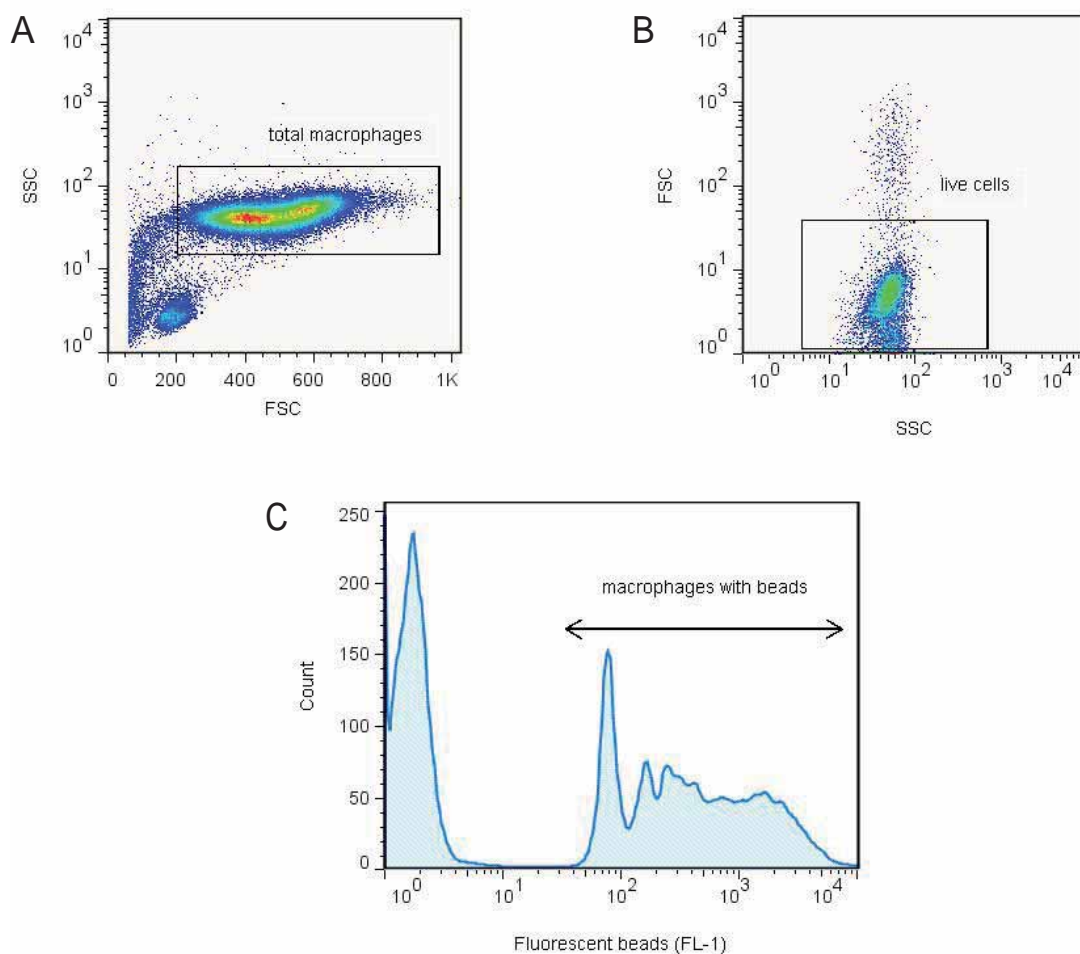


**Figure 4.5. Gating strategy for the study of macrophage phagocytosis with flow cytometry.** Macrophages were gated on FSC/SSC plot (A), and death cells were excluded with PI staining (B). Live cells were displayed in a histogram (C) based on the intensity of fluorescence on FL-1 channel. Cells that had phagocytosed beads exhibited a fluorescent signal, proportional to the number of intracellular beads.

#### 4.3.2. Phagocytosis of MSU crystals

Flow cytometers use the light scatter produced when one cell deflects the incident laser to determine its size and complexity, being the Side-Scattered Light (SSC) proportional to cell granularity or internal complexity. When macrophages phagocytose MSU crystals, SSC signal increases and these cells can be identified by flow cytometry (Figure 4.6).

M1 and M2 macrophages were cultured as previously described in 96 well culture plates. On day 7, after 18 hour incubation with MSU crystals (200  $\mu\text{g}/\text{mL}$ ), media was removed. Cells were washed, detached with Accutase™ and resuspended in FACS buffer. SSC was assessed using a FACScan flow cytometer.

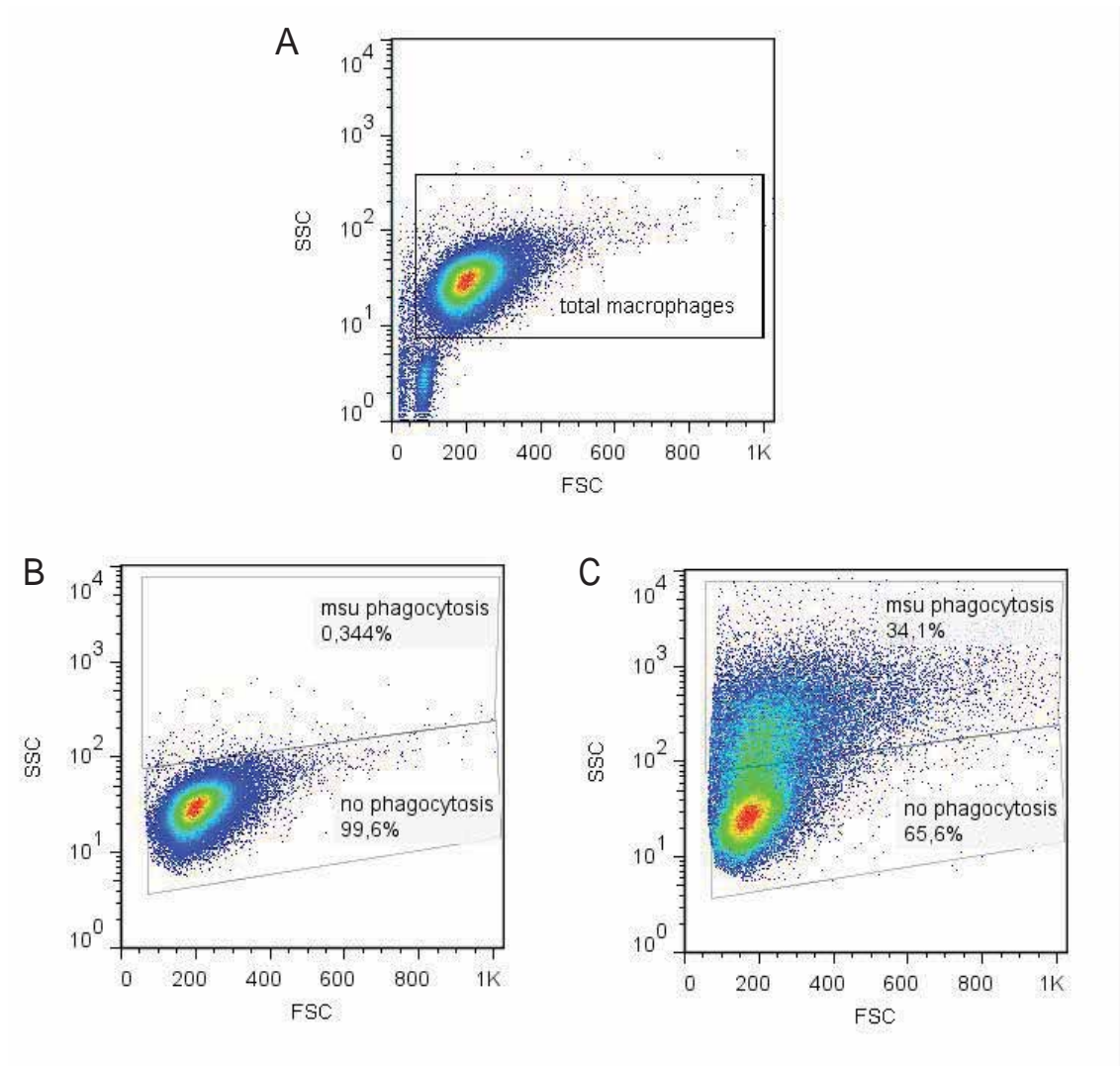


**Figure 4.6.** Assessment of MSU crystal phagocytosis by flow cytometry. First, total macrophages were gated on FSC/SSC plots (A). Samples of unstimulated macrophages were used to set the gates of macrophages with or without crystals (B). When MSU crystals were added (C), phagocytosed increased the SSC signal.

## 4.4. Cytokine analyses

### 4.4.1. Enzyme-linked immunosorbent assay (ELISA)

#### 4.4.1.1. ELISA IL-1 $\beta$

The inflammatory cytokine IL-1 $\beta$  was quantified in supernatants by ELISA (Mabtech), according to manufacturer's protocol. Briefly, 96 well high protein binding plates were coated with 100  $\mu$ l/well of capture antibody (mAb IL1 $\beta$ -1 diluted to 2  $\mu$ g/mL in PBS) and incubated overnight at 4°C. Plates were then washed with 200  $\mu$ l of Elisa Wash Buffer (0.05% PBS/Tween 20) and blocked with 200  $\mu$ l/well of incubation buffer (PBS with 0.05% Tween20 and 0.1% BSA) for 1 hour at RT. Eight point standard curve was prepared with the top standard of 300 pg/mL and serial dilutions 1:1. Samples were diluted 1:1 in incubation buffer. After washing each plate with Elisa Wash Buffer, 100  $\mu$ l/well of samples and standards were pipetted, as well as 100  $\mu$ l of incubation buffer as blank. Plates were covered and incubated at RT for 2 hours. After washing with Elisa Wash Buffer, 100  $\mu$ l/well of detection antibody (mAb IL1 $\beta$ -II-biotin diluted at 1  $\mu$ g/mL in incubation buffer) were added, and plates were incubated 1 hour at RT. Plates were washed and 100  $\mu$ l/well of Streptavidin-HRP diluted 1:1000 in incubation buffer were added, incubating 1 hour at RT. After washing, 100  $\mu$ l/well of TMB substrate solution (BD Bioscience) were added and plates were left 20-30 minutes at RT in the dark. 50  $\mu$ l of H<sub>2</sub>SO<sub>4</sub> 1M were added to stop the reaction and plates were read at 450 nm in an spectrophotometer (Epoch Microplate Spectrophotometer, Biotek). Readings at 540 nm were subtracted from the readings at 450 nm to correct optical imperfections in the plate. By using the optical density (OD) of pre-quantified standards, the concentration of each sample was determined by using a point-by-point calculation software.

#### 4.4.1.2. ELISA IL-10

Interleukin-10 was quantified using an ELISA kit (R&D Systems) , following the next protocol supplied by the manufacturer. 96 well high protein binding plates were coated with 100  $\mu$ l/well of capture antibody (diluted to 2  $\mu$ g/mL in PBS) and incubated overnight at 4°C. Plates were then washed with Elisa Wash Buffer (200  $\mu$ l/well) and blocked with 200  $\mu$ l/well of reagent diluent (1% BSA in PBS). Plates were incubated for 1 hour at RT. Eight point standard curve was prepared with the top standard of 2000 pg/mL and serial dilutions 1:1 in reagent diluent. Samples were diluted 1:2 in reagent diluent. After washing each plate, 100  $\mu$ l/well of samples and standards were pipetted, as well as 100  $\mu$ l of reagent diluent as blank. Plates were covered and incubated at RT for 2 hours. After two washes with Elisa Wash Buffer, 100  $\mu$ l/well of detection antibody diluted at 150 ng/mL in reagent diluent were added, and plates were incubated 2 hours at RT. Plates were washed with Elisa Wash Buffer and 100  $\mu$ l/well of



Streptavidin-HRP diluted 1:200 in reagent diluent were added, incubating 1 hour at RT. After washing each plate, 100  $\mu\text{l}$ /well of TMB substrate solution were added and plates were left 20-30 minutes at RT in the dark. The reaction was stopped with 50  $\mu\text{l}$  of H<sub>2</sub>SO<sub>4</sub> 1M and plates were read as exposed for IL-1 $\beta$  Elisa.

#### 4.4.1.3. Luminex<sup>®</sup> assays

Luminex<sup>®</sup> is, like ELISA, a technique that quantifies the concentration of an analyte (usually an antibody or an antigen) in a sample using a standard curve prepared with serial dilutions of one known concentration of the antigen. But, whereas with ELISA only one analyte can be detected in each plate, with Luminex<sup>®</sup> technology multiplex assays can be performed, measuring multiple analytes per well. Luminex<sup>®</sup> is based on polystyrene microspheres which are internally dyed with a unique combination of red and infrared dyes. Beads have in their surface antibodies to capture a specific analyte. Once analytes are bound to the bead, a fluorescent detection antibody binds to the complex. Samples are analyzed in an instrument similar to a flow cytometer, with a fluidics system that creates a line of beads that pass through the detection chamber and can be analyzed one by one. Then, beads are illuminated by two lasers, one to detect the type of bead, and the other to detect the amount of analyte bound to each bead.

To quantify the concentrations of TNF- $\alpha$ , IL-6, IL-8, IL-10, IL-12p40, IL-RA and GM-CSF, Luminex<sup>®</sup> Assays (Invitrogen) were used. Briefly, standards were reconstituted and serial dilutions were prepared (1:2). After mixing well with 30 seconds of vortex and 30 seconds of sonication, beads were diluted in Luminex Buffer (0.625  $\mu\text{l}$  each cytokine beads per well and 50  $\mu\text{l}$  buffer per well). The plate was pre-wet with 200  $\mu\text{l}$  of buffer and then dried by vacuum. After mixing well again with a vortex mixer and a sonicator, 50  $\mu\text{l}$  of beads were added to each well. Plate was washed twice with 200  $\mu\text{l}$  of buffer, applying the vacuum after each wash. In sample wells, 50  $\mu\text{l}$  of buffer were added to dilute the samples (1:1) and then 50  $\mu\text{l}$  of samples and 100  $\mu\text{l}$  of standards were pipetted. Plate was incubated 2 hours at RT in a shaker at 500 rpm. After washing the plate twice, the Biotinylated Detector Antibody was added to each well (2.5  $\mu\text{l}$  of each antibody per well and 50  $\mu\text{l}$  buffer/well) and incubated for 1 hour at RT in a shaker. Then, the plate was washed twice and Streptavidin-PE was added (50  $\mu\text{l}$ /well), incubating the plate for 30 minutes at RT in a shaker. Finally the plate was washed three times and 100  $\mu\text{l}$ /well of buffer were pipetted, leaving the plate in the shaker for 2-3 minutes. Then the plate was ready to be run in a Bio-Plex<sup>®</sup> 200 plate reader (Bio-Rad).

## 4.5. Flow cytometry

### 4.5.1. Cell surface antigens

To confirm macrophage polarization, the expression of surface markers associated with M1 (CD11b) and M2 (CD14 and CD163) was determined by flow cytometry. Macrophages were cultured as previously described with GM-CSF or M-CSF to obtain M1 or M2 macrophages respectively. On day 7, culture plates were centrifuged at 1500 rpm for 2 minutes and media was removed, washing each well once with PBS at 37°C and adding Accutase™ to detach macrophages. Cells were then harvested with PBS at 4°C and put in a 5 mL polystyrene tube. After one wash at 1500 rpm for 5 minutes with PBS, Fc receptors were blocked by adding 10 µl of heat-inactivated mouse serum (Sigma-Aldrich) for 15 minutes at 4°C. Then, cells were stained with the monoclonal antibodies anti-CD11b PE-Cy7 (eBioscience), anti-CD14 APC (eBioscience) and anti-CD163 PE (eBioscience), incubating tubes at 4°C for 30 minutes in the dark. Finally, after washing the tubes with 2 mL of PBS at 4°C, cells were resuspended in 400 µl of Isotone® (Beckman Coulter) and analyzed in a FACSCanto flow cytometer (BD Biosciences). Results were analyzed with the software FlowJo (TreeStar Inc).

### 4.5.2. Caspase-1 activity in macrophages

The intracellular levels of active caspase-1 (p20) were assessed with the Caspase-1 FLICA™ Detection Kit (Immunochemistry) that contains the reagent FAM-YVAD-FMK, a Fluorochrome Inhibitor of Caspases (FLICA) that is fluorescent, cell permeable and non-toxic. Once inside the cell, binds covalently to a reactive cysteine residue that resides on the large subunit of the caspase heterodimer, thereby inhibiting further activity. The fluorescent signal emitted can be analyzed by flow cytometry to assess the number of active enzyme present in the cell.

M1 and M2 macrophages were cultured in 96 well cell culture plates at an initial concentration of  $0.5 \times 10^6$  monocytes/mL. On day 7, plates were centrifuged at 1500 rpm 2 minutes and media was replaced by 100 µl of new cRPMI media. Some macrophages remained unstimulated and the rest were stimulated with four different agents: 200 µg/mL MSU for 1 hour, 100 ng/mL LPS for 1 hour, 5 mM ATP (Invivogen) for 15 minutes or 20 µg/mL nigericin (Invivogen) for 15 minutes. Cultured plates remained at 37°C, 5% CO<sub>2</sub> during incubation times. Once stimulated, 3.3 µl of FLICA 30X were added to each well, except unstained samples, and plates were incubated at 37°C, 5% CO<sub>2</sub> in the dark for one hour, gently shaking the plates every 15 minutes. After washing the plates with 200 µl of Wash Buffer FLICA at 1500 rpm 2 minutes, macrophages were detached as previously described using Accutase™. Cells were harvested and



put in 5 mL polystyrene tubes. Once washed with 1 mL of Wash Buffer FLICA at 1500 rpm 5 minutes, cells were resuspended in 300  $\mu$ l Isotone<sup>®</sup> and analyzed in a FACSCanto flow cytometer. Macrophages were gated on SSC/FSC plot and cells with MSU crystals were gated based on their increase on the SSC scale, as previously described. Mean fluorescent intensity values (MFI) in FITC channel, that corresponds to active caspase-1, were obtained from each sample using FACSDiva Software (BD Biosciences). Baseline levels of active caspase-1 were calculated in M1 and M2 macrophages using this formula:

$$\frac{\text{MFI non stimulated} - \text{MFI unstained}}{\text{MFI unstained}}$$

Changes in caspase-1 activation after challenging with MSU, ATP and nigericine were normalized to non stimulated samples after subtracting the background:

$$\frac{\text{MFI stimulated} - \text{MFI unstained}}{\text{MFI non stimulated} - \text{MFI unstained}}$$

## 4.6. Western Blot

### 4.6.1. Sample preparation

Peripheral blood mononuclear cells from healthy volunteers were separated with the density gradient Polymorphprep<sup>™</sup> (Medica Pacifica Ltd). Easysep<sup>™</sup> Human Monocyte Enrichment kit was then used to isolate CD14<sup>+</sup> monocytes. Cells were cultured in 12 well culture plates (1x10<sup>6</sup> cells/well) at a concentration of 0.5x10<sup>6</sup> cells/mL in cRPMI at 37°C, 5% CO<sub>2</sub>. Monocytes were polarized to M1 or M2 macrophages by adding GM-CSF (1000 I.U./mL) or M-CSF (20 ng/mL) on days 0, 2 and 5. On day 6, media was removed and replaced by 1 mL of Macrophage Culture Medium without FBS after washing each well with HBSS. Macrophages were then stimulated first with MSU (200  $\mu$ g/mL) and after one hour LPS (100 ng/mL) was added. Culture plates remained in the incubator at 37°C, 5% CO<sub>2</sub>. On day 7, after 18 hours of stimulation, plates were centrifuged at 1500 rpm 2 minutes, and supernatants removed and stored at -20°C. Cells were washed once with HBSS (1500 rpm, 5 minutes), adding 500  $\mu$ l of Accutase<sup>™</sup> to detach them from the plate as previously described. Macrophages were harvested and put in a new tube, washing each well with HBSS at 4°C to ensure complete recovery of the cells. Tubes were centrifuged at 1500 rpm 5 minutes, supernatants were removed and tubes were washed again with 2 mL of HBSS.

#### 4.6.1.1. Isolation of cytoplasmic protein

To prepare 500 µl of Lysis Buffer, 455 µl of Reactive A and 40 µl of Reactive B were mixed and before use 5 µl of 1 mM PMSF (phenylmethylsulfonyl fluoride) diluted in ethanol were added.

Reactive A (4°C)	10 mM HEPES pH 7.9, 1.5 mM MgCl <sub>2</sub> , 10 mM KCl, 10 mM NaMoO <sub>4</sub>
Reactive B (-20°C)	proteinase inhibitor cocktail 1X, 20 mM β-glycerophosphate, 2 mM Na <sub>3</sub> VO <sub>4</sub>

Table 4.1. Reactives used for preparation of lysis buffer

After washing the tubes with HBSS, supernatants were aspirated carefully and 40-60 µl of lysis buffer added, depending on pellet's size. Tubes were incubated on ice for 20 minutes, tapping them intermittently to mix. After a quick spin, 2.5 µl of 10% Igepal CA-630 were added. Cells were mixed with vortex. After a quick spin, tubes were placed on ice for 2 minutes and after that, centrifuged at 13000 rpm for 30 seconds at 4°C. Lysates were transferred to 1.5 mL Eppendorf® tubes and stored at -80°C.

#### 4.6.1.2. Protein quantification with Bio-Rad DC™ Protein Assay

The kit is based on the Bradford method, measuring protein by determining the staining of the solution by an acidic dye. Triplicates of samples and duplicates of standards were performed. Bovine serum albumin (BSA) was used as a standard in serial dilutions from 1.6 µg/µl to 0.2 µg/µl.

The amount of working reagent A needed to perform the assay was calculated as:

$$[(\text{number of samples} \times 3) + (\text{number of standards} \times 2) + 2] \times 25 \mu\text{L}$$

To make up working reagent A', 20 µl of reagent S were added to each millilitre of reagent A. In a 96 well plate with round bottom, 5 µl of standards and 5 µl of samples, previously diluted in double distilled water 1:1, were aliquoted. In each well, 25 µl of reactive A' and 200 µl of reactive B were added, mixing well. Plate was incubated at RT for 15 minutes. Absorbances were read in a microplate reader set at 750 nm. Total protein values were calculated using the standard curve. The linear range of the assay for BSA is 1.2 to 10.0 µg/mL.

#### 4.6.2. SDS-PAGE

In 1.5 mL Eppendorf® tubes, 20 µg of protein from each sample were incubated with 4.6 µl of 4X protein loading buffer and 1.8 µl of 10X reducing buffer at 95°C for 6 minutes using the dry heat block with 300 rpm shaking. After a quick spin, tubes were put on ice and were ready for loading. A gel was prepared in an electrophoresis tank with standard MES buffer in the outer chamber and MES buffer with antioxidant in the inner chamber. Samples and ladder were loaded and run at 150 V for 1 hour.

#### 4.6.3. Transferring to PVDF membrane

Transfer buffer (TB) was made on the day with 10X TG stock (3% Tris, 14.4% Glycine), methanol and 10% SDS. Paper filters and PVDF membrane were cut according to the size of the gel. Filters and nylon pads were soaked in TB. Membrane was activated in methanol for 1 minute and soaked in TB. Gels were carefully removed from the tanks and the glass plates. A sandwich was constructed in transfer cassette, keeping everything moist and removing all air bubbles by rolling a pipette over each layer. Gel was placed close to the negative electrode, and the membrane close to the positive electrode. Cassette was inserted into transfer tank and run at 300 mA for 2 hours.

#### 4.6.4. Western Blotting

Membranes were washed twice with TPBS (PBS 1X + 0.1% Tween 20) and blocked with Blocking Buffer (50 mL TPBS + 2.5 g milk powder) for 30 minutes at RT on shaker. Membranes were incubated with primary antibody diluted in blocking buffer overnight at 4°C or for 2 hours at RT. After three washes with TPBS, membranes were incubated with secondary antibody goat anti-rabbit or goat anti-mouse (diluted 1:5000 in blocking buffer) for 1 hour at RT on shaker. Membrane was washed three times with TPBS and two more times with PBS. Finally the membrane was placed in a glass and Pierce ECL Western Blotting substrate was added. After 5 minutes membranes were visualized in a reader and blots were analyzed with the software Photoshop. Membranes were stripped with 10 mL of glycine and 10 mL of Tween 20 at 70°C for 30 minutes and stored at 4°C in PBS and 1% Sodium Azide.

## 4.7. Expression of genes involved in inflammation

### 4.7.1. Preparation of samples

M1 and M2 macrophages were cultured in 12 or 24 well culture plates at an initial concentration of  $0.5 \times 10^6$  cells/mL. On day 6, plates were centrifuged at 1500 rpm for 2 minutes and media was replaced by new cRPMI media. Macrophages were then stimulated with MSU (200  $\mu\text{g/mL}$ ), LPS (100  $\text{ng/mL}$ ) or both. Based on time course experiments performed previously, the stimulation time of 4 hours was chosen as the best to see expression of our mRNAs of interest. After 4 hours of incubation, plates were centrifuged again at 1500 rpm for 2 minutes and supernatants were harvested and stored at  $-20^\circ\text{C}$ . Cells were washed once with PBS at  $37^\circ\text{C}$ , detached with Accutase™ and put into new tubes. After wash each tube with PBS at  $4^\circ\text{C}$  (1500 rpm 5 minutes), cells were transferred into new 1.5 mL RNase-free microtubes and washed twice with cold PBS at 300 g for 10 minutes. Pellets were then ready for RNA extraction.

### 4.7.2. RNA extraction

NucleoSpin® RNA XS kit (Macherey-Nagel), a commercial column-based system specially designed for total RNA isolation from small samples, was used according to the protocol supplied by the manufacturer (Figure 4.7). Briefly, to lyse and homogenize cells, sample pellets were mixed vigorously by vortex with 100  $\mu\text{l}$  Buffer RA1 and 2  $\mu\text{l}$  TCEP. Then 5  $\mu\text{l}$  of Carrier RNA working solution were added, mixing again by vortex. After a quick spin, 100  $\mu\text{l}$  of ethanol 70% were added to each sample pipetting up and down. The mixture was loaded to a NucleoSpin® RNA XS column and centrifuged at 11,000 g for 30 seconds. Columns were placed in a new collection tube and 100  $\mu\text{l}$  of MDB (Membrane Desalting Buffer) were added. Columns were centrifuged again at 11,000 g for 30 seconds. The rDNase Reaction Mixture was prepared by adding 3  $\mu\text{l}$  reconstituted rDNase to 27  $\mu\text{l}$  Reaction Buffer for rDNase, and 25  $\mu\text{l}$  of the mixture were added to each column. After an incubation of 15 minutes at RT, columns were incubated for 2 minutes with 100  $\mu\text{l}$  of Buffer RA2 and centrifuged at 11,000 g for 30 seconds. Then, were put in a new collection tubes and washed with 400  $\mu\text{l}$  of RA3 at 11,000 g for 30 seconds. After changing the collection tube, columns were washed again with 200  $\mu\text{l}$  of Buffer RA3 at 11,000 g for 2 minutes and were placed into nuclease-free 1.5 mL collection tubes. Samples were eluted in RNase-free water, 30  $\mu\text{l}$  for M1 and 16  $\mu\text{l}$  for M2, centrifuged at 11,000 g for 30 seconds and put immediately on ice.














1	Supply sample		Use up to 10 <sup>5</sup> cultured cells or 5 mg tissue samples
2	Lyse and homogenize cells		100 µL RA1 2 µL TCEP Mix
3	Add Carrier RNA		5 µL Carrier RNA working solution Mix
4	Filtrate lysate (optional)	 	11,000 x g, 30 s
5	Adjust RNA binding condition		100 µL 70% ethanol Mix
6	Bind RNA	 	Load lysate 11,000 x g, 30 s
7	Desalt silica membrane	 	100 µL MDB 11,000 x g, 30 s
8	Digest DNA		25 µL DNase reaction mixture RT, 15 min
9	Wash and dry silica membrane	 	1 <sup>st</sup> wash 100 µL RA2 RT, 2 min 11,000 x g, 30 s 2 <sup>nd</sup> wash 400 µL RA3 11,000 x g, 30 s 3 <sup>rd</sup> wash 200 µL RA3 11,000 x g, 2 min
10	Elute highly pure RNA	 	10 µL RNase-free H <sub>2</sub> O 11,000 x g, 30 s

Figure 4.7. Protocol for RNA extraction using the NucleoSpin® RNA XS kit

### 4.7.3. Quantification of RNA

Extracted RNA was quantified with the NanoVue Plus spectrophotometer (GE Healthcare Life Sciences) at 260 nm with a path length of 0.5 mm, and after that, samples were stored at -80°C. Table 3.2 shows RNA concentration of each sample.

### 4.7.4. Assessment of RNA quality

RNA quality was determined by analysis of the A260/A280 and A260/230 ratios obtained with the NanoVue Plus spectrophotometer. The first ratio informs about protein contamination and should be between 1.8 and 2.2, the lower the ratio, the more contaminated the sample is. The second decreases when the sample contains other contaminants such as phenolate ions, thiocyanates and other organic compounds that absorb at 230 nm, being the desirable value 2.0-2.2. As showed in Table 4.2, samples with MSU had higher absorbances at 260 nm with low purity ratios, probably due to the presence of this salt. As concentration of RNA could be overestimated, in these samples the maximum amount of RNA (12 µl) during reverse transcriptase reaction was employed.

### 4.7.5. First strand cDNA synthesis

The reactions of reverse transcriptase and the real time PCR were performed "uncoupled", that means, using two different tubes. First, the reverse transcriptase synthesized cDNA in a first tube, under optimal conditions using oligo-dT primers. Then, an aliquot of the RT reaction was transferred to a 96 well plate containing the thermostable DNA polymerase, DNA polymerase buffer and PCR primers, being the conditions of the reaction optimal for the DNA polymerase. This two enzyme protocol has an increase flexibility, because the optimal conditions of both reactions can be settled independently.

The protocol used for the reverse transcription is the following: RNA samples and reagents of the Transcriptor Reverse Transcriptase kit (Roche) were thawed and put on ice. Reactions were prepared in a laminar flow hood to avoid DNA contamination. The following components were pipetted into a thin-walled RNase and DNase-free reaction tube: molecular biology water up to 13 µl of total reaction, 1 µl of Oligo (dT) primer 100 µM and 1 µg RNA sample (12 µl in samples with low concentrations or samples with MSU). Tubes were incubated at 65°C for 10 minutes and then placed immediately on ice. Reverse transcriptase mix was prepared with the following reagents per sample: 4 µl Transcriptor RT Reaction Buffer, 0.5 µl Protector RNase inhibitor (40 U/µl), 2.5 µl dNTP-mix 10 mM and 0.5 µl Transcriptor Reverse Transcriptase. 7 µl of the mix were pipetted into each tube and after mixing well by vortex and a quick spin, tubes were incubated for 30 minutes at 55°C and the reaction was stopped at 85°C for 5

minutes. Tubes were put on ice. Samples were diluted 1:2 with molecular biology water, aliquoted (7.5 µl/tube) into PCR tubes and stored at -20°C.

<i>Sample name</i>	<i>Macrophage subset</i>	<i>Stimulation</i>	<i>RNA (µg/mL)</i>	<i>A260/A280</i>	<i>A260/A230</i>
S-40	M1	medium	71	NA	NA
S-40	M1	LPS	88	NA	NA
S-40	M1	MSU	66	NA	NA
S-40	M1	MSU+LPS	50	NA	NA
S-40	M2	medium	27.4	NA	NA
S-40	M2	LPS	43.8	NA	NA
S-40	M2	MSU	23.9	NA	NA
S-40	M2	MSU+LPS	14.1	NA	NA
S-41	M1	medium	122.1	1.779	2.096
S-41	M1	LPS	96.4	1.785	1.975
S-41	M1	MSU	151.2	0.737	0.629
S-41	M1	MSU+LPS	128.4	0.875	0.819
S-41	M2	medium	91.6	1.832	1.422
S-41	M2	LPS	127.2	1.817	1.767
S-41	M2	MSU	124.8	0.485	0.369
S-41	M2	MSU+LPS	112.8	0.558	0.493
S-42	M1	medium	51.6	1.792	0.908
S-42	M1	LPS	77.2	1.787	1.771
S-42	M1	MSU	66	0.829	0.317
S-42	M1	MSU+LPS	80.8	0.745	0.608
S-42	M2	medium	104	1.769	1.757
S-42	M2	LPS	97.6	1.768	1.968
S-42	M2	MSU	113.6	0.529	0.457
S-42	M2	MSU+LPS	32.4	0.368	0.303
S-43	M1	medium	174.4	1.832	2.106
S-43	M2	medium	81.2	1.829	2.115
S-44	M1	medium	99.6	1.818	1.649
S-43	M2	medium	74	1.832	1.341

Table 4.2. Quantification and purity of RNA assessed by spectrophotometry. (NA) not available

#### 4.7.6. Real Time PCR

The effect of MSU on macrophage expression of genes *IL-10*, *IL-1 $\beta$* , *casp-1* and *NLRP3* was assessed by qRT-PCR (quantitative real time polymerase chain reaction), taking as a reference gene *GAPD*. Reactions were prepared in a laminar flow hood in 96 well plates, with a total volume per reaction of 10  $\mu$ l, and run in a LightCycler<sup>®</sup>480 (Roche). Triplicates of each condition as well as a no template control and a mixture sample (calibrator) were run in each plate.

##### 4.7.6.1. Taqman probes for *IL-1 $\beta$* and *caspase-1* RT-PCR

RealTime ready assays (Roche) were used for *IL-1 $\beta$*  (ID 100950) and *caspase-1* (ID 100201) quantification. These assays contain primers and hydrolysis probes, labelled at the 5'-end with fluorescein (FAM) and at the 3'-end with a dark quencher dye. When the probe is intact, the quencher is close enough to the dye to suppress its fluorescence. During the PCR the probe binds to the target sequence and the 5' nuclease activity of the polymerase cleaves the hydrolysis probe. Then the reporter dye is no longer inhibited by the quencher and its fluorescence can be detected.

PCR reactions with the following reagents per reaction: 2  $\mu$ l of cDNA, 0.5  $\mu$ l of the solution primers+probes, 5  $\mu$ l of master mix (Roche) and 2.5  $\mu$ l of RNase-free distilled water per reaction. The programs and cycle conditions set for the reaction in the LightCycler<sup>®</sup>480 are listed on Table 4.3.

<i>Program name</i>	<i>Cycles</i>	<i>Analysis mode</i>	<i>Target</i> (°C)	<i>Acquisition</i> <i>mode</i>	<i>Hold</i> (hh:mm:ss)	<i>Ramp Rate</i> (°C/s)
Pre incubation	1	none	95	none	00:10:00	4.40
Amplification	50	quantification	95	none	00:00:10	4.40
			60	none	00:00:30	2.20
			72	single	00:00:01	4.40
Cooling	1	none	40	none	00:01:01	2.20

Table 4.3. Cycle conditions of RT-PCR for *IL-1 $\beta$*  and *caspase-1* using Taqman<sup>®</sup> probes

##### 4.7.6.2. RT-PCR with SYBR Green for *IL-10* and *NLRP3* expression

SYBR Green, a dye that binds to all double-stranded DNA molecules, together with specific primers (Table 4.4), were used for *IL-10* and *NLRP3* gene expression. Primers were gently provided by Dr. Rosa Faner.



	Sequence (5'→3')	Length	T <sub>m</sub>	GC%
<i>IL-10</i> forward primer	GTGATGCCCAAGCTGAGA	19	53.87	57.89%
<i>IL-10</i> reverse primer	CACGGCCTTGCTCTGTTTT	20	53.87	50.00%
<i>NLRP3</i> forward primer	GCGATCAACAGGAGAGACCTTTA	23	54.23	47.83%
<i>NLRP3</i> reverse primer	GCTGTCTTCTGGCATATCACA	22	54.52	50.00

Table 4.4. Primers for *IL-10* and *NLRP3* gene expression. Primers were used with SYBR Green fluorescent dye

For each RT-PCR reaction the following components were added: 2 µl cDNA, 0.5 µl of each primer (forward and reverse), 5 µl master mix SYBR Green (Roche) and 2 µl RNA-free distilled water. The programs used in the LightCycler®480 and cycle conditions are listed in Table 4.5.

Program name	Cycles	Analysis mode	Target (°C)	Acquisition mode	Hold (hh:mm:ss)	Ramp Rate (°C/s)	Acquisitions (per °C)
Pre incubation	1	none	95	none	00:10:00	4.40	
Amplification	50	quantification	95	none	00:00:05	4.40	
			62	none	00:00:05	2.20	
			72	single	00:00:15	4.40	
Melting curve	1	melting curve	95	none	00:00:05	4.40	
			65	none	00:00:15	2.20	
			95	continuous		0.11	5
Cooling	1	none	40	none	00:01:01	2.20	

Table 4.5. Cycle conditions of RT-PCR for *IL10* and *NLRP3* expression with SYBR Green

#### 4.7.6.3. Universal Probe Library for *GAPD* expression

For relative quantification, the *GAPD* gene was used as a reference gene. Its expression was measured with the Universal ProbeLibrary Human *GAPD* Gene kit (Roche). This assay is based in an hydrolisis probe too, but this time the 5'-end is labelled with LightCycler® Yellow 555 that can be detected with longer-wavelength emission filter (usually 560 nm or 568 nm).

For each reaction, the following reagents were added: 2 µl DNA, 0.2 µl primers, 0.2 µl probe, 5 µl master mix (Roche), 2.6 µl RNA-free distilled water, up to a total volume of 10 µl. Programs and cycle conditions of the LightCycler®480 are listed on Table 4.6.

Program name	Cycles	Analysis mode	Target (°C)	Acquisition mode	Hold (hh:mm:ss)	Ramp Rate (°C/s)
Pre incubation	1	none	95	none	00:07:00	4.80
Amplification	45	quantification	95	none	00:00:10	4.80
			60	none	00:00:30	2.50
			72	single	00:00:01	4.80
Cooling	1	none	40	none	00:00:10	2

Table 4.6. Cycle conditions of RT-PCR for GAPD using the UPL kit

#### 4.7.6.4. Analysis of results

Cp values were obtained from each sample. Quantification relative to the housekeeping gene *GAPD* was calculated using the formula:

$$2^{-(Cp \text{ target gene} - Cp \text{ reference gene})}$$

Being the Cp values inversely proportional to the initial amount of cDNA, that means that the lower the Cp value is, the higher the initial concentration of cDNA molecules.

#### 4.7.6.5. Agarose gel electrophoresis

To confirm specificity of the amplification, RT-PCR products were run in an agarose gel (Figure 4.8). Briefly, a 2% agarose gel was prepared with 100 mL Tris-borate-EDTA (TBE) buffer, 2gr of agarose and 5 µl SYBR® Safe (Life Technologies). 3 µl of each sample with 1 µl of Gel Loading Solution type I (Sigma-Aldrich) were loaded, as well as a molecular-weight size marker (Invitrogen). Samples were then run at 200 V. Visualization of cDNA fragments after electrophoresis was performed under ultraviolet light in a BioDoc-it® Imaging System (UVP).

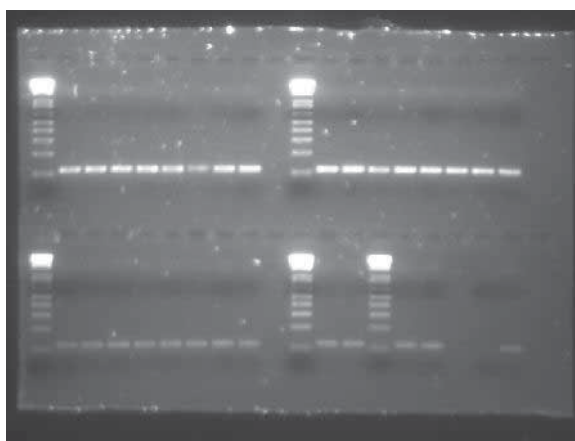


Figure 4.8. Gel electrophoresis of the amplification product of the *GAPD* gene after real time PCR.

## 4.8. Patients and controls

Patients with gout were recruited from the Emergency Department of Hospital Clínic Barcelona and the Rheumatology Department of Hospital Sant Pau in Barcelona, Spain. Patients were diagnosed by a clinical rheumatologist, according to the criteria set by the American Rheumatism Association<sup>[278]</sup>. A control group of healthy donors was recruited among workers of Hospital Clínic Barcelona. The study protocol was approved by the ethics committee of both hospitals and informed consent was obtained from each participant. Patients were classified into two groups: asymptomatic gout, with no clinical evidence of arthritis in the moment of the interview, and patients with an acute flare of arthritis. Patients and controls were interviewed with a protocol of questions regarding demographic data and, in the case of gout patients, with questions about articular disease, such as age of diagnosis of gout and treatment. After physical examination, number of tender and swollen joints were recorded. Seventeen patients with gout entered the study, 4 of them during an acute flare of gout. Table 3.7 shows demographic characteristics of these three groups.

### 4.8.1. Determination of uric acid, creatinine and CRP in sera

Analysis of sera from patients and controls was performed in the Biomedical Diagnosis Center (CORE laboratory) in the Hospital Clínic Barcelona. Method of quantification as well as normal ranges are listed in Table 4.8.

	<i>Method</i>	<i>Units</i>	<i>Normal range</i>
<b>Creatinine</b>	molecular absorption spectrometry	mg/dL	1.9-7.4
<b>Uric acid</b>	molecular absorption spectrometry	mg/dL	0.3-1.3
<b>CRP</b>	immunospectrometry	mg/dL	< 0.5 mg/dL

Table 4.8. Methods of quantification and normal ranges of uric acid, creatinine and CRP in sera

## 4.9. Inflammasome activity in monocytes of patients with gout

The purpose of these experiments was to compare the reactivity of the inflammasome to MSU crystals and other inflammasome activators between patients with gout and healthy controls. As the final product of inflammasome activation is cleavage and activation of caspase-1, intracellular levels of active caspase-1 were quantified as an approximation of inflammasome activity.

### 4.9.1. Selection of samples

To minimize the effect that an ongoing inflammation or the use of anti-inflammatory drugs could exert over the results, we selected asymptomatic patients with gout and patients with any painful or swollen joint on examination or those treated with non-steroidal anti-inflammatory analgesics (NSAIDs), aspirin or colchicine were excluded. For comparison purposes, we selected as controls healthy men over 40 years old, free of inflammatory diseases and without any anti-inflammatory treatment. Seven volunteers were recruited in each group.

### 4.9.2. Quantification of active caspase-1 in monocytes

The same reagent used to assess the activity of caspase-1 in macrophages (Caspase-1 FLICA Detection Kit) was employed, but this time to study peripheral blood monocytes, as these cells have been involved in gout pathogenesis and can be easily isolated from peripheral blood.

Twenty millilitres of blood into heparinised tubes were obtained by vein puncture. Mononuclear peripheral cells were isolated by a density gradient with Ficoll-Paque PLUS as previously described, adjusted to  $1 \times 10^6$  cells/mL in cRPMI and placed in 5 mL polystyrene tubes (100,000 cells/tube). Duplicates of each condition, as well as non-stained and non-stimulated controls, were performed. Cells were stimulated with MSU (200  $\mu\text{g}/\text{mL}$  for 1 hour), ATP (5 nM for 15 minutes) or nigericin (20  $\mu\text{g}/\text{mL}$  for 15 minutes) at 37°C, 5% CO<sub>2</sub>, following intracellular staining with 3.3  $\mu\text{l}$  of FLICA 30X for 1 hour at 37°C, 5% CO<sub>2</sub> in the dark. After two washes with Wash Buffer FLICA (1500 rpm, 5 minutes), cells were resuspended in 300  $\mu\text{l}$  of Wash Buffer FLICA and analyzed in a FACSCanto flow cytometer. The population of monocytes was gated in the FSC/SSC dot plot. Voltage of the 488 nm laser was adjusted with the unstained sample to obtain a mean intensity of FITC signal of  $10^2$ . Mean value of FITC signal, indicative of intracellular activated caspase-1, was obtained from each sample using the software FACSDiva. Baseline levels of active caspase-1 as well as the effect of stimulation on caspase-1 activation were analyzed as exposed previously for macrophages in section 5.2.

## 4.10. Monocyte subpopulations in patients with gout

Monocytes in peripheral blood were analyzed by flow cytometry according to their expression of CD14 and CD16, identifying three different subpopulations: classical ( $CD4^{++} CD16^{-}$ ), intermediate ( $CD14^{++} CD16^{+}$ ) and non-classical ( $CD14^{+} CD16^{++}$ ). We used the protocol proposed by Heimbeck *et al.* for whole blood staining, as the avoidance of density-gradient isolation minimizes variability. Percentages of each subpopulation were compared between asymptomatic patients, patients during an acute flare of arthritis and healthy controls.

### 4.10.1. Selection of samples

Patients with gout were classified into 2 groups: asymptomatic patients (n= 13) or patients with an acute flare (n=4). As controls, we selected men or women of any age, free of inflammatory diseases and anti-inflammatory treatment (n=19).

### 4.10.2. Assessment of monocyte subpopulations in peripheral blood

Ten millilitres of venous blood were obtained in tubes with EDTA by venipuncture. Blood was aliquoted in 5 mL polystyrene tubes, 50 $\mu$ l/tube. Cells were stained with anti-CD45 PE-Cy7 (Beckman Coulter), anti-HLA DR FITC (Becton Dickinson), anti-CD16 AlexaFluor<sup>®</sup>647 (BD Pharmigen) and anti-CD14 PE (Miltenyi Biotec) for 15 minutes at RT in the dark. One tube remained unstained as a control and another was stained with all the antibodies except anti-CD16. Lysis of erythrocytes was performed adding 2 mL of lysing solution (BD Biosciences) for 15 minutes at RT. Tubes were centrifuged at 1500 rpm 5 minutes and then washed with 2 mL of PBS at 4°C (1500 rpm 5 minutes). Cells were analyzed in a FACSCanto flow cytometer and the software FACSDiva.

To analyze the subsets of monocytes, the gating protocol of Heimbeck *et al.* was used (Figure 4.9) because this approximation minimizes contamination of granulocytes and NK cells as it is performed with whole blood, avoiding alteration of the results from manipulation. First, monocytes were gated from hematopoietic cells were gated based on their CD45 positivity and SSC values and then monocytes were gated as HLA-DR<sup>+</sup> cells. One fluorescent minus one (FMO) control tube, stained with all the antibodies except anti-CD16, was used to establish the borderline between CD16<sup>+</sup> and CD16<sup>-</sup> monocytes. Percentages from total monocytes of the three subpopulations ( $CD14^{++}CD16^{-}$ ,  $CD14^{++}CD16^{+}$  and  $CD14^{+}CD16^{++}$ ) were then obtained from each participant and compared between groups.

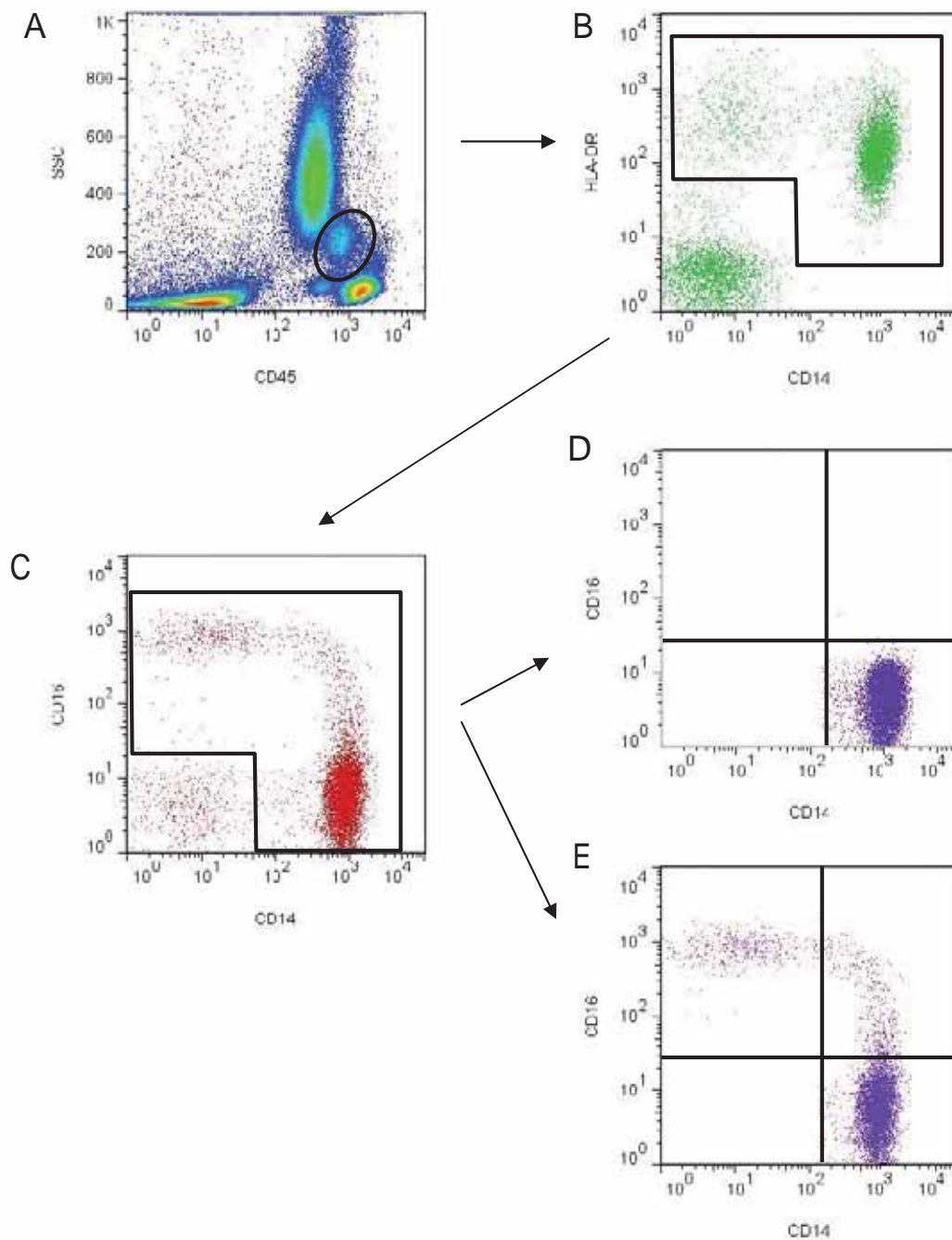


**Figure 4.9. Analysis of monocyte subpopulations by flow cytometry.** Peripheral blood was stained with monoclonal antibodies against CD45, HLA-DR, CD14 and CD16 and samples were analyzed in a flow cytometer. First, population of monocytes was identified based on their expression of CD45 and SSC values (A). Some lymphocytes were gated too, as intermediate monocytes are small and tend to localize in the lymphocyte area. Then, HLA-DR-positive cells were gated (B) in order to avoid contamination with NK cells, that are also CD16<sup>+</sup>. These monocytes were displayed based on their expression of CD16 and CD14 (C). Double negative cells were excluded and the remaining cells were considered total monocytes. An FMO control without CD16 staining was used to set CD16 positivity, as showed in (D). Finally, monocytes were classified according CD14 and CD16 positivity (E).

## 4.11. Analysis of *NLRP3* gene in patients with gout

### 4.11.1. Sample preparation

Venous blood was obtained in EDTA tubes by venipuncture from all patients with gout (n=17). Genomic DNA was extracted using the Roche MagNAPure Compact (Roche Diagnostics, Indianapolis, IN) and adjusted to a final concentration of 50 ng/mL.

### 4.11.2. Genomic DNA amplification

To avoid DNA contamination PCR reactions were prepared in a laminar flow hood. As most of gain-of-function mutations associated with autoinflammatory diseases in *NLRP3* are located in exon 3, this fragment was amplified using the primers listed in Table 4.9 and the Expand High Fidelity PCR System kit (Roche). Briefly, each reaction contained the following reagents: primers (1 μM), dNTPs (200 μM), Taq polymerase (1 U.I.) and PCR Buffer (1X) with  $MgCl_2$ . PCR conditions were as follows: initial denaturation at 95 °C for 5 minutes followed by 10 cycles of 95°C for 30 seconds, touchdown annealing (1°C decrease per cycle) between 65 °C and 55 °C for 30 seconds and extension at 72 °C for 1 minute. For the remaining 25 cycles, we used an annealing temperature of 55 °C and finished with a final extension cycle at 72 °C for 7 min. The specificity of the reaction was then assessed by electrophoresis of the PCR product in an agarose gel.

<i>Primer</i>	<i>Sequence</i>
Exon 3 forward	5'-GTTACCACTCGCTTCCGATG-3'
Exon 3 reverse	5'-GCTGTGGCAACAGTATTTGG-3'

Table 4.9. Primers for exon 3 amplification

### 4.11.3. PCR sequencing reaction

The product of amplification was purified with ExoSAP-IT for PCR Product Cleanup (Affymetrix), according to manufacturer. Briefly, 2.5 μl of amplification were pipetted into a PCR tube together with 1 μl ExoSAP reagent. Samples were then incubated at 37°C for 15 minutes, followed by a 15 minute incubation period at 80°C to inactivate the enzymes.

Bidirectional fluorescence sequencing was performed using BigDye Terminator version 3.1 Cycle Sequencing kit (Applied Biosystems). For each sample amplification, four different sequencing reactions were performed to reach all exon 3 (Table 4.10). One batch of the master mix with 0.5 μl BigDye Terminator, 0.75 μl Sequencing Buffer, 4.25 μl of water per sample was prepared and 5.5 μl were added to each tube containing 3.5 μl of amplification product



previously purified. Finally, 1  $\mu$ l of primer was pipetted, reaching a final volume of 10  $\mu$ l per reaction. Conditions of the PCR were: initial denaturation at 95 °C for one minute followed by 30 cycles of 96°C for 10 seconds, 50 °C for 5 seconds and extension at 60 °C for 4 minutes. Sequencing was performed on a 3730XL DNA Analyzer (Applied Biosystems).

<i>Primer</i>	<i>Sequence</i>
CIAS 3-A-3'	5'-CCATCCACAAGATCGTGAGA-3'
CIAS 3-B-5'	5'-GTCGGGGACACTCTACCAAG-3'
CIAS 3-NGB-F	5'-CATGTGGAGATCCTGGGTTT-3'
CIAS 3-S2	5'-GGGTATTTGATTTTGTGT-3'

Table 4.10. Primers for exon 3 sequencing

#### 4.11.4. Analysis of results

Gene sequences obtained with the software Chromas Lite 2.1.1 (Technelysium Pty Ltd) were first read manually and compared to NLRP3 wild type sequence (GeneBank AY051114). Then, were analyzed with the sequence alignment program ClustalW2. As control population, the Iberian samples from 1,000 Genome Project (n=14) were used. Frequencies of each polymorphism were compared between gout patients and controls using Fisher's exact test with the software GraphPad Prism®.

#### 4.12. Statistical analysis

Statistical analysis was performed with Prism 5 (GraphPad Software). Variables are described through this thesis as mean +/- standard error or the mean (SEM). Normality of variables was assessed by Shapiro-Wilk or Kolmogorov-Smirnov tests. For comparison between two groups, two-tailed Student t-test or Mann-Whitney test were applied depending on normality of the distribution of the variables. For paired observations, we used paired t-test or the non-parametric Willcoxon matched pairs test. We compared three or more groups with one-way analysis of variance (ANOVA). The post Hoc tests Dunnett's T3 test or Bonferroni's test were chosen depending on homogeneity of variances. Correlation analysis was performed with Spearman or Pearson's tests. Minor allele frequencies of *NLRP3* polymorphism were compared with Fisher's test.



# 5.

**Role of M2 macrophages in  
early stages of gout flares**



Macrophages are cells of the mononuclear phagocyte system that reside in every tissue of the body and, together with its phagocytic function, can also have both inflammatory and anti-inflammatory functions depending on the environment and the stimuli they receive. Because of this dual role, these cells have been involved in both initiation and resolution of gout flares. Resident macrophages in the peritonitis mice model initiate the inflammatory response to MSU crystals and their depletion abolishes the production of inflammatory cytokines and neutrophil infiltration<sup>[259]</sup>. Regarding gout resolution, Landis *et al.* demonstrated that maturation of monocytes to macrophages switches their response to MSU crystals towards an anti-inflammatory function that could dampen the inflammatory process and explain the self-remitting course of gout<sup>[279]</sup>.

Different macrophage phenotypes or polarization states can be obtained *in vitro* depending on the environment where cells undergo maturation. In the presence of IFN- $\gamma$ , TNF- $\alpha$  or GM-CSF, macrophages acquire an inflammatory phenotype and are referred as M1 macrophages. By contrast, M2 macrophages, polarized with IL -4, IL -10 or M-CSF exhibit anti-inflammatory functions<sup>[196]</sup>.

Our hypothesis is that changes in polarization state of macrophages are involved in initiation of gout flares. The presence and concentration of cytokines in synovial fluid, that changes through the course of the arthritis flare<sup>[280]</sup>, could modulate macrophage phenotype towards inflammatory or anti-inflammatory roles. In this chapter, we focused our attention in the initiation of gout flares taking as starting point M2 macrophages polarized with M-CSF, which are considered by some authors to represent the population of tissue resident macrophages in the steady state<sup>[199]</sup>. The first part of this chapter describes the experiments performed to characterize M1 and M2 macrophages, ensuring the proper polarization of macrophages. In the second part we investigated the effect of MSU crystals on M2 macrophages and how hyperuricemia may affect this response. Finally, as MSU crystals induce IL-1 $\beta$  production through NLRP3 inflammasome activation<sup>[98]</sup>, in the last section we analyzed in more detail inflammasome activation in M1 and M2 macrophages and the effect of MSU crystals on the inflammasome of M2 macrophages.

## 5.1. Characterization of M1 and M2 macrophages

Although one could roughly differentiate between M1 and M2 macrophages by optical microscope, it seemed conceivable to spend time and efforts making sure that macrophages were properly polarized, as these cells are the cornerstone of the experiments in this chapter. Thus, different laboratory techniques such as flow cytometry, ELISA, Luminex® and real time PCR (RT-PCR) were performed to confirm the state of macrophage polarization. This section describes the results obtained, providing at the same time an overview of the main differences between M1 and M2 phenotypes.

As described previously in methods section, macrophages were derived from peripheral blood monocytes of healthy donors. Briefly, peripheral blood mononuclear cells were separated from whole blood by centrifugation with a density gradient. Monocytes were then isolated by negative selection with magnetic beads and cultured with GM-CSF (1000 I.U./mL) or M-CSF (20 ng/mL) to obtain M1 or M2 macrophages respectively. After one week of incubation at 37°C and 5% CO<sub>2</sub>, cell morphology, surface antigens, phagocytic activity, response to LPS and IL-10 gene expression were assessed to confirm polarization towards M1 and M2 phenotypes.

### 5.1.1. Differences in macrophage morphology

After 6 days of incubation, cell cultures were examined in an inverted optical microscope (Figure 5.1 A and B) and, as expected, M1 and M2 macrophages differed in their morphology. Whereas M1 macrophages were rounded and bigger than the M2, with the typical “fried egg” morphology described by other authors<sup>[201,203]</sup>, M2 macrophages had a spindle-like shape.

Size and internal complexity were then assessed by flow cytometry, as laser light scattering depends on physical properties of the cell, namely its size and internal complexity. Forward-scattered light (FSC), detected just off the axis of the incident laser beam, is proportional to cell-surface area or size. Side-scattered light (SSC) is collected at 90 degrees to the laser beam, being proportional to cell granularity or internal complexity. Figure 5.1 C-D shows results obtained from 5 independent experiments. Higher values of FSC were observed in M1 macrophages (mean +/- SEM: M1 271.4 +/- 5.57, M2 228 +/- 10.17, p=0.0087), confirming our previous observations with the microscope. On the other hand, M1 macrophages exhibited higher SCC values, although these differences were not statistically significant (M1 39.16 +/- 1.44, M2 34.26 +/- 2.56, p=0.1377).

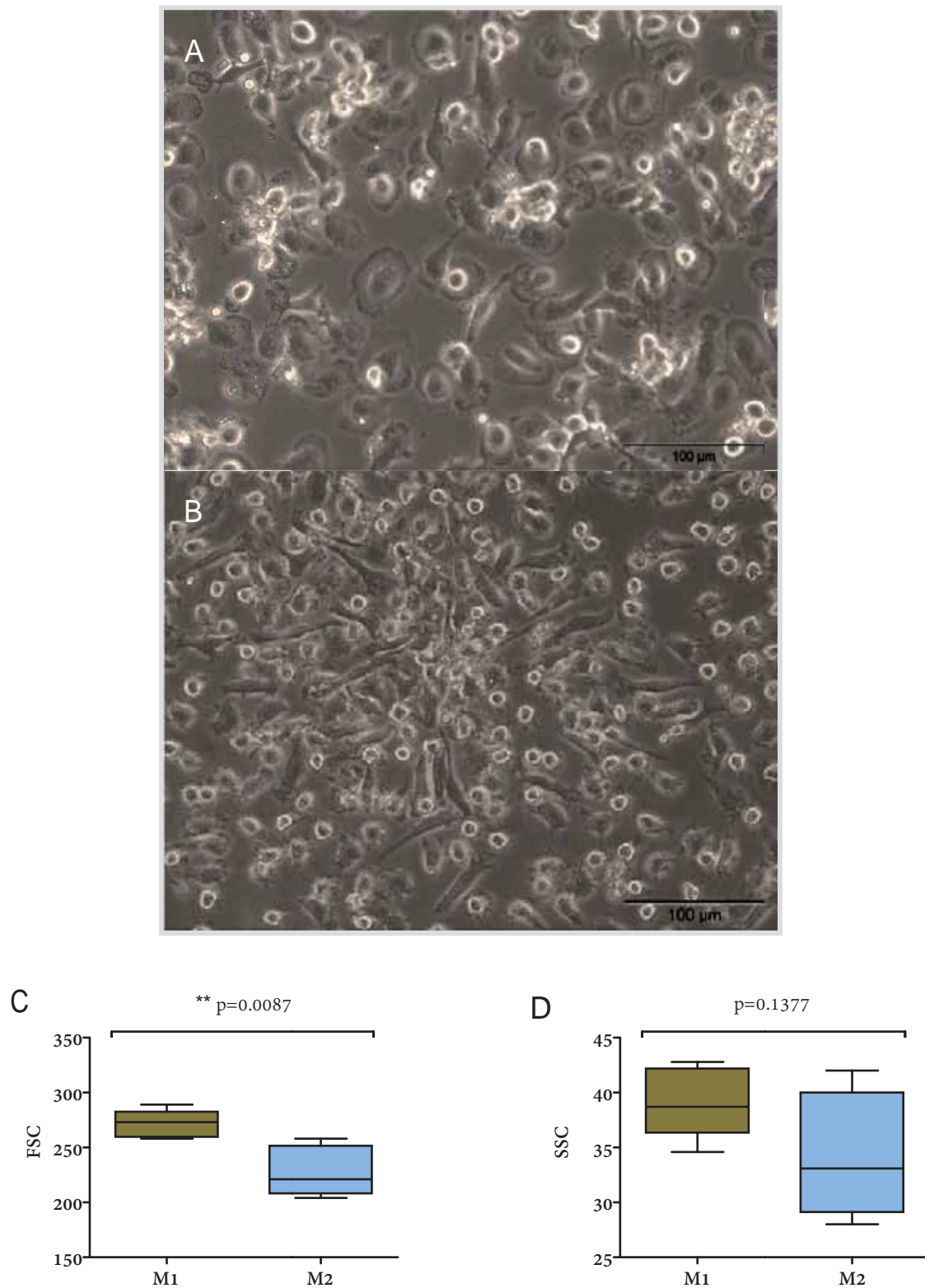


**Figure 5.1. Assessment of cell morphology in M1 and M2 macrophages.** Observed in an inverted optical microscope, M1 macrophages (A) had the typical “fried egg” morphology and M2 macrophages (B) had a stretched shape. Size and internal granularity were then analyzed by flow cytometry, comparing FSC (C) and SSC values (D). No differences were observed in internal complexity or SSC signal whereas M1 macrophages exhibit higher FSC values suggestive of higher cellular size. Graph boxes represent median with first and third quartiles with whiskers representing 10 and 90 percentiles. p values obtained from 5 different experiments by Student's t-test.

### 5.1.2. Expression of cell surface antigens in polarized macrophages

Cell surface antigens are molecules within plasma membrane that, as cell markers, help identify and classify cells due to the fact that, for one type of cell, a unique combination of this antigens is present in its surface. To differentiate between both macrophage subtypes, fluorescent antibodies against antigens associated with M1 (CD11b) and M2 phenotypes (CD14 and CD163) were used<sup>[203]</sup>. Fluorescent signal was detected by flow cytometry and mean fluorescent intensity (MFI) values of each antigen were analyzed and compared, as shown in Figure 5.2 .

Our results were consistent with previous literature: CD11b expression was higher in M1 macrophages and CD14 in M2, whereas the antigen CD163 was only expressed in M2 macrophages.

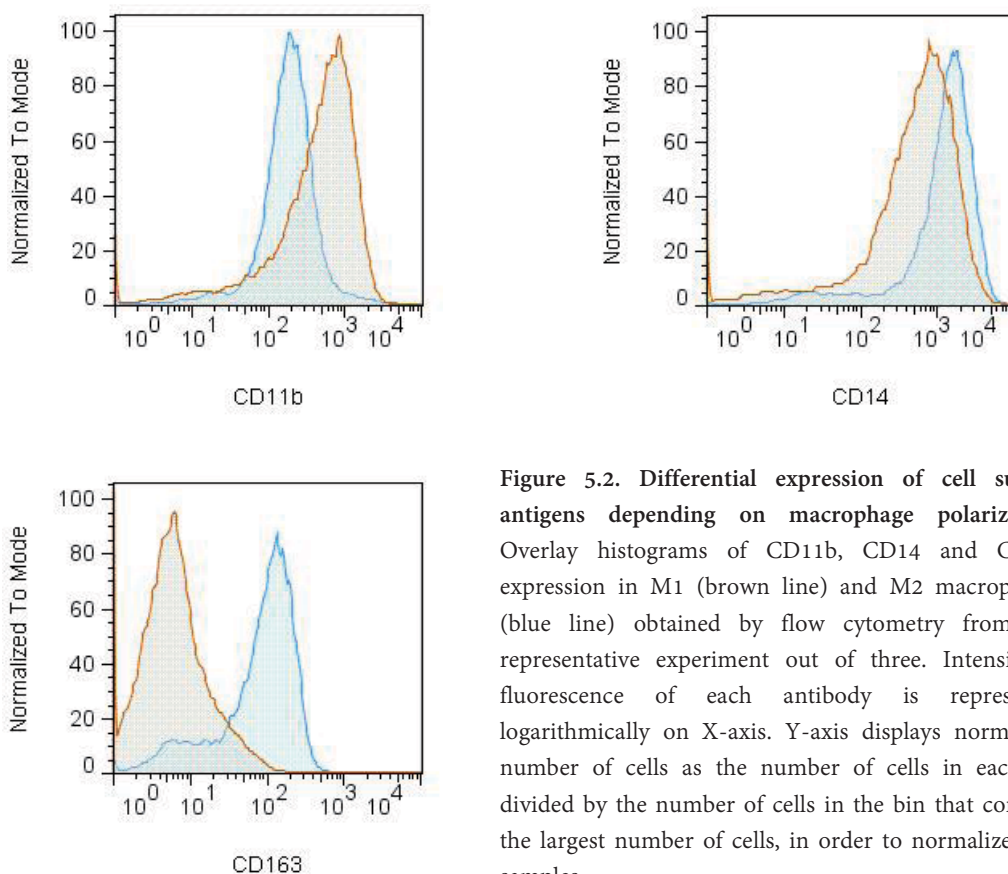


**Figure 5.2. Differential expression of cell surface antigens depending on macrophage polarization.** Overlay histograms of CD11b, CD14 and CD163 expression in M1 (brown line) and M2 macrophages (blue line) obtained by flow cytometry from one representative experiment out of three. Intensity of fluorescence of each antibody is represented logarithmically on X-axis. Y-axis displays normalized number of cells as the number of cells in each bin divided by the number of cells in the bin that contains the largest number of cells, in order to normalize both samples.

### 5.1.3. Phagocytic capacity of M1 and M2 macrophages

Macrophages are phagocytic cells that engulf and digest cellular debris and pathogens, maintaining tissue homeostasis. As M1 and M2 macrophages have different functions, they also differ in their phagocytic capacity<sup>[203]</sup>.

In our experiments, phagocytic activity of cultured macrophages was quantified using two different approaches, both involving flow cytometry. In the first one, phagocytosis was analyzed using fluorescent polystyrene beads (FluoSpheres® fluorescent microspheres) that can be detected by flow cytometry. We next assessed MSU crystal phagocytosis as cells that phagocyte crystals increase their SSC signal<sup>[271]</sup>, as previously described in methods chapter .

#### 5.1.3.1. Phagocytosis of fluorescent beads

Macrophages were cultured for 1 hour with fluorescent beads. After washing several times to avoid binding of beads to cell surface, samples were analyzed in a FACSCalibur flow cytometer. Percentage of fluorescent cells and MFI values from beads were obtained for each sample. Figure 5.3 presents the results from 2 independent experiments from different macrophage cultures.

M2 macrophages not only demonstrated a higher phagocytic capacity in terms of higher percentage of cells showing fluorescence (mean +/- SEM: M1 58.25 +/- 1.25, M2 96.4 +/- 0.60,  $p=0.0013$ ), but also higher MFI values (M1 768 +/- 62, M2 2239 +/- 747,  $p=0.1887$ ), suggesting that M2 macrophages can uptake more beads per cell.

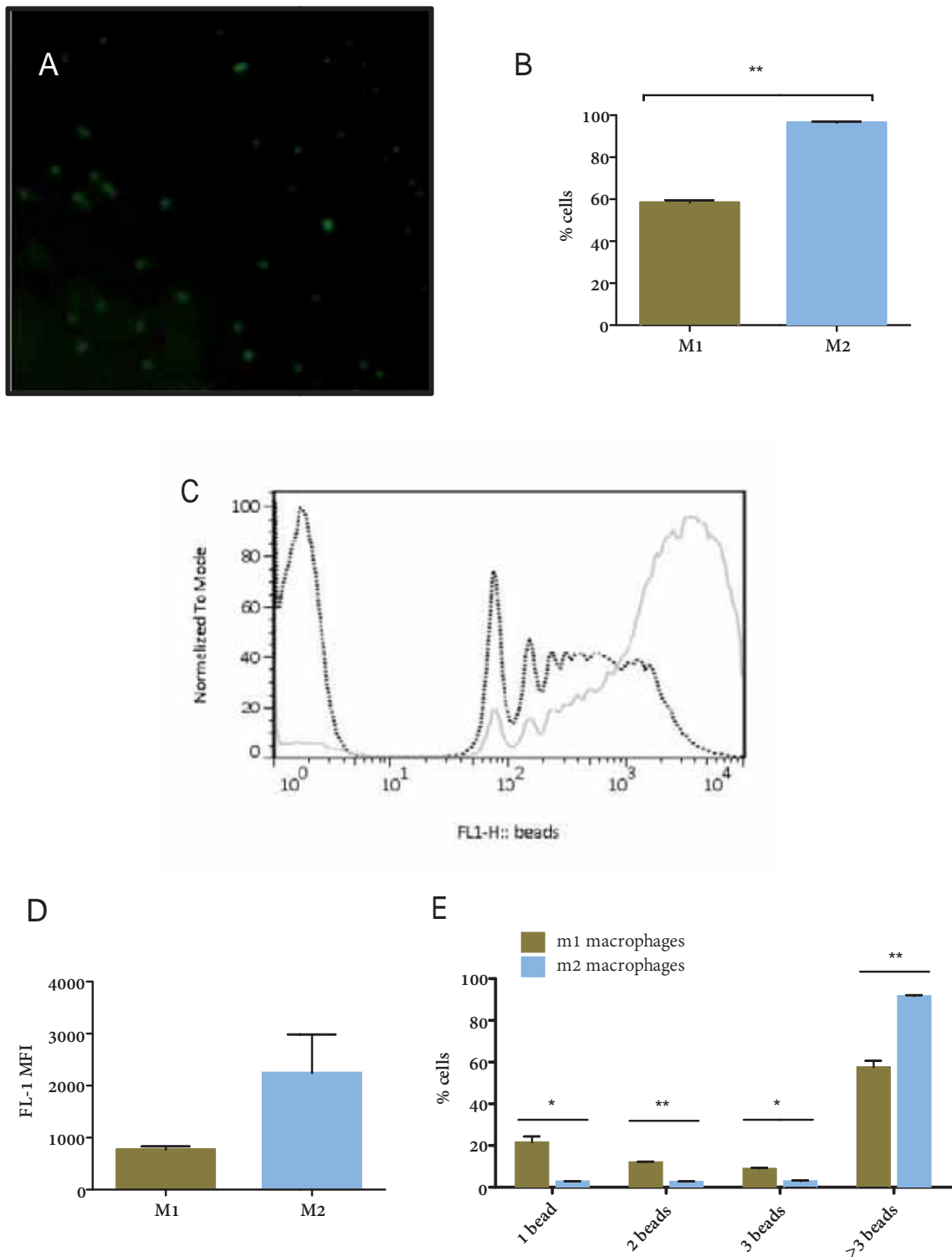


**Figure 5.3. Phagocytosis of fluorescent beads in macrophage cultures.** Image (A), obtained with an immunofluorescence microscope, shows incubation of macrophages with fluorescent beads. Cells with fluorescent signal were identified by flow cytometry. Graph (B) shows the percentage of M1 and M2 macrophages containing fluorescent beads. Histogram (C) displays the intensity of fluorescent signal from beads (on FL-1 channel) on X-axis and on Y-axis the number of cells as the percentage of the maximum bin. M2 macrophages (grey line) exhibited higher levels of fluorescence comparing with M1 macrophages (black dotted line), as compared in (D). Graph (E) shows number of beads per cell obtained from flow cytometry histogram according with fluorescent peaks. Results from 2 independent experiments. MFI: mean fluorescence intensity. \*  $p=0.01-0.05$ , \*\*  $p=0.001-0.01$ , \*\*\*  $p<0.001$  by Student's t-test.



### 5.1.3.2. Phagocytosis of MSU crystals

On day 7, MSU (200  $\mu\text{g}/\text{mL}$ ) was added to M1 and M2 macrophages and phagocytosis of these needle-shape crystals was first observed in an optical microscope. Figure 5.4 A and B shows differences observed in MSU clearance between both subtypes of macrophages, that were obvious after only one hour of incubation. M2 macrophages were more effective in MSU phagocytosis, with nearly all the cells loaded with crystals, whereas in the case of M1 more crystals remained in the extracellular media. In the follow up of M2 macrophages (Figure 5.4 C-E) almost all MSU crystals had been phagocytosed after 18 hours of incubation.

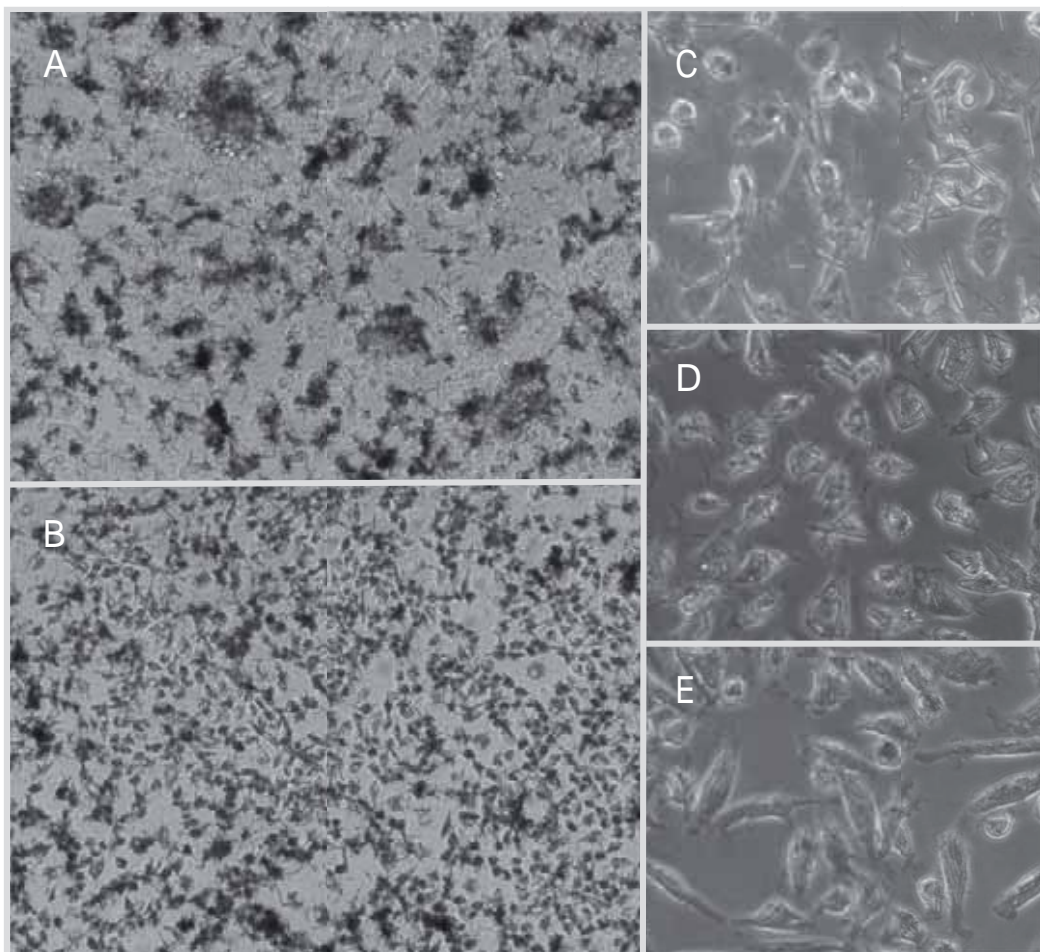


**Figure 5.4.** MSU phagocytosis in M1 and M2 macrophages. M1 (A) and M2 (B) macrophage cultures after one hour of incubation with MSU crystals (200  $\mu\text{g}/\text{mL}$ ). Pictures were taken in an inverted optical microscope with a 10X objective. M2 macrophages were incubated with 200  $\mu\text{g}/\text{mL}$  of MSU crystals and pictures were taken using the 20X objective just after the addition of crystals (C), after 1 hour (D) and at 18 hours (E).

Flow cytometry was then used to quantify MSU phagocytosis, confirming the observations made by microscopy. As described in the methods chapter, this technique can identify cells that uptake MSU crystals as they increase their internal complexity and therefore their SSC signal (Figure 5.5). Macrophages were incubated for 2 (5 experiments) or 18 hours (2 experiments) with MSU crystals (200  $\mu\text{g}/\text{mL}$ ) and, after washing, the percentage of cells with crystals was analyzed. The same experiment was performed with peripheral blood monocytes from healthy donors (7 experiments) exposed to MSU crystals for 2 hours. Monocytes had a higher capacity for MSU phagocytosis, only achieved by M2 macrophages after 18 hours (Figure 5.6 and Table 5.1). As in our previous experiments with fluorescent beads, M2 macrophages were more phagocytic than M1, but these differences were not statistically significant (at 2 hours  $p=0.0625$ , at 18 hours  $p=0.0757$ ). Cell death was analyzed by PI staining and higher mortality was observed in M2 macrophages at 18 hours (mean live cells  $\pm$  SEM: M1  $80.95 \pm 1.050$  and M2  $64.35 \pm 2.850$ ,  $p=0.0319$ ), probably related to their higher phagocytic capacity, dying after MSU phagocytosis.

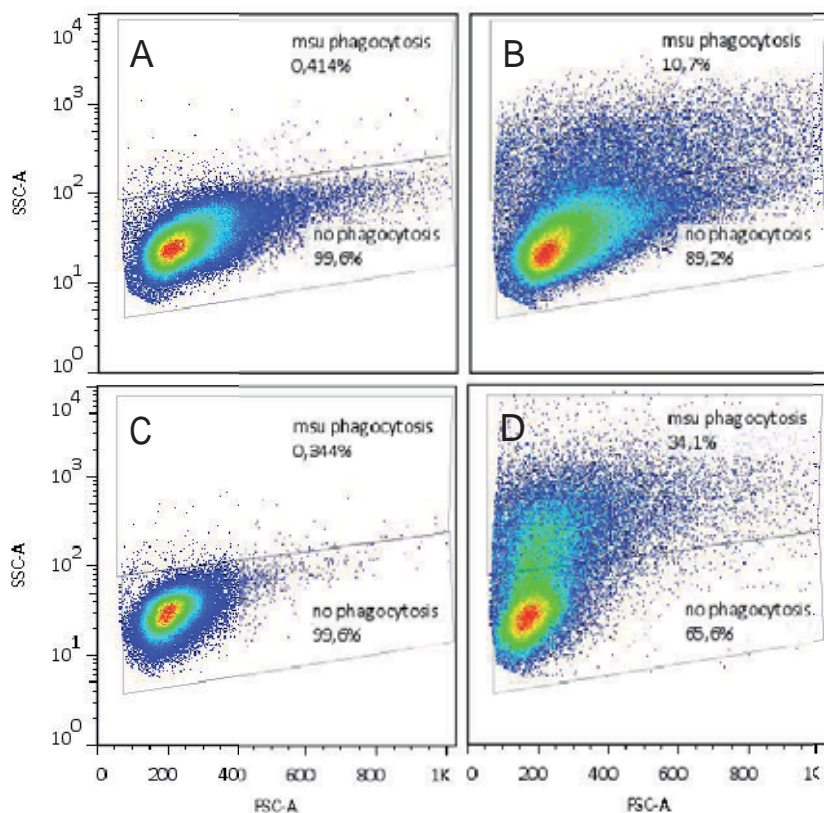


**Figure 5.5.** Analysis of MSU phagocytosis by flow cytometry. Cultures of M1 macrophages without (A) and with (B) crystals, and M2 macrophages without (C) and with (D) crystals. Phagocytic cells were identified by an increase in SSC values.

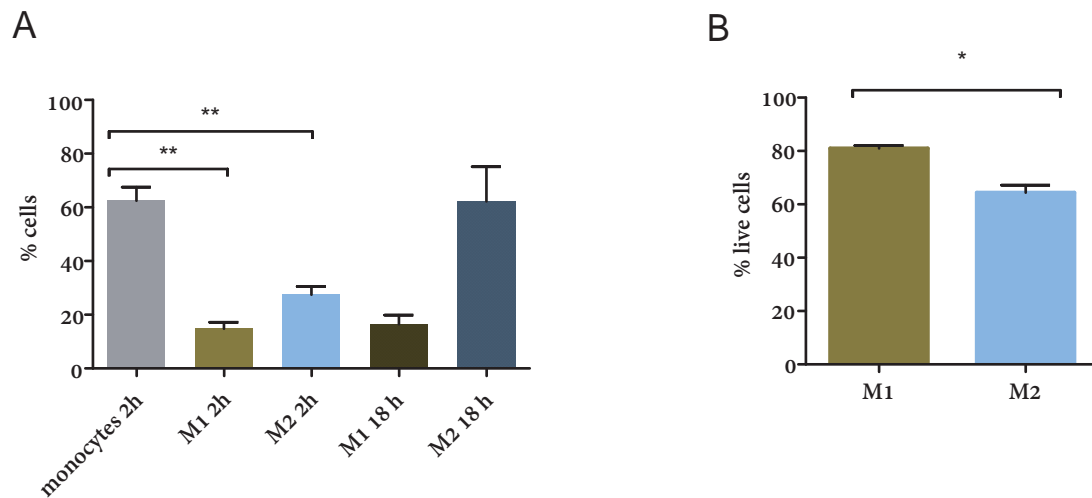


**Figure 5.6. Quantification of MSU crystal phagocytosis in macrophages.** (A) Percentage of cells that uptake MSU crystals after 2 or 18 hours of incubation with MSU (200 µg/mL) analyzed by flow cytometry. (B) Cell viability after 18 hours of incubation with MSU, assessed by PI staining by flow cytometry. \*  $p=0.01-0.05$ , \*\*  $p=0.001-0.01$ , \*\*\*  $p<0.001$  by Mann Whitney for comparison of 2 hours experiments and Student's t-test for cell viability analysis.

	<i>Mean (%)</i>	<i>SD</i>	<i>CI</i>
Monocytes 2 hours	62.44	13.48	49.97-74.90
M1 macrophages 2 hours	14.80	5.30	8.22-21.38
M2 macrophages 2 hours	27.44	6.94	18.82-36.06
M1 macrophages 18 hours	16.45	4.88	-27.39-60.29
M2 macrophages 18 hours	62.20	18.24	-101.7-226.1

**Table 5.1. Statistics of MSU phagocytosis.** M1 and M2 macrophages were incubated with MSU crystals (200 µg/mL) for 2 or 18 hours. Table shows mean, standard deviation (SD) and 95% confidence interval (CI) of the percentage of cells with MSU crystals, analyzed by flow cytometry.

#### 5.1.4. Cytokine profile in response to LPS

M1 macrophages are characterized by the production of inflammatory cytokines such as IL-1 $\beta$ , IL-6 or TNF- $\alpha$ , whereas M2 macrophages are considered anti-inflammatory because of the secretion of IL-10 in response to LPS<sup>[200,203]</sup>. To analyze the cytokine profile of our M1 and M2 differentiated macrophages, cells were stimulated with LPS (100 ng/mL) for 18 hours and production of IL-1 $\beta$ , IL-10, IL-12 p40, IL-8 and GM-CSF were quantified by ELISA and Luminex® in culture supernatants.

M1 macrophages were the main producers of the inflammatory cytokines IL-1 $\beta$ , IL12 p40 and the growth factor GM-CSF, that was produced even in non-stimulated macrophages (Figure 5.7). On the other hand, supernatants of M2 macrophages had higher concentrations of the anti-inflammatory cytokine IL-10. The chemokine IL-8 was equally produced after stimulation by M1 and M2 macrophages, although significant higher levels were found in unstimulated M1 cultures. Results obtained are consistent with previous literature and confirm the proper polarization of macrophages.

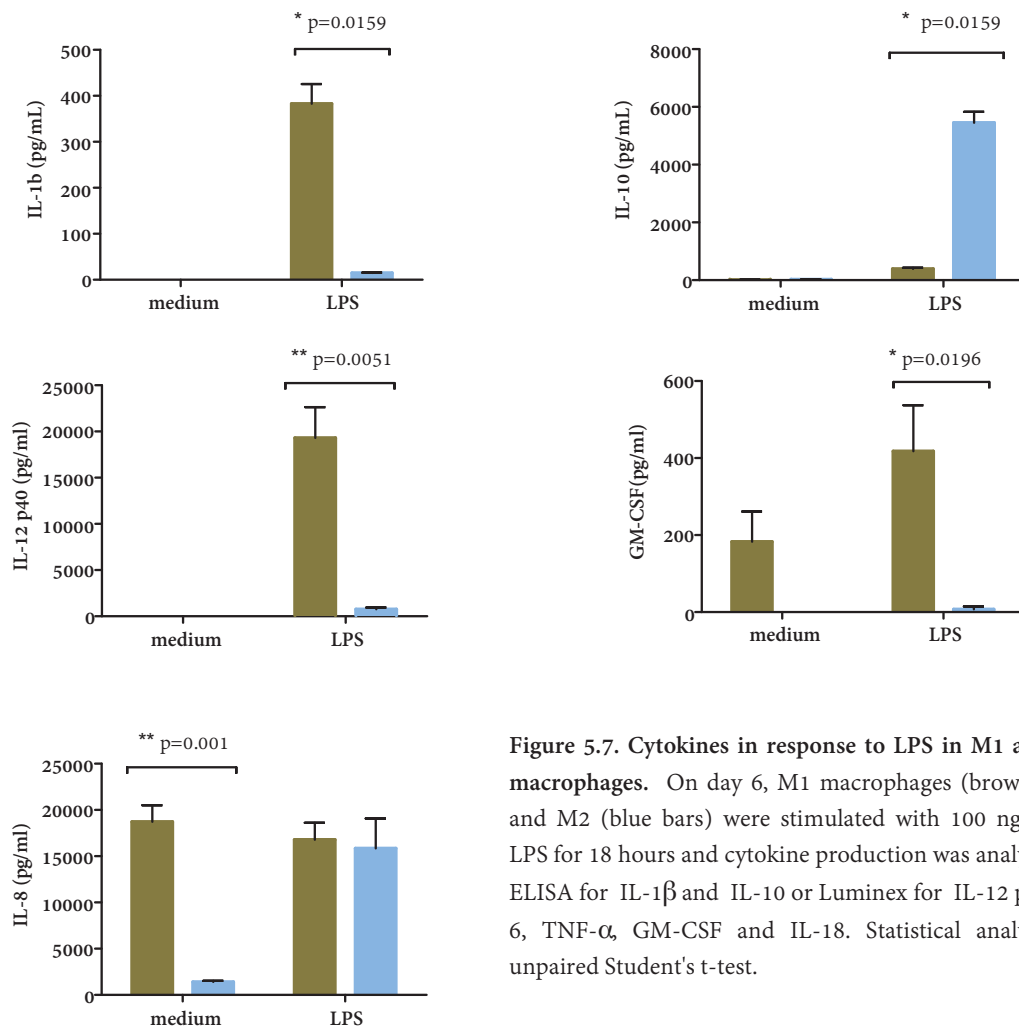


**Figure 5.7. Cytokines in response to LPS in M1 and M2 macrophages.** On day 6, M1 macrophages (brown bars) and M2 (blue bars) were stimulated with 100 ng/mL of LPS for 18 hours and cytokine production was analyzed by ELISA for IL-1 $\beta$  and IL-10 or Luminex for IL-12 p40, IL-6, TNF- $\alpha$ , GM-CSF and IL-18. Statistical analysis by unpaired Student's t-test.

As M2 macrophages produce of IL-10 but not IL-1 $\beta$  after LPS challenging, levels of both cytokines were quantified during differentiation of monocytes through M2 macrophages (days 0, 3, and 6). Figure 5.8 presents the evolution of these cytokines over time, showing that as monocytes differentiate IL-1 $\beta$  production decrease and IL-10 increase.

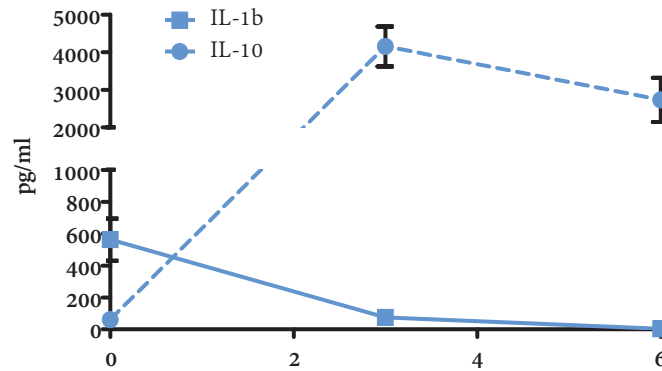


Figure 5.8. Cytokine production in response to LPS through M2 polarization. Peripheral blood monocytes cultured with M-CSF for M2 macrophage polarization were stimulated with LPS (100 ng/mL) for 18 hours on days 0, 3 and 6. Graphs shows IL-1 $\beta$  and IL-10 production on supernatants, quantified by ELISA. Results from one experiment.

### 5.1.5. Differential *IL-10* gene expression

M1 and M2 macrophages can be differentiated by their gene expression profiles. One of the most differentially expressed genes is *IL-10*<sup>[281]</sup>, thus its mRNA was analyzed by RT-PCR, as described in methods section. Briefly, RNA isolation was performed with a column system, and the resulting RNA was used as a template for the synthesis of cDNA for the RT-PCR. Relative quantification was calculated using the Ct method, with *GAPD* as a reference gene. As seen in Figure 5.9, M2 macrophages exhibited higher *IL-10* gene expression at baseline, compared with M1 macrophages.

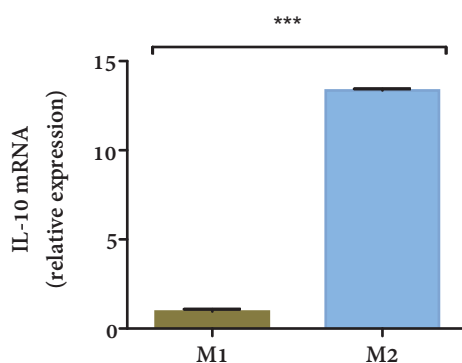


Figure 5.9. Basal *IL-10* RNA expression in M2 macrophages. Graph represents relative gene *IL-10* expression in unstimulated M1 and M2 macrophages calculated as  $2^{-\Delta\Delta CT}$  with *GAPD* as reference gene. Results from 2 independent experiments. \*\*\*  $p=0.0002$  by Student's t-test.

## 5.2. Role of M2 macrophages in gout initiation

Having verified that our macrophages were correctly polarized, we investigated the role of M2 macrophages in the initiation of the inflammatory response to MSU crystals. M2 macrophages, considered by some authors as resident macrophages in tissues, could uptake MSU crystals without IL-1 $\beta$  production. This fact could explain the presence of MSU crystals or MSU deposits in asymptomatic joints<sup>[270,282,283]</sup>. But MSU phagocytosis could turn them more “M1-like”, being able to produce IL-1 $\beta$  when stimulated again with a TLR agonist.

This section tries to confirm this hypothesis. In the first part, M2 macrophages were challenged with LPS, MSU or both together to study the effect of MSU phagocytosis on macrophage function, specifically on IL-1 $\beta$  and IL-10 production, and on cell surface antigens. These results were confirmed with a macrophage-like cell line (THP-1 cells). In the second part, the same experiments were performed using calcium pyrophosphate (CPP) crystals, which are also a well known cause of crystal-induced arthritis. Finally, M2 macrophages were cultured with soluble uric acid to investigate the effect of hyperuricemia in the response of M2 macrophages to MSU crystals.

### 5.2.1. Effect of MSU crystals on cytokine production

#### 5.2.1.1. Macrophages and MSU

Our previous results showed that M2 macrophage response to LPS is characterized by production of IL-10 but not IL-1 $\beta$ . As macrophages have been involved in the initiation of the inflammatory response in gout arthritis, we wondered if M2 macrophages could produce the inflammatory cytokine IL-1 $\beta$  after MSU phagocytosis. Thus, M2 macrophages were challenged on day 6 with LPS (100 ng/mL), MSU (200  $\mu$ g/mL) or both for 18 hours, and the production of IL-1 $\beta$  and IL-10 was analyzed on cell culture supernatants by ELISA. Results from 9 independent experiments are summarized in Figure 5.10.

As expected, M2 macrophages did not produce IL-1 $\beta$  when LPS was added, neither with MSU alone. This fact agrees with published observations that MSU crystals can be found in asymptomatic joints<sup>[270]</sup>. However, MSU and LPS together induced IL-1 $\beta$  secretion ( $p=0.0078$ ). The opposite effect was observed on IL-10, as incubation of macrophage cultures with MSU and LPS decreased production of this anti-inflammatory cytokine ( $p=0.0039$ ).

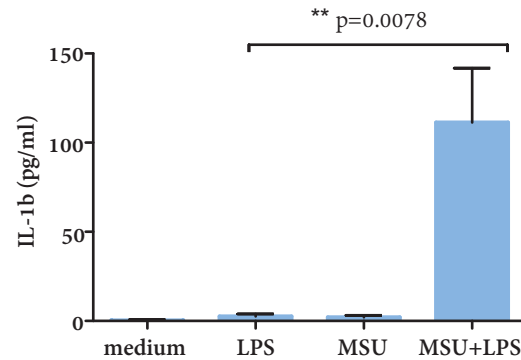
To exclude the possibility that the decline in IL-10 production could be secondary to cell death after MSU phagocytosis, cell viability was analyzed together with changes in this cytokine. Five independent experiments were performed and each sample was analyzed by flow cytometry



using PI staining. As seen in graph 5.10 C, the drop in IL-10 was more pronounced than the decrease in the number of live cells (mean  $\pm$  SEM: percentage of decrease in live cells 30.18  $\pm$  3.22, decrease in IL-10 64.45  $\pm$  7.820,  $p=0.030$ ), suggesting than other factors rather than cell death are involved in the down regulation of IL-10.

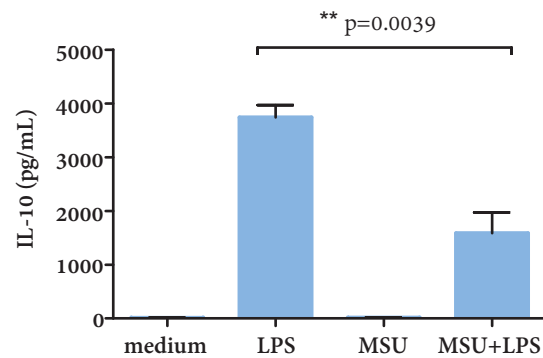
A

	Mean (pg/mL)	SD	CI
Medium	0.3193	0.90	-0.4357-1.074
LPS	2.587	3.88	-0.6581-5.832
MSU	2.003	3.50	-0.9270-4.933
MSU+LPS	111.4	86.10	39.39-183.4



B

	Mean (pg/mL)	SD	CI
Medium	10.70	15.25	-1.019-22.42
LPS	3738	692.1	3206-4270
MSU	12.80	21.57	-3.784-29.38
MSU+LPS	1587	1159	696.4-2478



C

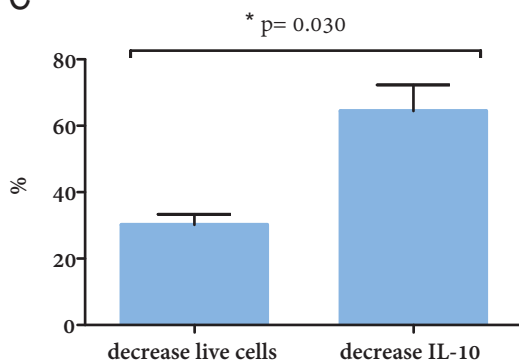
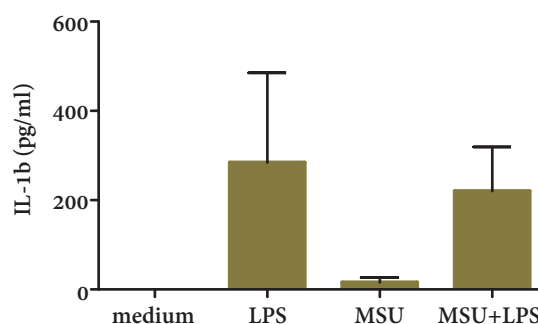


**Figure 5.10. Effect of MSU on IL-1 $\beta$  and IL-10 production in M2 macrophages.** Macrophages were stimulated with LPS (100 ng/mL), MSU (200  $\mu$ g/mL) or both for 18 hours and cytokines were quantified in cell culture supernatants by ELISA. Graph (A) shows production of IL-1 $\beta$  in 8 independent experiments. (B) Results of IL-10 levels in 9 independent experiments. (C) Shows the relation between cell death and the decrease in IL-10 production. Cell viability was analyzed by flow cytometry with PI and IL-10 was quantified by ELISA. SD: standard deviation, CI: 95% confidence interval. Statistic analysis by Willcoxon's test.

The effect of MSU crystals on M1 macrophages was also analyzed with the same stimulation protocol previously used for M2 macrophages. M1 macrophages fail to produce cytokines when challenged with MSU (Figure 5.11). When stimulated with MSU and LPS, whereas there was a homogeneity in the results in M2 macrophages with a clear trend towards an increase in IL-1 $\beta$  and a decrease in IL-10 in all of the experiments performed, it was not the case with M1 macrophages. Four different experiments were performed, and the poor agreement between experiments did not allow us to draw a conclusion about the effect of MSU on response to LPS.

A

	Mean (pg/mL)	SD	CI
Medium	0	0	0
LPS	284.4	401.3	-354.1-922.9
MSU	15.54	22.60	-20.42-51.50
MSU+LPS	220.5	197.5	-93.85-534.8



B

	Mean (pg/mL)	SD	CI
Medium	0	0	0
LPS	652.3	455.3	-478.8-1783
MSU	0.77	1.34	-2.55-4.1
MSU+LPS	861.6	1125	-1932-3655

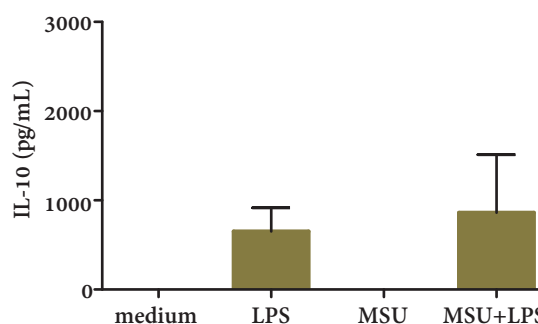


**Figure 5.11. Effect of MSU on IL-1 $\beta$  and IL-10 production in M1 macrophages.** Macrophages were stimulated with LPS (100 ng/mL), MSU (200  $\mu$ g/mL) or both for 18 hours and cytokines were quantified in cell culture supernatants by ELISA. Graphs show production of IL-1 $\beta$  (A) and IL-10 (B) in 4 independent experiments. SD: standard deviation. CI: 95% confidence interval.



Production of other cytokines after MSU and LPS stimulation was then analyzed in supernatants of stimulated macrophages by Bioplex (Figure 5.12). M2 macrophages did not secrete IL-12 p40 even in the presence of MSU and LPS together. The chemokine IL-8 was detected in stimulated macrophages but not in unstimulated M2. IL-1Ra was produced in unstimulated M1 macrophages and after LPS challenging in both macrophage subtypes, whereas the addition of MSU resulted in a decreased levels. Interestingly, although M1 macrophages were the main producers of GM-CSF, it could be induced in M2 macrophages by the presence of LPS and MSU.

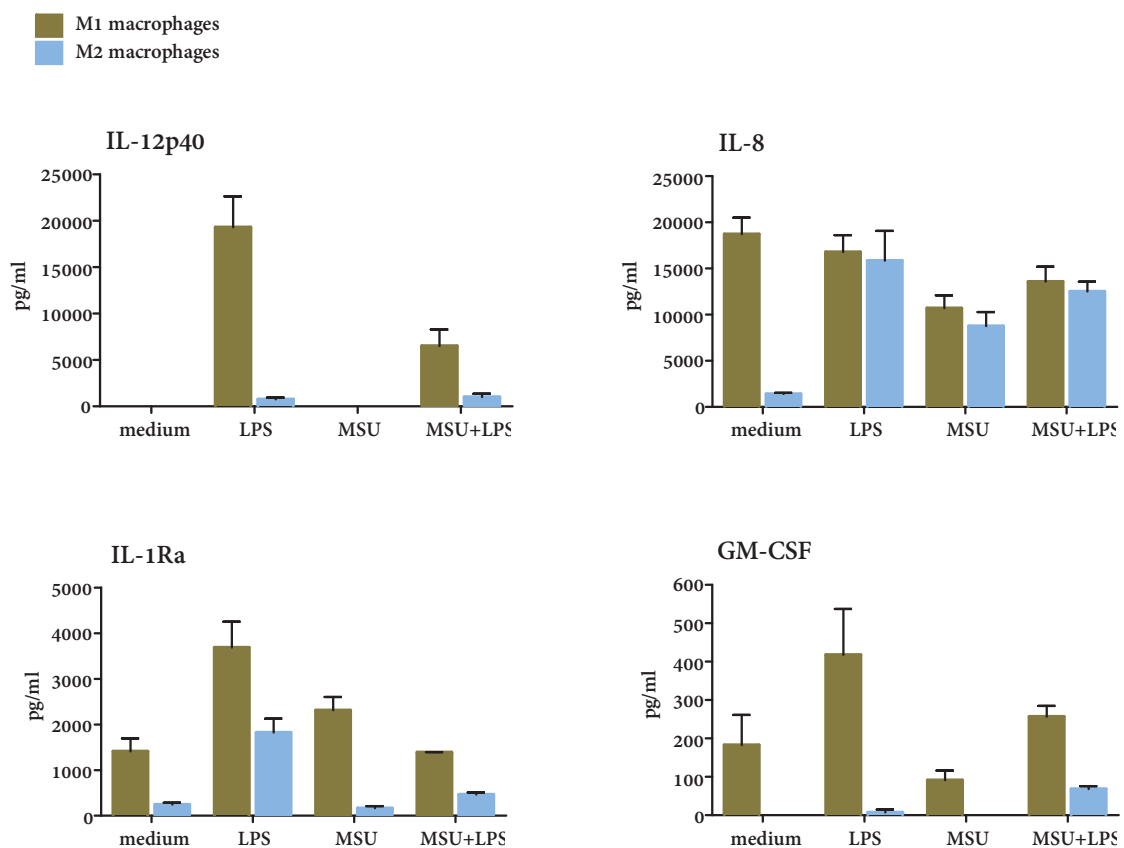
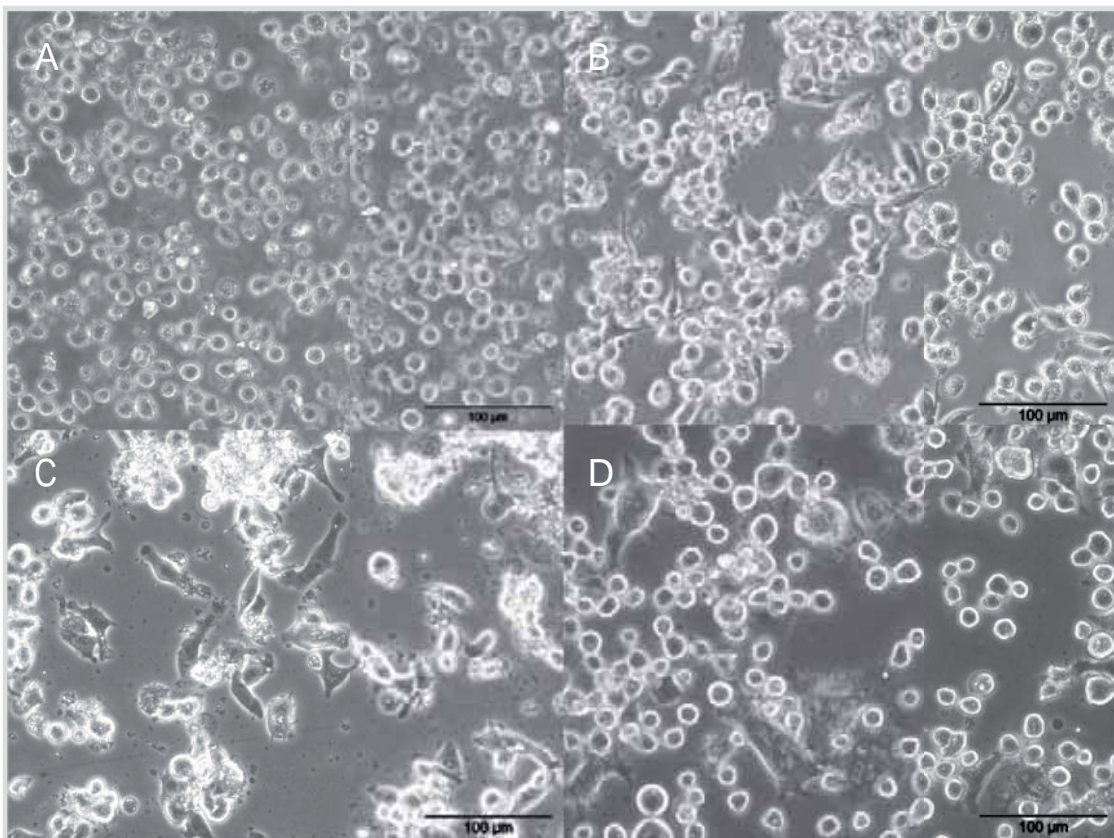


Figure 5.12. Effect of MSU on production of IL-12p40, IL-8, IL-1Ra and GM-CSF in M1 and M2 macrophages. Macrophages were stimulated with LPS (100 ng/mL), MSU (200  $\mu$ g/mL) or both for 18 hours and cytokines were quantified in cell culture supernatants by Bioplex.

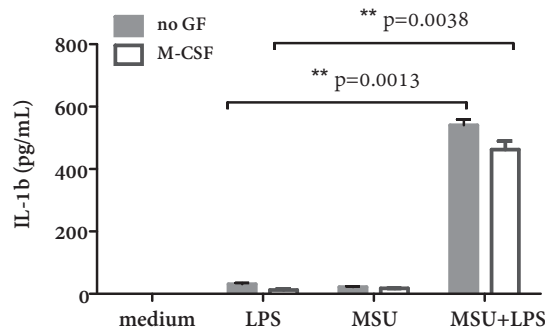
### 5.2.1.2. THP-1 cells and MSU

Experiments performed with M2 macrophages were replicated with the cell line THP-1. Cells were first differentiated to macrophages with PMA and some of them were then polarized towards an M2 phenotype with M-CSF for one week. The resulting “macrophage-like” cells (Figure 5.13) were stimulated as previously described with LPS (100 ng/mL), MSU crystals (200  $\mu$ g/mL) or both for 18 hours and IL-1 $\beta$  and IL-10 production was assessed in cell supernatants by ELISA.

THP-1 cells activated with PMA exhibited the same behaviour than M2 macrophages, producing IL-1 $\beta$  only when challenging with LPS and MSU together (mean  $\pm$  SEM: LPS 30.91  $\pm$  4.416 ng/mL, MSU+LPS 540.5  $\pm$  18.21 ng/mL,  $p=0.0013$ ), as seen in Figure 5.14. The same pattern was observed when cells were cultured with M-CSF (without growth factor 540.5  $\pm$  18.21 ng/mL, with M-CSF 462.1  $\pm$  27.58 ng/mL,  $p=0.1412$ ). However, unlike M2 macrophages, THP-1 cells activated with PMA did not produce any IL-10, even when cultured in the presence of M-CSF.



**Figure 5.13. Activation of THP-1 cells with PMA.** (A) Suspension of THP-1 cells at baseline. When exposed to PMA these cells become activated and differentiate into macrophage-like cells: (B) THP-1 after 5 hours of PMA stimulation, (C) after 24 hours and (D) on day 10 after polarization with M-CSF. Pictures taken with an Olympus Inverted Fluorescent Microscope IX51.



	THP-1 cells			THP-1 cells with M-CSF		
	mean	SD	CI	mean	SD	CI
LPS	30.91	6.245	-25.20-87.2	12.53	4.070	-24.04-49.10
MSU	21.68	3.673	-11.32-54.68	17.42	0.6562	11.52-23.32
MSU+LPS	540.5	25.76	309-771.9	462.1	39.00	111.7-812.5

**Figure 5.14. Effect of MSU on IL-1 $\beta$  production in THP-1 cells.** Graph compares IL-1 $\beta$  production in THP-1 cells activated with PMA cultured without growth factors (grey bars) or with M-CSF (white bars) after stimulation with LPS (100 ng/mL), MSU (200  $\mu$ g/mL) or both for 18 hours. Table shows mean, standard deviation (SD) and 95% confidence interval (CI) of IL-1 $\beta$  levels, quantified by ELISA. \*\* by unpaired Student's t-test. Results from one experiment.

### 5.2.2. Effect of MSU crystals in cell surface markers

As M2 macrophages acquire the capacity to produce IL-1 $\beta$  after MSU phagocytosis, we investigated if MSU could modify the expression of cell surface antigens towards an M1 phenotype described as higher CD11b, lower CD14 and no expression of CD163.

On day 6, we stimulated M2 macrophages with LPS (100 ng/mL) and MSU (200  $\mu$ g/mL) for 18 hour and expression of CD11b, CD14 and CD163 was analyzed by flow cytometry. Our results showed that MSU crystals decreased both CD11b and CD14 expression and slightly CD163 (Figure 5.15 A). However, no statistically significant differences were founded when analyzed the effect of stimulation in each cell surface antigen (CD11b  $p=0.5647$ , CD14  $p=0.1801$ , CD163  $p=0.5647$ ).

To investigate the paracrine effects of soluble factors produced by M2 macrophages after stimulation, we cultured M2 macrophages for 24 hours in conditioned media from M2 macrophages previously stimulated with LPS and MSU (Figure 5.15 B). Interestingly, conditioned media of unstimulated M2 macrophages or macrophages with MSU up-regulated M2 markers and decreased CD11b. The presence of LPS resulted in a decreased of CD163 and CD11b. CD14 increased specially in conditioned media from macrophages with both LPS and MSU. Again, these differences were not statistically significant (CD11b  $p=0.4463$ , CD14  $p=0.7274$ , CD163  $p=0.4462$ ).

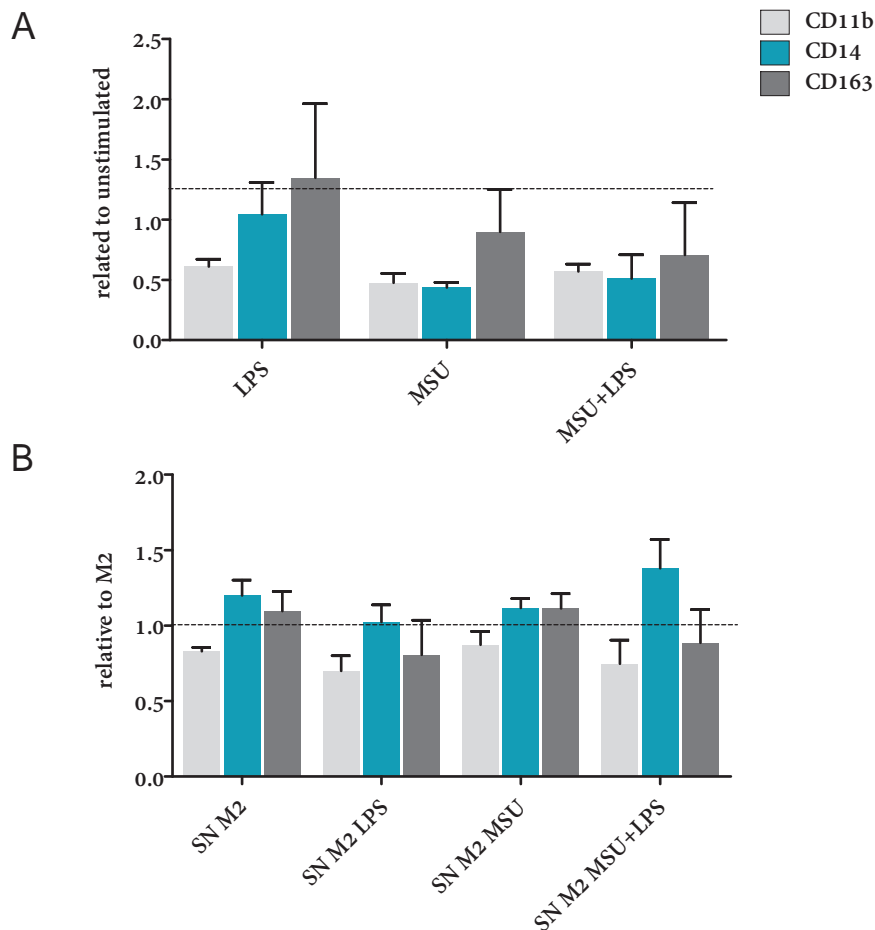
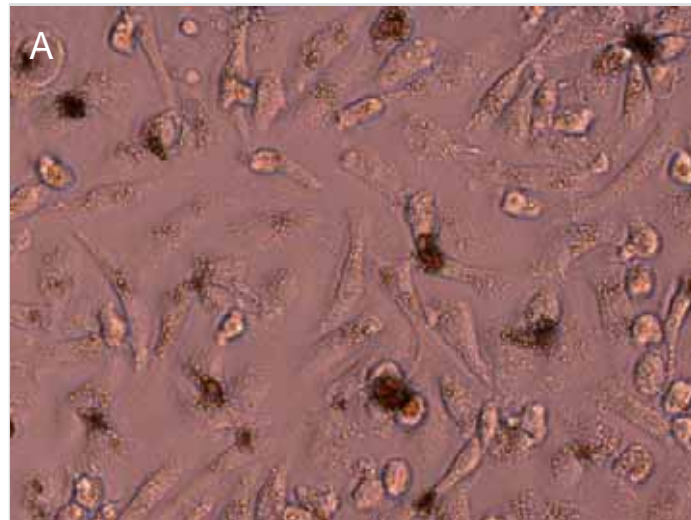


**Figure 5.15.** Effect of MSU in cell surface antigens. (A) M2 macrophages on day 7 were challenged with LPS, MSU or both (n=2) or (B) were cultured for 24 hours in conditioned media from M2 macrophages stimulated with LPS or MSU (n=3) and expression of CD11b, CD14 and CD163 was analyzed by flow cytometry. SN: supernatant.

### 5.2.3. Effect of CPP crystals on M2 macrophages

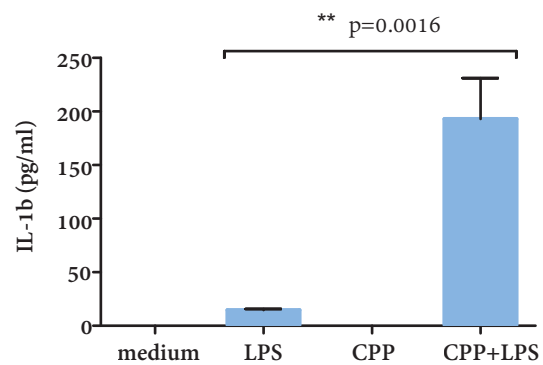
Calcium pyrophosphate (CPP) crystals are, as MSU crystals, associated with rheumatic diseases. The deposition of these crystals in connective tissues is known as chondrocalcinosis, pseudogout or pyrophosphate arthropathy, and symptoms range from an asymptomatic deposition of crystals, to acute arthritis or destructive arthropathy. On polarized light microscopy these crystals usually have a rhomboid shape and are only weakly birefringent. The activation of NLRP3 inflammasome has also been involved in the pathogenesis of CPP related arthropathies.

In order to see if results obtained with MSU crystals were specific for this crystal, the same experiments were performed using CPP crystals. As presented in Figure 5.16, M2 macrophages produced the inflammatory cytokine IL-1 $\beta$  only in the presence of both CPP and LPS ( $p=0.0016$ ), whereas a less pronounced decrease of IL-10 production was observed ( $p=0.1396$ ).



B

	Mean (pg/mL)	SD	CI
Medium	0	0	0
LPS	14.78	1.978	12.32-17.23
MSU	0	0	0
MSU+LPS	193.00	85.48	86.88-299.1



C

	Mean (pg/mL)	SD	CI
Medium	23.62	8.920	12.54-34.69
LPS	5450.0	844.6	4401-6498
MSU	51.23	9.679	39.21-63.25
MSU+LPS	4507.0	968.5	3304-5710

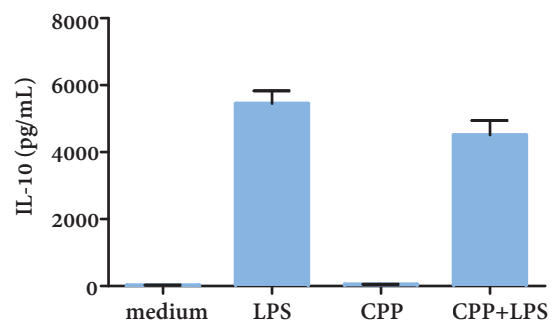


**Figure 5.16. Production of IL-1 $\beta$  and IL-10 in M2 macrophages after stimulation with CCP crystals.** Phagocytosis of CPP crystals (A), that are visualized as small granules by optic inverted microscopy (20X objective). Macrophages were challenged with CCP (200  $\mu$ g/mL), LPS (100 ng/mL) or both for 18 hours and production of IL-1 $\beta$  (B) and IL-10 (C) was quantified in supernatants by ELISA. Results from one representative experiment out of 5. SD: standard deviation, CI: 95% confidence interval. \*\* unpaired Student's t-test.

Then, we analyzed cell viability after MSU or CPP incubation in order to investigate if the lower effect in IL-10 down-regulation observed with CPP crystals could be secondary to lower cell death. No differences between MSU and CPP were observed when macrophages were cultured with these crystals for 18 hours, as shown in Figure 5.17.

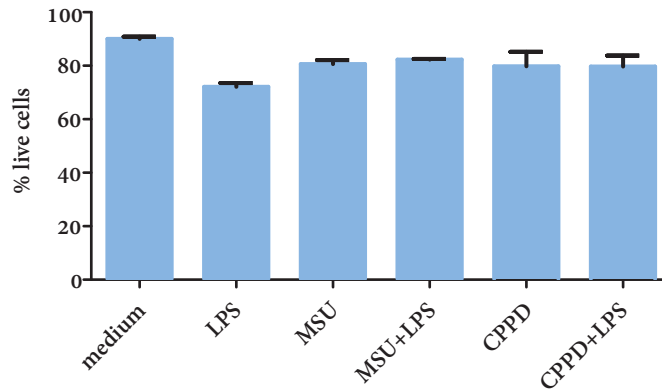


**Figure 5.17.** Effect of MSU and CPP crystals on cell viability. M2 macrophages were cultured with MSU (200  $\mu\text{g}/\text{mL}$ ), CPP (200  $\mu\text{g}/\text{mL}$ ) and LPS (100  $\text{ng}/\text{mL}$ ) for 18 hours, and cell viability was quantified by flow cytometry with PI.

#### 5.2.4. Effect of soluble uric acid on M2 macrophage function

Whereas an extensive literature has been published about the interaction of MSU crystals with immune cells, less information exists about the impact of soluble uric acid (SUA) over these cells. Uric acid has been associated with deleterious effects like arterial hypertension, ischemic cardiomyopathy and obesity, but it seems to have a protector role in some pathologies, especially on brain damage in the settings of multiple sclerosis, Parkinson and ischemic stroke.

In patients with gout, both an increase and a decrease in uric acid levels can initiate an arthritis flare. To explore if SUA could have any effect on the response of M2 macrophages to MSU crystals, two sets of *in vitro* experiments were designed. First we investigated the role of uric acid on macrophage polarization. Monocytes were polarized towards M2 macrophages in the presence of uric acid and, after 7 days of culture, cells were stimulated with MSU and LPS and production of IL-1 $\beta$  and IL-10 was quantified as in previous experiments. Additionally, we studied the effect of an acute increase of uric acid levels in M2 macrophages, adding different concentrations of SUA to already polarized macrophages 24 hours before stimulation with MSU and LPS. As 0.3 mM is the physiological concentration of uric acid in human blood, we would refer to this condition as normouricemia, whereas concentrations of 0.6 mM would be considered hyperuricemia. Results of these experiments are detailed in the next paragraphs.

#### 5.2.4.1. Effect of chronic exposure to SUA on macrophage polarization

Monocytes were polarized towards M2 macrophages in the presence of two different concentrations of SUA (0.3 and 0.6 mM). On day 6, LPS (100 ng/mL) and MSU (200 µg/mL) were added as previously described. After 18 hours supernatants were harvested and levels of IL-1 $\beta$  and IL-10 were analyzed by ELISA.

As showed in Figure 5.18, M2 macrophages polarized in the presence of SUA produced less IL-1 $\beta$  upon challenging with MSU and LPS, especially in conditions of hyperuricemia. A modest effect was observed in IL-10 production, with macrophages exposed to high uric acid concentrations tending to produce less IL-10 after LPS or MSU and LPS stimulation. A slightly increase after incubation with MSU and LPS was observed in conditions of normouricemia compared with hyperuricemia.

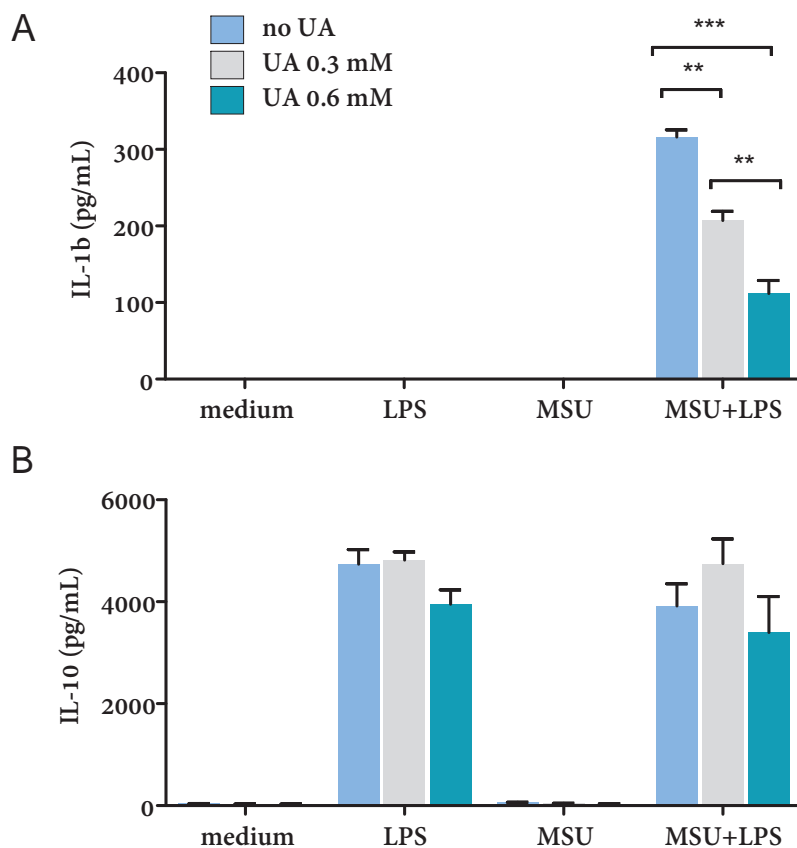
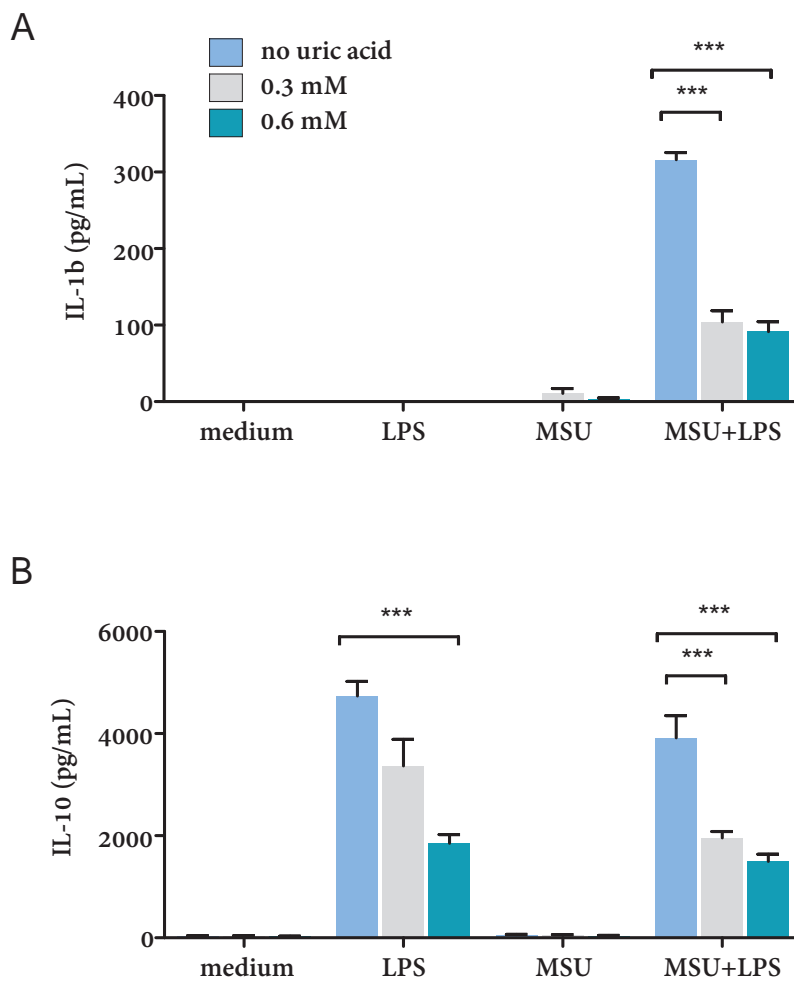


Figure 5.18. Effect of chronic exposure to soluble uric acid on cytokine production in M2 macrophages. Peripheral blood monocytes were polarized to M2 macrophages in the presence of different concentrations of soluble uric acid (0.3 mM or 0.6 mM). On day 6, M2 macrophages were challenged MSU (200 µg/mL), LPS (100 ng/mL) or both for 18 hours and production of IL-1 $\beta$  (A) and IL-10 (B) was quantified in supernatants by ELISA. Results from one representative experiment out of 3. \*\*\*  $p < 0.001$  by one-way ANOVA and Bonferroni's post-test.



#### 5.2.4.2. Effect of acute exposure to SUA

As an acute increase in uric acid levels can trigger gout flares, we analyzed the effect of culturing M2 macrophages in the presence of soluble uric acid for 24 hours. The presence of SUA had a suppressive effect on both IL-1 $\beta$  and IL-10 production. No differences were observed between uric acid concentrations regarding IL-1 $\beta$  suppression, while culture with high concentrations or uric acid had the highest effect in IL-10 down regulation (Figure 5.19).



**Figure 5.19.** Effect of acute exposure to SUA on cytokine production in M2 macrophages. Peripheral blood monocytes were polarized to M2 macrophages with M-CSF. On day 6, macrophages were incubated with different concentrations of SUA (0.3 mM or 0.6 mM) for 24 hours. Then were challenged with LPS (100 ng/mL) or MSU (200  $\mu$ g/mL) for 18 hours and production of IL-1 $\beta$  (A) and IL-10 (B) was assessed in supernatants by ELISA. \*\*\*  $p < 0.001$  by one-way ANOVA and Bonferroni's or T3 Dunnett's post-test.



#### 5.2.4.3. Effect of SUA on cell viability and phagocytic capacity of M2 macrophages

As the effect of MSU crystals largely depends on their phagocytosis, the phagocytic capacity of M2 macrophages cultured with uric acid was assessed by flow cytometry using fluorescent beads. No differences in phagocytosis were observed with any of the concentrations of SUA in both chronic and acute exposure to soluble uric acid, as shown in Figure 5.20 A.

Cell death could be another confounding factor that could decrease the production of cytokines. Using the viability PI staining (Figure 5.20 B), cell viability was analyzed by flow cytometry, and no differences were found between different uric acid concentrations.

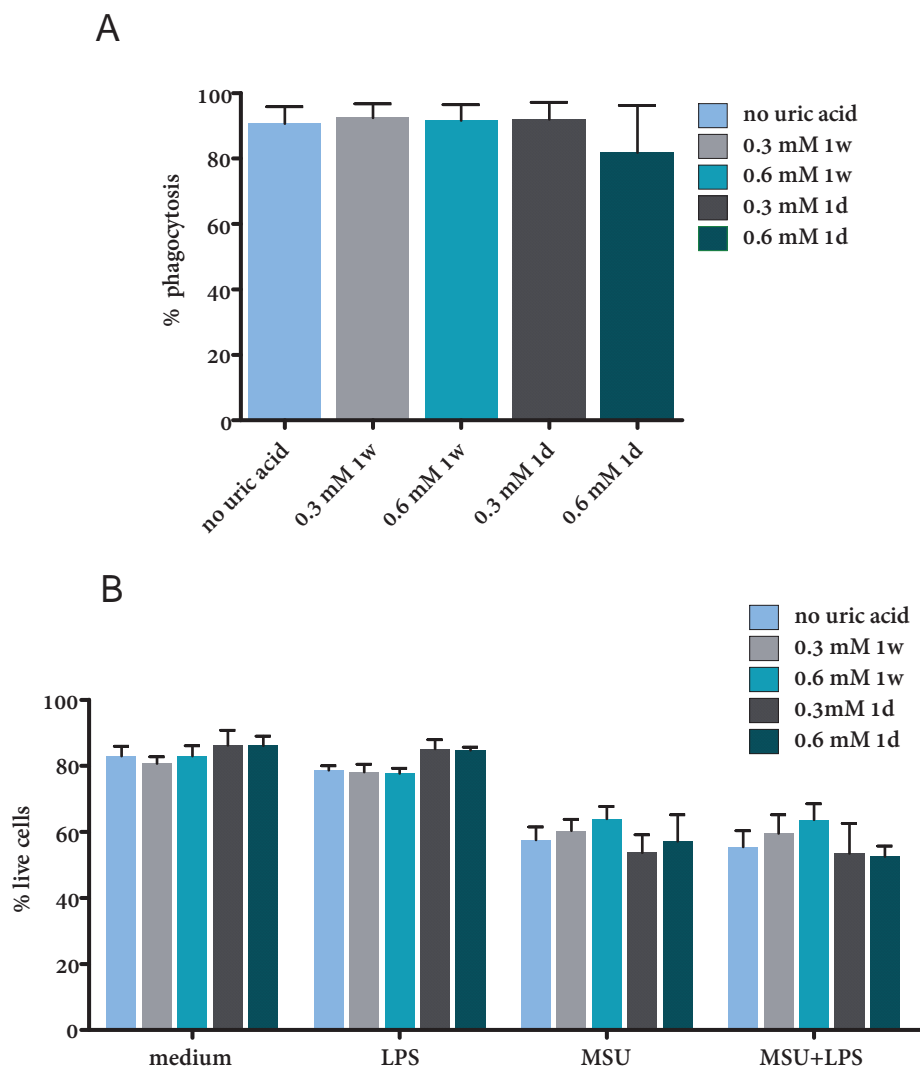


Figure 5.20. Phagocytic capacity and cell viability of M2 macrophages cultured with soluble uric acid. Phagocytosis was analyzed by flow cytometry using fluorescent beads. Graph (A) shows percentage of cells that uptake beads. On figure (B) percentage of live cells assessed by flow cytometry with the viability PI staining is represented. Results from 4 independent experiments. 1w: one week, 1d: one day.

### 5.3. The inflammasome in the inflammatory response of M2 macrophages

The purpose of this section is to clarify why M2 macrophages acquire an "M1-like" inflammatory phenotype and produce IL-1 $\beta$  after MSU phagocytosis. IL-1 $\beta$  is a pro-inflammatory cytokine tightly regulated, being necessary the presence of two signals for its production. One signal, through TLR receptors and transcription factor Nf- $\kappa$ B, is responsible for transcription and translation of pro-IL-1 $\beta$ , the inactive form of the protein. A second signal activates the inflammasome, a protein complex that cleaves the inactive form of the enzyme caspase-1. Its active form, an heterodimer formed by two larger subunits (p20) and two smaller subunits (p10), cleaves and activates pro-IL-1 $\beta$ . In a considerable number of publications stimulation of monocytes with a TLR agonist such as LPS results in IL-1 $\beta$  secretion but macrophages fail to produce this cytokine. According to Netea *et al.*, differences observed in IL-1 $\beta$  production between monocytes and monocyte-derived macrophages can be explained because monocytes constitutively express active caspase-1 and they only need one signal to secrete this cytokine, whereas in macrophages the inflammasome needs to be activated<sup>[284]</sup>. Our hypothesis to explain that M2 macrophages produce IL-1 $\beta$  only after LPS and MSU stimulation, is that M1 and M2 macrophages differ in the state of inflammasome activation and MSU crystals could be necessary in M2 macrophages to activate the inflammasome. Once caspase-1 has been activated, the stimulation with LPS could lead to IL-1 $\beta$  production. Conversely, M1 macrophages could have, like monocytes, pre-activated caspase-1, being able to produce IL-1 $\beta$  when challenged with LPS alone. To test this hypothesis, the state of inflammasome activation was analyzed in M1 and M2 macrophages, comparing baseline levels of both active and inactive forms of caspase-1 and its gene expression. Moreover, in order to understand the capacity of M2 macrophages to produce IL-1 $\beta$  after MSU phagocytosis and LPS challenging we investigated the effect of MSU crystals in inflammasome activation of this macrophage subset.

#### 5.3.1. Analysis of intracellular active caspase-1

Intracellular levels of active caspase-1 were assessed in M1 and M2 monocyte-derived macrophages from healthy donors by flow cytometry with a fluorescent antibody (FAM-FLICA caspase-1 assay). The interest of using flow cytometry is that macrophages that engulf MSU crystals can be identified, as they increase their SSC values, and be separately analyzed. Once gated, MFI values of the fluorescent antibody, representative of the levels of active caspase-1, were analyzed. Baseline levels of active caspase-1, as well as the degree of inflammasome activation after MSU challenging, reflected by an increase in active caspase-1,

were compared between M1 and M2 macrophages. Results of five different macrophage cultures are summarized in next paragraphs.

When comparing constitutively levels of active caspase-1, M1 macrophages exhibited higher levels than M2 as seen in Figures 5.21 A and 5.22 A, although these differences were not statistically significant (mean  $\pm$  SEM: M1 3.25  $\pm$  1.03, M2 2.13  $\pm$  0.144,  $p = 0.3573$  by Student's t-test). Macrophages were then challenged with MSU (200  $\mu\text{g}/\text{mL}$  for 1 hour), LPS (100  $\text{ng}/\text{mL}$  for 1 hour) or both. As positive controls of NLRP3 inflammasome activation macrophages were stimulated with ATP (5 mM 15 minutes) or nigericin (20  $\mu\text{g}/\text{mL}$  15 minutes). In both M1 and M2 macrophages, MSU increased the levels of active caspase-1 in cells with crystals (Figures 5.21 C, 5.22 C and 5.23) whereas cells that had not phagocytosed crystals exhibited the same inflammasome activation than unstimulated macrophages.

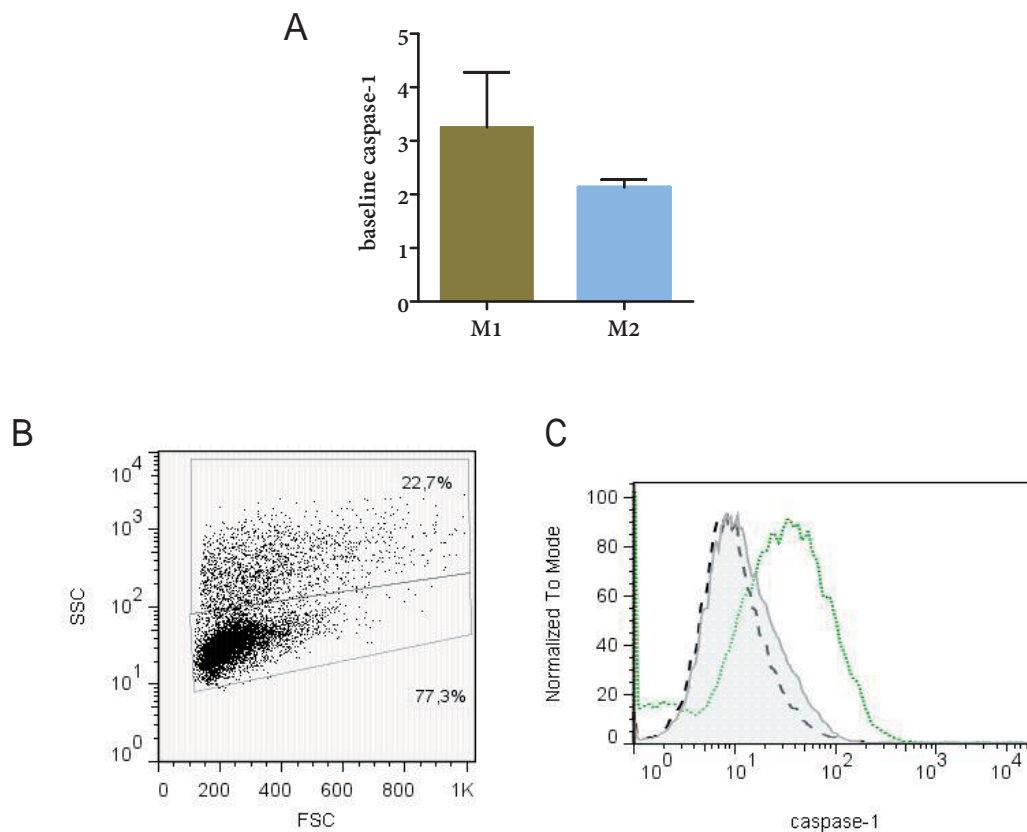


**Figure 5.21. Baseline state of caspase-1 activation in M1 and M2 macrophages and effect of MSU crystals on caspase-1 activation.** The presence of intracellular active caspase-1 was assessed by flow cytometry using a fluorescent antibody against this enzyme. Graph (A) compares levels of active caspase-1 in M1 and M2 macrophages from 5 different healthy donors, with MFI values normalized to unstained samples. Macrophages were then incubated with MSU crystals (200  $\mu\text{g}/\text{mL}$ ) for 1 hour and samples were analyzed by flow cytometry, gating macrophages with crystals as they increase their SSC signal (B). Histogram (C) shows on X-axis the fluorescent signal of the antibody against active caspase-1 and on Y-axis the % of cells normalized for the maximum bin. Macrophages with crystals (green dotted line) exhibited higher levels of active caspase-1 compared with macrophages without crystals (black dashed line) and unstimulated macrophages (grey line).

Caspase-1 activation was then visualized in an immunofluorescent microscope (Figure 4.22). Unstimulated macrophages showed and enhanced stained for caspase-1 compared with M2, in which active caspase-1 was concentrated in one or two cytoplasmic locations. In M2 macrophages, after phagocytosis of MSU crystals, intracellular staining of active caspase-1 increased.

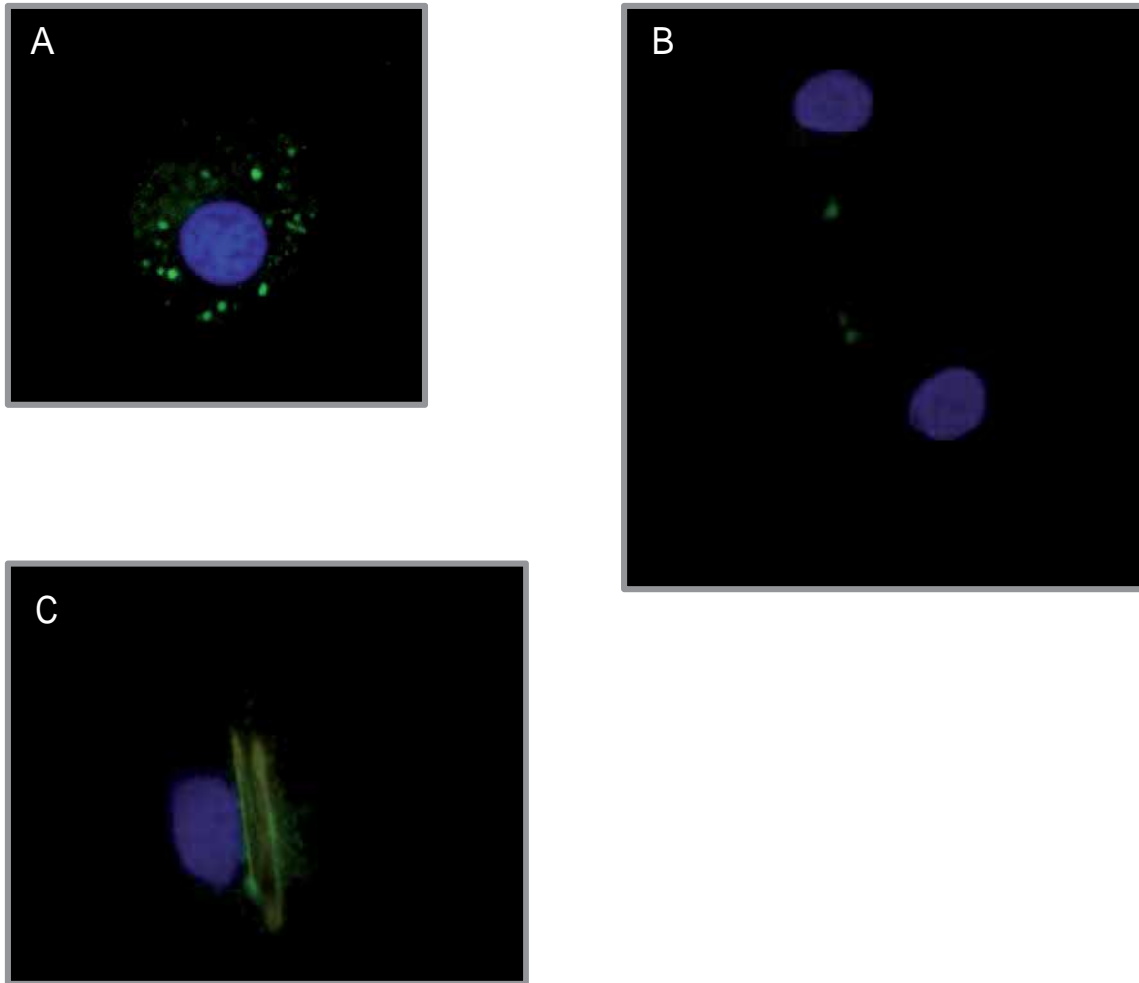
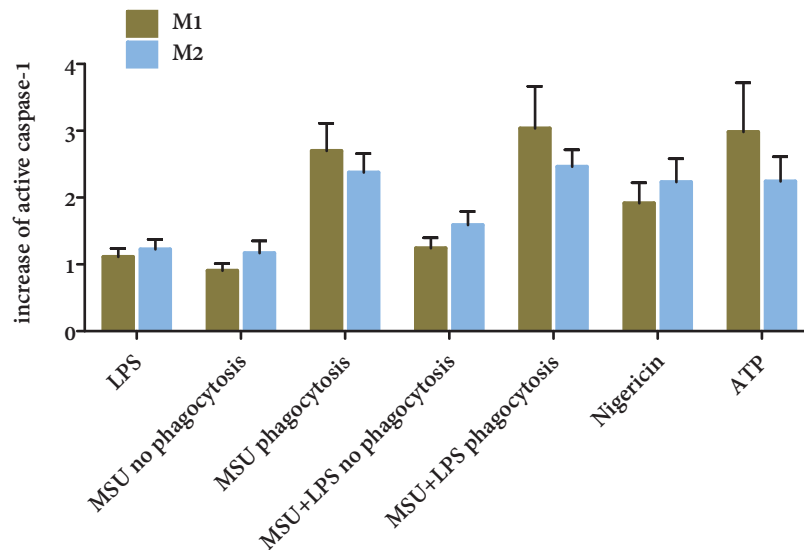


**Figure 5.22. Active caspase-1 in M1 and M2 macrophages.** FAM-FLICA caspase-1 assay was used for the staining of active caspase-1 whereas nuclei were stained with Hoechst provided in the same assay. Cells were concentrated on a glass slide using the cytopsin technique. Samples of unstimulated M1 (B), unstimulated M2 (B) and MSU cultured with MSU crystals (C) (200  $\mu\text{g}/\text{mL}$  for 1 hour) were then analyzed in an immunofluorescence microscope. Fluorescent images from caspase-1 (green), Hoechst (blue) and images of MSU crystals obtained without fluorescent filters were overlaid using the software ImageJ.

The increase in caspase-1 after MSU challenging was independent on the presence of LPS, which did not have any additive effect in caspase-1 activation. No differences were observed between caspase-1 activation with MSU and other activators the inflammasome such as nigericin or ATP (Figure 5.23 and Table 5.2). When comparing between M1 and M2 macrophages, the same degree of activation after stimulation with MSU crystals, nigericine and ATP was observed, with no significant differences.



	M1 macrophages			M2 macrophages			P
	Mean	SD	CI	Mean	SD	CI	
LPS	1.11	0.28	0.76-1.46	1.22	0.33	0.81-1.64	0.4421
MSU phagocytosis	2.70	0.92	1.55-3.85	2.37	0.64	1.58-3.16	0.3802
MSU+LPS phagocytosis	3.04	1.4	1.29-4.78	2.46	0.56	1.76-3.62	0.2978
Nigericin	1.91	0.69	1.06-2.77	2.23	0.78	1.26-3.20	0.5673
ATP	2.98	1.65	0.93-5.03	2.24	0.83	1.21-3.27	0.4193

**5.23. Comparison of caspase-1 activation between M1 and M2 macrophages after stimulation with MSU, nigericin and ATP.** M1 and M2 macrophages were challenged with MSU (200 µg/mL 1 hour), LPS (100 ng/mL 1 hour), ATP (5 mM 15 minutes) or nigericin (20 µg/mL 15 minutes) and, after incubation with a fluorescent antibody against active caspase-1, the presence of this active enzyme was quantified by flow cytometry. Graph presents MFI values obtained after subtracting the unstained sample were normalized to unstimulated cells. Table displays main statistics in both populations such as mean, standard deviation (SD) and 95% confidence interval (CI), as well as p values obtained after comparing M1 and M2 subgroups with paired t-test.

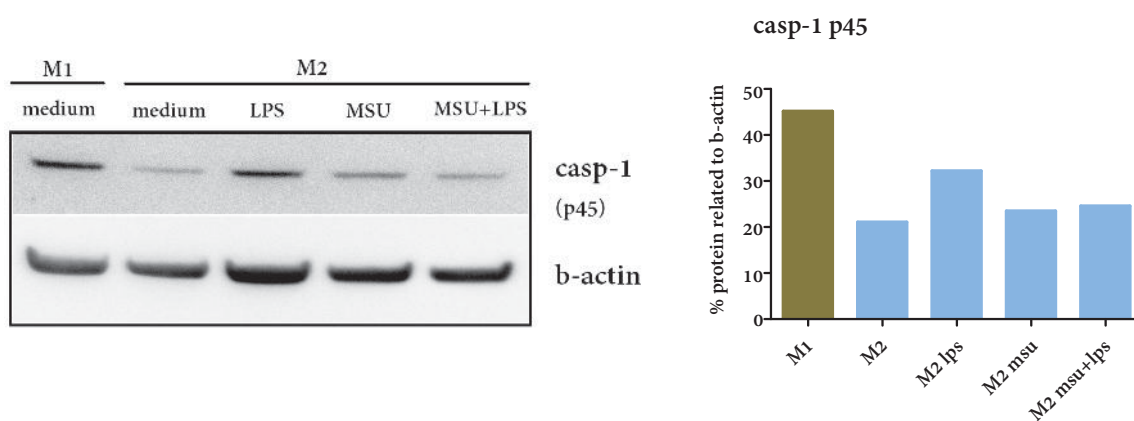
	<i>M1</i>	<i>M2</i>
Repeated measures ANOVA	p<0.0001	p=0.0003
<hr/>		
Tukey's Multiple comparison test	Significant? p<0.05	Significant? p<0.05
medium vs LPS	No	No
medium vs MSU no phagocytosis	No	No
medium vs MSU phagocytosis	Yes *	Yes *
medium vs MSU+LPS no phagocytosis	No	No
medium vs MSU+LPS phagocytosis	Yes **	Yes **
medium vs nigericin	No	Yes *
medium vs ATP	Yes **	Yes *
LPS vs MSU no phagocytosis	No	No
LPS vs MSU phagocytosis	No	No
LPS vs MSU+LPS no phagocytosis	No	No
LPS vs MSU+LPS phagocytosis	Yes *	Yes *
LPS vs nigericin	No	No
LPS vs ATP	Yes *	No
MSU no phagocytosis vs MSU phagocytosis	Yes *	Yes *
MSU no phagocytosis vs MSU+LPS no phagocytosis	No	No
MSU no phagocytosis vs MSU+LPS phagocytosis	Yes **	Yes *
MSU no phagocytosis vs nigericin	No	No
MSU no phagocytosis vs ATP	Yes **	No
MSU phagocytosis vs MSU+LPS no phagocytosis	No	No
MSU phagocytosis vs MSU+LPS phagocytosis	No	No
MSU phagocytosis vs nigericin	No	No
MSU phagocytosis vs ATP	No	No
MSU+LPS no phagocytosis vs MSU+LPS phagocytosis	Yes *	No
MSU+LPS no phagocytosis vs nigericin	No	No
MSU+LPS no phagocytosis vs ATP	Yes *	No
MSU+LPS phagocytosis vs nigericin	No	No
MSU+LPS phagocytosis vs ATP	No	No
nigericin vs ATP	No	No

Table 5.2. Statistical analysis of inflammasome activation in M1 and M2 macrophages. Intracellular active caspase-1 levels were analyzed by flow cytometry after staining with a fluorescent antibody against caspase-1 (FAM-FLICA caspase-1 assay). MFI values obtained after subtracting the unstained sample were normalized to unstimulated cells. (\*\*\*)p<0.001, (\*\*) p=0.001-0.01, (\*) p=0.01-0.05, not significant if p>0.05.

### 5.3.2. Inactive forms of caspase-1 and IL-1 $\beta$

Once known that M1 macrophages exhibit higher levels of active caspase-1, levels of the inactive protein pro-caspase-1 were quantified in M1 and M2 macrophages. For this purpose, cytoplasm protein was extracted from macrophage cultures and the presence of caspase-1 and other inflammasome related proteins such as ASC and pro-IL $\beta$  were detected by western blot.

As shown in Figure 5.24, M1 macrophages exhibited higher levels of pro-caspase 1 (p45) when compared with M2 macrophages. Stimulation of the later with LPS increased the expression of this inactive enzyme. Apoptosis-associated speck-like protein containing a caspase recruitment domain (ASC), is a reversible adaptor molecule that connects nucleotide-binding oligomerization-domain proteins (NODs), such as NLRP3 with pro-caspase-1. ASC was undetectable in unstimulated M2 macrophages and was induced after LPS and to a lesser extend MSU stimulation (Figure 5.25). When analyzing the presence of IL-1 $\beta$ , its inactive form (pro-IL-1 $\beta$ ), showed the same pattern than ASC, increasing after LPS stimulation (Figure 5.25). But interestingly, a synergistic effect was observed in the presence of MSU and LPS. This result agrees with the higher levels of IL-1 $\beta$  observed our previous experiments when M2 macrophages were challenged with LPS and MSU together. This inactive cytokine was undetectable when macrophages were stimulated with MSU, explaining the lack of IL-1 $\beta$  production even these crystals can activate the inflammasome and increase the levels of active caspase-1, as previously showed by flow cytometry. Levels of the active form of IL-1 $\beta$  showed small differences between groups, probably because once activated, nearly all the cytokine is excreted to the extracellular media, and it is better to determine it in the supernatant.



**Figure 5.24.** Quantification of intracellular levels of inactive caspase-1 (p45) in M1 and M2 macrophages. Presence of pro-caspase-1 in M1 and M2 analyzed by western blot. Cells were stimulated with MSU (200  $\mu$ g/mL), LPS (100 ng/mL) for 18 hours. Intensity of each band was quantified with Photoshop software and values normalized to  $\beta$ -actin are represented in graph.

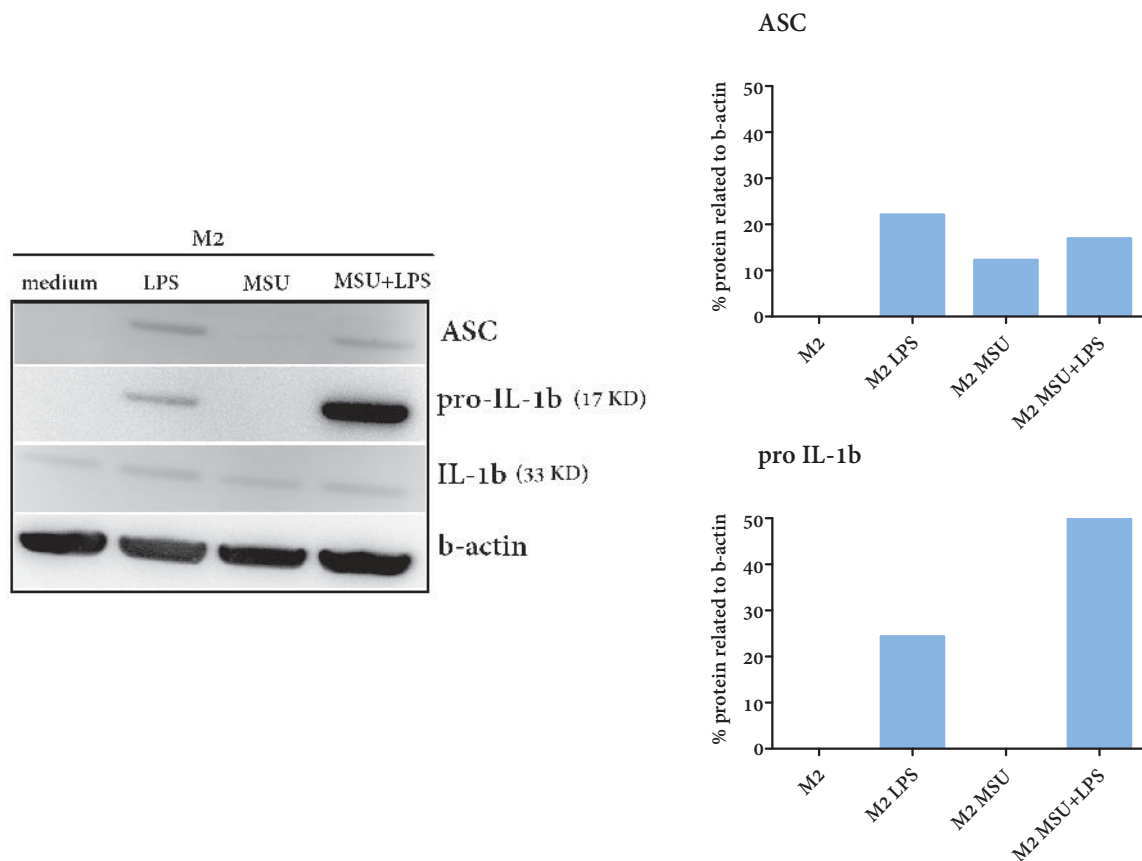


**Figure 5.25. Quantification of intracellular levels of ASC and pro-IL-1 $\beta$  in M2 macrophages.** Expression of ASC, pro-IL-1 $\beta$  and active IL-1 $\beta$  in cytoplasm of M2 macrophages was detected by western blot. Cells were stimulated with MSU (200  $\mu$ g/mL), LPS (100 ng/mL) for 18 hours. Intensity of each band was quantified with Photoshop software and values normalized to  $\beta$ -actin are represented in graph.

### 5.3.3. Expression of inflammasome related genes

As results obtained in previous experiments show that M1 macrophages exhibit higher levels of both the precursor and active caspase-1 compared with M2 macrophages, we wondered about the state of transcription of genes involved in the inflammasome in different polarization states. Thus, mRNA levels of caspase-1, IL-1 $\beta$  and NLRP3 were assessed by Real-Time PCR.

Briefly, M1 and M2 macrophage cultures were challenged on day 6 with MSU (200  $\mu$ g/mL), LPS (100 ng/mL) or both for 4 hours. RNA was isolated with NucleoSpin<sup>®</sup> RNA XS kit and after inverse transcriptase reaction cDNA was obtained. Selected sequences were amplified with primers designed for *caspase-1*, *IL-1 $\beta$*  and *NLRP3* genes and the amplification process was monitored in a LightCycler 480 using fluorescent probes or SYBRGreen. Next paragraphs expose the results from 5 independent experiments.



### 5.3.3.1. Caspase-1 gene expression

First, assessment of baseline expression of caspase-1 was performed comparing samples of non-stimulated macrophages (Figure 5.26). Our results showed that M1 macrophages had at baseline less expression of caspase-1 than M2 (mean +/- SEM: M1 0.85 +/- 0.17, M2 1.44 +/- 0.11,  $p=0.0216$ ). Both macrophage subtypes doubled mRNA expression when stimulated with LPS, whereas MSU did not have any effect, even decreased mRNA expression in M2 macrophages. M1 and M2 macrophages had the same behaviour after stimulation, with no statistically significant differences ( $p=0.7$  for LPS,  $p=0.1$  for MSU and  $p=1$  for MSU and LPS)

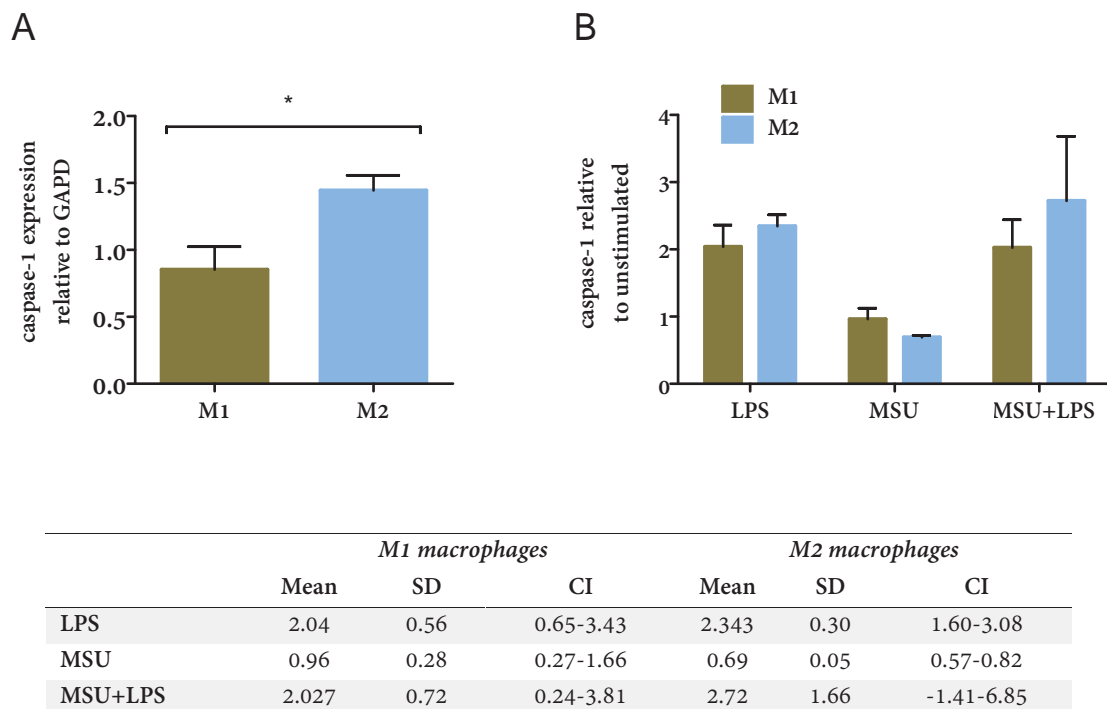
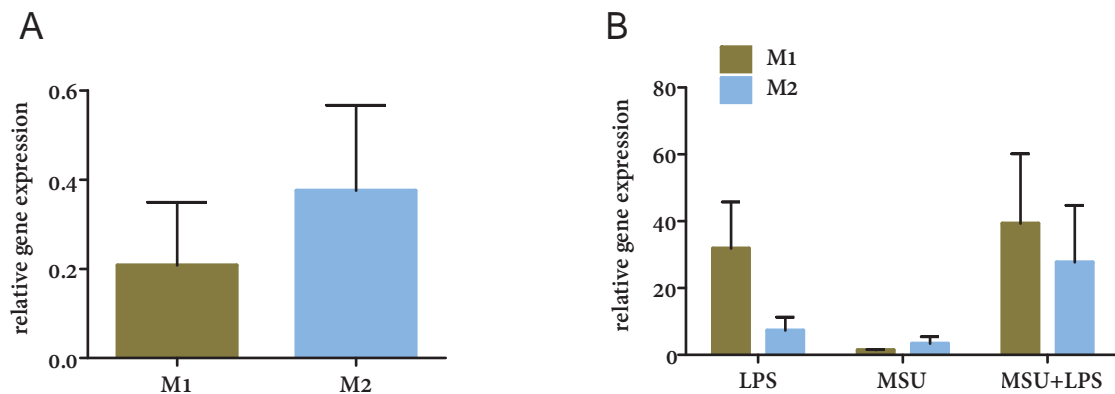


**Figure 5.26. Caspase-1 gene expression in M1 and M2 macrophages.** Macrophage cultures were stimulated with LPS (100 ng/mL), MSU (200  $\mu$ g/mL) or both for 4 hours. After RNA extraction and reverse transcriptase reaction, amplification was performed in a LightCycler 480 using a specific fluorescent probe. Quantification of RNA was normalized to *GADP* gene expression. Graph (A) represents caspase-1 expression in non-stimulated macrophages. Graph (B) represents the effect of LPS and MSU stimulation, relative to baseline levels. Table shows statistics from graph (B) in order to compare between M1 and M2 macrophages. \*  $p=0.0216$ .

### 5.3.3.2. *IL-1 $\beta$* gene expression

As shown in Figure 5.27, M1 and M2 macrophages exhibited similar levels of *IL-1 $\beta$*  mRNA (mean  $\pm$  SEM: M1 0.29  $\pm$  0.14, M2 0.37  $\pm$  0.19,  $p = 0.6250$ ). Once stimulated with LPS, expression of this gene increased, although differences between different experimental conditions did not reach significance (M1  $p = 0.0665$ , M2  $p = 0.1579$ ) probably due to the variability of the samples, that showed more deviation than previous experiments with caspase-1. This fact could also explain that the differences observed in LPS response between M1 and M2 macrophages were not statistically significant ( $p = 0.4$  for LPS,  $p = 0.7$  for MSU and  $p = 1$  for MSU+LPS). Of note, in M2 macrophages, although MSU crystals alone had a slightly effect of *IL-1 $\beta$*  expression, in combination with LPS increased mRNA values eight times.

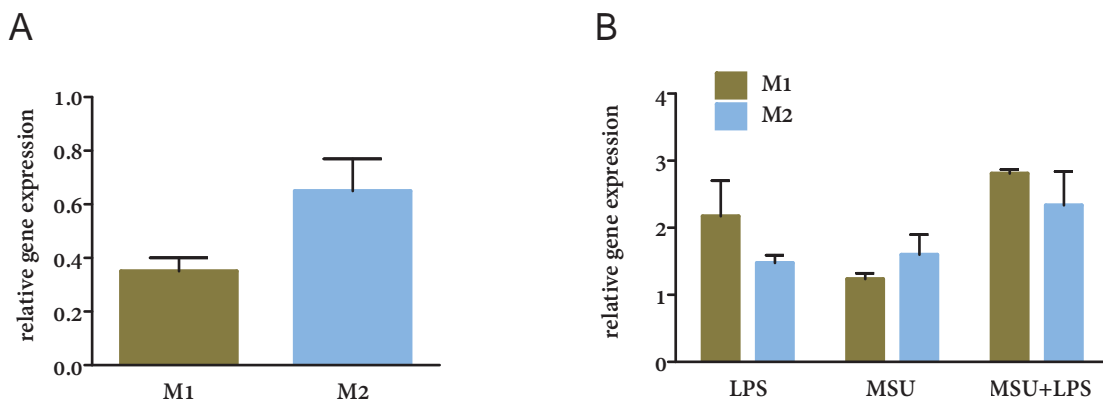


	<i>M1 macrophages</i>			<i>M2 macrophages</i>		
	Mean	SD	CI	Mean	SD	CI
LPS	31.80	24.17	-28.25-91.85	7.27	6.98	-10.07-24.61
MSU	1.45	0.19	0.97-1.94	3.37	3.54	-5.44-12.18
MSU+LPS	39.30	36.17	-50.54-129.2	24.70	29.56	-45.73-101.1

**Figure 5.27. *IL-1 $\beta$*  gene expression in M1 and M2 macrophages.** Macrophage cultures were stimulated with LPS (100 ng/mL), MSU (200  $\mu$ g/mL) or both for 4 hours. qRT-PCR was performed in a LightCycler 480 using a specific fluorescent probe and quantification of RNA was normalized to *GADP* gene expression. Graph (A) represents *IL-1 $\beta$*  expression in non-stimulated macrophages. Graph (B) represents the effect of LPS and MSU stimulation, relative to baseline levels. Table shows statistics from graph (B) in order to compare between M1 and M2 macrophages.

### 5.3.3.3. *NLRP3* relative gene expression

Although M2 macrophages had higher levels at the baseline (Figure 5.28), these differences were not statistically significant (mean $\pm$  SEM: M1 0.35  $\pm$  0.05, M2 0.65  $\pm$  0.12,  $p=0.1474$ ). Again, as with IL-1 $\beta$  expression, although LPS stimulation increased *NLRP3* gene expression, this differences were not statistically significant compared with MSU and MSU with LPS (M1  $p=0.107$ , M2= 0.3679) and no differences were observed between M1 and M2 responses.



	<i>M1 macrophages</i>			<i>M2 macrophages</i>		
	Mean	SD	CI	Mean	SD	CI
LPS	2.17	0.75	-4.56-8.9	1.47	0.16	0.01-2.936
MSU	1.23	0.12	0.15-2.31	1.6	0.42	-2.21-5.41
MSU+LPS	2.81	0.08	2.05-3.57	2.33	0.71	-4.08-8.752

**Figure 5.28. *NLRP3* gene expression in M1 and M2 macrophages.** Macrophage cultures were stimulated with LPS (100 ng/mL), MSU (200  $\mu$ g/mL) or both for 4 hours. qRT-PCR was performed in a LightCycler 480 using a specific the fluorescent dye SYBR Green. Gene expression relative to the housekeeping gene GAPD was then calculated. Graph (A) represents *NLRP3* expression in non-stimulated macrophages. Graph (B) represents the effect of LPS and MSU stimulation, relative to baseline levels. Table shows statistics from graph (B) in order to compare between M1 and M2 macrophages.



6.

**The mononuclear phagocyte  
system in patients with gout**



The central role of the mononuclear phagocyte system in gout has been highlighted during the last years. Macrophages initiate the inflammatory response to MSU crystals and produce inflammatory cytokines and chemokines that induce migration of blood monocytes to further amplify the inflammatory response. One of the questions that remain unanswered in gout is why some individuals with hyperuricemia, and even with MSU deposits, remain asymptomatic. In the first part of this chapter we investigated the possibility that it could be due to a greater reactivity of blood monocytes to MSU crystals in patients who develop gout. With this aim, we compared inflammasome activation in monocytes from patients with gout and healthy donors. Additionally, the possibility of polymorphisms in *NLRP3* gene, that could modify inflammasome activation, was explored by genotyping this gene in patients with gout.

Different monocyte subpopulations in peripheral blood with differential functions have been described based on CD14 and CD16 expression. Of them, intermediate monocytes (CD14<sup>++</sup>CD16<sup>+</sup>) are expanded in inflammatory diseases such as rheumatoid arthritis, sarcoidosis, sepsis and seem to be involved in atherosclerosis but no studies have analyzed monocyte subpopulations in gout. In the last part of this chapter we analyzed the distribution of monocyte subpopulations in gout in asymptomatic patients or during an acute flare and its relation with uric acid levels and inflammation.

## 6.1. Demographic data

We recruited 19 healthy controls and 17 patients with gout, of them 13 patients were asymptomatic and in 4 patients samples were obtained during a gout flare. Demographic characteristics of subjects are summarized in Table 6.1.

All patients with gout were males, whereas women represented 42% of the control group. Patients with asymptomatic group were older ( $p=0.0006$ ) and had higher uric acid ( $p=0.033$ ) and creatinine levels ( $p=0.015$ ) when compared with the control group. Of note, CRP levels were higher in patients, whether or not they had an acute flare (asymptomatic  $p=0.0099$ , acute gout  $p=0.0072$ ), although mean levels in asymptomatic patients were below the normal range of CRP, considered 0.5 mg/mL.

Most patients with asymptomatic gout were on ULT therapy, mainly with allopurinol (600 mg/daily in one patient, 300 mg/daily in two, 200 mg/daily in one and 100 mg/daily in five patients). Other reported treatments were febuxostat in two patients and benzbromarone in one. On the other hand, in the group with an acute flare only half of them were on hypouricemic treatment. Gout flare was monoarticular in three patients and three joints were affected in one. Mean duration of gout was longer in the asymptomatic group ( $p=0.4662$ ). Of note, none of the patients recruited had tophi on physical examination.

	<i>Asymptomatic gout</i>	<i>Acute gout</i>	<i>Controls</i>
<b>n</b>	13	4	19
<b>Male sex, n (%)</b>	13 (100)	4 (100)	11 (57,9)
<b>Age, mean years</b>	64,9 ***	56,5	40,7
<b>Uric acid , mean mg/dL</b>	6,39 *	6,93	4,97
<b>Creatinine, mean mg/dL</b>	1,06 **	0,90	0,75
<b>CRP, mean mg/dL</b>	0,32 *	4,94 **	0,06
<b>Hypouricemic treatment, n (%)</b>	12 (92.3)	2 (50)	
	Allopurinol 9	Allopurinol 2	
	Febuxostat 2		
	Benzbromarone 1		
<b>Duration of gout, mean years</b>	23,6	15,3	

**Table 6.1. Demographic data of gout patients and controls.** Statistical analysis between groups was performed using Kruskal-Wallis test with Dunn's test to compare pairs of columns. Pairs with statistical differences were then compared with Mann-Whitney test, adjusting p values with the Bonferroni's correction to counteract the problem of multiple comparisons. CPR: C-reactive protein. . (\*\*\*) $p<0.001$ , (\*\*) $p=0.001-0.01$ , (\*) $p=0.01-0.05$ .



## 6.2. Caspase-1 activity in patients with gout

Hyperuricemia is the main risk factor of gout, increasing the possibility of arthritis with uric acid levels. Nevertheless, not all patients with high uric acid will develop clinical gout. Non-invasive imaging techniques such as ultrasonography have demonstrated that some patients, even in the presence of MSU deposits, remain asymptomatic. The reason of this phenomenon is still unknown. Our hypothesis is that patients with clinical gout could exhibit a higher inflammatory response to MSU crystals than asymptomatic individuals. As IL-1 $\beta$  has been considered the main inflammatory cytokine in gout and MSU crystals activate NLRP3 inflammasome, we explored the possibility that differences in inflammasome functionality could play a role. We compared inflammasome activation and IL-1 $\beta$  production between a cohort of patients with gout and a group of healthy controls. Moreover, to investigate the possibility that polymorphisms in *NLRP3* gene could be involved in the response to MSU crystals, we analyzed this gene in the group of patients with gout.

### 6.2.1. Demographic data

For these experiments, we selected 7 patients with gout, without arthritis in the moment of the interview and without any anti-inflammatory treatment such as NSAIDs, colchicine or aspirin. On the other hand, the control group included 7 healthy males, over 40 years old, without any anti-inflammatory treatment. Demographic data of these patients are summarized in Table 6.2.

All subjects were men and the mean age in gout group was higher. Uric acid, creatinine and CRP levels were higher in the group of patients, but these differences did not reach statistical significance. All patients except one were treated with ULT therapy, mainly allopurinol, three of them with 100 mg daily and the other two required higher doses of 300 mg daily.

	<i>Gout</i>	<i>Controls</i>
<b>Male sex (n)</b>	7	7
<b>Mean age, mean years</b>	66.5 **	52.7
<b>Uric acid , mean mg/dL</b>	6.69	5.75
<b>Creatinine, mean mg/dL</b>	0.94	0.81
<b>CRP, mean mg/dL</b>	0.32	0.08
<b>Time evolution gout, mean years</b>	22.01	
<b>Uric acid lowering therapy (n)</b>	6	
Febuxostat	1	
Allopurinol	5	

Table 6.2. Demographic characteristics of gout patients and controls. (\*\*)  $p=0.0044$  by Student's t-test.

### 6.2.2. Assessment of inflammasome activity

Cleavage and activation of caspase-1 depends upon inflammasome assembly and consequently, the increase of active caspase-1 levels after stimulation can reflect the degree of inflammasome activation. Therefore, to compare inflammasome functionality between patients with gout and healthy donors, we quantified caspase-1 levels by flow cytometry. Analysis was performed in peripheral blood monocytes because these cells migrate into the joint to take part in the inflammatory response to MSU crystals and they can also differentiate towards macrophages.

PBMCs were stimulated with MSU (200  $\mu\text{g}/\text{mL}$  for 1 hour) and LPS (100  $\text{ng}/\text{mL}$  for 1 hour) and as positive controls we used nigericin (20  $\mu\text{g}/\text{mL}$  for 15 minutes) and ATP (5  $\text{mM}$  for 15 minutes). After stimulation, active caspase-1 was labelled with the Caspase-1 FLICA™ Detection Kit (Immunochemistry Technologies) and mean fluorescence intensity (MFI) of each sample was analyzed by flow cytometry, gating the population of blood monocytes as shown in Figure 6.1 A.

#### 6.2.2.1. Baseline levels of active caspase-1

First, we compared the presence of active caspase-1 in unstimulated monocytes. As showed in graph 6.1 B, no differences were founded between patients with gout and healthy controls (mean  $\pm$  SEM: controls 22.01  $\pm$  0.81, gout 22.34  $\pm$  1.72,  $p=0.8650$ ).

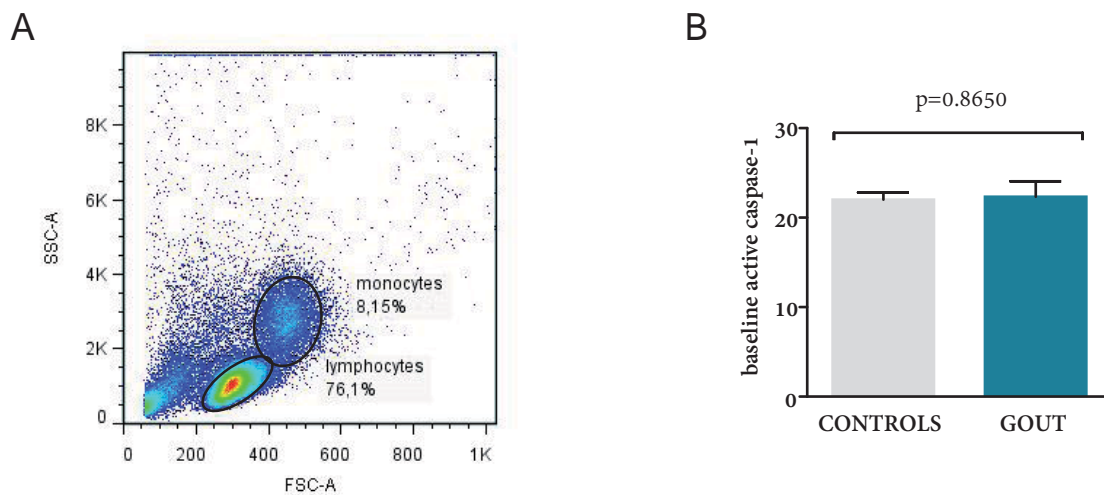


**Figure 6.1. Caspase-1 levels in monocytes at steady state.** Intracellular active caspase-1 was assessed in PBMCs by flow cytometry using the fluorescent antibody FAM-FLICA. (A) Monocytes were gated based on their SSC and FSC values. Graph (B) presents mean fluorescent intensity values of active caspase-1 from each sample normalized to unstained sample. Statistical analysis was performed with unpaired t test.

### 6.2.2.2. Caspase-1 activation in stimulated monocytes

Then, we compared inflammasome activation in both groups, analyzing the increase of active caspase-1 after stimulation with MSU crystals (200  $\mu\text{g}/\text{mL}$ ) for 1 hour. As expected, MSU crystals increased active caspase-1 in both patients and controls (Figure 6.2). However, patients with gout exhibited higher levels of active caspase-1 after stimulation ( $p=0.0419$ ), suggesting higher inflammasome activity (Figure 6.3). No differences were observed in caspase-1 activation when monocytes were challenged with other inflammasome activators such as ATP ( $p=0.7730$ ) or nigericine ( $p=0.0842$ ).

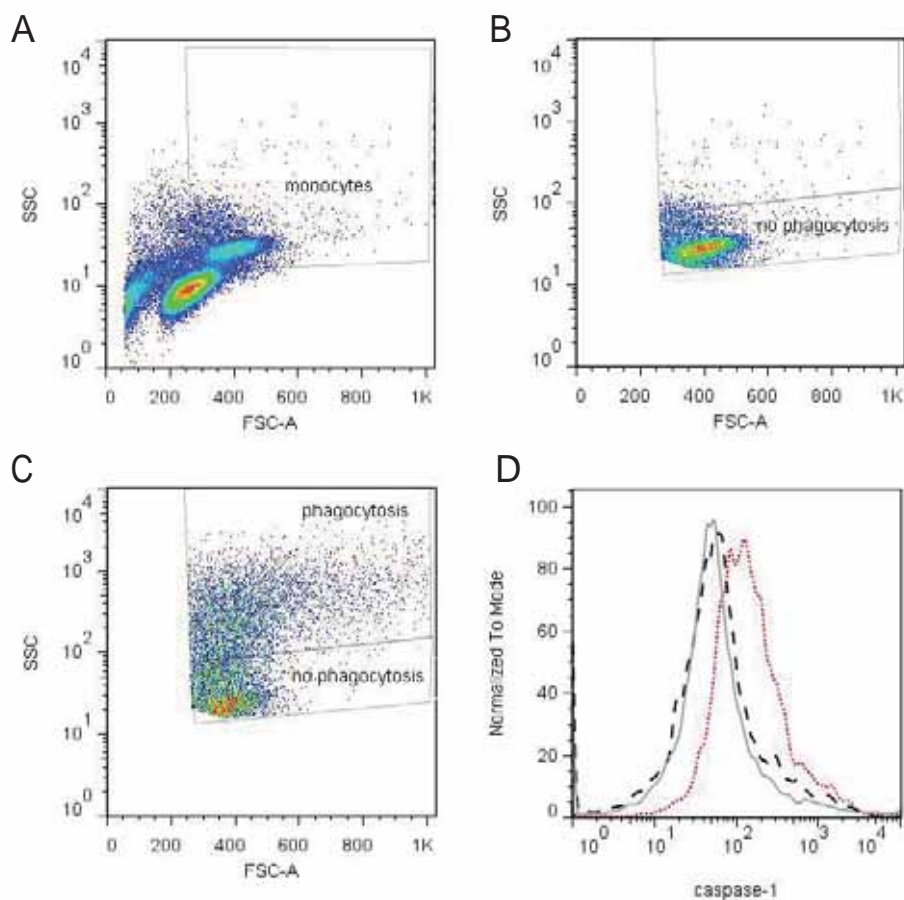
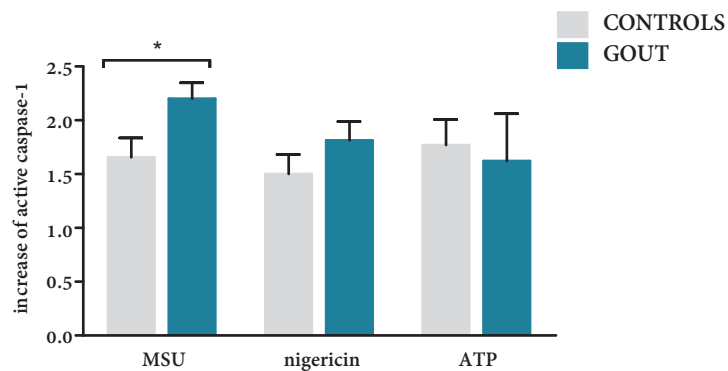


**Figure 6.2.** Analysis of inflammasome activation in monocytes after MSU phagocytosis. PBMCs were stimulated with MSU crystals (200  $\mu\text{g}/\text{mL}$ ) for one hour and then stained with a fluorescent antibody that binds to active caspase-1. Samples were analyzed by flow cytometry, gating the monocyte population on FSC/SSC plot (A). Taking as a reference the monocytes in unstimulated sample (B), monocytes that phagocyte crystals were gated as they increase their SSC signal (C). Histogram (D) shows fluorescent signal of active caspase-1 on X-axis and the number of cells as the percentage of maximum bin on the Y-axis. Monocytes with MSU crystals (red dotted line) increased their active caspase-1 levels comparing with monocytes without crystals (black dashed line) and unstained sample (grey line).

When comparing the effect of the different stimulations in each group, in patients with gout response to MSU crystals was higher than stimulation with nigericin ( $p=0.0313$ ) but no differences were observed comparing MSU and ATP ( $p=0.4375$ ) or nigericin with ATP ( $p=0.4775$ ). On the other hand, in the group of healthy donors, no differences were observed between the three activators of the inflammasome ( $p=0.9537$ ). Table 6.3 summarises the results obtained from our stimulation experiments.



<i>Stimulation</i>	<i>Group</i>	<i>Mean</i>	<i>SD</i>	<i>CI</i>	<i>p value</i>
MSU	Healthy	1.66	0.40	1.15-2.16	0.0419 (†)
	Gout	2.20	0.36	1.82-2.58	
Nigericin	Healthy	1.50	0.48	1.06-1.94	0.0842 (‡)
	Gout	1.81	0.47	1.38-2.24	
ATP	Healthy	1.77	0.63	1.19-2.35	0.7730 (†)
	Gout	1.62	1.16	0.55-2.70	

**Figure 6.3. Inflammasome activation in monocytes.** PBMCs from gout patients and healthy controls were stimulated with MSU (200  $\mu\text{g}/\text{mL}$  for 1 hour), nigericin (20  $\mu\text{g}/\text{mL}$  for 15 minutes) or ATP (5 mM for 15 minutes) and activation of inflammasome was analyzed by flow cytometry by quantification active caspase-1 in monocyte population. Graph shows the increase of active caspase-1 relative to baseline levels. Table shows the results from comparison between gouty patients and healthy controls. Statistical analysis was performed by unpaired t-test (†) or Mann Whitney test (‡). SD: standard deviation, CI: 95% confidence interval.

Phagocytic capacity of monocytes could influence the effect of these crystals, therefore we compared the percentage of phagocytosis in monocytes from patients and healthy controls. We observed no differences regarding MSU phagocytosis (Figure 6.4), so we could conclude that MSU crystals have a higher effect on caspase-1 activation in monocytes from patients with gout and that this effect is independent of their phagocytic activity.

We next correlated activation of caspase-1 after MSU challenging with uric acid levels, creatinine and CRP. A positive relation was observed with uric acid levels ( $r=0.27$ ,  $p=0.449$ ), creatinine ( $r=0.12$ ,  $p=0.7589$ ), and especially with CRP ( $r=0.45$ ,  $p=0.1912$ ), although none of them reach statically significance, probably due to the sample size, and we could not demonstrate correlation.

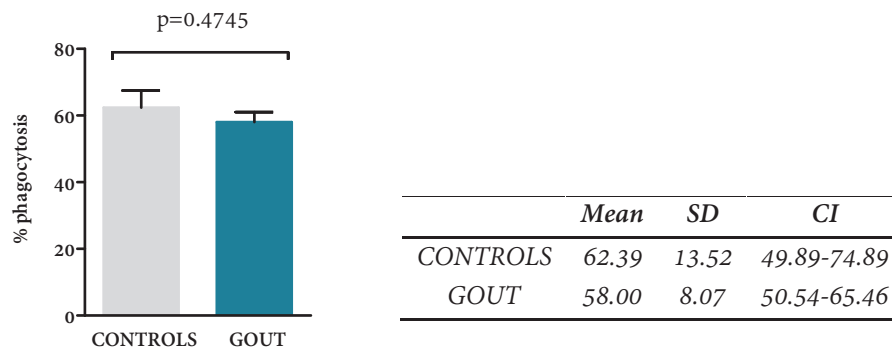


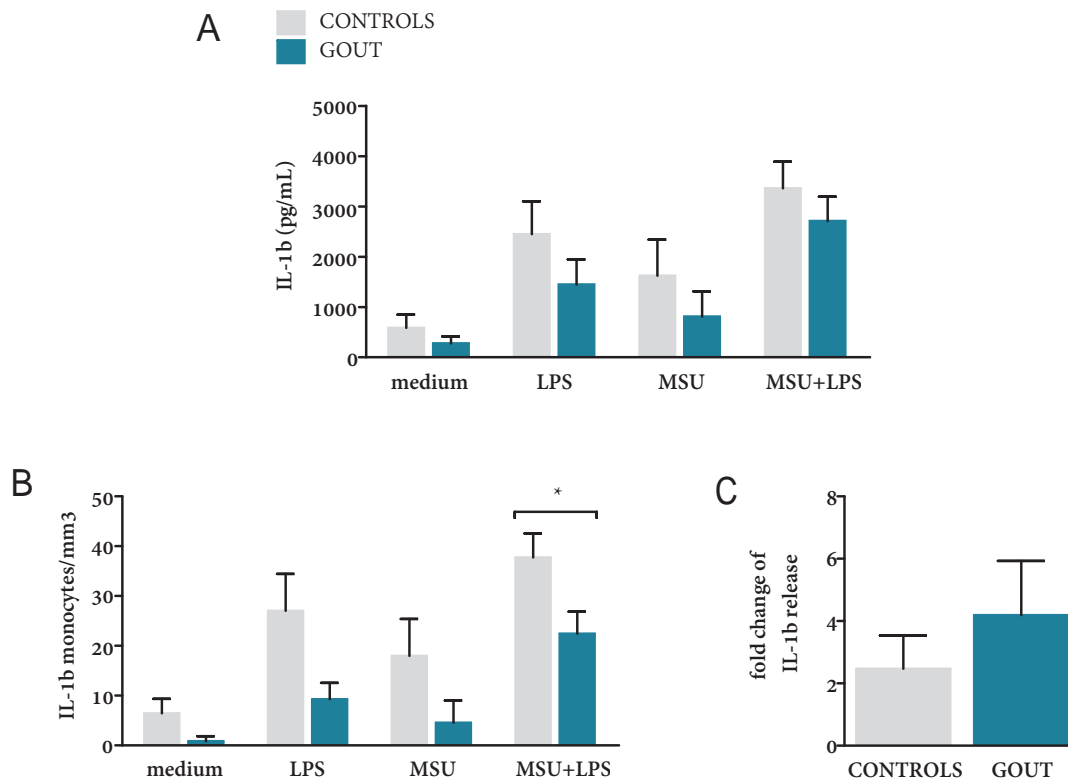
Figure 6.4. MSU phagocytosis in monocytes from patients with gout and healthy donors. Phagocytosis of MSU was quantified by flow cytometry as cells with crystals increase their SSC values. SD: standard deviation, CI: 95% confidence interval.

### 6.2.3. IL-1 $\beta$ production after MSU stimulation

Peripheral blood mononuclear cells were cultured on 96 well plates and stimulated with MSU (200  $\mu\text{g}/\text{mL}$ ), LPS (100  $\text{ng}/\text{mL}$ ) or both together for 24 hours. Levels of IL-1 $\beta$  in supernatants were compared between patients with gout ( $n=6$ ) and healthy donors ( $n=6$ ). Unexpectedly, patients with gout exhibited a higher production of IL-1 $\beta$  when exposed to MSU or LPS, although these differences were not statistically significant (Figure 6.5). As samples from patients with gout had higher number of monocytes (mean $\pm$ -SEM controls 87.50 $\pm$ -7.55, gout 111 $\pm$ -10.32 cells/ $\text{mm}^3$ ,  $p=0.093$ ), IL-1 $\beta$  production was normalized to monocytes/ $\text{mm}^3$ , making these differences even more pronounced. However, the synergism between MSU and LPS was more important in gouty patients although differences did not reach significance (mean $\pm$ -SEM, controls 2.47 $\pm$ -1.07, gout 4.19 $\pm$ -1.74,  $p=0.1255$ ).

As our experiments with soluble uric acid and M2 macrophages had showed that uric acid has a suppressive effect on IL-1 $\beta$  production, we correlated our results with serum uric acid levels.

We a negative relation between IL-1 $\beta$  production after stimulation with MSU and LPS and uric acid but correlation was not statistically significant ( $r = -0.233$  and  $p = 0.5170$ ).



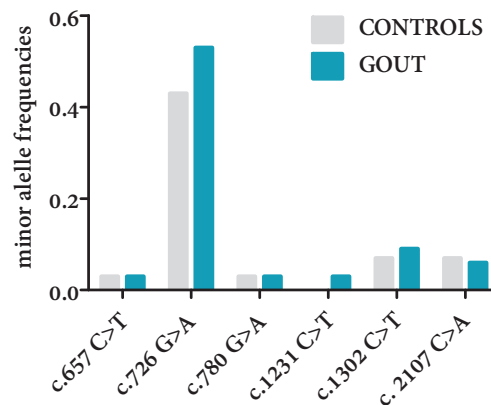
Stimulation	Group	Mean	SD	CI	p
medium	Healthy	6.55	6.98	-0.77 - 13.88	0.1404 (†)
	Gout	1.32	1.83	-0.96 - 3.60	
LPS	Healthy	27.03	18.09	8.04 - 46.02	0.0714 (†)
	Gout	9.28	7.34	0.17 - 18.39	
MSU	Healthy	18.15	17.97	-0.71 - 37.01	0.3109 (‡)
	Gout	4.76	9.88	-7.51 - 17.02	
MSU+LPS	Healthy	37.74	11.81	25.35 - 50.14	0.0473 (†)
	Gout	22.45	9.89	10.17 - 34.73	

**Figure 6.5. IL-1 $\beta$  production in patients with gout.** PBMCs were challenged with LPS (100 ng/mL), MSU (200  $\mu$ g/mL) or both for 24 hours, and IL-1 $\beta$  was quantified in supernatants by ELISA (A). In graph (B) IL-1 $\beta$  production was normalized to monocytes/mm<sup>3</sup> and results from statistical analysis are depicted in the table. Graph (C) represents the fold change in IL-1 $\beta$  production with MSU and LPS compared with LPS alone. Results from 6 patients with gout and 6 healthy donors. Comparison between gouty patients and healthy controls was performed by unpaired t-test (†) or Mann Whitney test (‡). SD: standard deviation, CI: 95% confidence interval. \*  $p = 0.0473$ .

#### 6.2.4. Polymorphisms of *NLRP3* gene in gout patients

In order to understand why PBMCs from patients with gout exhibit a higher inflammasome activity after MSU stimulation, we investigated the possibility that *NLRP3* polymorphisms could influence the response to MSU crystals. Cryopyrin-associated periodic fever syndromes (CAPS) are inherited autoinflammatory diseases caused by heterozygous gain-of-function mutations in *NLRP3* gene that lead to a higher response of the inflammasome after stimulation. As most of mutations in CAPS syndromes are located in exon 3, which encodes de NACHT domain of *NLRP3*, we analyzed this segment in the group of patients with gout (n=16). For each polymorphism, frequencies of the minor allele (MAF) were compared with the control population of Iberian ancestry from the 1,000 Genome Project.

As shown in Figure 6.7, The majority of polymorphisms founded in our patients consisted in nucleotide changes that did not translated in amino acid changes. One variation that results in an amino acid change was observed in two patients. This variant, the Q703K, has been associated with spondyloarthritis. When comparing with the control population (n=14), no differences were observed.



Sequence change	Protein name	rs number	MAF GOUT	MAF controls	p	Odds ratio (95%CI)
c.657 C>T	p.Thr219Thr	rs7525979	0.03	0.03	1	0.82 (0.05-13.71)
c.726 G>A	p.Ala242Ala	rs3806268	0.53	0.43	0.46	1.5 (0.55-4.11)
c.780 G>A	p.Arg260Arg	rs4925543	0.03	0.03	1	0.82 (0.05-13.71)
c.1231 C>T	p.Leu411Leu	rs148478875	0.03	0.0059	1	2.55 (0.1-65.18)
c.1302 C>T	p.Ser434Ser	rs34298354	0.09	0.07	1	1.26 (0.19-8.11)
c.2107 C>A	p.Gln703Lys	rs35829419	0.027	0.041	1	0.81 (0.11-6.17)

Figure 6.7. Analysis of *NLRP3* gene in gout. Exon 3 of *NLRP3* was sequenced in a group of patients with gout (n=16). The Iberian population of Spain from 1000 Genome Project was taken as a reference. Statistical analysis was performed with Fisher exact test. MAF: minor allele frequency.

### 6.3. Monocyte subpopulations in gout

Blood monocytes have a variety of functions such as tissue repair and defence against infections or neoplastic cells. This heterogeneity is explained by the existence of monocyte subsets with phenotypic and functional differences. Scientific community has recognized three different monocyte subsets based on the expression of the cell surface antigens CD14 and CD16: classical ( $CD4^{++} CD16^{-}$ ), intermediate ( $CD14^{++} CD16^{+}$ ) and non-classical ( $CD14^{+} CD16^{++}$ ) monocytes. Of them, intermediate and non-classical monocytes are expanded in inflammatory diseases such as rheumatoid arthritis, sepsis, HIV infection and atherosclerosis. In the case of rheumatoid arthritis, the expansion of the  $CD16^{+}$  population correlates with disease activity and decreases after treatment. It is unknown, however if these "inflammatory" monocytes are the cause of the burden or if they expand in response to the inflammatory milieu. Our hypothesis is that  $CD16^{+}$  monocytes could be expanded during gout flares and these monocytes could migrate into the joint to participate in the inflammatory response to MSU crystals. With this aim we analyzed monocyte subpopulations in 4 gouty patients during an acute flare.

As gout has been associated with an increase in cardiovascular risk, our hypothesis is that the expansion of the intermediate phenotype, even in the absence of arthritis, could reflect subclinical inflammation and play a role in the development of atherosclerosis. Therefore, we analyzed monocyte subpopulations in a group of asymptomatic patients compared with healthy donors.

#### 6.3.1. Analysis of monocyte subpopulations

Peripheral blood monocyte subpopulations were assessed in 19 healthy controls, 13 patients diagnosed of gout but asymptomatic and 4 patients with gout during an acute flare. Samples of peripheral blood were collected in EDTA tubes by venipuncture, and staining with monoclonal antibodies against CD45, HLA-DR, CD14 and CD16 was performed as explained in methods section. Samples were analyzed by flow cytometry using the gate strategy proposed by Ziegler-Heitbrock *et al.* <sup>[249]</sup>. Uric acid, creatinine and PCR were quantified in serum. Tables 6.3, 6.4 and 6.4 show the results from participants in each group.



<i>code</i>	<i>sex</i>	<i>age</i>	<i>Classical</i> <i>CD14<sup>++</sup>CD16<sup>-</sup></i>	<i>Intermediate</i> <i>CD14<sup>++</sup>CD16<sup>+</sup></i>	<i>Non-classical</i> <i>CD14<sup>+</sup>CD16<sup>++</sup></i>	<i>Cr</i>	<i>UA</i>	<i>CPR</i>
G-6	W	61	94.8	1.7	3.4	0.72	3.9	0.03
G-9	M	63	89.9	3.9	5.1	1.01	6.5	0.02
G-10	W	23	86.1	4.7	9.2	0.49	5.5	0.03
G-11	W	24	86.4	3.2	10.4	0.57	3.4	0.01
G-12	W	30	88.2	4.3	7.3	0.65	4	0.06
G-13	W	47	82.4	6.9	10.7	0.6	2.8	0.01
G-14	W	42	85.9	4	9.7	0.8	6.1	0.12
G-17	M	29	90.1	5.6	4.2	0.96	5.4	0.06
G-18	M	51	88.3	2.3	9.2	0.81	5.8	0.04
G-22	M	52	72.7	8.7	18.5	0.59	4.3	0.26
G-25	M	48	85.7	5	9.3	0.74	5.5	0.05
G-30	M	28	89.7	3.1	7	0.93	6.1	0.01
G-31	M	46	75	7	17.9	0.94	5.8	0.03
G-32	M	55	85.4	3.4	11.2	0.75	6.6	0.09
G-34	M	32	87.7	7.5	4.8	0.69	5.9	0.12
G-35	M	54	72.9	9.5	17.6	NA	NA	NA
G-36	M	30	90	3.9	6	0.9	5.3	0.02
G-37	W	31	90.5	4.2	5.6	0.66	2.9	0.03
G-38	W	28	86.1	4.1	9.7	0.61	3.7	0.02
<b>Mean</b>		<b>40.7</b>	<b>85.67</b>	<b>4.89</b>	<b>9.31</b>	<b>0.74</b>	<b>4.97</b>	<b>0.056</b>
<b>SEM</b>		<b>3.01</b>	<b>1.38</b>	<b>0.49</b>	<b>1.04</b>	<b>0.04</b>	<b>0.29</b>	<b>0.01</b>

**Table 6.3. Monocyte subpopulations in healthy donors.** Results are expressed as percentage from total monocytes. W: women, M: men, SEM: standard error, Cr: creatinine (mg/dL), UA: uric acid (mg/dL), CRP: C-reactive protein (mg/dL), NA: non-available.

<i>code</i>	<i>sex</i>	<i>age</i>	<i>Classical</i> <i>CD14<sup>++</sup>CD16<sup>-</sup></i>	<i>Intermediate</i> <i>CD14<sup>++</sup>CD16<sup>+</sup></i>	<i>Non-classical</i> <i>CD14<sup>+</sup>CD16<sup>++</sup></i>	<i>Cr</i>	<i>UA</i>	<i>CPR</i>
G-7	M	57	88.8	3.7	7.1	1.04	4.4	0.88
G-16	M	67	86.3	5.7	8	1.03	4.8	0.11
G-19	M	66	86.7	4.6	8.6	1.19	6.7	0.81
G-20	M	50	83.2	5	11.7	0.98	7.1	0.03
G-24	M	68	81.2	6.7	12.1	0.8	7.1	0.24
G-26	M	41	88.2	4.2	7.6	1.02	4	0.42
G-29	M	85	90.6	3.4	5.9	0.97	5.9	0.12
G-33	M	54	83.7	4.3	12	0.83	6.5	0.06
G-39	M	NA	88.2	3.4	8.4	0.74	9.3	0.82
G-40	M	69	82.1	3.5	14.3	0.95	7.6	0.08
G-41	M	75	90.7	2.6	6.6	1.36	8.6	0.06
G-43	M	75	88.7	3	12	0.82	6.5	0.57
G-44	M	72	93.1	4.6	2.3	2.06	4.5	0.02
<b>Mean</b>		<b>64.9</b>	<b>87.04</b>	<b>4.21</b>	<b>8.97</b>	<b>1.061</b>	<b>6.38</b>	<b>0.32</b>
<b>SEM</b>		<b>3.55</b>	<b>1.00</b>	<b>0.32</b>	<b>0.91</b>	<b>0.095</b>	<b>0.45</b>	<b>0.09</b>

**Table 6.4. Monocyte subpopulations in asymptomatic gouty patients.** Results are expressed as percentage from total monocytes. W: women, M: men, SEM: standard error, Cr: creatinine (mg/dL), UA: uric acid (mg/dL), CRP: C-reactive protein (mg/dL), NA: non-available.

<i>code</i>	<i>sex</i>	<i>age</i>	<i>Classical</i> <i>CD14<sup>++</sup>CD16<sup>-</sup></i>	<i>Intermediate</i> <i>CD14<sup>++</sup>CD16<sup>+</sup></i>	<i>Non-classical</i> <i>CD14<sup>+</sup>CD16<sup>++</sup></i>	<i>Cr</i>	<i>UA</i>	<i>PCR</i>
G-21	M	69	77.4	9.6	13	1.22	5.1	7.21
G-23	M	46	77	11.3	11.7	0.73	8.8	5.04
G-27	M	51	88.3	7.1	4.6	0.7	6.9	5.66
G-28	M	60	85.7	6.4	7.9	0.95	6.9	1.83
<b>Mean</b>		<b>56.5</b>	<b>82.1</b>	<b>8.6</b>	<b>9.3</b>	<b>0.9</b>	<b>6.9</b>	<b>4.9</b>
<b>SEM</b>		<b>5.07</b>	<b>2.88</b>	<b>1.13</b>	<b>1.90</b>	<b>0.12</b>	<b>0.75</b>	<b>1.13</b>

**Table 6.5. Monocyte subpopulations during acute gout.** Results are expressed as percentage from total monocytes. W: women, M: men, SEM: standard error, Cr: creatinine (mg/dL), UA: uric acid (mg/dL), CRP: C-reactive protein (mg/dL).

Percentages of classical and non-classical monocytes did not significantly differ between groups but, as expected, the intermediate subset was expanded in patients with an acute flare of gout (Figure 6.8), with a trend towards a decrease of classical monocytes in these patients. Statistical analysis showed differences in numbers of intermediate monocytes between patients with acute gout and both healthy donors and asymptomatic patients ( $p=0.0501$  and  $p=0.0165$  respectively). Figure 6.9 presents results from one healthy donor and one patient with arthritis and illustrates the increment of the intermediate phenotype. Of note, no differences were observed in the percentage of intermediate monocytes between asymptomatic patients and healthy controls.

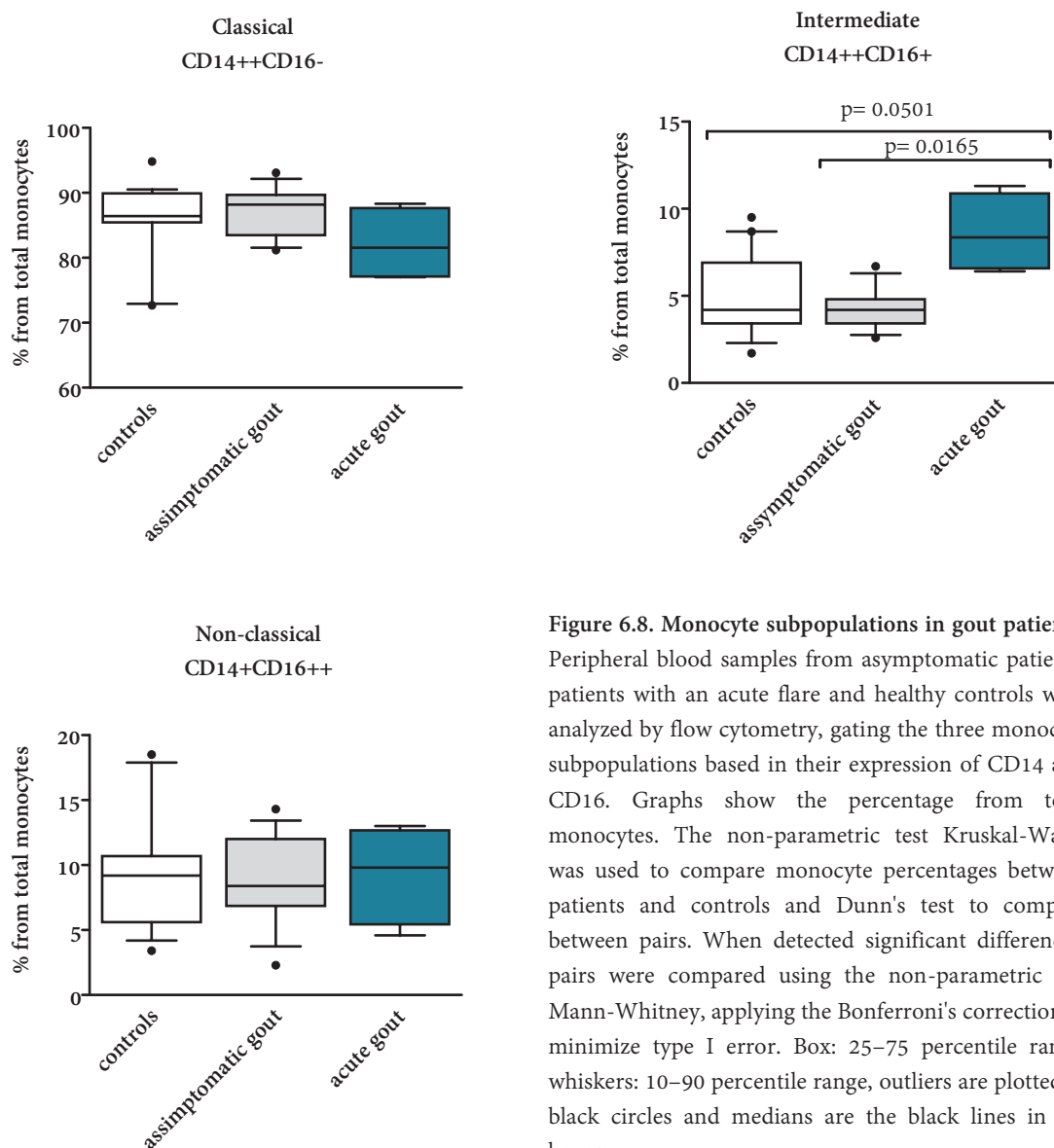


**Figure 6.8. Monocyte subpopulations in gout patients.** Peripheral blood samples from asymptomatic patients, patients with an acute flare and healthy controls were analyzed by flow cytometry, gating the three monocyte subpopulations based in their expression of CD14 and CD16. Graphs show the percentage from total monocytes. The non-parametric test Kruskal-Wallis was used to compare monocyte percentages between patients and controls and Dunn's test to compare between pairs. When detected significant differences, pairs were compared using the non-parametric test Mann-Whitney, applying the Bonferroni's correction to minimize type I error. Box: 25–75 percentile range, whiskers: 10–90 percentile range, outliers are plotted as black circles and medians are the black lines in the boxes.

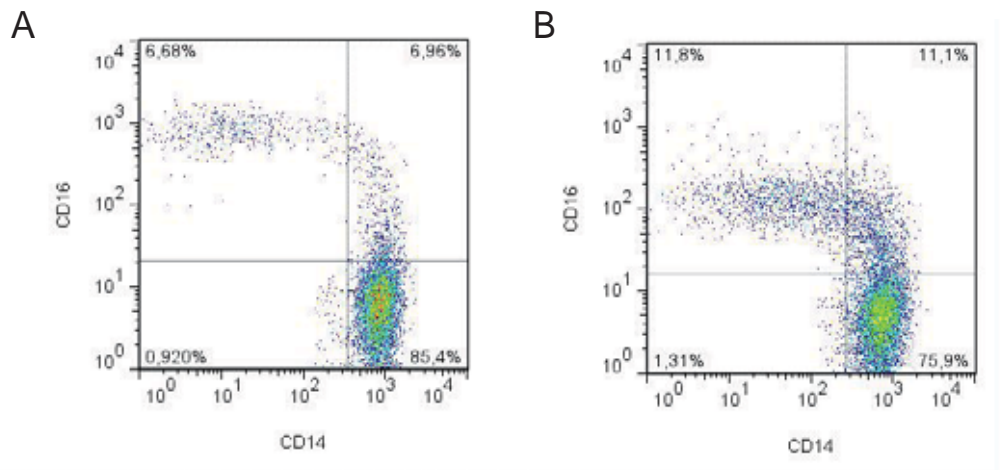


Figure 6.9. Flow cytometry analysis of blood monocyte subsets. Results of monocyte subpopulations in one healthy donor (A) and in one patient with an acute flare of gout (B), showing that the population of CD14<sup>++</sup>CD16<sup>+</sup> monocytes is expanded in patients with active arthritis.

### 6.3.1.1. Relation of monocytes with uric acid, creatinine and CRP

To investigate a possible relation between monocyte subpopulations and age, uric acid, creatinine and CRP, correlation between percentage of monocytes and these variables was evaluated using the Spearman coefficient rank ( $r_s$ ). Only a weak positive relation was observed between intermediate monocytes and CRP levels, but results were not significant and therefore no correlation could be demonstrated (Figure 6.10). This result is consistent with our previous observation about the expansion of intermediate population in patients with arthritis and suggests that, in the context of inflammation, this subpopulation tends to rise.

	<i>Classical</i>	<i>Intermediate</i>	<i>Non-classical</i>
<b>Age</b>	$r_s = -0.01036$ $p = 0.9536$	$r_s = -0.1101$ $p = 0.5353$	$r_s = 0.08349$ $p = 0.6388$
<b>Creatinine</b>	$r_s = 0.2349$ $p = 0.1744$	$r_s = -0.1075$ $p = 0.5388$	$r_s = -0.1626$ $p = 0.3506$
<b>Uric acid</b>	$r_s = -0.1890$ $p = 0.2770$	$r_s = -0.0074$ $p = 0.9662$	$r_s = -0.1957$ $p = 0.2598$
<b>CRP</b>	$r_s = -0.2434$ $p = 0.1588$	$r_s = 0.3135$ $p = 0.0667$	$r_s = 0.1735$ $p = 0.3190$

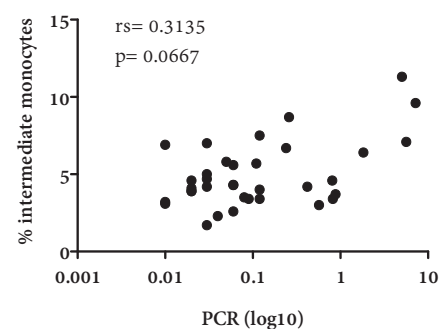
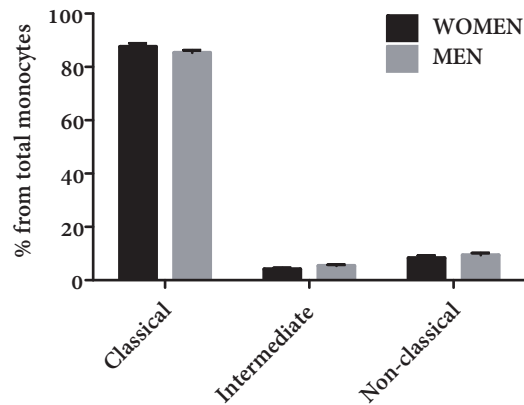


Figure 6.10 Correlation analysis of monocyte subpopulations, age and biochemical parameters in sera. Monocyte subpopulations from peripheral venous blood were assessed by flow cytometry, and results were correlated with age and levels of creatinine, uric acid and CPR. Only a weak positive relation was found between CPR and intermediate monocytes.  $r_s$ : Spearman coefficient rank. Statistical analysis by Spearman's correlation.

### 6.3.1.2. Influence of gender on monocytes

To exclude the influence of gender in our results, data were analyzed in men and women separately. Although Ziegler-Heitbrock *et al.* founded lower CD14<sup>+</sup>CD16<sup>++</sup> monocytes in females [249], in our analysis no differences were observed between men and women (Figure 6.11).



		<i>Classical</i> CD14 <sup>++</sup> CD16 <sup>-</sup>	<i>Intermediate</i> CD14 <sup>++</sup> CD16 <sup>+</sup>	<i>Non-classical</i> CD14 <sup>+</sup> CD16 <sup>++</sup>
Men	mean	85.29	5.338	9.403
	SEM	1.03	0.428	0.775
Women	mean	87.55	4.138	8.250
	SEM	1.31	0.514	0.918
p values		0.5925 <sup>‡</sup>	0.2928 <sup>‡</sup>	0.4649 <sup>†</sup>

**Table 6.11. Distribution of monocyte subpopulations in men and women.** Percentage of each population was obtained by flow cytometry according to CD14 and CD16 expression. Results from men and women were compared with t-student (†) or Mann-Whitney (‡) tests depending on normality of the variables.

### 6.3.1.3. Monocyte subpopulations in synovial fluid

In one patient with an acute flare of arthritis we had the opportunity to analyze the distribution of monocyte subpopulations in a sample of synovial fluid obtained after joint aspiration. Surprisingly, the population of non-classical monocytes was inexistent, whereas one third of the monocytes had an intermediate phenotype.

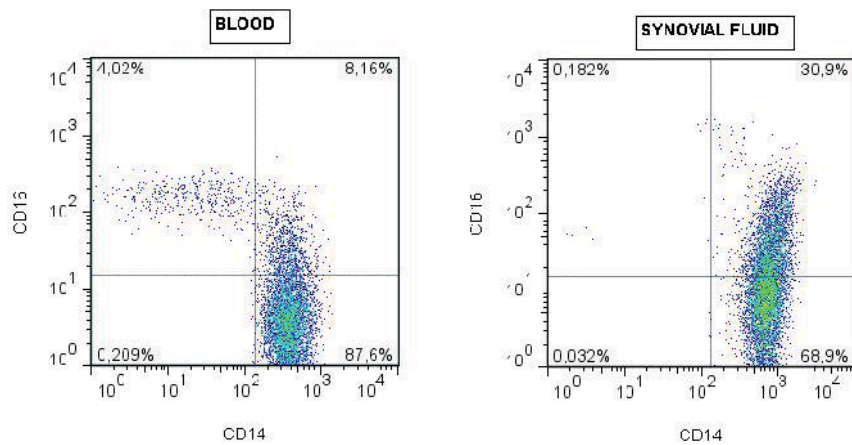


**Figure 6.12. Monocyte subpopulations in synovial fluid from a gout patient.** Analysis by flow cytometry, plots show monocyte subpopulations according to CD14 and CD16 expression in blood and synovial fluid of one patient with an acute flare of gout.

*"The important thing in science is  
not so much to obtain new facts  
as to discover new ways of thinking about them."*

William Lawrence Bragg

7.

**Discussion**





## 7.1. Role of M2 macrophages in gout initiation

The role of monocytes and macrophages in the pathogenesis of gout has been known for decades. However, the exact contribution of each one in the initiation of gout flares has not been analyzed until the last 10 years. Based in the observation that MSU crystals can be found in asymptomatic joints<sup>[270,285]</sup>, Yagnik *et al.* demonstrated that the maturation state of monocytes and macrophages determines their response to MSU crystals<sup>[271,279,286]</sup>. They proposed that, whereas blood monocytes would initiate the inflammatory response to MSU crystals, macrophages would contribute to its resolution. But during the last years the role of macrophages as the initiators of MSU-induced inflammation has been highlighted<sup>[259]</sup>. In an attempt to try to explain these contradictory facts, and as the interaction of MSU crystals and macrophages with different polarization states has not yet been assessed, we decided to investigate the effect of these crystals on M1 and M2 macrophages. We hypothesised that changes in polarization states of macrophages could be involved in the initiation and resolution of this inflammatory process. Focusing in the initiation, MSU crystals could modify macrophages' phenotype, turning them more "M1-like" and increasing their inflammatory functions. A second signal could then lead to production of inflammatory cytokines and the initiation of an inflammatory response. To explore this idea, we studied the effect of MSU crystals in a population of cells resembling resident macrophages in synovial structures *in vitro*.

### *M2 macrophages as a model of tissue resident macrophages*

Because it is difficult to obtain and culture significant numbers of human macrophages, we performed our experiments with *in vitro* monocyte-derived macrophages as, *in vivo*, blood monocytes give rise to tissue resident macrophages.

This factor has to be considered when interpreting our results, as *in vitro* experiments do not always translate to *in vivo* reality. Conditions of monocyte differentiation, such as the specific employed growth factor, affect the phenotype of the resulting macrophages, and consequently, the protocol applied for *in vitro* macrophage cultures has to be taken into account when results are analyzed and compared.

We considered different maturation protocols and we chose the one that we considered more "physiological". The reasons that justify the election of M2 macrophages polarized with M-CSF are discussed in the next paragraph.

*In vitro*, monocytes differentiate into macrophage-like cells during a process that lasts from 5 to 10 days and requires the presence of growth factors such as M-CSF, GM-CSF or IL-3. Other cytokines such as G-CSF, IL-1, IL-2, IL-4, IL-6, IFN- $\beta$ , TNF- $\alpha$  and bacterial LPS have proved to be ineffective in promoting monocyte survival and differentiation, and in the absence of growth factors, monocytes do not survive more than 3-5 days<sup>[201]</sup>. However, some groups do not use any growth factor to culture monocyte-derived macrophages<sup>[272]</sup>. In our hands, culture of monocytes in the presence of autologous serum without growth factors resulted in high mortality and lack of differentiation. This prompted us to consider the idea to add growth factors to our cultures, in order to obtain fully differentiated macrophages as similar as possible to resting synovial macrophages. With this aim, we decided to follow the concept of macrophage polarization towards M1 and M2 phenotypes<sup>[195]</sup>. In the presence of microbial products and IFN- $\gamma$  macrophages acquire an inflammatory phenotype characterized by an increased ability to kill intracellular pathogens and produce inflammatory cytokines. These macrophages are termed "classical activated" or "M1" macrophages. On the other hand, macrophages cultured with IL-4, IL-13, IL-10, TGF- $\beta$ , IgG immunocomplexes or vitamin D3 receive the name of "alternatively activated" or "M2" macrophages. These macrophages are anti-inflammatory and immune regulatory, playing a role in tissue repair and angiogenesis. Similarly, culture of macrophages with GM-CSF or M-CSF results in cells with inflammatory M1 or anti-inflammatory M2 phenotypes respectively<sup>[200,203]</sup>. M-CSF is a growth factor present at detectable levels in blood stream at steady state<sup>[199]</sup> and it has a main role in the maintenance of macrophage populations, as has been highlighted by the effects of its absence in M-CSF-deficient osteopetrotic mice (*Csf1<sup>op</sup>/Csf1<sup>op</sup>*) that exhibit a severe deficiency in macrophages<sup>[208]</sup>. These facts, together with the anti-inflammatory functions of macrophages cultured with M-CSF, have led to postulate that these macrophages resemble the population of resident macrophages in tissues at steady state<sup>[199]</sup>. Moreover, macrophages cultured with M-CSF and synovial macrophages share the expression of CD163<sup>[257]</sup>. For all these reasons, we chose a culture protocol of monocyte-derived M2 macrophages in the presence of M-CSF in order to obtain macrophages that could represent the resident population in the joint that is exposed to MSU crystals *in vivo*. Additionally, for comparison purposes, we cultured M1 macrophages polarized by GM-CSF.

### ***M1 and M2 macrophages can be differentiated by their morphology, cell surface antigens, phagocytic capacity, cytokine profile and gene expression***

Phenotype of our M1 and M2 macrophages was consistent with previous reports from other groups regarding cell morphology, surface antigens, phagocytic capacity, cytokine profile and gene expression, confirming the proper polarization of our macrophages<sup>[200,201,203,287]</sup>.

M1 macrophages in our cultures were bigger and rounded, with the typical "fried egg" morphology. They expressed higher levels of CD11b, the  $\alpha$ -subunit that together with the  $\beta$  subunit CD18 forms the heterodimeric integrin  $\alpha M\beta 2$  molecule<sup>[288]</sup>. On the other hand, M2 macrophages were smaller and stretched and expressed higher levels of CD14, that acts as a co-receptor in the response to bacterial LPS<sup>[172]</sup>. The scavenger receptor CD163 was only present in M2 macrophages. It is involved in the clearance of hemoglobin-haptoglobin complexes, preventing the oxidative stress caused by heme compound<sup>[289]</sup>. CD163 is up-regulated by M-CSF, IL-10, IL-6 and glucocorticoids and down-regulated by GM-CSF, IL-4, LPS, IFN- $\gamma$  and TNF- $\alpha$ <sup>[290]</sup> and has been considered a marker of alternative macrophage activation<sup>[291]</sup>.

M2 macrophages presented higher phagocytic capacity of polystyrene beads compared with M1 macrophages. This results agree with Verrek *et al.*: they demonstrated that M2 macrophages uptake more mycobacteria and support their outgrowth when compared with M1<sup>[200]</sup>. Subsequently, M2 macrophages have been involved in chronic mycobacterial infection.

Regarding cytokine production by our M1 macrophages after LPS challenging, they produced inflammatory cytokines such as IL-1 $\beta$  and the p40 subunit of IL-12 and IL-23, as has previously been reported<sup>[200]</sup>. Interleukin-12 is a heterodimer of p40 and p35 chains, whereas IL-23 is a cytokine composed by the common p40 next to the specific p19 chain. Verreck *et al.* showed that M1 macrophages secrete IL-23 but not IL-12, as they can produce p40 and p19 chains but not p35, requiring the presence of IFN- $\gamma$  to induce IL12 p35 gene transcription.

On the other hand, no detectable levels of inflammatory cytokines, such as IL-1 $\beta$  or IL-12, were found in our M2 cultures, and instead, they were the main producers of IL-10. This cytokine is secreted by almost all leukocytes, but especially by monocytes and macrophages after stimulation with danger signals or after clearance of apoptotic cells. It acts on monocytes and macrophages inhibiting LPS- and IFN- $\gamma$  induced secretion of pro-inflammatory cytokines such as IL-1 $\beta$ , TNF- $\alpha$ , IL-6, IL-8, G-CSF and GM-CSF. IL-10 also induces the release of anti-inflammatory mediators such as IL-1Ra, increases the phagocytic capacity of macrophages and down regulates major histocompatibility complex class II (MHCII) and adhesion molecules on cell surface, decreasing the chemotaxis of monocytes. On neutrophils, IL-10 inhibits the production of inflammatory cytokines and decreases their chemotaxis by downregulating the production of chemokines responsible of their migration<sup>[292]</sup>.

In our cultures, both M1 and M2 macrophages produced IL-8, and in the case of M1 macrophages, even in non-stimulated cultures, accordingly with previous reports<sup>[203]</sup>. IL-8 is one of the main chemokines responsible for the recruitment of neutrophils. The production of

IL-8 in M2 macrophages has been explained as it could play a role in the homeostatic functions of M2 macrophages, facilitating their interaction with neutrophils<sup>[203]</sup>.

To analyze the production of IL-1 $\beta$  and IL-10 through polarization of peripheral blood monocytes towards a M2 phenotype, we quantified these cytokines after LPS stimulation on days 0, 3 and 6 of differentiation. As expected, maturation of monocytes resulted in a decrease of IL-1 $\beta$ , but an increase in IL-10 secretion through time. Similar results have been reported by Yagnik *et al.*, with a significant reduction of IL-1 $\beta$  on day 3 and complete inhibition on day 5 in monocyte-derived macrophages in the absence of growth factors<sup>[279,286]</sup>.

M1 and M2 macrophages exhibit different transcriptional profiles, according to their different functions. It has been previously reported that macrophages polarized with M-CSF show minor differences when compared with IL-4 macrophages, as they both lead to the acquisition of an M2 phenotype<sup>[197]</sup>. Hamilton *et al.* compared basal cytokine gene expression in GM-CSF macrophages and M-CSF macrophages<sup>[281]</sup>. In accordance with their findings, higher levels of IL-10 mRNA were obtained from our M2 macrophages when compared with M1.

However, our results of MSU phagocytosis and GM-CSF production provide new data about the phenotypic differences between M1 and M2 macrophages. In our experiments, M2 macrophages showed an increased capacity for MSU phagocytosis. This fact was linked to a higher mortality. Viability of osteoblasts after MSU stimulation has been analyzed by Dalbeth *et al.* and mechanisms involved in cell death of osteoblasts seem to be independent of phagocytosis<sup>[293]</sup>.

Interestingly, M1 macrophages in our cell cultures were the main producers of GM-CSF, detectable in supernatants of unstimulated cells. It seems reasonable that M1 macrophages, once activated in the setting of an inflammatory process, could secrete more GM-CSF to polarize infiltrating monocytes to M1 macrophages. This communication between macrophages and neighbouring cells in the site of inflammation through growth factors and cytokines has received the name of "CSF network"<sup>[199,294]</sup>. Macrophages activated by danger signals and products from T lymphocytes produce inflammatory cytokines such as IL-1 $\beta$  and TNF- $\alpha$  that activate non-hematopoietic cells like fibroblasts or endothelial cells to produce inflammatory cytokines, GM-CSF, G-CSF and M-CSF. These growth factors can act systemically or locally on granulocyte and macrophage precursors, promoting their proliferation, differentiation and activation. In turn, macrophages produce GM-CSF and M-CSF that act in an autocrine manner. The final result is a positive feedback loop that could explain the chronic characteristics of the inflammatory process.

### ***Culture of macrophages with MSU crystals does not result in IL-1 $\beta$ production***

Once properly polarized, macrophages were exposed to MSU crystals but in our experiments neither M1 nor M2 macrophages produced the inflammatory cytokine IL-1 $\beta$ . Our results are consistent with the presence of phagocytosed MSU crystals inside mononuclear cells in asymptomatic joints of patients with gout<sup>[270]</sup>. Moreover, they agree with previous work from Yagnik *et al.* reporting that monocyte-derived macrophages, contrarily to fresh monocytes, fail to produce inflammatory cytokines in response to MSU<sup>[279,286]</sup>.

Conflicting data about the effect of MSU crystals on IL-1 $\beta$  production in monocytes and macrophages have been published. Some groups have reported that human PBMCs produce IL-1 $\beta$  after MSU challenging<sup>[136,279,295]</sup>, whereas work from Netea's group has demonstrated the requirement of another signal besides MSU stimulation<sup>[275,296]</sup>. On the other hand, THP-1 cells require activation with PMA<sup>[295]</sup>. Mice peritoneal macrophages collected after lavage with LPS do not need any priming<sup>[175,297]</sup>, whereas macrophages obtained 3 days after intraperitoneal injection of thioglycolate do not exhibit enough levels of pro-IL-1 $\beta$  and require priming with LPS to produce IL-1 $\beta$  after MSU stimulation<sup>[295]</sup>. The concentration of MSU crystals could be a confounding factor too, as intra-articular injection of 600  $\mu\text{g}/\text{mL}$  MSU crystals fails to induce inflammation according to Netea's work<sup>[275]</sup>, whereas in other groups injection of 1 or 3 mg in the peritoneal and air pouch mice models leads to an inflammatory reaction<sup>[173,175,259,295]</sup>. Taken together, these data suggest that, when analyzing the results of these studies, one should consider factors such as the specific subtype of cell, the methods used for harvesting these cells, MSU concentrations, the site of injection (air-pouch, peritoneal, intraarticular) and mainly if these experiments are performed with mouse or human samples. Differences between mouse and human cells are a major controversial aspect for the immunology of XXI-century, and differences in inflammation and inflammatory mechanisms between these models should be also taken into account when concepts derived from articles are used to understand pathogenesis of diseases<sup>[298]</sup>.

But even using similar protocols, contradictory results have been reported. Amaral *et al.* showed that intra-articular injection of 100  $\mu\text{g}/\text{mL}$  of MSU crystals in C57BL/6 mice is followed by neutrophil infiltration and IL-1 $\beta$  detection at 3 hours<sup>[299]</sup>. On the contrary, using the same mouse strain, Netea's group did not found IL-1 $\beta$  production or signs of inflammation in histological examination 4 hours after intra-articular injection of 300  $\mu\text{g}/\text{mL}$ <sup>[275]</sup>.

### ***M2 macrophages after MSU stimulation acquire and M1-like phenotype, producing IL-1 $\beta$ and decreasing IL-10 secretion after LPS challenging***

When we challenged M2 macrophages with LPS, as expected, we did not detect IL-1 $\beta$  production. However, the combination of MSU and LPS led to IL-1 $\beta$  secretion and the same pattern was observed with CPP crystals. As previously reported by Martinon *et al.*, THP-1 cells required the presence of MSU and LPS for IL-1 $\beta$  production<sup>[295]</sup>.

The requirement of two signals for IL-1 $\beta$  production has been already described. One signal induces pro-IL-1 $\beta$  production and the second signal is responsible of inflammasome activation and IL-1 $\beta$  secretion<sup>[164]</sup>. Netea *et al.* demonstrated that monocytes constitutively express enough levels of active caspase-1 and therefore they only need one signal through TLR receptors (LPS or Pam3Cys) to produce IL-1 $\beta$ . On the other hand, macrophages exhibit low levels of active caspase-1 and therefore they need one signal for pro-IL-1 $\beta$  induction and a second signal for inflammasome activation, pro-IL-1 $\beta$  cleavage and IL-1 $\beta$  secretion. This second signal is provided by ATP or MSU crystals. In their experiments, MSU and the free fatty acid (FFA) C18:0 were necessary for IL-1 $\beta$  production *in vitro* in human PBMCs and mice macrophages and for induction of gouty arthritis *in vivo* when injecting MSU crystals into mice joints<sup>[275]</sup>. The relation of FFA and activation via TIR, especially with TLR2 and 4, is well documented in type 2 diabetes<sup>[300]</sup>. As ingestion of an abundant meal, alcohol consumption and fasting are associated with an increase in FFA concentration; Netea's results explain the role of these situations as triggers of gout flares.

Harper *et al.*<sup>[297]</sup> suggests that one of the reasons of the lack of response to MSU could be that cell lines or monocyte-derived macrophages differentiated *in vitro* in sterile media, in the absence of TLR ligands, would lack pro-IL-1 $\beta$ . One of the limitations of our study is that macrophages have been derived *in vitro* and we cannot rule out the possibility that this could have affected experimentally pro-IL-1 $\beta$  levels. However, based on Netea's results, in which two signals were required for MSU induction of inflammation *in vivo*, and in the clinical finding of MSU crystals in asymptomatic joints, we suggest that, due to the lack of pro-IL-1 $\beta$  or other regulatory mechanisms, *in vivo* resident macrophages in the steady state could exhibit the same behaviour. However, research with human synovial macrophages is needed to confirm this hypothesis.

In our experiments macrophages produced lower levels of IL-1 $\beta$  (100 pg/mL) than monocytes, and the relevance of this fact could be questionable. However, Scanu *et al.* analyzed the presence of inflammatory and anti-inflammatory cytokines in synovial fluid of patients with



gout flares and found similar levels of IL-1 $\beta$  at early stages<sup>[280]</sup>. Thus we can conclude that the low IL-1 $\beta$  production by M2 macrophages could be biologically relevant in the setting of gout flares.

On the other hand, stimulation of M2 macrophages with MSU and LPS led to a decrease in IL-10 production. To rule out the effect of cell mortality on IL-10, we compared cell viability with IL-10 production, and as IL-10 reduction was much more higher than cell mortality, we suggest that other factors than just a decrease in cell viability are involved in down regulation of IL-10. One of this regulators of M2 phenotype could be the presence of NF- $\kappa$ B p50, that has been involved the development of LPS tolerance and is necessary for the expression of M2 related genes<sup>[301]</sup>. NF- $\kappa$ B induces transcription of inflammatory cytokines and comprises five members: NF-kB1 (p105), NF-kB2 (p100), RelA, RelB, c-Rel. NF-kB1 and NF-kB2 are post-transcriptionally processed to the subunits p50 and p52 respectively. In the canonical pathway, inflammatory cytokines and PAMPS activate the IKK complex, resulting in the nuclear translocation of p50/p65 heterodimers that activate transcription of genes involved in inflammation. However, p50 homodimers act like negative regulators, as they carry a nuclear localization sequence but lack a transcription activation domain<sup>[302]</sup>. Accordingly with this suppressive function, p50 has been involved in the induction of tolerance, that is associated with and M2 phenotype, inducing the transcription of M2 associated genes and repressing M1 genes. On the other hand, p50<sup>-/-</sup> mice fail to develop tolerance, and exhibit a restoration of M1 mediators and inhibition of M2 cytokines and chemokines due to the increase of IFN- $\gamma$ <sup>[301]</sup>. We suggest that changes in p50 could be one of the possible mechanisms participating in the M1-skewing of the inflammatory response in M2 macrophages after MSU phagocytosis.

Unfortunately, when we analyzed the effect of MSU crystals on LPS-induced IL-1 $\beta$  production by M1 macrophages, it was impossible to reach any conclusion due to the heterogeneity of the results. In some experiments MSU and LPS decreased IL-1 $\beta$  compared with production with LPS alone, whereas in others their combination resulted in an increased IL-1 $\beta$  secretion.

### ***Changes in cytokine production are not associated with the acquisition of M1-associated cell surface markers***

As macrophages stimulated with MSU seemed to acquire an "M1-like" cytokine phenotype in terms of cytokine production, we analyzed the expression of cell surface markers associated with M1 macrophages.

M2 macrophages cultured with MSU for 18 hours down-regulated CD11b and CD14 and to a lesser extend CD163. The engulfment of the membrane after MSU phagocytosis could explain

that the surface expression of these antigens decreased. As both markers, CD11b and CD14, have been involved in phagocytosis, another possible explanation could be the internalization of these receptors after binding with MSU crystals<sup>[303]</sup>. Interaction of MSU and Mac-1 integrin (CD11b)<sup>[304]</sup> or CD14<sup>[172]</sup> have described, and down-regulation of these surface molecules after ligand-binding has been extensively documented, even in situations where simultaneous binding occurs<sup>[305]</sup>.

To study the paracrine effect of soluble factors released by M2 macrophages after stimulation, we cultured unstimulated M2 macrophages with conditioned media from M2 macrophages exposed to MSU or LPS. This conditioned media was previously centrifuged to remove MSU and, as expected, no crystals could be observed in the microscope. However, the possibility of small crystals cannot be excluded. Conditioned media of unstimulated M2 macrophages resulted in up-regulation of markers associated with M2 polarization and the same effect was observed with conditioned media from macrophages stimulated with MSU. This fact could suggest that macrophages after MSU phagocytosis do not produce inflammatory cytokines to induce M1 macrophages, supporting the idea of non-inflammatory phagocytosis of MSU crystals by M2 macrophages. We expected to see a change towards an M1 phenotype when macrophages were exposed to conditioned media after MSU and LPS stimulation, but we observed an up-regulation of CD14 with down-regulation of CD11b and to a lesser extent CD163. Therefore, the results of these experiments were no-conclusive, although the changes in CD14 and Mac-1 suggest some paracrine effect.

### ***MSU activate the inflammasome in M2 macrophages and M1 and M2 macrophages exhibit differences in inflammasome proteins***

Changes in inflammasome activation could be involved in the production of IL-1 $\beta$  after stimulation of M2 macrophages with MSU and LPS. It has been proposed that macrophages need two signals for IL-1 $\beta$  production: one for pro-IL1 $\beta$  transcription and translation through activation of TLR receptors and a second signal for inflammasome assembly and caspase-1 activation. On contrary, in monocytes the presence of active caspase-1 in steady state allows them to produce IL-1 $\beta$  after only one signal through TLR receptors<sup>[284]</sup>. As M1 macrophages exhibited the same behaviour that monocytes, we hypothesized that M1 and M2 macrophages could be differentiated by their inflammasome activation state: resting M1 macrophages have already activated caspase-1, whereas in M2 macrophages, MSU crystals would induce inflammasome activation and cleavage of caspase-1, resulting in the presence of active caspase-1.



First, we assessed the effect of MSU crystals in the inflammasome of M2 macrophages. As expected, MSU crystals increased active caspase-1 levels, whereas LPS increased intracellular levels of inactive caspase-1 and pro-IL-1 $\beta$ , confirming our hypothesis. Of note, the combination of MSU and LPS had a synergistic effect on pro-IL-1 $\beta$  production. The same synergic effect has been described in human synovial fibroblasts cultured with MSU and serum amyloid A protein (SAA)<sup>[276]</sup>. Thus, we can conclude that M2 macrophages are able to produce the inflammatory cytokine IL-1 $\beta$  after LPS stimulation when MSU crystals have already activated the inflammasome.

Then, we investigated the differences in inflammasome activation between M1 and M2 macrophages, analyzing the presence of active and inactive forms of caspase-1 and its gene expression. We observed a trend towards increased levels of active caspase-1 in M1 macrophages, although our results did not reach significance, and intracellular levels of inactive caspase-1 were higher in M1. Unexpectedly, when we compared gene expression of *caspase-1*, *NLRP3* and *IL-1 $\beta$* , M2 macrophages exhibited higher mRNA levels compared with M1. Focusing on caspase-1, M1 macrophages exhibited higher levels of inactive caspase-1 but lower mRNA levels, and therefore our results suggest that a negative regulatory posttranscriptional mechanism could be involved. One of these regulatory mechanisms are microRNA (miRNA), short regulatory RNAs of approximately 21 nucleotides in length that regulate the expression of target mRNA containing complementary sequences<sup>[306]</sup>. In association with Argonaute proteins (Ago), miRNA form the RNA-induced silencing complex (RISC) that represses RNA expression. miRNA exert their suppressive effect by inhibiting mRNA translation or by promoting degradation of target mRNA<sup>[307]</sup>. miRNA have been involved in inflammasome regulation and specifically miR-223, a miRNA highly expressed in human macrophages, has demonstrated that it regulates *NLRP3* expression. Levels of miR-223 are inversely correlated with NLRP3 protein, exerting an inhibitory effect on IL-1 $\beta$  production. According to that, mice lacking miR-223 have enhanced sterile inflammation<sup>[308,309]</sup>. Culture of macrophages with GM-CSF results in decreased expression of miR-223 and higher levels of NLRP3 protein<sup>[309]</sup>. However, the relation of miR-223 with mRNA *NLRP3* is not so clear, as it has been associated with both an increase or a decrease in *NLRP3* mRNA, and thus it is not known if it exerts its negative effects through inhibiting translation with a consequent accumulation of mRNA, or if it induces mRNA degradation resulting in low *NLRP3* expression. As the same miRNA can modulate different mRNAs that are involved in the same biological process<sup>[307]</sup>, miR-223 could be involved in posttranscriptional regulation of caspase-1 too. We suggest that the higher caspase-1 gene expression observed in M2 macrophages with low levels of NLRP3 protein could be explained by the presence of higher levels of miR-223 that repress mRNA translation. On the contrary, macrophages polarized

with GM-CSF could exhibit lower miR-223 expression resulting in higher translation and higher protein levels. This could be a protective mechanism to prevent excessive inflammation in resident macrophages. Future work analyzing the association of MSU with miRNA could shed light into this phenomenon.

Our gene expression results differ from previous published work from Pelegrin *et al.* using mice macrophages and a different polarization protocol. In their experiments, mice peritoneal macrophages polarized towards M1 macrophages with IFN- $\gamma$  and LPS had higher expression of the inflammasome related genes caspase-1 and *NLRP3* compared with M2 macrophages polarized with IL-4. Harper's group have recently published their results using mice bone marrow derived macrophages polarized with GM-CSF and M-CSF<sup>[277]</sup>. In their experiments, pro-IL-1 $\beta$ , active IL-1  $\beta$ , inactive caspase-1 and active caspase-1 were higher in GM-CSF macrophages than M-CSF macrophages. However, their macrophages had cytoplasmic pro-IL-1 $\beta$  and produced IL-1 $\beta$  after MSU stimulation, especially the GM-CSF macrophages. Differences between mice and human inflammatory pathways could explain the differences observed between our experiments with human samples and mice experiments<sup>[298]</sup>.

### ***Soluble uric acid has a suppressive effect on M2 macrophages***

When we polarized M2 macrophages in the presence of soluble uric acid, conditions of normouricemia, and especially hyperuricemia, decreased IL-1 $\beta$  production, whereas IL-10 was scarcely affected. Thus, uric acid seemed to induce a less inflammatory phenotype. Uric acid lowering therapy has been associated with an increased risk of gout flares, and this fact has been explained as the dissolution of MSU deposits causes a dispersion of crystals that could increase interaction with leukocytes<sup>[310]</sup>. Based in our results, another possible mechanism could be that the disappearance of the regulatory effect of soluble uric acid could favour the development of gout flares.

We expected to see the opposite effect of the acute exposure of soluble uric acid, as an acute increase of uric acid has been associated with gout flares. However, our results showed that cultured of M2 macrophages with uric acid for 24 hours resulted in the suppression of both IL-1 $\beta$  and IL-10 production. To our knowledge this is the first time that the effect of soluble uric acid on macrophages has been analyzed and we have not found any explanation for this suppressive effect.

### ***Proposed model for the initiation of gout flares***

Based on our results, we propose the following model to explain the initiation of the inflammatory response to MSU crystals: (1) M2 macrophages or resident macrophages *in vivo*, would phagocytose MSU crystals without the production of inflammatory cytokines, but MSU crystals would increase their cytoplasmic levels of active caspase-1, resembling M1 macrophages. (2) A concomitant trigger for gout flares such as an infection, fasting, a copious meal or alcohol intake, would activate TLR receptors and induce transcription and translation of pro-IL-1 $\beta$ . (3) In the presence of active caspase-1, pro-IL-1 $\beta$  would be cleaved into its active form and released to the joint space. (4) Other inflammatory cytokines and chemokines produced by macrophages would act on other non-hematopoietic cells such as endothelial cells, to promote migration of monocytes and neutrophils. (5) Moreover, IL-1 $\beta$  would promote the production of GM-CSF by endothelial or synovial cells that in turn could activate recently recruited monocytes towards an inflammatory M1 phenotype, resulting in the amplification of the inflammatory response. In this line, Harper *et al.* have demonstrated recently the requirement of GM-CSF for the acquisition of an inflammatory phenotype in recruited monocytes<sup>[277]</sup>.

## **7.2. The monocyte-phagocyte system in patients with gout**

### ***Patients with gout exhibit an enhanced inflammasome response to MSU crystals***

We had the hypothesis that the reason why some individuals with hyperuricemia develop arthritis whereas others remain asymptomatic is that monocytes and macrophages of patients with gout exhibit a greater inflammatory response to MSU crystals. As these crystals activate NLRP3 inflammasome, resulting in the production of the inflammatory cytokine IL-1 $\beta$ , in this thesis we investigated the possibility of enhanced inflammasome reactivity in patients with gout. With this aim, we analyzed caspase-1 activation and IL-1 $\beta$  production in PBMCs from gouty patients and healthy donors.

No differences were observed regarding baseline levels of active caspase-1 between gouty patients and controls. Although IL-1 $\beta$  has a central role in gouty arthritis, to our concern no studies analyzing activation of caspase-1 in gout have been published. Our results contrast with previous work from Cascão *et al.* in patients with rheumatoid arthritis<sup>[311,312]</sup>. Using the same fluorescent antibody, they analyzed the presence of active caspase-1 in patients with early arthritis (EA), early rheumatoid arthritis (ERA) and established rheumatoid arthritis (RA).

Leukocytes from patients with ERA and RA exhibited higher levels of active caspase-1 at baseline compared with healthy controls. The reason of the discrepancy between this study and our patients with gout could be that we selected asymptomatic patients, without tender or swollen joints, whereas disease activity scores (DAS28) of rheumatoid arthritis patients suggested moderate disease activity.

In our experiments, gouty patients exhibited an enhanced up-regulation of active caspase-1 after MSU stimulation, but no differences were observed with other inflammasome activators such as ATP or nigericine. NLRP3 activation by ATP and nigericine is secondary to the decrease in intracellular levels of potassium<sup>[147]</sup>, in the case of ATP through binding to the ionophore receptor P2X<sub>7</sub>R, whereas nigericin is a potassium-proton ionophore<sup>[313]</sup>. This mechanism of K<sup>+</sup> efflux is also shared with particulate elements such as alum, silica and calcium pyrophosphate crystals<sup>[314]</sup>. Whereas phagocytosis is necessary for IL-1 $\beta$  production by MSU, cytochalasin D, that inhibits phagocytosis, does not have any effect on IL-1 $\beta$  production induced by ATP and nigericine<sup>[176]</sup>. These facts could prompt us to speculate that an increased phagocytic capacity of monocytes in gouty patients could account for the differences observed in caspase-1 activation in our experiments. However, we observed no differences in MSU phagocytosis between monocytes from gouty patients and healthy controls. Therefore, other molecules involved specifically in MSU phagocytosis differentially expressed in monocytes from patients with gout could explain the enhanced inflammasome activation in response to MSU in gouty patients.

Unexpectedly, we found that PBMCs of gouty patients after stimulation with TLR4 agonist LPS and MSU produced less IL-1 $\beta$  than healthy controls. Proportion of monocytes in PBMCs was higher in gout group, and thus, differences between patients and controls were more evident after adjusting IL-1 $\beta$  production to monocytes/mm<sup>3</sup>. We have previously demonstrated that uric acid has a suppressive effect on IL-1 $\beta$  production in M2 macrophages. When we correlated uric acid levels with this cytokine and in this assay, we observed a negative effect of uric acid on IL-1 $\beta$ , although we did not find significant correlation. The results of our cytokine experiments contrast with work of Mylona *et al.*<sup>[315]</sup>. They reported that PBMCs from gouty patients produced more IL-1 $\beta$  when stimulated with TLR1/2 ligand Pam3Cys, especially in the presence of MSU crystals. However, we agree with their finding that the synergism between MSU crystals and TLR agonists is enhanced in gout group. This increased response could be secondary to differences in pro-IL-1 $\beta$  synthesis or to an enhanced activation of this immature cytokine by caspase-1. In their work Mylona *et al.* ruled out the first possibility, as they analyzed mRNA IL-1 $\beta$  by RT-PCR without finding any difference and suggesting that in gouty patients NLRP3 inflammasome could be activated more readily. Our experiments with

caspase-1 demonstrate that gouty patients exhibit an enhanced inflammasome activity after MSU and LPS stimulation that could explain this increased synergism.

Based on our results we conclude that patients with gout, although exhibiting a greater inflammasome reactivity after challenging with MSU and LPS, they produce lower levels of IL-1 $\beta$ , suggesting that other mechanisms that regulate IL-1 $\beta$  secretion could be involved. A possible candidate could be soluble uric acid, which modulate this pathway. One of the limitations of our experiments is that we compared gouty patients with healthy donors and not with individuals with asymptomatic hyperuricemia. However, our results open the possibility that the magnitude of inflammasome activation induced by MSU could result in clinical differences, encouraging future research with larger cohorts including hyperuricemic individuals.

### ***Gout is not associated with NLRP3 polymorphisms in exon 3***

Gout has been associated with polymorphisms in genes involved in renal urate transport, such as *SLC2A9*, *SLC22A12* and *ABCG2* that affect serum levels of uric acid. However, it seems conceivable that other factors apart from uric acid could influence the development of clinical gout, as not all individuals with hyperuricemia develop clinical gout. Equivalently, polymorphisms in genes related to inflammatory process could affect the magnitude of the response as they may affect cytokine production. Accordingly, polymorphisms in TLR4, IL-8, IL-12, TGF- $\beta$  and TNF- $\alpha$  genes have been associated with gout<sup>[316–319]</sup>. Regarding *NLRP3*, gain-of-function mutations in this gene are responsible of the CAPS syndromes and polymorphisms of *NLRP3* have been involved in inflammatory conditions such as Alzheimer's disease, asbestos pulmonary fibrosis, diabetes and insulin resistance, psoriasis, pneumoconiosis, nodular melanoma, celiac disease, Crohn's disease, HIV-1 infection, food allergy and aspirin induced asthma, juvenile idiopathic arthritis and rheumatoid arthritis<sup>[320–332]</sup>. We had the hypothesis that *NLRP3* polymorphisms could affect the reactivity to MSU crystals and increase the risk of gout. One limitation of our study is that the sample of patients is small (n=16). We genotyped *NLRP3* exon 3, which is this the region is where most of gain-of-function mutations in CAPS syndromes are located. We found several polymorphisms, but none of them was significantly associated with gout. Only one patient was heterozygous for the Q703K variant, that in the presence of the *CARD8* variant C10X, has been associated with an increased risk of inflammatory diseases due to increased IL-1 $\beta$  mRNA levels, increased IL-1 $\beta$  secretion after stimulation, delayed apoptosis of neutrophils and impaired clearance of apoptotic neutrophils<sup>[328,329,331,333,334]</sup>.

### ***Gouty flares are associated with an expansion of CD14<sup>++</sup>CD16<sup>+</sup> monocytes***

Of the three monocyte subpopulations recognised in humans, the intermediate and the non-classical monocytes are increased in infectious and inflammatory conditions such as sepsis, HIV infection, asthma and Crohn's disease<sup>[335]</sup>. In rheumatoid arthritis (RA), CD16<sup>+</sup> monocytes are expanded and correlate with disease activity, decreasing in patients who respond to therapy<sup>[253]</sup>. Rossol *et al.* demonstrated that specifically the intermediate subpopulation is expanded in RA, although in this study no correlation with clinical parameters was found. These monocytes were the main producers of LPS-induced IL-1 $\beta$ , IL-1 $\alpha$  and TNF- $\alpha$  and exhibited a greater capacity for Th17 cell differentiation through the production of IL-1 $\beta$  and IL-23<sup>[240]</sup>. Accordingly, we found an expansion of the intermediate subpopulation in patients with acute gout. One of the limitations of our study is the small sample size, as we could only obtain four samples from patients during a gout flare. No correlation was demonstrated between intermediate monocytes and CPR values, neither with uric acid levels, creatinine or age. However a tendency towards a positive effect of CPR values on intermediate monocytes was observed. Thus, one factor to take into account is that this monocyte subset could be expanded in response to the inflammatory milieu as an "innocent bystander" and not be involved in the inflammatory response.

The majority of authors suggest that some classical monocytes leave the circulation and develop into tissue macrophages, whereas other classical monocytes might develop into intermediate monocytes which in turn, can leave the circulation or develop into non-classical monocytes patrolling the endothelial-blood interface<sup>[254]</sup>. CD14<sup>++</sup>CD16<sup>+</sup> monocytes are the responsible of production of inflammatory cytokines and express a variety of chemokine receptors such as CCR2, CCR5 and CX3CR1 that facilitate their migration. We propose that during an acute flare of gout factors released from joints, such as M-CSF<sup>[252,253]</sup>, increase the generation of this inflammatory subset, that migrate into tissues and amplifies the inflammatory response to MSU crystals.

Although it has been reported that women have lower counts of intermediate monocytes due to the effect of estrogens<sup>[249,336]</sup>, we and others<sup>[337]</sup> have not found any difference between men and women, and the mean age of women in our study was 35 years.

We had the opportunity to analyze one synovial fluid from a patient with an acute flare and surprisingly, we found a lack of non-classical monocytes and an important expansion of the intermediate ones, from 8% in peripheral blood to 31% in synovial fluid. This fact was reported by Kawanaka *et al.*, who found significant differences between CD16<sup>+</sup> cells in blood and

synovial fluid in 7 patients with active RA, with percentages of CD16<sup>+</sup> monocytes of 15% and 59% respectively.

Intermediate monocytes have been involved in the inflammation developed along atherosclerosis, as they express a broader panel of chemokine receptors, produce inflammatory cytokines and have a high capacity for the uptake of oxidised LDL. This implication is supported by the beneficial effect of blocking monocyte chemokine receptors such as CCR2, CCR5 and CX3CR1 in atherosclerosis models<sup>[254]</sup>. CD16<sup>+</sup> monocytes are associated with cardiovascular risk factors such as obesity<sup>[338,339]</sup>, coronary artery disease<sup>[246]</sup>, plaque instability<sup>[340]</sup> and in-stent restenosis<sup>[341]</sup>. In patients with chronic kidney disease, intermediate monocytes have been associated with cardiovascular events and overall survival<sup>[342]</sup>. One proposed model is that endothelial cells become activated after an initial injury induced by smoking, hyperglycaemia or hypertension. Activated endothelial cells express adhesion molecules and produce chemokines that induce migration of monocytes into the endothelial space. Once there, monocytes differentiate into macrophages that engulf lipoproteins and become foam cells, producing inflammatory cytokines and chemokines and initiating a redundant cycle. For these reasons our hypothesis was that in patients with asymptomatic hyperuricemia the expansion of the intermediate subpopulation could be involved in the cardiovascular risk associated with gout. However, we did not find any differences when comparing with healthy donors and this result could suggest that systemic inflammation in gout is restricted to the acute episodes.



### 7.3. Future work

Results obtained in this thesis reinforce the relevance of the inflammatory differentiation of macrophages and monocytes in the pathogenesis of the gout and contribute in the current knowledge of the pathogenic mechanisms of gout. However, they open new questions and further studies are still required in this field to obtain targets for prevention and a more personalized treatment of gouty patients.

The necessity of studies with human resident macrophages is one factor to consider, as probably one of the limitations of this thesis is that macrophages were derived *in vitro* from blood monocytes. Moreover, advances in the knowledge of macrophage maturation *in situ* could help to design better *in vitro* protocols in order to obtain macrophages as close as possible to tissue resident macrophages.

We have demonstrated that M2 macrophages modify their IL-1  $\beta$  and IL-10 production towards a more M1-like phenotype. However we did not find changes in cell surface markers. The analysis of the effect of MSU crystals on gene transcription profiles in M2 macrophages could help to elucidate the extension of changes exerted by these crystals on M2 macrophages. Investigation on the effects of MSU crystals on Nf- $\kappa$ B and miRNA in polarized macrophages could expand the results obtained in this thesis.

Furthermore, the results of our studies regarding caspase-1 activation and distribution of monocyte subpopulations encourage future research with larger cohorts including hyperuricemic individuals.



*Happiness does not come from doing easy work  
but from the afterglow of satisfaction  
that comes after the achievement  
of a difficult task that demanded our best*

Theodore Isaac Rubin

8.

**Conclusions**



1. M2 macrophages, in the presence of MSU crystals, change their anti-inflammatory phenotype and acquire inflammatory functions. After stimulation with a TLR agonist, such as LPS, these inflammatory macrophages are then able to produce IL-1 $\beta$  whereas its IL-10 secretion is reduced. Activation of the inflammasome by MSU crystals is the responsible of this effect on IL-1 $\beta$ .
2. Soluble uric acid exerts a suppressive effect on both IL-1b and IL-10 production in M2 macrophages.
3. M1 macrophages exhibit higher levels of inactive caspase-1 and a tendency towards higher levels of active caspase-1 at baseline, compared with M2 macrophages. On the other hand, gene expression of caspase-1 is higher in M2.
4. PBMCs from gouty patients have enhanced inflammasome activation after MSU stimulation when compared with healthy controls. These differences are not associated with *NLRP3* polymorphisms.
5. The subpopulation of intermediate monocytes is expanded in peripheral blood of gout patients during an acute flare of arthritis. However, in asymptomatic patients, distribution of monocyte subpopulations shows no differences with healthy controls.



## **Bibliography**



- [1] Perez-Ruiz F, Castillo E, Chinchilla SP, Herrero-Beites AM. Clinical Manifestations and Diagnosis of Gout. *Rheum Dis Clin North Am*. 2014 May;40(2):193–206.
- [2] Doherty M, Jansen TL, Nuki G, Pascual E, Perez-Ruiz F, Punzi L, So AK, Bardin T. Gout: why is this curable disease so seldom cured? *Ann Rheum Dis*. 2012 Nov;71(11):1765–70.
- [3] Wortmann RL. Gout and Hyperuricemia. In: Firestein GS, Gabriel SE, Budd RC, Harris J, Edward D, McInnes IB et al., editors. *Kelley's textbook of rheumatology*. 8th ed. Philadelphia: Saunders; 2008. p. 1481–506.
- [4] Rothschild B, Tanke D, Carpenter K. Tyrannosaurs suffered from gout. *Nature*. 1997;387(6631):357.
- [5] Gritzalis KC, Karamanou M, Androutsos G. Gout in the writings of eminent ancient Greek and Byzantine physicians. *Acta Med Hist Adriat*. 2011 Jan;9(1):83–8.
- [6] Nuki G, Simkin P a. A concise history of gout and hyperuricemia and their treatment. *Arthritis Res Ther*. 2006 Jan;8 Suppl 1(Table 1):S1.
- [7] McCarthy D. A historical note: Leeuwenhoek's description of crystals from a gouty tophus. *Arthritis Rheum*. 1970;13(4):414–8.
- [8] Wollaston W. On gouty and urinary concretions. *Philos Trans R Soc London*. 1797;87(1797):386–400.
- [9] Garrod AB, Storey GD. Alfred Baring Garrod (1819–1907). *Rheumatology*. 2001;40(10):1189–90.
- [10] McCarty D, Hollander J. Identification of urate crystals in gouty synovial fluid. *Ann Intern Med*. 1961;54(3):452–60.
- [11] Faires J, DJ M. Acute arthritis in man and dog after intrasynovial injection of sodium urate crystals. *Lancet*. 1962;280(7258):682–5.
- [12] Richette P, Bardin T. Gout. *Lancet*. 2010 Jan 23;375(9711):318–28.
- [13] Martinon F. Mechanisms of uric acid crystal- mediated autoinflammation. *Immunol Rev*. 2010;233(1):218–32.
- [14] Motojima K, Kanaya S, Goto S. Cloning and sequence analysis of cDNA for rat liver uricase. *J Biol Chem*. 1988 Nov 15;263(32):16677–81.

- [15] Kratzer JT, Lanasa M a, Murphy MN, Cicerchi C, Graves CL, Tipton P a, Ortlund E a, Johnson RJ, Gaucher E a. Evolutionary history and metabolic insights of ancient mammalian uricases. *Proc Natl Acad Sci U S A*. 2014 Mar 11;111(10):3763–8.
- [16] Oda M, Satta Y, Takenaka O, Takahata N. Loss of urate oxidase activity in hominoids and its evolutionary implications. *Mol Biol Evol*. 2002 May;19(5):640–53.
- [17] Johnson RJ, Sautin YY, Oliver WJ, Roncal C, Mu W, Gabriela Sanchez-Lozada L, Rodriguez-Iturbe B, Nakagawa T, Benner S a. Lessons from comparative physiology: could uric acid represent a physiologic alarm signal gone awry in western society? *J Comp Physiol B*. 2009 Jan;179(1):67–76.
- [18] Álvarez-Lario B, Macarrón-Vicente J. Uric acid and evolution. *Rheumatology (Oxford)*. 2010 Nov;49(11):2010–5.
- [19] Champion E, Glynn R, DeLabry L. Asymptomatic hyperuricemia. Risks and consequences in the Normative Aging Study. *Am J Med*. 1987;82(3):421–6.
- [20] Smith EUR, Díaz-Torné C, Perez-Ruiz F, March LM. Epidemiology of gout: an update. *Best Pract Res Clin Rheumatol*. Elsevier Ltd; 2010 Dec;24(6):811–27.
- [21] Doherty M. New insights into the epidemiology of gout. *Rheumatology (Oxford)*. 2009 May;48 Suppl 2:ii2–ii8.
- [22] Lawrence RC, Helmick CG, Arnett FC, Deyo R a, Felson DT, Giannini EH, Heyse SP, Hirsch R, Hochberg MC, Hunder GG, Liang MH, Pillemer SR, Steen VD, Wolfe F. Estimates of the prevalence of arthritis and selected musculoskeletal disorders in the United States. *Arthritis Rheum*. 1998 May;41(5):778–99.
- [23] Wallace KL, Riedel AA, Joseph-ridge N, Wortmann R. Increasing Prevalence of Gout and Hyperuricemia Over 10 Years Among Older Adults in a Managed Care Population. *J Rheumatol*. 2004;31(8):1582–7.
- [24] Zhu Y, Pandya BJ, Choi HK. Prevalence of gout and hyperuricemia in the US general population: the National Health and Nutrition Examination Survey 2007-2008. *Arthritis Rheum*. 2011 Oct;63(10):3136–41.
- [25] Currie WJ. Prevalence and incidence of the diagnosis of gout in Great Britain. *Ann Rheum Dis*. 1979 Apr;38(2):101–6.
- [26] Steven MM. Prevalence of chronic arthritis in four geographical areas of the Scottish Highlands. *Ann Rheum Dis*. 1992 Feb;51(2):186–94.



- [27] Harris C. The prevalence and prophylaxis of gout in England. *J Clin Epidemiol*. 1995;48(9):1153–8.
- [28] Annemans L, Spaepen E, Gaskin M, Bonnemaire M, Malier V, Gilbert T, Nuki G. Gout in the UK and Germany: prevalence, comorbidities and management in general practice 2000-2005. *Ann Rheum Dis*. 2008 Jul;67(7):960–6.
- [29] Trifirò G, Morabito P, Cavagna L, Ferrajolo C, Pecchioli S, Simonetti M, Bianchini E, Medea G, Cricelli C, Caputi AP, Mazzaglia G. Epidemiology of gout and hyperuricaemia in Italy during the years 2005-2009: a nationwide population-based study. *Ann Rheum Dis*. 2013 May;72(5):694–700.
- [30] Nan H, Qiao Q, Dong Y, Gao W, Tang B, Qian R, Tuomilehto J. The prevalence of hyperuricemia in a population of the coastal city of Qingdao, China. *J Rheumatol*. 2006;33(7):1346–50.
- [31] Miao Z, Li C, Chen Y, Zhao S, Wang Y, Wang Z, Chen X, Xu F, Wang F, Sun R, Hu J, Song W, Yan S, Wang C. Dietary and lifestyle changes associated with high prevalence of hyperuricemia and gout in the Shandong coastal cities of Eastern China. *J Rheumatol*. 2008;35(9):1859–64.
- [32] Winnard D, Wright C, Taylor WJ, Jackson G, Te Karu L, Gow PJ, Arroll B, Thornley S, Gribben B, Dalbeth N. National prevalence of gout derived from administrative health data in Aotearoa New Zealand. *Rheumatology (Oxford)*. 2012 May;51(5):901–9.
- [33] Arromdee E, Michet CJ, Crowson CS, O’Fallon WM, Gabriel SE. Epidemiology of gout: is the incidence rising? *J Rheumatol*. 2002;29(11):2403–6.
- [34] Klemp P, Stansfield S a, Castle B, Robertson MC. Gout is on the increase in New Zealand. *Ann Rheum Dis*. 1997;56(1):22–6.
- [35] Choi HK, Atkinson K, Karlson EW, Willett W, Curhan G. Purine-rich foods, dairy and protein intake, and the risk of gout in men. *N Engl J Med*. 2004 Mar 11;350(11):1093–103.
- [36] Zhang Y, Chen C, Choi H, Chaisson C, Hunter D, Niu J, Neogi T. Purine-rich foods intake and recurrent gout attacks. *Ann Rheum Dis*. 2012;71:1448–53.
- [37] Choi HK, Curhan G. Soft drinks, fructose consumption, and the risk of gout in men: prospective cohort study. *BMJ*. 2008 Feb 9;336(7639):309–12.
- [38] Choi HK, Willett W, Curhan G. Fructose-rich beverages and risk of gout in women. *JAMA*. 2010 Nov 24;304(20):2270–8.

- [39] Khanna D, Fitzgerald JD, Khanna PP, Bae S, Singh MK, Neogi T, Pillinger MH, Merrill J, Lee S, Prakash S, Kaldas M, Gogia M, Perez-Ruiz F, Taylor W, Lioté F, Choi H, Singh J a, ... Terkeltaub R. 2012 American College of Rheumatology guidelines for management of gout. Part 1: systematic nonpharmacologic and pharmacologic therapeutic approaches to hyperuricemia. *Arthritis Care Res (Hoboken)*. 2012 Oct;64(10):1431–46.
- [40] Choi HK, Willett W, Curhan G. Coffee consumption and risk of incident gout in men: a prospective study. *Arthritis Rheum*. 2007 Jun;56(6):2049–55.
- [41] Study H. Coffee consumption and risk of incident gout in women: the Nurses' Health study. *Am J Clin Nutr*. 2010;92(4):922–7.
- [42] Kiyohara C, Kono S, Honjo S, Todoroki I, Sakurai Y, Nishiwaki M, Hamada H, Nishikawa H, Koga H, Ogawa S, Nakagawa K. Inverse association between coffee drinking and serum uric acid concentrations in middle-aged Japanese males. *Br J Nutr*. 1999 Aug;82(2):125–30.
- [43] Dalbeth N, Ames R, Gamble GD, Horne A, Wong S, Kuhn-Sherlock B, MacGibbon A, McQueen FM, Reid IR, Palmano K. Effects of skim milk powder enriched with glycomacropeptide and G600 milk fat extract on frequency of gout flares: a proof-of-concept randomised controlled trial. *Ann Rheum Dis*. 2012 Jun;71(6):929–34.
- [44] Jacob RA, Spinozzi GM, Vicky A, Kelley DS, Prior RL, Ars A, Children A. Consumption of cherries lowers plasma urate in healthy women. *J Nutr*. 2003;2(January):1826–9.
- [45] Zhang Y, Neogi T, Chen C, Chaisson C, Hunter DJ, Choi HK. Cherry Consumption and Decreased Risk of Recurrent Gout Attacks. *Arthritis Rheum*. 2012;64(12):4004–11.
- [46] Choi H, Gao X, Curham G. Vitamin C Intake and the Risk of Gout in Men. A prospective study. *Arch Intern Med*. 2009;169(5):502–7.
- [47] Gao X, Curhan G, Forman JP, Ascherio A, Choi HK. Vitamin C intake and serum uric acid concentration in men. *J Rheumatol*. 2008 Sep;35(9):1853–8.
- [48] Gibson T, Rodgers A, Simmonds H, Toseland P. Beer drinking and its effect on uric acid. *Br J Rheumatol*. 1984;23(3):203.
- [49] Zhang Y, Woods R, Chaisson CE, Neogi T, Niu J, McAlindon TE, Hunter D. Alcohol consumption as a trigger of recurrent gout attacks. *Am J Med*. 2006 Sep;119(9):800.e13–8.

- [50] Neogi T, Chen C, Niu J, Chaisson C, Hunter DJ, Zhang Y. Alcohol quantity and type on risk of recurrent gout attacks: an internet-based case-crossover study. *Am J Med.* Elsevier Inc; 2014 Apr;127(4):311–8.
- [51] Choi HK, Atkinson K, Karlson EW, Willett W, Curhan G. Alcohol intake and risk of incident gout in men: a prospective study. *Lancet.* 2004 Apr 17;363(9417):1277–81.
- [52] Zhang W, Doherty M, Bardin T, Pascual E, Barskova V, Conaghan P, Gerster J, Jacobs J, Leeb B, Lioté F, McCarthy G, Netter P, Nuki G, Perez-Ruiz F, Pignone A, Pimentão J, Punzi L, ... Zimmermann-Gòrska I. EULAR evidence based recommendations for gout. Part II: Management. Report of a task force of the EULAR Standing Committee for International Clinical Studies Including Therapeutics (ESCISIT). *Ann Rheum Dis.* 2006 Oct;65(10):1312–24.
- [53] Zhu Y, Pandya BJ, Choi HK. Comorbidities of gout and hyperuricemia in the US general population: NHANES 2007-2008. *Am J Med.* Elsevier Inc.; 2012 Jul;125(7):679–687.e1.
- [54] Khosla UM, Zharikov S, Finch JL, Nakagawa T, Roncal C, Mu W, Krotova K, Block ER, Prabhakar S, Johnson RJ. Hyperuricemia induces endothelial dysfunction. *Kidney Int.* 2005 May;67(5):1739–42.
- [55] Corry D, Eslami P, Yamamoto K, Nyby M, Makino H, Tuck M. Uric acid stimulates vascular smooth muscle cell proliferation and oxidative stress via the vascular renin-angiotensin system. *J Hypertens.* 2008;26(2):269–75.
- [56] Feig D. Uric acid. A novel mediator and marker of risk in chronic kidney disease? *Curr Opin Nephrol Hypertens.* 2009;18(6):526–30.
- [57] Feig DI, Soletsky B, Johnson RJ. Effect of Allopurinol on Blood Pressure Essential Hypertension. *JAMA.* 2008;300(8):924–32.
- [58] Soletsky B, Feig DI. Uric acid reduction rectifies prehypertension in obese adolescents. *Hypertension.* 2012 Nov;60(5):1148–56.
- [59] Gois P, Souza E. Pharmacotherapy for hyperuricemia in hypertensive patients. *Cochrane database Syst Rev.* 2013;(1):CD008652.
- [60] Bhole V, Choi JW, Kim SW, de Vera M, Choi H. Serum uric acid levels and the risk of type 2 diabetes: a prospective study. *Am J Med.* Elsevier Inc.; 2010 Oct;123(10):957–61.
- [61] Sattui SE, Singh J a, Gaffo AL. Comorbidities in Patients with Crystal Diseases and Hyperuricemia. *Rheum Dis Clin North Am.* 2014 May;40(2):251–78.

- [62] Montalcini T, Gorgone G, Gazzaruso C, Sesti G, Perticone F, Pujia A. Relation between serum uric acid and carotid intima-media thickness in healthy postmenopausal women. *Intern Emerg Med*. 2007 Mar;2(1):19–23.
- [63] Tavit Y, Kaya MG, Oktar SO, Sen N, Okyay K, Yazici HU, Cengel A. Uric acid level and its association with carotid intima-media thickness in patients with hypertension. *Atherosclerosis*. 2008 Mar;197(1):159–63.
- [64] Wang H, Jacobs DR, Gaffo a L, Gross MD, Goff DC, Carr JJ. Longitudinal association between serum urate and subclinical atherosclerosis: the Coronary Artery Risk Development in Young Adults (CARDIA) study. *J Intern Med*. 2013 Dec;274(6):594–609.
- [65] Neogi T, Terkeltaub R, Ellison R, Hunt S, Zhang Y. Serum urate is not associated with coronary artery calcification: the NHLBI Family Heart Study. *J Rheumatol*. 2011;38(1):111–7.
- [66] Kim SY, Guevara JP, Kim KM, Choi HK, Heitjan DF, Albert D a. Hyperuricemia and coronary heart disease: a systematic review and meta-analysis. *Arthritis Care Res (Hoboken)*. 2010 Feb;62(2):170–80.
- [67] Zhao G, Huang L, Song M, Song Y. Baseline serum uric acid level as a predictor of cardiovascular disease related mortality and all-cause mortality: a meta-analysis of prospective studies. *Atherosclerosis*. Elsevier Ltd; 2013 Nov;231(1):61–8.
- [68] Choi HK, Zhu Y, Mount DB. Genetics of gout. *Curr Opin Rheumatol*. 2010 Mar;22(2):144–51.
- [69] Krishnan E, Lessov-Schlaggar CN, Krasnow RE, Swan GE. Nature versus nurture in gout: a twin study. *Am J Med*. Elsevier Inc.; 2012 May;125(5):499–504.
- [70] Kolz M, Johnson T, Sanna S, Teumer A, Vitart V, Perola M, Mangino M, Albrecht E, Wallace C, Farrall M, Johansson A, Nyholt DR, Aulchenko Y, Beckmann JS, Bergmann S, Bochud M, Brown M, ... Gieger C. Meta-analysis of 28,141 individuals identifies common variants within five new loci that influence uric acid concentrations. *PLoS Genet*. 2009 Jun;5(6):e1000504.
- [71] Yang Q, Köttgen A, Dehghan A, Smith A V, Glazer NL, Chen M-H, Chasman DI, Aspelund T, Eiriksdottir G, Harris TB, Launer L, Nalls M, Hernandez D, Arking DE, Boerwinkle E, Grove ML, Li M, ... Coresh J. Multiple genetic loci influence serum urate levels and their relationship with gout and cardiovascular disease risk factors. *Circ Cardiovasc Genet*. 2010 Dec;3(6):523–30.

- [72] Tin A, Woodward OM, Kao WHL, Liu C-T, Lu X, Nalls M a, Shriner D, Semmo M, Akyzbekova EL, Wyatt SB, Hwang S-J, Yang Q, Zonderman AB, Adeyemo A a, Palmer C, Meng Y, Reilly M, ... Köttgen A. Genome-wide association study for serum urate concentrations and gout among African Americans identifies genomic risk loci and a novel URAT1 loss-of-function allele. *Hum Mol Genet.* 2011 Oct 15;20(20):4056–68.
- [73] Okada Y, Sim X, Go MJ, Wu J-Y, Gu D, Takeuchi F, Takahashi A, Maeda S, Tsunoda T, Chen P, Lim S-C, Wong T-Y, Liu J, Young TL, Aung T, Seielstad M, Teo Y-Y, ... Tanaka T. Meta-analysis identifies multiple loci associated with kidney function-related traits in east Asian populations. *Nat Genet.* Nature Publishing Group; 2012 Aug;44(8):904–9.
- [74] Köttgen A, Albrecht E, Teumer A, Vitart V, Krumsiek J, Hundertmark C, Pistis G, Ruggiero D, O’Seaghdha CM, Haller T, Yang Q, Tanaka T, Johnson AD, Kutalik Z, Smith A V, Shi J, Struchalin M, ... Gieger C. Genome-wide association analyses identify 18 new loci associated with serum urate concentrations. *Nat Genet.* 2013 Feb;45(2):145–54.
- [75] Sulem P, Gudbjartsson DF, Walters GB, Helgadóttir HT, Helgason A, Gudjonsson S a, Zanon C, Besenbacher S, Bjornsdóttir G, Magnusson OT, Magnusson G, Hjartarson E, Saemundsdóttir J, Gylfason A, Jonasdóttir A, Holm H, Karason A, ... Stefansson K. Identification of low-frequency variants associated with gout and serum uric acid levels. *Nat Genet.* Nature Publishing Group; 2011 Nov;43(11):1127–30.
- [76] Reginato AM, Olsen BR. Genetics and experimental models of crystal-induced arthritis. Lessons learned from mice and men: is it crystal clear? *Curr Opin Rheumatol.* 2007;19(2):134–45.
- [77] Hak a E, Curhan GC, Grodstein F, Choi HK. Menopause, postmenopausal hormone use and risk of incident gout. *Ann Rheum Dis.* 2010 Jul;69(7):1305–9.
- [78] Nicholls a, Snaith ML, Scott JT. Effect of oestrogen therapy on plasma and urinary levels of uric acid. *Br Med J.* 1973 Feb 24;1(5851):449–51.
- [79] Lioté F, Lancrenon S, Lanz S, Guggenbuhl P, Lambert C, Saraux A, Chiarelli P, Delva C, Aubert J-P, Ea H-K. GOSPEL: prospective survey of gout in France. Part I: design and patient characteristics (n = 1003). *Joint Bone Spine.* Elsevier Masson SAS; 2012 Oct;79(5):464–70.
- [80] Kim H-R, Lee JH, Oh J, Kim NR, Lee S-H. Clinical images: detection of gouty arthritis in the atlantoaxial joint using dual-energy computed tomography. *Arthritis Rheum.* 2012 Apr;64(4):1290.

- [81] Simkin P, Campbell P, Larson E. Gout in Heberden's nodes. *Arthritis Rheum.* 1983;26(1):94-7.
- [82] Parhami N, Greenstein N, Juozevicius J. Erosive osteoarthritis and gout: gout in 36 joints. *J Rheumatol.* 1986;13(2):469-71.
- [83] Baer P, Tenenbaum J, Fam A, Little H. Coexistent septic and crystal arthritis. Report of four cases and literature review. *J Rheumatol.* 1986;13(3):604-7.
- [84] Kobayashi S, Taniguchi A, Okamoto H, Momohara S, Tomatsu T. A case of isolated gouty tophus in a patient without a previous history of gouty arthritis. *J Clin Rheumatol.* 2009 Oct;15(7):373.
- [85] Zhang W, Doherty M, Pascual E, Bardin T, Barskova V, Conaghan P, Gerster J, Jacobs J, Leeb B, Lioté F, McCarthy G, Netter P, Nuki G, Perez-Ruiz F, Pignone A, Pimentão J, Punzi L, ... Zimmermann-Gòrska I. EULAR evidence based recommendations for gout. Part I: Diagnosis. Report of a task force of the Standing Committee for International Clinical Studies Including Therapeutics (ESCISIT). *Ann Rheum Dis.* 2006 Oct;65(10):1301-11.
- [86] Pascual E, Batlle-Guardia E, Martínez A, Rosas J, Vela P. Synovial fluid analysis for diagnosis of intercritical gout. *Ann Intern Med.* 1999;131(10):756-9.
- [87] Pascual E, Sivera F, Andrés M. Synovial fluid analysis for crystals. *Curr Opin Rheumatol.* 2011 Mar [cited 2014 Jan 23];23(2):161-9.
- [88] Olivé A, Garcia-Melchor E. On Raynaud's phenomenon. *Med Clin (Barc).* 2009 May 16;132(18):712-8.
- [89] Dalbeth N, Fransen J, Jansen TL, Neogi T, Schumacher HR, Taylor WJ. New classification criteria for gout: a framework for progress. *Rheumatology (Oxford).* 2013 Oct [cited 2014 Jul 9];52(10):1748-53.
- [90] Urano W, Yamanaka H, Tsutani H, Nakajima H, Matsuda Y, Taniguchi A, Hara M, Kamatani N. The inflammatory process in the mechanism of decreased serum uric acid concentrations during acute gouty arthritis. *J Rheumatol.* 2002;29(9):1950-3.
- [91] Yu KH, Luo SF, Liou LB, Wu Y-JJ, Tsai WP, Chen JY, Ho HH. Concomitant septic and gouty arthritis--an analysis of 30 cases. *Rheumatology (Oxford).* 2003 Sep;42(9):1062-6.
- [92] Tejera B, Riveros A, Martínez-Morillo M, Cañellas J. Septic arthritis associated to gout and pseudogout: the importance of arthrocentesis. *Reumatol Clin.* 2014;10(1):61-2.

- [93] Bellamy N, Downie WW, Buchanan WW. Observations on spontaneous improvement in patients with podagra: implications for therapeutic trials of non-steroidal anti-inflammatory drugs. *Br J Clin Pharmacol*. 1987 Jul;24(1):33–6.
- [94] Khanna D, Khanna PP, Fitzgerald JD, Singh MK, Bae S, Neogi T, Pillinger MH, Merrill J, Lee S, Prakash S, Kaldas M, Gogia M, Perez-Ruiz F, Taylor W, Lioté F, Choi H, Singh J a, ... Terkeltaub R. 2012 American College of Rheumatology guidelines for management of gout. Part 2: therapy and antiinflammatory prophylaxis of acute gouty arthritis. *Arthritis Care Res (Hoboken)*. 2012 Oct;64(10):1447–61.
- [95] Neogi T. Gout. *N Engl J Med*. 2011;364(5):443–52.
- [96] Schlesinger N. Treatment of Acute Gout. *Rheum Dis Clin North Am*. Elsevier Inc; 2014 May;40(2):329–41.
- [97] Schlesinger N, Detry M, Holland B, Baker D, Beutler A, Rull M, Hoffman B, Schumacher H. Local ice therapy during bouts of acute gouty arthritis. *J Rheumatol*. 2002;29(2):331–4.
- [98] Martinon F, Pétrilli V, Mayor A, Tardivel A, Tschopp J. Gout-associated uric acid crystals activate the NALP3 inflammasome. *Nature*. 2006 Mar 9;440(7081):237–41.
- [99] Terkeltaub R a, Furst DE, Bennett K, Kook K a, Crockett RS, Davis MW. High versus low dosing of oral colchicine for early acute gout flare: Twenty-four-hour outcome of the first multicenter, randomized, double-blind, placebo-controlled, parallel-group, dose-comparison colchicine study. *Arthritis Rheum*. 2010 Apr;62(4):1060–8.
- [100] Perez-Ruiz F, Herrero-Beites AM. ACTH analogues medications for the treatment of crystal-induced acute inflammation. A target to be explored? *Joint Bone Spine*. Elsevier Masson SAS; 2013 May;80(3):236–7.
- [101] Daoussis D, Antonopoulos I, Yiannopoulos G, Andonopoulos AP. ACTH as first line treatment for acute gout in 181 hospitalized patients. *Joint Bone Spine*. Elsevier Masson SAS; 2013 May;80(3):291–4.
- [102] Axelrod D, Preston S. Comparison of parenteral adrenocorticotrophic hormone with oral indomethacin in the treatment of acute gout. *Arthritis Rheum*. 1988;31(6):803–5.
- [103] Siegel L, Alloway J, Nashel D. Comparison of adrenocorticotrophic hormone and triamcinolone acetonide in the treatment of acute gouty arthritis. *J Rheumatol*. 1994;21(7):1325–7.
- [104] Terkeltaub R, Sundry JS, Schumacher HR, Murphy F, Bookbinder S, Biedermann S, Wu R, Mellis S, Radin A. The interleukin 1 inhibitor rilonacept in treatment of chronic



- gouty arthritis: results of a placebo-controlled, monosequence crossover, non-randomised, single-blind pilot study. *Ann Rheum Dis.* 2009 Oct;68(10):1613–7.
- [105] Edwards NL, So A. Emerging Therapies for Gout. *Rheum Dis Clin North Am.* Elsevier Inc; 2014 May;40(2):375–87.
- [106] So A, De Meulemeester M, Pikhak A, Yücel a E, Richard D, Murphy V, Arulmani U, Sallstig P, Schlesinger N. Canakinumab for the treatment of acute flares in difficult-to-treat gouty arthritis: Results of a multicenter, phase II, dose-ranging study. *Arthritis Rheum.* 2010 Oct;62(10):3064–76.
- [107] Schlesinger N, De Meulemeester M, Pikhak A, Yücel a E, Richard D, Murphy V, Arulmani U, Sallstig P, So A. Canakinumab relieves symptoms of acute flares and improves health-related quality of life in patients with difficult-to-treat Gouty Arthritis by suppressing inflammation: results of a randomized, dose-ranging study. *Arthritis Res Ther.* BioMed Central Ltd; 2011 Jan;13(2):R53.
- [108] Schlesinger N, Alten RE, Bardin T, Schumacher HR, Bloch M, Gimona A, Krammer G, Murphy V, Richard D, So AK. Canakinumab for acute gouty arthritis in patients with limited treatment options: results from two randomised, multicentre, active-controlled, double-blind trials and their initial extensions. *Ann Rheum Dis.* 2012 Nov;71(11):1839–48.
- [109] Tran A, Edelman J. Interleukin-1 inhibition by anakinra in refractory chronic tophaceous gout. *Int J Rheum Dis.* 2011;14(3):e33–7.
- [110] Chen K, Fields T, Mancuso C a, Bass AR, Vasanth L. Anakinra's efficacy is variable in refractory gout: report of ten cases. *Semin Arthritis Rheum.* Elsevier Inc.; 2010 Dec;40(3):210–4.
- [111] Singh D, Huston KK. IL-1 inhibition with anakinra in a patient with refractory gout. *J Clin Rheumatol.* 2009 Oct;15(7):366.
- [112] Gratton SB, Scalapino KJ, Fye KH. Case of anakinra as a steroid-sparing agent for gout inflammation. *Arthritis Rheum.* 2009 Sep 15;61(9):1268–70.
- [113] McGonagle D, Tan a L, Shankaranarayana S, Madden J, Emery P, McDermott MF. Management of treatment resistant inflammation of acute on chronic tophaceous gout with anakinra. *Ann Rheum Dis.* 2007 Dec;66(12):1683–4.
- [114] So A, De Smedt T, Revaz S, Tschopp J. A pilot study of IL-1 inhibition by anakinra in acute gout. *Arthritis Res Ther.* 2007 Jan;9(2):R28.
- [115] So A, Busso N. A magic bullet for gout? *Ann Rheum Dis.* 2009 Oct;68(10):1517–9.



- [116] Doherty T a, Brydges SD, Hoffman HM. Autoinflammation: translating mechanism to therapy. *J Leukoc Biol.* 2011 Jul [cited 2014 Jul 10];90(1):37–47.
- [117] Chaichian Y, Chohan S, Becker M a. Long-Term Management of Gout: Nonpharmacologic and Pharmacologic Therapies. *Rheum Dis Clin North Am.* Elsevier Inc; 2014 May;40(2):357–74.
- [118] Perez-Ruiz F, Calabozo M, Pijoan JI, Herrero-Beites AM, Ruibal A. Effect of urate-lowering therapy on the velocity of size reduction of tophi in chronic gout. *Arthritis Rheum.* 2002 Aug;47(4):356–60.
- [119] Rees F, Jenkins W, Doherty M. Patients with gout adhere to curative treatment if informed appropriately: proof-of-concept observational study. *Ann Rheum Dis.* 2013 Jun;72(6):826–30.
- [120] Rees F, Hui M, Doherty M. Optimizing current treatment of gout. *Nat Rev Rheumatol.* Nature Publishing Group; 2014 May;10(5):271–83.
- [121] Burns CM, Wortmann RL. Gout therapeutics: new drugs for an old disease. *Lancet.* Elsevier Ltd; 2011 Jan 8;377(9760):165–77.
- [122] Becker M a, Schumacher HR, Wortmann RL, MacDonald P a, Palo W a, Eustace D, Vernillet L, Joseph-Ridge N. Febuxostat, a novel nonpurine selective inhibitor of xanthine oxidase: a twenty-eight-day, multicenter, phase II, randomized, double-blind, placebo-controlled, dose-response clinical trial examining safety and efficacy in patients with gout. *Arthritis Rheum.* 2005 Mar;52(3):916–23.
- [123] Schumacher HR, Becker M a, Wortmann RL, Macdonald P a, Hunt B, Streit J, Lademacher C, Joseph-Ridge N. Effects of febuxostat versus allopurinol and placebo in reducing serum urate in subjects with hyperuricemia and gout: a 28-week, phase III, randomized, double-blind, parallel-group trial. *Arthritis Rheum.* 2008 Nov 15;59(11):1540–8.
- [124] Mayer M, Khosravan R, Vernillet L, Wu J, Joseph-Ridge N, Mulford D. Pharmacokinetics and pharmacodynamics of febuxostat, a new non-purine selective inhibitor of xanthine oxidase in subjects with renal impairment. *Am J Ther.* 2005;12(1):22–34.
- [125] Perez-Ruiz F, Alonso-Ruiz A, Calabozo M, Herrero-Beites A, García-Erauskin G, Ruiz-Lucea E. Efficacy of allopurinol and benzbromarone for the control of hyperuricaemia. A pathogenic approach to the treatment of primary chronic gout. *Ann Rheum Dis.* 1998 Sep;57(9):545–9.

- [126] Yood RA, Edwards NL, Gutierrez-urena SR, Treadwell EL, White WB, Lipsky PE, Horowitz Z, Maroli AN, Ii RWW, Hamburger SA, Becker MA. Efficacy and Tolerability of Pegloticase for the Treatment of Chronic Gout in Patients. *JAMA*. 2011;306(7):711–20.
- [127] Schumacher HR, Sundy JS, Terkeltaub R, Knapp HR, Mellis SJ, Stahl N, Yancopoulos GD, Soo Y, King-Davis S, Weinstein SP, Radin AR. Riloncept (interleukin-1 trap) in the prevention of acute gout flares during initiation of urate-lowering therapy: results of a phase II randomized, double-blind, placebo-controlled trial. *Arthritis Rheum*. 2012 Mar;64(3):876–84.
- [128] Schumacher HR, Evans RR, Saag KG, Clower J, Jennings W, Weinstein SP, Yancopoulos GD, Wang J, Terkeltaub R. Riloncept (interleukin-1 trap) for prevention of gout flares during initiation of uric acid-lowering therapy: results from a phase III randomized, double-blind, placebo-controlled, confirmatory efficacy study. *Arthritis Care Res (Hoboken)*. 2012 Oct;64(10):1462–70.
- [129] Mitha E, Schumacher HR, Fouche L, Luo S-F, Weinstein SP, Yancopoulos GD, Wang J, King-Davis S, Evans RR. Riloncept for gout flare prevention during initiation of uric acid-lowering therapy: results from the PRESURGE-2 international, phase 3, randomized, placebo-controlled trial. *Rheumatology (Oxford)*. 2013 Jul;52(7):1285–92.
- [130] Schlesinger N, Mysler E, Lin H-Y, De Meulemeester M, Rovensky J, Arulmani U, Balfour A, Krammer G, Sallstig P, So A. Canakinumab reduces the risk of acute gouty arthritis flares during initiation of allopurinol treatment: results of a double-blind, randomised study. *Ann Rheum Dis*. 2011 Jul;70(7):1264–71.
- [131] McDermott MF, Aksentijevich I, Galon J, McDermott EM, Ogunkolade BW, Centola M, Mansfield E, Gadina M, Karenko L, Pettersson T, McCarthy J, Frucht DM, Aringer M, Torosyan Y, Teppo a M, Wilson M, Karaarslan HM, ... Kastner DL. Germline mutations in the extracellular domains of the 55 kDa TNF receptor, TNFR1, define a family of dominantly inherited autoinflammatory syndromes. *Cell*. 1999 Apr 2;97(1):133–44.
- [132] Galon J, Aksentijevich I, McDermott MF, O'Shea JJ, Kastner DL. TNFRSF1A mutations and autoinflammatory syndromes. *Curr Opin Immunol*. 2000 Aug;12(4):479–86.
- [133] Dinarello C a. Immunological and inflammatory functions of the interleukin-1 family. *Annu Rev Immunol*. 2009 Jan;27:519–50.
- [134] McGonagle D, McDermott MF. A proposed classification of the immunological diseases. *PLoS Med*. 2006 Aug;3(8):e297.

- [135] Ryan JG, Goldbach-Mansky R. The spectrum of autoinflammatory diseases: recent bench to bedside observations. *Curr Opin Rheumatol*. 2008;20(1):66–75.
- [136] Di Giovine F, Malawista S, Nuki G, GW D. Interleukin 1 (IL-1) as a mediator of crystal arthritis. Stimulation of T cell and synovial fibroblast mitogenesis by urate crystal-induced IL 1. *J Immunol*. 1987;138(10):3213–8.
- [137] Pétrilli V, Martinon F. The inflammasome, autoinflammatory diseases and gout. *Jt Bone Spine*. 2007;74:571–6.
- [138] Franchi L, Eigenbrod T, Muñoz-Planillo R, Nuñez G. The inflammasome: a caspase-1-activation platform that regulates immune responses and disease pathogenesis. *Nat Immunol*. 2009 Mar;10(3):241–7.
- [139] Martinon F, Mayor A, Tschopp J. The inflammasomes: guardians of the body. *Annu Rev Immunol*. 2009 Jan;27:229–65.
- [140] Sidiropoulos PI, Goulielmos G, Voloudakis GK, Petraki E, Boumpas DT. Inflammasomes and rheumatic diseases: evolving concepts. *Ann Rheum Dis*. 2008 Oct;67(10):1382–9.
- [141] Medzhitov R. Toll-like receptors and innate immunity. *Nat Rev Immunol*. 2001 Nov;1(2):135–45.
- [142] Martinon F, Burns K, Tschopp J. The inflammasome: a molecular platform triggering activation of inflammatory caspases and processing of proIL-beta. *Mol Cell*. 2002;10(2):417–26.
- [143] Martinon F, Tschopp J. Inflammatory caspases: linking an intracellular innate immune system to autoinflammatory diseases. *Cell*. 2004;117(5):561–74.
- [144] Hoffman HM, Mueller JL, Broide DH, Wanderer a a, Kolodner RD. Mutation of a new gene encoding a putative pyrin-like protein causes familial cold autoinflammatory syndrome and Muckle-Wells syndrome. *Nat Genet*. 2001 Nov;29(3):301–5.
- [145] Aganna E, Martinon F, Hawkins PN, Ross JB, Swan DC, Booth DR, Lachmann HJ, Bybee A, Gaudet R, Woo P, Feighery C, Cotter FE, Thome M, Hitman G a, Tschopp J, McDermott MF. Association of mutations in the NALP3/CIAS1/PYPAF1 gene with a broad phenotype including recurrent fever, cold sensitivity, sensorineural deafness, and AA amyloidosis. *Arthritis Rheum*. 2002 Sep;46(9):2445–52.
- [146] Agostini L, Martinon F, Burns K, Mcdermott MF, Hawkins PN, Boveresses C, Epalinges C-. NALP3 Forms an IL-1b-Processing Inflammasome with Increased Activity in Muckle-Wells Autoinflammatory Disorder. 2004;20(3):319–25.

- [147] Perregaux D, Gabels A. Interleukin-1 $\beta$  Maturation and Release in Response to ATP and Nigericin. *J Biol Chem*. 1994;269(21):15195–203.
- [148] Mariathasan S, Weiss DS, Newton K, McBride J, O'Rourke K, Roose-Girma M, Lee WP, Weinrauch Y, Monack DM, Dixit VM. Cryopyrin activates the inflammasome in response to toxins and ATP. *Nature*. 2006 Mar 9;440(7081):228–32.
- [149] Hornung V, Bauernfeind F, Halle A, Samstad EO, Kono H, Rock KL, Fitzgerald K a, Latz E. Silica crystals and aluminum salts activate the NALP3 inflammasome through phagosomal destabilization. *Nat Immunol*. 2008 Aug;9(8):847–56.
- [150] Eisenbarth SC, Colegio OR, O'Connor W, Sutterwala FS, Flavell R a. Crucial role for the Nalp3 inflammasome in the immunostimulatory properties of aluminium adjuvants. *Nature*. 2008 Jun 19;453(7198):1122–6.
- [151] Dostert C, Pétrilli V, Van Bruggen R, Steele C, Mossman BT, Tschopp J. Innate immune activation through Nalp3 inflammasome sensing of asbestos and silica. *Science*. 2008 May 2;320(5876):674–7.
- [152] Kanneganti T-D, Ozören N, Body-Malapel M, Amer A, Park J-H, Franchi L, Whitfield J, Barchet W, Colonna M, Vandenabeele P, Bertin J, Coyle A, Grant EP, Akira S, Núñez G. Bacterial RNA and small antiviral compounds activate caspase-1 through cryopyrin/Nalp3. *Nature*. 2006 Mar 9;440(7081):233–6.
- [153] Kanneganti T-D, Body-Malapel M, Amer A, Park J-H, Whitfield J, Franchi L, Taraporewala ZF, Miller D, Patton JT, Inohara N, Núñez G. Critical role for Cryopyrin/Nalp3 in activation of caspase-1 in response to viral infection and double-stranded RNA. *J Biol Chem*. 2006 Dec 1;281(48):36560–8.
- [154] Berlin R, Wood B. Studies on the pathogenesis of fever. XII. Electrolytic factors influencing the release of endogenous pyrogen from polymorphonuclear leucocytes. *J ex*. 1964;119:697–714.
- [155] Pétrilli V, Papin S, Dostert C, Mayor A, Martinon F, Tschopp J. Activation of the NALP3 inflammasome is triggered by low intracellular potassium concentration. *Cell Death Differ*. 2007 Sep;14(9):1583–9.
- [156] Pelegrin P, Surprenant A. Pannexin-1 couples to maitotoxin- and nigericin-induced interleukin-1 $\beta$  release through a dye uptake-independent pathway. *J Biol Chem*. 2007 Jan 26;282(4):2386–94.
- [157] Rubartelli A. Redox control of NLRP3 inflammasome activation in health and disease. *J Leukoc Biol*. 2012 Nov;92(5):951–8.

- [158] Haneklaus M, O'Neill L a J, Coll RC. Modulatory mechanisms controlling the NLRP3 inflammasome in inflammation: recent developments. *Curr Opin Immunol*. Elsevier Ltd; 2013 Feb;25(1):40–5.
- [159] Hoffman HM, Scott P, Mueller JL, Misaghi A, Stevens S, Yancopoulos GD, Murphy A, Valenzuela DM, Liu-Bryan R. Role of the leucine-rich repeat domain of cryopyrin/NALP3 in monosodium urate crystal-induced inflammation in mice. *Arthritis Rheum*. 2010 Jul;62(7):2170–9.
- [160] McDermott MF. A common pathway in periodic fever syndromes. *Trends Immunol*. 2004 Sep;25(9):457–60.
- [161] Contassot E, Beer H-D, French LE. Interleukin-1, inflammasomes, autoinflammation and the skin. *Swiss Med Wkly*. 2012 Jan [cited 2014 May 26];142(May):w13590.
- [162] Sims JE, Smith DE. The IL-1 family: regulators of immunity. *Nat Rev Immunol*. Nature Publishing Group; 2010 Feb;10(2):89–102.
- [163] Guma M, Ronacher L, Liu-Bryan R, Takai S, Karin M, Corr M. Caspase 1-independent activation of interleukin-1beta in neutrophil-predominant inflammation. *Arthritis Rheum*. 2009 Dec;60(12):3642–50.
- [164] Netea MG, Nold-Petry C a, Nold MF, Joosten L a B, Opitz B, van der Meer JHM, van de Veerdonk FL, Ferwerda G, Heinhuis B, Devesa I, Funk CJ, Mason RJ, Kullberg BJ, Rubartelli A, van der Meer JWM, Dinarello C a. Differential requirement for the activation of the inflammasome for processing and release of IL-1beta in monocytes and macrophages. *Blood*. 2009 Mar 5;113(10):2324–35.
- [165] Gabay C, Lamacchia C, Palmer G. IL-1 pathways in inflammation and human diseases. *Nat Rev Rheumatol*. Nature Publishing Group; 2010 Apr;6(4):232–41.
- [166] Horai R, Saijo S, Tanioka H, Nakae S, Sudo K, Okahara A, Ikuse T, Asano M, Iwakura Y. Development of chronic inflammatory arthropathy resembling rheumatoid arthritis in interleukin 1 receptor antagonist-deficient mice. *J Exp Med*. 2000 Jan 17;191(2):313–20.
- [167] Almeida de Jesus A, Goldbach-Mansky R. Monogenic autoinflammatory diseases: concept and clinical manifestations. *Clin Immunol*. Elsevier B.V.; 2013 Jun;147(3):155–74.
- [168] Janeway C a, Medzhitov R. Innate immune recognition. *Annu Rev Immunol*. 2002 Jan;20(2):197–216.

- [169] Matzinger P. The danger model: a renewed sense of self. *Science*. 2002 Apr 12;296(5566):301–5.
- [170] Shi Y, Evans JE, Rock KL. Molecular identification of a danger signal that alerts the immune system to dying cells. *Nature*. 2003;425(6957):516–21.
- [171] Tran T, Pham J, Shafeeq H, Manigault K, Arya V. Role of interleukin-1 inhibitors in the management of gout. *Pharmacotherapy*. 2013;33(7):744–53.
- [172] Scott P, Ma H, Viriyakosol S, Terkeltaub R, Liu-Bryan R. Engagement of CD14 mediates the inflammatory potential of monosodium urate crystals. *J Immunol*. 2006 Nov 1;177(9):6370–8.
- [173] Liu-Bryan R, Scott P, Sydlaske A, Rose DM, Terkeltaub R. Innate immunity conferred by Toll-like receptors 2 and 4 and myeloid differentiation factor 88 expression is pivotal to monosodium urate monohydrate crystal-induced inflammation. *Arthritis Rheum*. 2005 Sep;52(9):2936–46.
- [174] Liu-bryan R, Pritzker K, Firestein GS, Terkeltaub R. TLR2 signalling in chondrocytes drives calcium pyrophosphate dihydrate and monosodium urate crystal-induced nitric oxide generation. *J Immunol*. 2010;174(8):5016.
- [175] Chen C-J, Shi Y, Hearn A, Fitzgerald K, Golenbock D, Reed G, Akira S, Rock KL. MyD88-dependent IL-1 receptor signaling is essential for gouty inflammation stimulated by monosodium urate crystals. *J Clin Invest*. 2006;116(8):2262–71.
- [176] Riteau N, Baron L, Villeret B, Guillou N, Savigny F, Ryffel B, Rassendren F, Le Bert M, Gombault a, Couillin I. ATP release and purinergic signaling: a common pathway for particle-mediated inflammasome activation. *Cell Death Dis*. Nature Publishing Group; 2012 Jan [cited 2014 Jun 4];3(10):e403.
- [177] Schorn C, Frey B, Lauber K, Janko C, Stryio M, Keppeler H, Gaip US, Voll RE, Springer E, Munoz LE, Schett G, Herrmann M. Sodium overload and water influx activate the NALP3 inflammasome. *J Biol Chem*. 2011 Jan 7;286(1):35–41.
- [178] Geissmann F, Manz MG, Jung S, Sieweke MH, Merad M, Ley K. Development of monocytes, macrophages, and dendritic cells. *Science*. 2010 Feb 5;327(5966):656–61.
- [179] Mononuclear phagocytes in immune defence. *Immunology*. p. 147–61.
- [180] Ziegler-Heitbrock L. Monocyte subsets in man and other species. *Cell Immunol*. Elsevier Inc.; 2014;289(1-2):135–9.

- [181] Van Furth R, Cohn Z a. The origin and kinetics of mononuclear phagocytes. *J Exp Med.* 1968 Sep 1;128(3):415–35.
- [182] Van Furth R, Cohn Z, Hirsch J, Humphrey J, Spector W, Langevoort H. The mononuclear phagocyte system: a new classification of macrophages, monocytes, and their precursor cells. *Bull World Heal Organ.* 1972;46(6):845–52.
- [183] Chorro L, Sarde A, Li M, Woollard KJ, Chambon P, Malissen B, Kissenpfennig A, Barbaroux J-B, Groves R, Geissmann F. Langerhans cell (LC) proliferation mediates neonatal development, homeostasis, and inflammation-associated expansion of the epidermal LC network. *J Exp Med.* 2009 Dec 21;206(13):3089–100.
- [184] Davies LC, Jenkins SJ, Allen JE, Taylor PR. Tissue-resident macrophages. *Nat Immunol.* 2013 Oct;14(10):986–95.
- [185] Galli SJ, Borregaard N, Wynn T a. Phenotypic and functional plasticity of cells of innate immunity: macrophages, mast cells and neutrophils. *Nat Immunol.* Nature Publishing Group; 2011 Nov;12(11):1035–44.
- [186] Mackaness GB. The immunological basis of acquired cellular resistance. *J Exp Med.* 1964;120(3):105–20.
- [187] Nathan C., Murray HW, Wlebe IE, Rubin BY. Identification of interferon-gamma as the lymphokine that activates human macrophage oxidative metabolism and antimicrobial activity. *J Emerg Med.* 1983;158(September):670–89.
- [188] Dalton DK, Pitts-meeck S, Keshav S, Figari IS, Bradley A, Stewart TA. Multiple Defects of Immune Cell Function in Mice with Disrupted Interferon- $\gamma$  Genes. *Science (80- ).* 1993;259(5102):1739–42.
- [189] Gordon S. Alternative activation of macrophages. *Nat Rev Immunol.* 2003 Jan;3(1):23–35.
- [190] Stein M, Keshav S, Harris N, Gordon S. Interleukin 4 Potently Enhances Murine Macrophage Mannose Receptor Activity: A Marker of Alternative Immunologic Macrophage Activation. *J Exp Med.* 1992;176(1):287–92.
- [191] Xue J, Schmidt S V, Sander J, Draffehn A, Krebs W, Quester I, De Nardo D, Gohel TD, Emde M, Schmidleithner L, Ganesan H, Nino-Castro A, Mallmann MR, Labzin L, Theis H, Kraut M, Beyer M, ... Schultze JL. Transcriptome-based network analysis reveals a spectrum model of human macrophage activation. *Immunity.* Elsevier Inc.; 2014 Feb 20 [cited 2014 May 28];40(2):274–88.



- [192] Mosser DM. The many faces of macrophage activation. *J Leukoc Biol.* 2003 Feb 1;73(2):209–12.
- [193] Mantovani A, Sozzani S, Locati M, Allavena P, Sica A. Macrophage polarization: tumor-associated macrophages as a paradigm for polarized M2 mononuclear phagocytes. *Trends Immunol.* 2002;23(11):549–55.
- [194] Krausgruber T, Blazek K, Smallie T, Alzabin S, Lockstone H, Sahgal N, Hussell T, Feldmann M, Udalova I a. IRF5 promotes inflammatory macrophage polarization and TH1-TH17 responses. *Nat Immunol.* Nature Publishing Group; 2011 Mar;12(3):231–8.
- [195] Mosser DM, Edwards JP. Exploring the full spectrum of macrophage activation. *Nat Rev Immunol.* Nature Publishing Group; 2008 Dec;8(12):958–69.
- [196] Mantovani A, Sica A, Sozzani S, Allavena P, Vecchi A, Locati M. The chemokine system in diverse forms of macrophage activation and polarization. *Trends Immunol.* 2004 Dec;25(12):677–86.
- [197] Martinez FO, Gordon S, Locati M, Mantovani A. Transcriptional Profiling of the Human Monocyte-to-Macrophage Differentiation and Polarization: New Molecules and Patterns of Gene Expression. *J Immunol.* 2006 Nov 2;177(10):7303–11.
- [198] Metcalf D. Hematopoietic cytokines. *Blood.* 2008 Jan 15;111(2):485–91.
- [199] Hamilton J a. Colony-stimulating factors in inflammation and autoimmunity. *Nat Rev Immunol.* 2008 Jul;8(7):533–44.
- [200] Verreck F a W, de Boer T, Langenberg DML, Hoeve M a, Kramer M, Vaisberg E, Kastelein R, Kolk A, de Waal-Malefyt R, Ottenhoff THM. Human IL-23-producing type 1 macrophages promote but IL-10-producing type 2 macrophages subvert immunity to (myco)bacteria. *Proc Natl Acad Sci U S A.* 2004;101(13):4560–5.
- [201] Young D, Lowe L, Clark S. Comparison of the effects of IL-3, granulocyte-macrophage colony-stimulating factor, and macrophage colony-stimulating factor in supporting monocyte differentiation in culture. Analysis of macrophage antibody-dependent cellular cytotoxicity. *J Immunol.* 1990;145(2):607–15.
- [202] Ambarus C a, Krausz S, van Eijk M, Hamann J, Radstake TRDJ, Reedquist K a, Tak PP, Baeten DLP. Systematic validation of specific phenotypic markers for in vitro polarized human macrophages. *J Immunol Methods.* Elsevier B.V.; 2012 Jan 31;375(1-2):196–206.
- [203] Verreck F a W, de Boer T, Langenberg DML, van der Zanden L, Ottenhoff THM. Phenotypic and functional profiling of human proinflammatory type-1 and anti-



- inflammatory type-2 macrophages in response to microbial antigens and IFN-gamma- and CD40L-mediated costimulation. *J Leukoc Biol.* 2006;79(2):285–93.
- [204] Hamilton J a, Achuthan A. Colony stimulating factors and myeloid cell biology in health and disease. *Trends Immunol.* Elsevier Ltd; 2013 Feb;34(2):81–9.
- [205] Stanley ER, Berg KL, Einstein DB, Lee PS, Yeung YG. The biology and action of colony stimulating factor-1. *Stem Cells.* 1994;12 Suppl 1(July 1996):15–24; discussion 25.
- [206] Sherr CJ, Rettenmier CW, Sacca R, Roussel MF, Look a T, Stanley ER. The c-fms proto-oncogene product is related to the receptor for the mononuclear phagocyte growth factor, CSF-1. *Cell.* 1985;41(3):665–76.
- [207] Lenzo J, Turner A, Cook A, Vlahos R, Anderson G, Reynolds E, Hamilton J. Control of macrophage lineage populations by CSF-1 receptor and GM-CSF in homeostasis and inflammation. *Immunol Cell Biol.* 2012;90(4):429–40.
- [208] Wiktor-Jedrzejczak W, Bartocci a, Ferrante a W, Ahmed-Ansari a, Sell KW, Pollard JW, Stanley ER. Total absence of colony-stimulating factor 1 in the macrophage-deficient osteopetrotic (op/op) mouse. *Proc Natl Acad Sci U S A.* 1990;87(12):4828–32.
- [209] Cecchini MG, Dominguez MG, Mocci S, Wetterwald a, Felix R, Fleisch H, Chisholm O, Hofstetter W, Pollard JW, Stanley ER. Role of colony stimulating factor-1 in the establishment and regulation of tissue macrophages during postnatal development of the mouse. *Development.* 1994;120(6):1357–72.
- [210] Ryan GR, Dai XM, Dominguez MG, Tong W, Chuan F, Chisholm O, Russell RG, Pollard JW, Stanley ER. Rescue of the colony-stimulating factor 1 (CSF-1)-nullizygous mouse (Csf1(op)/Csf1(op)) phenotype with a CSF-1 transgene and identification of sites of local CSF-1 synthesis. *Blood.* 2001 Jul 1;98(1):74–84.
- [211] Chitu V, Stanley ER. Colony-stimulating factor-1 in immunity and inflammation. *Curr Opin Immunol.* 2006 Feb;18(1):39–48.
- [212] Campbell IK, Bendele A, Smith D a, Hamilton J a. Granulocyte-macrophage colony stimulating factor exacerbates collagen induced arthritis in mice. *Ann Rheum Dis.* 1997 Jun;56(6):364–8.
- [213] Campbell IK, Rich MJ, Bischof RJ, Hamilton J a. The colony-stimulating factors and collagen-induced arthritis: exacerbation of disease by M-CSF and G-CSF and requirement for endogenous M-CSF. *J Leukoc Biol.* 2000;68(1):144–50.
- [214] Hamilton J. CSF-1 signal transduction. *J Leukoc Biol.* 1997;62(August):145–55.

- [215] Yang YH, Hamilton J a. Dependence of interleukin-1-induced arthritis on granulocyte-macrophage colony-stimulating factor. *Arthritis Rheum.* 2001 Jan;44(1):111–9.
- [216] Baran CP, Opalek JM, McMaken S, Newland C a, O'Brien JM, Hunter MG, Bringardner BD, Monick MM, Brigstock DR, Stromberg PC, Hunninghake GW, Marsh CB. Important roles for macrophage colony-stimulating factor, CC chemokine ligand 2, and mononuclear phagocytes in the pathogenesis of pulmonary fibrosis. *Am J Respir Crit Care Med.* 2007 Jul 1;176(1):78–89.
- [217] Lenda DM, Kikawada E, Stanley ER, Kelley VR. Reduced Macrophage Recruitment, Proliferation, and Activation in Colony-Stimulating Factor-1-Deficient Mice Results in Decreased Tubular Apoptosis During Renal Inflammation. *J Immunol.* 2003 Mar 15;170(6):3254–62.
- [218] Lenda DM, Stanley ER, Kelley VR. Negative Role of Colony-Stimulating Factor-1 in Macrophage, T Cell, and B Cell Mediated Autoimmune Disease in MRL-Fas<sup>lpr</sup> Mice. *J Immunol.* 2004 Sep 21;173(7):4744–54.
- [219] Hercus TR, Thomas D, Guthridge M a, Ekert PG, King-Scott J, Parker MW, Lopez AF. The granulocyte-macrophage colony-stimulating factor receptor: linking its structure to cell signaling and its role in disease. *Blood.* 2009 Aug 13;114(7):1289–98.
- [220] Stanley E, Lieschke GJ, Grail D, Metcalff D, Hodgson G, Gall JAM, Maher DW, Cebon J, Sinickas V, I ARD. Granulocyte/macrophage colony-stimulating factor-deficient mice show no major perturbation of hematopoiesis but develop a characteristic pulmonary pathology. *Proc Natl Acad Sci.* 1994;91(June):5592–6.
- [221] Campbell IK, Rich MJ, Bischof RJ, Dunn a R, Grail D, Hamilton J a. Protection from collagen-induced arthritis in granulocyte-macrophage colony-stimulating factor-deficient mice. *J Immunol.* 1998 Oct 1;161(7):3639–44.
- [222] Cook a D, Braine EL, Campbell IK, Rich MJ, Hamilton J a. Blockade of collagen-induced arthritis post-onset by antibody to granulocyte-macrophage colony-stimulating factor (GM-CSF): requirement for GM-CSF in the effector phase of disease. *Arthritis Res.* 2001 Jan;3(5):293–8.
- [223] McQualter JL, Darwiche R, Ewing C, Onuki M, Kay TW, Hamilton J a, Reid HH, Bernard CC. Granulocyte macrophage colony-stimulating factor: a new putative therapeutic target in multiple sclerosis. *J Exp Med.* 2001 Oct 1;194(7):873–82.
- [224] Manczak M, Mao P, Nakamura K, Bebbington C, Park B, Reddy PH. Neutralization of granulocyte macrophage colony-stimulating factor decreases amyloid beta 1-42 and suppresses microglial activity in a transgenic mouse model of Alzheimer's disease. *Hum Mol Genet.* 2009 Oct 15;18(20):3876–93.

- [225] Kellar R, Lancaster J, Thai H, Juneman E, Johnson N, Byrne H, Stansifer M, Arsanjani R, Baer M, Bebbington C, Flashner M, Yarranton G, Goldman S. Antibody to granulocyte macrophage colony-stimulating factor reduces the number of activated tissue macrophages and improves left ventricular function after myocardial infarction in a rat coronary artery ligation model. *J Cardiovasc Pharmacol*. 2011;57(5):568–74.
- [226] Kim D, Sandoval D, Reed JA, Matter EK, Tolod EG, Woods SC, Seeley RJ. The role of GM-CSF in adipose tissue inflammation. *Am J Physiol Endocrinol Metab*. 2008;295(5):1038–46.
- [227] Vlahos R, Bozinovski S, Hamilton J a, Anderson GP. Therapeutic potential of treating chronic obstructive pulmonary disease (COPD) by neutralising granulocyte macrophage-colony stimulating factor (GM-CSF). *Pharmacol Ther*. 2006 Oct;112(1):106–15.
- [228] Yamashita N, Tashimo H, Ishida H, Kaneko F, Nakano J, Kato H, Hirai K, Horiuchi T, Ohta K. Attenuation of airway hyperresponsiveness in a murine asthma model by neutralization of granulocyte-macrophage colony-stimulating factor (GM-CSF). *Cell Immunol*. 2002 Oct;219(2):92–7.
- [229] Haghghat A, Weiss D, Whalin MK, Cowan DP, Taylor WR. Granulocyte colony-stimulating factor and granulocyte macrophage colony-stimulating factor exacerbate atherosclerosis in apolipoprotein E-deficient mice. *Circulation*. 2007 Apr 17;115(15):2049–54.
- [230] Ditiatkovski M, Toh B-H, Bobik A. GM-CSF deficiency reduces macrophage PPAR-gamma expression and aggravates atherosclerosis in ApoE-deficient mice. *Arterioscler Thromb Vasc Biol*. 2006 Oct;26(10):2337–44.
- [231] Nebiker C a, Han J, Eppenberger-Castori S, Iezzi G, Hirt C, Amicarella F, Cremonesi E, Huber X, Padovan E, Angrisani B, Drosler R a, Rosso R, Bolli M, Oertli D, von Holzen U, Adamina M, Muraro MG, ... Spagnoli GC. GM-CSF Production by Tumor Cells Is Associated with Improved Survival in Colorectal Cancer. *Clin Cancer Res*. 2014 Apr 15;Epub ahead of print.
- [232] Takeda K, Hatakeyama K, Tsuchiya Y, Rikiishi H, Kumagai K. A correlation between GM-CSF gene expression and metastases in murine tumors. *Int J cancer*. 1991;47(3):413–20.
- [233] Sheng JR, Muthusamy T, Prabhakar BS, Meriggioli MN. GM-CSF-induced regulatory T cells selectively inhibit anti-acetylcholine receptor-specific immune responses in experimental myasthenia gravis. *J Neuroimmunol*. Elsevier B.V.; 2011 Dec 15;240-241:65–73.

- [234] Hu X, Sun H, Han C, Wang X, Yu W. Topically applied rhGM-CSF for the wound healing: a systematic review. *Burns*. 2011 Aug;37(5):729–41.
- [235] Schäbitz W-R, Krüger C, Pitzer C, Weber D, Laage R, Gassler N, Aronowski J, Mier W, Kirsch F, Dittgen T, Bach A, Sommer C, Schneider A. A neuroprotective function for the hematopoietic protein granulocyte-macrophage colony stimulating factor (GM-CSF). *J Cereb Blood Flow Metab*. 2008 Jan;28(1):29–43.
- [236] Takahashi T, Kalka C, Masuda H, Chen D, Silver M, Kearney M, Magner M, Isner JM, Asahara T. Ischemia- and cytokine-induced mobilization of bone marrow-derived endothelial progenitor cells for neovascularization. *Nat Med*. 1999 Apr;5(4):434–8.
- [237] Passlick B, Flieger D, Ziegler-Heitbrock L. Identification and characterization of a novel monocyte subpopulation in human peripheral blood. *Blood*. 1989;74(7):2527–34.
- [238] Ziegler-Heitbrock L, Ancuta P, Crowe S, Dalod M, Grau V, Hart DN, Leenen PJM, Liu Y-J, MacPherson G, Randolph GJ, Scherberich J, Schmitz J, Shortman K, Sozzani S, Strobl H, Zembala M, Austyn JM, Lutz MB. Nomenclature of monocytes and dendritic cells in blood. *Blood*. 2010 Oct 21;116(16):e74–80.
- [239] Cros J, Cagnard N, Woollard K, Patey N, Zhang S-Y, Senechal B, Puel A, Biswas SK, Moshous D, Picard C, Jais J-P, D’Cruz D, Casanova J-L, Trouillet C, Geissmann F. Human CD14<sup>dim</sup> monocytes patrol and sense nucleic acids and viruses via TLR7 and TLR8 receptors. *Immunity*. 2010 Sep 24;33(3):375–86.
- [240] Rossol M, Kraus S, Pierer M, Baerwald C, Wagner U. The CD14<sup>(bright)</sup> CD16<sup>+</sup> monocyte subset is expanded in rheumatoid arthritis and promotes expansion of the Th17 cell population. *Arthritis Rheum*. 2012 Mar;64(3):671–7.
- [241] Shantsila E, Wrigley B, Tapp L, Apostolakis S, Montoro-Garcia S, Drayson MT, Lip GYH. Immunophenotypic characterization of human monocyte subsets: possible implications for cardiovascular disease pathophysiology. *J Thromb Haemost*. 2011 May;9(5):1056–66.
- [242] Ancuta P, Rao R, Moses A, Mehle A, Shaw SK, Luscinskas FW, Gabuzda D. Fractalkine preferentially mediates arrest and migration of CD16<sup>+</sup> monocytes. *J Exp Med*. 2003 Jun 16;197(12):1701–7.
- [243] Fingerle G, Pforte A, Passlick B, Blumenstein M, Ströbel M, Ziegler-Heitbrock HW. The novel subset of CD14<sup>+</sup>/CD16<sup>+</sup> blood monocytes is expanded in sepsis patients. *Blood*. 1993 Nov 15;82(10):3170–6.

- [244] Herra CM, Keane CT, Whelan A. Increased expression of Fc gamma receptors on neutrophils and monocytes may reflect ongoing bacterial infection. *J Med Microbiol.* 1996 Feb;44(2):135–40.
- [245] Saleh MN, Goldman SJ, LoBuglio a F, Beall a C, Sabio H, McCord MC, Minasian L, Alpaugh RK, Weiner LM, Munn DH. CD16+ monocytes in patients with cancer: spontaneous elevation and pharmacologic induction by recombinant human macrophage colony-stimulating factor. *Blood.* 1995 May 15;85(10):2910–7.
- [246] Schlitt A, Heine GH, Blankenberg S, Espinola-Klein C, Dopheide JF, Bickel C, Lackner KJ, Iz M, Meyer J, Darius H, Rupprecht HJ. CD14+CD16+ monocytes in coronary artery disease and their relationship to serum TNF-alpha levels. *Thromb Haemost.* 2004 Jun 2;92(2):419–24.
- [247] Heron M, Grutters JC, van Velzen-Blad H, Veltkamp M, Claessen AME, van den Bosch JMM. Increased expression of CD16, CD69, and very late antigen-1 on blood monocytes in active sarcoidosis. *Chest.* 2008 Nov;134(5):1001–8.
- [248] Moniuszko M, Bodzenta-Lukaszyk A, Kowal K, Lenczewska D, Dabrowska M. Enhanced frequencies of CD14++CD16+, but not CD14+CD16+, peripheral blood monocytes in severe asthmatic patients. *Clin Immunol.* Elsevier Inc.; 2009 Mar;130(3):338–46.
- [249] Heimbeck I, Hofer TPJ, Eder C, Wright AK, Frankenberger M, Marei A, Boghdadi G, Scherberich J, Ziegler-Heitbrock L. Standardized single-platform assay for human monocyte subpopulations: Lower CD14+CD16++ monocytes in females. *Cytometry A.* 2010 Sep;77(9):823–30.
- [250] Fingerle-Rowson G, Angstwurm M, Andreesen R, Ziegler-Heitbrock HW. Selective depletion of CD14+ CD16+ monocytes by glucocorticoid therapy. *Clin Exp Immunol.* 1998 Jun;112(3):501–6.
- [251] Siedlar M, Strach M, Bukowska-Strakova K, Lenart M, Szaflarska A, Węglarczyk K, Rutkowska M, Baj-Krzyworzeka M, Pituch-Noworolska A, Kowalczyk D, Grodzicki T, Ziegler-Heitbrock L, Zembala M. Preparations of intravenous immunoglobulins diminish the number and proinflammatory response of CD14+CD16++ monocytes in common variable immunodeficiency (CVID) patients. *Clin Immunol.* 2011 May;139(2):122–32.
- [252] Korkosz M, Bukowska-Strakova K, Sadis S, Grodzicki T, Siedlar M. Monoclonal antibodies against macrophage colony-stimulating factor diminish the number of circulating intermediate and nonclassical (CD14(++)CD16+)/CD14(+)CD16(++) monocytes in rheumatoid arthritis patient. *Blood.* 2012 May 31;119(22):5329–30.

- [253] Kawanaka N, Yamamura M, Aita T, Morita Y, Okamoto A, Kawashima M, Iwahashi M, Ueno A, Ohmoto Y, Makino H. CD14+,CD16+ blood monocytes and joint inflammation in rheumatoid arthritis. *Arthritis Rheum.* 2002 Oct;46(10):2578–86.
- [254] Heine GH, Ortiz A, Massy Z a, Lindholm B, Wiecek A, Martínez-Castelao A, Covic A, Goldsmith D, Süleymanlar G, London GM, Parati G, Sicari R, Zoccali C, Fliser D. Monocyte subpopulations and cardiovascular risk in chronic kidney disease. *Nat Rev Nephrol.* Nature Publishing Group; 2012 Jun;8(6):362–9.
- [255] Athnasou NA. Synovial macrophages. *Ann Rheum Dis.* 1995;54(5):392–4.
- [256] Hume DA, Unit MRCR, Gordon S. The mononuclear phagocyte system of the mouse defined by immunohistochemical localization of antigen F4/80: macrophages of bone and associated connective tissue. *J Cell Sci.* 1984;66:189–94.
- [257] Smith MD. The normal synovium. *Open Rheumatol J.* 2011 Jan;5:100–6.
- [258] Edwards J. The origin of type A synovial lining cells. *Immunobiology.* 1982;161(3-4):227–31.
- [259] Martin WJ, Walton M, Harper J. Resident macrophages initiating and driving inflammation in a monosodium urate monohydrate crystal-induced murine peritoneal model of acute gout. *Arthritis Rheum.* 2009 Jan;60(1):281–9.
- [260] Duff G, Atkins E, Malawista S. Trans Assoc Am Physicians. 1983;96:234-45. The fever of gout: urate crystals activate endogenous pyrogen production from human and rabbit mononuclear phagocytes. *Trans Assoc Am Physicians.* 1983;96:234–45.
- [261] Wood DD, Ihrie EJ, Dinarello C a, Cohen PL. Isolation of an interleukin-1-like factor from human joint effusions. *Arthritis Rheum.* 1983 Aug;26(8):975–83.
- [262] Guerne P, Terkeltaub R, Zuraw B, Lotz M. Inflammatory microcrystals stimulate interleukin-6 production and secretion by human monocytes and synoviocytes. *Arthritis Rheum.* 1989;32(11):1443–52.
- [263] Di Giovine F, Malawista S, Thornton E, Duff G. Urate Crystals Stimulate Production of Tumor Necrosis Factor Alpha from Human Blood Monocytes and Synovial Cells. *J Clin Invest.* 1991;87(4):1375–81.
- [264] Terkeltaub R, Zachariae C, Santoro D, Martin J, Peveri P, Matsushima K. Monocyte-derived neutrophil chemotactic factor/interleukin-8 is a potential mediator of crystal-induced inflammation. *Arthritis Rheum.* 1991;34(7):984.

- [265] Amaral F a, Costa V V, Tavares LD, Sachs D, Coelho FM, Fagundes CT, Soriani FM, Silveira TN, Cunha LD, Zamboni DS, Quesniaux V, Peres RS, Cunha TM, Cunha FQ, Ryffel B, Souza DG, Teixeira MM. NLRP3 inflammasome-mediated neutrophil recruitment and hypernociception depend on leukotriene B(4) in a murine model of gout. *Arthritis Rheum.* 2012 Feb;64(2):474–84.
- [266] Jaramillo M, Godbout M, Naccache PH, Olivier M. Signaling events involved in macrophage chemokine expression in response to monosodium urate crystals. *J Biol Chem.* 2004 Dec 10 [cited 2014 Jun 16];279(50):52797–805.
- [267] Harigai M, Hara M, Yoshimura T, Leonard E, Inoue K, Kashiwazaki S. Monocyte chemoattractant protein-1 (MCP-1) in inflammatory joint diseases and its involvement in the cytokine network of rheumatoid synovium. *Clin Immunol Immunopathol.* 1993;69(1):83–91.
- [268] Matsukawa A, Miyazaki S, Maeda T, Tanase S, Feng L, Ohkawara S, Yoshinaga M, Yoshimura T. Production and regulation of monocyte chemoattractant protein-1 in lipopolysaccharide- or monosodium urate crystal-induced arthritis in rabbits: roles of tumor necrosis factor alpha, interleukin-1, and interleukin-8. *Lab Invest.* 1998;78(8):973–85.
- [269] Scanu A, Oliviero F, Gruaz L, Sfriso P, Pozzuoli A, Frezzato F, Agostini C, Burger D, Punzi L. High-density lipoproteins downregulate CCL2 production in human fibroblast-like synoviocytes stimulated by urate crystals. *Arthritis Res Ther.* 2010;12(1):R23.
- [270] Pascual E, Jovaní V. A quantitative study of the phagocytosis of urate crystals in the synovial fluid of asymptomatic joints of patients with gout. *Br J Rheumatol.* 1995;34(8):724–6.
- [271] Yagnik DR, Hillyer P, Marshall D, Smythe CD, Krausz T, Haskard DO, Landis RC. Noninflammatory phagocytosis of monosodium urate monohydrate crystals by mouse macrophages. Implications for the control of joint inflammation in gout. *Arthritis Rheum.* 2000;43(8):1779–89.
- [272] Landis RC, Yagnik DR, Florey O, Philippidis P, Emons V, Mason JC, Haskard DO. Safe disposal of inflammatory monosodium urate monohydrate crystals by differentiated macrophages. *Arthritis Rheum.* 2002 Nov;46(11):3026–33.
- [273] Yagnik DR, Evans BJ, Florey O, Mason JC, Landis RC, Haskard DO. Macrophage release of transforming growth factor beta1 during resolution of monosodium urate monohydrate crystal-induced inflammation. *Arthritis Rheum.* 2004 Jul;50(7):2273–80.



- [274] Jenner W, Motwani M, Veighey K, Newson J, Audzevich T, Nicolaou A, Murphy S, Macallister R, Gilroy DW. Characterisation of leukocytes in a human skin blister model of acute inflammation and resolution. *PLoS One*. 2014 Jan [cited 2014 Jul 12];9(3):e89375.
- [275] Joosten L a B, Netea MG, Mylona E, Koenders MI, Malireddi RKS, Oosting M, Stienstra R, van de Veerdonk FL, Stalenhoef AF, Giamarellou-Bourboulis EJ, Kanneganti T-D, van der Meer JWM. Engagement of fatty acids with Toll-like receptor 2 drives interleukin-1 $\beta$  production via the ASC/caspase 1 pathway in monosodium urate monohydrate crystal-induced gouty arthritis. *Arthritis Rheum*. 2010 Nov [cited 2014 Jan 21];62(11):3237–48.
- [276] Migita K, Koga T, Satomura K, Izumi M, Torigoshi T, Maeda Y, Izumi Y, Jiuchi Y, Miyashita T, Yamasaki S, Aiba Y, Komori A, Nakamura M, Motokawa S, Kawakami A, Nakamura T, Ishibashi H. Serum amyloid A triggers the monosodium urate -mediated mature interleukin-1 $\beta$  production from human synovial fibroblasts. *Arthritis Res Ther*. BioMed Central Ltd; 2012 Jan [cited 2014 Jun 15];14(3):R119.
- [277] Shaw O, Steiger S, Liu X, Hamilton JA, Harper JL. GM-CSF drives MSU crystal-induced inflammatory macrophage differentiation and NLRP3 inflammasome upregulation in vivo. *Arthritis Rheum*. 2014;
- [278] Wallace, SL, Robinson H, Masi A, Decker J, McCarty D, Yü T. Preliminary criteria for the classification of the acute arthritis of primary gout. *Arthritis Rheum*. 1977;20(3):895–900.
- [279] Landis RC, Yagnik DR, Florey O, Philippidis P, Emons V, Mason JC, Haskard DO. Safe disposal of inflammatory monosodium urate monohydrate crystals by differentiated macrophages. *Arthritis Rheum*. 2002 Nov;46(11):3026–33.
- [280] Scanu A, Oliviero F, Ramonda R, Frallonardo P, Dayer J-M, Punzi L. Cytokine levels in human synovial fluid during the different stages of acute gout: role of transforming growth factor  $\beta$ 1 in the resolution phase. *Ann Rheum Dis*. 2012 Apr [cited 2014 Jan 23];71(4):621–4.
- [281] Lacey DC, Achuthan A, Fleetwood AJ, Dinh H, Roiniotis J, Scholz GM, Chang MW, Beckman SK, Cook AD, Hamilton J a. Defining GM-CSF- and macrophage-CSF-dependent macrophage responses by in vitro models. *J Immunol*. 2012 Jun 1;188(11):5752–65.
- [282] Rouault T, Caldwell D, Holmes E. Aspiration of the asymptomatic metatarsophalangeal joint in gout patients and hyperuricemic controls. *Arthritis Rheum*. 1982;25(2):209–12.



- [283] Puig JG, de Miguel E, Castillo MC, Rocha a L, Martínez M a, Torres RJ. Asymptomatic hyperuricemia: impact of ultrasonography. *Nucleosides Nucleotides Nucleic Acids*. 2008 Jun;27(6):592–5.
- [284] Netea MG, Nold-petry CA, Nold MF, Joosten LAB, Opitz B, Meer JHM Van Der, Veerdonk FL Van De, Ferwerda G, Heinhuis B, Devesa I, Funk CJ, Mason RJ, Kullberg BJ, Rubartelli A, Meer JWM Van Der, Dinarello CA. Differential requirement for the activation of the inflammasome for processing and release of IL-1<sup>α</sup> in monocytes and macrophages. 2009;113(10):1–3.
- [285] De Miguel E, Puig JG, Castillo C, Peiteado D, Torres RJ, Martín-Mola E. Diagnosis of gout in patients with asymptomatic hyperuricaemia: a pilot ultrasound study. *Ann Rheum Dis*. 2012 Jan;71(1):157–8.
- [286] Yagnik DR, Evans BJ, Florey O, Mason JC, Landis RC, Haskard DO. Macrophage release of transforming growth factor beta1 during resolution of monosodium urate monohydrate crystal-induced inflammation. *Arthritis Rheum*. 2004 Jul;50(7):2273–80.
- [287] Pelegrin P, Surprenant A. Dynamics of macrophage polarization reveal new mechanism to inhibit IL-1beta release through pyrophosphates. *EMBO J*. Nature Publishing Group; 2009 Jul 22;28(14):2114–27.
- [288] Mazzone A, Ricevuti G. Leukocyte CD11/CD18 integrins: biological and clinical relevance. *Haematologica*. 1995;80:161–75.
- [289] Nielsen MJ, Moestrup SK. Receptor targeting of hemoglobin mediated by the haptoglobins: roles beyond heme scavenging. *Blood*. 2009 Jul 23 [cited 2014 Jan 23];114(4):764–71.
- [290] Buechler C, Ritter M, Orsó E, Langmann T, Klucken J, Schmitz G. Regulation of scavenger receptor CD163 expression in human monocytes and macrophages by pro- and antiinflammatory stimuli. *J Leukoc Biol*. 2000;67(1):97–103.
- [291] Moestrup SK, Møller HJ. CD163: a regulated hemoglobin scavenger receptor with a role in the anti-inflammatory response. *Ann Med*. 2004 Jan [cited 2014 Jan 23];36(5):347–54.
- [292] Sabat R, Grütz G, Warszawska K, Kirsch S, Witte E, Wolk K, Geginat J. Biology of interleukin-10. *Cytokine Growth Factor Rev*. 2010 Oct;21(5):331–44.
- [293] Chhana A, Callon KE, Pool B, Naot D, Watson M, Gamble GD, McQueen FM, Cornish J, Dalbeth N. Monosodium urate monohydrate crystals inhibit osteoblast viability and function: implications for development of bone erosion in gout. *Ann Rheum Dis*. 2011 Sep;70(9):1684–91.

- [294] Hamilton J. Rheumatoid arthritis : Opposing actions of haemopoietic growth factors and slow-acting anti-rheumatic drugs. *Lancet*. 1993;342(8870):536–9.
- [295] Martinon F, Pétrilli V, Mayor A, Tardivel A, Tschopp J. Gout-associated uric acid crystals activate the NALP3 inflammasome. *Nature*. 2006 Mar 9;440(7081):237–41.
- [296] Mylona EE, Mouktaroudi M, Crisan TO, Makri S, Pistiki A, Georgitsi M, Savva A, Netea MG, van der Meer JW, Giamarellos-Bourboulis EJ, Joosten LA. Enhanced interleukin-1 $\beta$  production of PBMCs from patients with gout after stimulation with Toll-like receptor-2 ligands and urate crystals. *Arthritis Res Ther. BioMed Central Ltd*; 2012 Jul 4;14(4):R158.
- [297] Martin WJ, Shaw O, Liu X, Steiger S, Harper JL. Monosodium urate monohydrate crystal-recruited noninflammatory monocytes differentiate into M1-like proinflammatory macrophages in a peritoneal murine model of gout. *Arthritis Rheum*. 2011 May;63(5):1322–32.
- [298] Seok J, Warren HS, Cuenca AG, Mindrinos MN, Baker H V, Xu W, Richards DR, McDonald-Smith GP, Gao H, Hennessy L, Finnerty CC, López CM, Honari S, Moore EE, Minei JP, Cuschieri J, Bankey PE, ... Tompkins RG. Genomic responses in mouse models poorly mimic human inflammatory diseases. *Proc Natl Acad Sci U S A*. 2013 Feb 26 [cited 2014 Jul 10];110(9):3507–12.
- [299] Amaral F a, Costa V V, Tavares LD, Sachs D, Coelho FM, Fagundes CT, Soriani FM, Silveira TN, Cunha LD, Zamboni DS, Quesniaux V, Peres RS, Cunha TM, Cunha FQ, Ryffel B, Souza DG, Teixeira MM. NLRP3 inflammasome-mediated neutrophil recruitment and hypernociception depend on leukotriene B(4) in a murine model of gout. *Arthritis Rheum*. 2012 Mar [cited 2014 Jun 29];64(2):474–84.
- [300] Yin J, Peng Y, Wu J, Wang Y, Yao L. Toll-like receptor 2/4 links to free fatty acid-induced inflammation and  $\beta$ -cell dysfunction. *J Leukoc Biol*. 2014;95(1):47–52.
- [301] Porta C, Rimoldi M, Raes G, Brys L, Ghezzi P, Di Liberto D, Dieli F, Ghisletti S, Natoli G, De Baetselier P, Mantovani A, Sica A. Tolerance and M2 (alternative) macrophage polarization are related processes orchestrated by p50 nuclear factor kappaB. *Proc Natl Acad Sci U S A*. 2009 Sep 1;106(35):14978–83.
- [302] Bonizzi G, Karin M. The two NF-kappaB activation pathways and their role in innate and adaptive immunity. *Trends Immunol*. 2004 Jun [cited 2014 May 30];25(6):280–8.
- [303] Underhill DM, Ozinsky A. Phagocytosis of microbes: complexity in action. *Annu Rev Immunol*. 2002 Jan [cited 2014 May 25];20(2):825–52.

- [304] Barabe RIC, Gilbert C, Liao N, Bourgoïn SG, Naccache PH. Crystal-induced neutrophil activation VI . Involvement of Fc  $\gamma$  RIIIB ( CD16 ) and CD11b in response to inflammatory microcrystals. :209–20.
- [305] Oliva C, Turnbough CL, Kearney JF. CD14-Mac-1 interactions in *Bacillus anthracis* spore internalization by macrophages. *Proc Natl Acad Sci U S A*. 2009 Aug 18;106(33):13957–62.
- [306] Pasquinelli AE. MicroRNAs and their targets: recognition, regulation and an emerging reciprocal relationship. *Nat Rev Genet*. Nature Publishing Group; 2012 Apr [cited 2014 May 25];13(4):271–82.
- [307] Mathonnet G, Fabian MR, Svitkin Y V, Parsyan A, Huck L, Murata T, Biffo S, Merrick WC, Darzynkiewicz E, Pillai RS, Filipowicz W, Duchaine TF, Sonenberg N. MicroRNA inhibition of translation initiation in vitro by targeting the cap-binding complex eIF4F. *Science*. 2007 Oct 21 [cited 2014 May 31];317(5845):1764–7.
- [308] Haneklaus M, Gerlic M, Kurowska-Stolarska M, Rainey A-A, Pich D, McInnes IB, Hammerschmidt W, O'Neill L a J, Masters SL. Cutting edge: miR-223 and EBV miR-BART15 regulate the NLRP3 inflammasome and IL-1 $\beta$  production. *J Immunol*. 2012 Oct 15 [cited 2014 May 23];189(8):3795–9.
- [309] Bauernfeind F, Rieger A, Schildberg F a, Knolle P a, Schmid-Burgk JL, Hornung V. NLRP3 inflammasome activity is negatively controlled by miR-223. *J Immunol*. 2012 Oct 15 [cited 2014 Jun 15];189(8):4175–81.
- [310] Latourte A, Bardin T, Richette P. Prophylaxis for acute gout flares after initiation of urate-lowering therapy. 2014;1–7.
- [311] Cascão R, Polido-Pereira J, Canhão H, Rodrigues A, Navalho M, Raquel H, Neves-Costa A, Mourão A, Resende C, da Silva J, Fonseca J, Moita L. Caspase-1 is active since the early phase of rheumatoid arthritis. *Clin Exp Rheumatol*. 2012 Jan;30(1):144.
- [312] Cascão R, Polido-Pereira J, Canhão H, Rodrigues A, Navalho M, Raquel H, Neves-Costa A, Mourão A, Resende C, da Silva J, Fonseca J, Moita L. Caspase-1 is active since the early phase of rheumatoid arthritis. *Ann Rheum Dis*. 2011;70(Suppl 2):A2.
- [313] Pelegrin P, Surprenant A. The P2X(7) receptor-pannexin connection to dye uptake and IL-1 $\beta$  release. *Purinergic Signal*. 2009 Jun;5(2):129–37.
- [314] Muñoz-Planillo R, Kuffa P, Martínez-Colón G, Smith BL, Rajendiran TM, Núñez G. K<sup>+</sup> efflux is the common trigger of NLRP3 inflammasome activation by bacterial toxins and particulate matter. *Immunity*. 2013 Jun 27 [cited 2014 May 23];38(6):1142–53.

- [315] Mylona EE, Mouktaroudi M, Crisan TO, Makri S, Pistiki A, Georgitsi M, Savva A, Netea MG, van der Meer JW, Giamarellos-Bourboulis EJ, Joosten LA. Enhanced interleukin-1 $\beta$  production of PBMCs from patients with gout after stimulation with Toll-like receptor-2 ligands and urate crystals. *Arthritis Res Ther. BioMed Central Ltd*; 2012 Jul 4;14(4):R158.
- [316] Qing Y, Zhou J, Zhang Q, Wang D, Li M, Yang Q, Huang P, Yin L, Pan S, Xie W, Zhang M, Pu M, Zeng M. Association of TLR4 Gene rs2149356 Polymorphism with Primary Gouty Arthritis in a Case-Control Study. 2013;8(5):1–9.
- [317] Liu S, Yin C, Chu N, Han L, Li C. IL-8 -251T/A and IL-12B 1188A/C polymorphisms are associated with gout in a Chinese male population. *Scand J Rheumatol*. 2013 Jan [cited 2014 Jun 23];42(2):150–8.
- [318] Chang S-J, Chen C-J, Tsai F-C, Lai H-M, Tsai P-C, Tsai M-H, Ko Y-C. Associations between gout tophus and polymorphisms 869T/C and -509C/T in transforming growth factor beta1 gene. *Rheumatology (Oxford)*. 2008 May [cited 2014 Jun 23];47(5):617–21.
- [319] Chang S-J, Tsai P-C, Chen C-J, Lai H-M, Ko Y-C. The polymorphism -863C/A in tumour necrosis factor-alpha gene contributes an independent association to gout. *Rheumatology (Oxford)*. 2007 Nov [cited 2014 Jun 23];46(11):1662–6.
- [320] Tan M-S, Yu J-T, Jiang T, Zhu X-C, Wang H-F, Zhang W, Wang Y-L, Jiang W, Tan L. NLRP3 polymorphisms are associated with late-onset Alzheimer's disease in Han Chinese. *J Neuroimmunol. Elsevier B.V.*; 2013 Dec 15 [cited 2014 Jun 12];265(1-2):91–5.
- [321] Kukkonen MK, Vehmas T, Piirilä P, Hirvonen A. Genes involved in innate immunity associated with asbestos-related fibrotic changes. *Occup Environ Med*. 2014 Jan [cited 2014 Jun 25];71(1):48–54.
- [322] Zheng Y, Zhang D, Zhang L, Fu M, Zeng Y, Russell R. Variants of NLRP3 gene are associated with insulin resistance in Chinese Han population with type-2 diabetes. *Gene. Elsevier B.V.*; 2013 Nov 1 [cited 2014 Jun 25];530(1):151–4.
- [323] Pontillo a, Brandao L, Guimaraes R, Segat L, Araujo J, Crovella S. Two SNPs in NLRP3 gene are involved in the predisposition to type-1 diabetes and celiac disease in a pediatric population from northeast Brazil. *Autoimmunity*. 2010 Dec [cited 2014 Jun 23];43(8):583–9.
- [324] Carlström M, Ekman A-K, Petersson S, Söderkvist P, Enerbäck C. Genetic support for the role of the NLRP3 inflammasome in psoriasis susceptibility. *Exp Dermatol*. 2012 Dec [cited 2014 Jun 25];21(12):932–7.

- [325] Ji X, Hou Z, Wang T, Jin K, Fan J, Luo C, Chen M, Han R, Ni C. Polymorphisms in inflammasome genes and risk of coal workers' pneumoconiosis in a Chinese population. *PLoS One*. 2012 Jan [cited 2014 Jun 15];7(10):e47949.
- [326] Verma D, Bivik C, Farahani E, Synnerstad I, Fredrikson M, Enerbäck C, Rosdahl I, Söderkvist P. Inflammasome polymorphisms confer susceptibility to sporadic malignant melanoma. *Pigment Cell Melanoma Res*. 2012 Jul [cited 2014 Jun 11];25(4):506–13.
- [327] Pontillo A, Vendramin A, Catamo E, Fabris A, Crovella S. The missense variation Q705K in CIAS1/NALP3/NLRP3 gene and an NLRP1 haplotype are associated with celiac disease. *Am J Gastroenterol*. 2011;106(3):539–44.
- [328] Roberts R, Topless R, Phipps-Green A, Geary R, Barclay M, Merriman T. Evidence of interaction of CARD8 rs2043211 with NALP3 rs35829419 in Crohn's disease. *Genes Immun*. 2010;11(4):351–6.
- [329] Schoultz I, Verma D, Halfvarsson J, Törkvist L, Fredrikson M, Sjöqvist U, Lördal M, Tysk C, Lerm M, Söderkvist P, Söderholm J. Combined polymorphisms in genes encoding the inflammasome components NALP3 and CARD8 confer susceptibility to Crohn's disease in Swedish men. *Am J Gastroenterol*. 2009;104(5):1180–8.
- [330] Villani A-C, Lemire M, Fortin G, Louis E, Silverberg MS, Collette C, Baba N, Libioulle C, Belaiche J, Bitton A, Gaudet D, Cohen A, Langelier D, Fortin PR, Wither JE, Sarfati M, Rutgeerts P, ... Franchimont D. Common variants in the NLRP3 region contribute to Crohn's disease susceptibility. *Nat Genet*. 2009 Jan [cited 2014 May 23];41(1):71–6.
- [331] Kastbom a, Verma D, Eriksson P, Skogh T, Wingren G, Söderkvist P. Genetic variation in proteins of the cryopyrin inflammasome influences susceptibility and severity of rheumatoid arthritis (the Swedish TIRA project). *Rheumatology (Oxford)*. 2008 Apr [cited 2014 Jun 25];47(4):415–7.
- [332] Yang C, Huang S-T, Chiang B-L. Association of NLRP3 and CARD8 genetic polymorphisms with juvenile idiopathic arthritis in a Taiwanese population. *Scand J Rheumatol*. 2014 Jan [cited 2014 Jun 25];43(2):146–52.
- [333] Verma D, Särndahl E, Andersson H, Eriksson P, Fredrikson M, Jönsson J-I, Lerm M, Söderkvist P. The Q705K polymorphism in NLRP3 is a gain-of-function alteration leading to excessive interleukin-1 $\beta$  and IL-18 production. *PLoS One*. 2012 Jan [cited 2014 Jun 12];7(4):e34977.
- [334] Blomgran R, Patcha Brodin V, Verma D, Bergström I, Söderkvist P, Sjöwall C, Eriksson P, Lerm M, Stendahl O, Särndahl E. Common genetic variations in the NALP3

- inflammasome are associated with delayed apoptosis of human neutrophils. *PLoS One*. 2012 Jan [cited 2014 Jun 23];7(3):e31326.
- [335] Wong KL, Yeap WH, Tai JY, Ong SM, Dang TM, Wong SC. The three human monocyte subsets: implications for health and disease. *Immunol Res*. 2012 Sep;53(1-3):41–57.
- [336] Ben-Hur H, Mor G, Insler V, Blickstein I, Amir-Zaltsman Y, Sharp A, Globerson A, Kohen F. Menopause is associated with a significant increase in blood monocyte number and a relative decrease in the expression of estrogen receptors in human peripheral monocytes. *Amer J Reprod Immunol*. 1995;34(6):363–9.
- [337] Tollerud D, Clark J, Brown L, Neuland C, Pankiw-Trost LK, Blattner W, Hoover R. The influence of age, race, and gender on peripheral blood mononuclear-cell subsets in healthy nonsmokers. *J Clin Immunol*. 1989;9(3):214–22.
- [338] Rogacev KS, Ulrich C, Blömer L, Hornof F, Oster K, Ziegelin M, Cremers B, Grenner Y, Geisel J, Schlitt A, Köhler H, Fliser D, Girndt M, Heine GH. Monocyte heterogeneity in obesity and subclinical atherosclerosis. *Eur Heart J*. 2010 Feb [cited 2014 Jul 2];31(3):369–76.
- [339] Poitou C, Dalmás E, Renovato M, Benhamo V, Hajduch F, Abdenour M, Kahn J-F, Veyrie N, Rizkalla S, Fridman W-H, Sautès-Fridman C, Clément K, Cremer I. CD14<sup>dim</sup>CD16<sup>+</sup> and CD14<sup>+</sup>CD16<sup>+</sup> monocytes in obesity and during weight loss: relationships with fat mass and subclinical atherosclerosis. *Arterioscler Thromb Vasc Biol*. 2011 Oct [cited 2014 Jun 10];31(10):2322–30.
- [340] Kashiwagi M, Imanishi T, Tsujioka H, Ikejima H, Kuroi A, Ozaki Y, Ishibashi K, Komukai K, Tanimoto T, Ino Y, Kitabata H, Hirata K, Akasaka T. Association of monocyte subsets with vulnerability characteristics of coronary plaques as assessed by 64-slice multidetector computed tomography in patients with stable angina pectoris. *Atherosclerosis*. Elsevier Ireland Ltd; 2010 Sep;212(1):171–6.
- [341] Liu Y, Imanishi T, Ikejima H, Tsujioka H, Ozaki Y, Kuroi A, Okochi K, Ishibashi K, Tanimoto T, Ino Y, Kitabata H, Akasaka T. Association Between Circulating Monocyte Subsets and In-Stent Restenosis After Coronary Stent Implantation in Patients With ST-Elevation Myocardial Infarction. *Circ J*. 2010;74(12):2585–91.
- [342] Rogacev KS, Seiler S, Zawada AM, Reichart B, Herath E, Roth D, Ulrich C, Fliser D, Heine GH. CD14<sup>++</sup>CD16<sup>+</sup> monocytes and cardiovascular outcome in patients with chronic kidney disease. *Eur Heart J*. 2011 Jan;32(1):84–92.